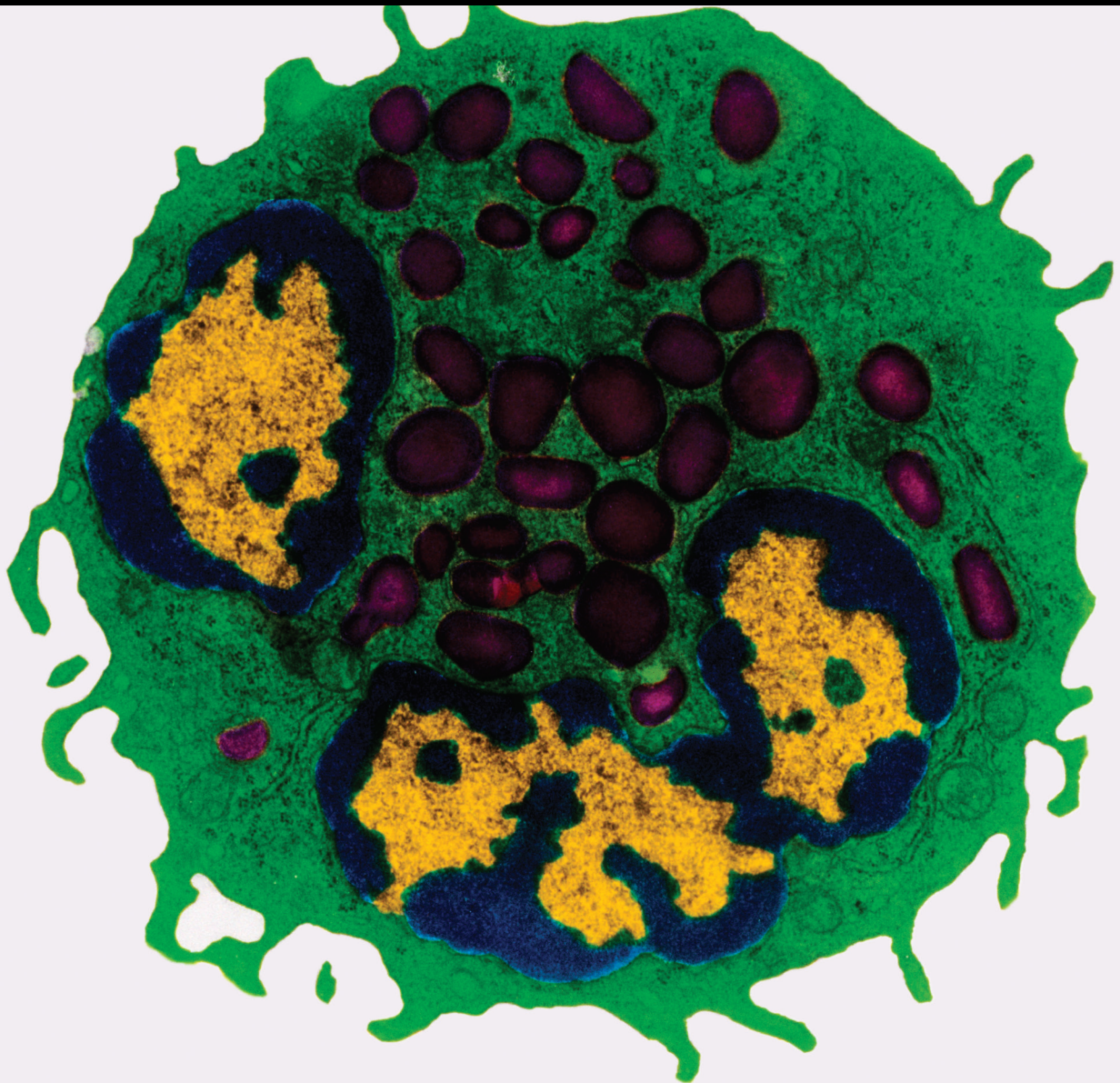


Inflammation and Regional Immune Balance in Autoimmune Disorders

Lead Guest Editor: Donghua Xu

Guest Editors: Shushan Yan, Xiaochen Wang, and Bingjie Gu





Inflammation and Regional Immune Balance in Autoimmune Disorders

Mediators of Inflammation

Inflammation and Regional Immune Balance in Autoimmune Disorders

Lead Guest Editor: Donghua Xu


Guest Editors: Shushan Yan, Xiaochen Wang, and
Bingjie Gu







Copyright © 2022 Hindawi Limited. All rights reserved.

This is a special issue published in “Mediators of Inflammation.” All articles are open access articles distributed under the Creative Commons Attribution License, which permits unrestricted use, distribution, and reproduction in any medium, provided the original work is properly cited.

Chief Editor






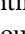

Anshu Agrawal , USA

Associate Editors

Carlo Cervellati , Italy
Elaine Hatanaka , Brazil
Vladimir A. Kostyuk , Belarus
Carla Pagliari , Brazil












Academic Editors

Amedeo Amedei , Italy
Emiliano Antiga , Italy
Tomasz Brzozowski , Poland
Daniela Caccamo , Italy
Luca Cantarini , Italy
Raffaele Capasso , Italy
Calogero Caruso , Italy
Robson Coutinho-Silva , Brazil
Jose Crispin , Mexico
Fulvio D'Acquisto , United Kingdom
Eduardo Dalmarco , Brazil
Agnieszka Dobrzyn, Poland
Ulrich Eisel , The Netherlands
Mirvat El-Sibai , Lebanon
Giacomo Emmi , Italy
Claudia Fabiani , Italy
Fabíola B Filippin Monteiro , Brazil
Antonella Fioravanti , Italy
Tânia Silvia Fröde , Brazil
Julio Galvez , Spain
Mirella Giovarelli , Italy
Denis Girard, Canada
Markus H. Gräler , Germany
Oreste Gualillo , Spain
Qingdong Guan , Canada
Tommaso Iannitti , United Kingdom
Byeong-Churl Jang, Republic of Korea
Yasumasa Kato , Japan
Cheorl-Ho Kim , Republic of Korea
Alex Kleinjan , The Netherlands
Martha Lappas , Australia
Ariadne Malamitsi-Puchner , Greece
Palash Mandal, India
Joilson O. Martins , Brazil
Donna-Marie McCafferty, Canada
Barbro N. Melgert , The Netherlands

Paola Migliorini , Italy
Vinod K. Mishra , USA
Eeva Moilanen , Finland
Elena Niccolai , Italy
Nadra Nilsen , Norway
Sandra Helena Penha Oliveira , Brazil
Michal A. Rahat , Israel
Zoltan Rakonczay Jr. , Hungary
Marcella Reale , Italy
Emanuela Roscetto, Italy
Domenico Sergi , Italy
Mohammad Shadab , USA
Elena Silvestri, Italy
Carla Sipert , Brazil
Helen C. Steel , South Africa
Saravanan Subramanian, USA
Veendamali S. Subramanian , USA
Taina Tervahartiala, Finland
Alessandro Trentini , Italy
Kathy Triantafilou, United Kingdom
Fumio Tsuji , Japan
Maria Letizia Urban, Italy
Giuseppe Valacchi , Italy
Kerstin Wolk , Germany
Soh Yamazaki , Japan
Young-Su Yi , Republic of Korea
Shin-ichi Yokota , Japan
Francesca Zimetti , Italy

Contents

Topical Treatment of Colquhounia Root Relieves Skin Inflammation and Itch in Imiquimod-Induced Psoriasiform Dermatitis in Mice

Fei Li , Dan Han , Bo Wang , Wentao Zhang , Yan Zhao , Jing Xu , Liesu Meng , Kuanhou Mou , Shemin Lu , Wenhua Zhu , and Yan Zhou 









Research Article (15 pages), Article ID 5782922, Volume 2022 (2022)

A Variant of sNASP Exacerbates Lymphocyte Subset Disorder and Nephritis in a Spontaneous Lupus Model Sle1.Yaa Mouse

Jianye Zhang, Xiaoping Du, Hui Wang, Yatao Bao, Meng Lian, Zhiwei Xu , and Jiyu Ju 



Research Article (9 pages), Article ID 8175863, Volume 2021 (2021)

Endangered Lymphocytes: The Effects of Alloxan and Streptozotocin on Immune Cells in Type 1 Induced Diabetes

Luiz A. D. Queiroz , Josiane B. Assis , João P. T. Guimarães , Emanuella S. A. Sousa , Anália C. Milhomem , Karen K. S. Sunahara , Anderson Sá-Nunes , and Joilson O. Martins 

Research Article (15 pages), Article ID 9940009, Volume 2021 (2021)

Gut Microbiota and Type 2 Diabetes Mellitus: Association, Mechanism, and Translational Applications

Lili Zhang, Jinjin Chu, Wenhao Hao, Jiaojiao Zhang, Haibo Li, Chunjuan Yang, Jinghan Yang, Xiaohua Chen , and Honggang Wang 


Review Article (12 pages), Article ID 5110276, Volume 2021 (2021)

Serum IgE Predicts Difference of Population and Allergens in Allergic Diseases: Data from Weifang City, China

Zhang Xu-De , Guo Bei-Bei , Wang Xi-Juan , Li Hai-Bo , Zhang Li-Li , and Liu Feng-Xia 






Research Article (9 pages), Article ID 6627087, Volume 2021 (2021)

Role of Extracellular Vesicles in Placental Inflammation and Local Immune Balance

Zengfang Wang, Ruizhen Yang, Jiaojiao Zhang, Pingping Wang, Zengyan Wang, Jian Gao , and Xue Liu 

Review Article (10 pages), Article ID 5558048, Volume 2021 (2021)

Investigation of Newly Diagnosed Drug-Naive Patients with Systemic Autoimmune Diseases Revealed the Cleaved Peptide Tyrosine Tyrosine (PYY 3-36) as a Specific Plasma Biomarker of Rheumatoid Arthritis

Jozsef A. Balog , Agnes Kemeny , Laszlo G. Puskas , Szilard Burcsar, Attila Balog , and Gabor J. Szebeni 

Research Article (9 pages), Article ID 5523582, Volume 2021 (2021)

Research Article

Topical Treatment of Colquhounia Root Relieves Skin Inflammation and Itch in Imiquimod-Induced Psoriasiform Dermatitis in Mice

Fei Li ¹, Dan Han ¹, Bo Wang ², Wentao Zhang ³, Yan Zhao ¹, Jing Xu ^{3,4}, Liesu Meng ^{3,4}, Kuanhou Mou ¹, Shemin Lu ^{3,4}, Wenhua Zhu ^{3,4} and Yan Zhou ¹

¹Department of Dermatology, The First Affiliated Hospital of Xi'an Jiaotong University, Xi'an, Shaanxi, China

²Center for Translational Medicine, The First Affiliated Hospital of Xi'an Jiaotong University, Xi'an, Shaanxi, China

³Institute of Molecular and Translational Medicine, and Department of Biochemistry and Molecular Biology, School of Basic Medical Sciences, Xi'an Jiaotong University Health Science Center, Xi'an, Shaanxi, China

⁴Key Laboratory of Environment and Genes Related to Diseases (Xi'an Jiaotong University), Ministry of Education, Xi'an, Shaanxi, China

Correspondence should be addressed to Wenhua Zhu; zhuwenhua@xjtu.edu.cn and Yan Zhou; yanzhou7798@xjtu.edu.cn

Fei Li and Dan Han contributed equally to this work.

Received 18 June 2021; Revised 15 December 2021; Accepted 27 December 2021; Published 11 January 2022

Academic Editor: Shushan Yan

Copyright © 2022 Fei Li et al. This is an open access article distributed under the Creative Commons Attribution License, which permits unrestricted use, distribution, and reproduction in any medium, provided the original work is properly cited.

Itch is one of the major clinical manifestations of psoriasis, which is closely related with neurogenic inflammation and difficult to control. Colquhounia Root (CR) is a Chinese herb exhibiting broad bioactivities on anti-inflammation. This study was designed to explore the antipsoriatic and anti-itch potential of CR and its underlying mechanisms. Mice in a model of imiquimod-induced psoriasiform dermatitis were treated topically with CR for 7 days, and the severity of skin lesions and itch was significantly ameliorated. CR reduced the inflammatory cell infiltration, as well as mast cells in skins. Particularly, the expression of inflammatory cytokines and chemokine including *Il17a*, *Il22*, and *Ccl20* and itch-related molecules such as *SP*, *CGRP*, and *NGF* in lesions were decreased in diseased mice upon application with CR. The normal human epidermal keratinocytes were stimulated with the M5 cytokine cocktail, the mixture of IL-17A, IL-22, Oncostatin M, IL-1 α , and TNF- α , and cell viability and mRNA expression levels of inflammatory factors and itch-related molecules were measured after being treated with CR. We found that CR inhibited both cell hyperproliferation and overexpression of inflammatory cytokines and itch-related molecules *in vitro*. Altogether, we conclude that CR relieves psoriatic lesions and itch via controlling immunological and neurogenic inflammation.

1. Introduction

Psoriasis is a chronic immune-mediated inflammatory disease mainly manifested as scaly erythema and patches in the skin. Patients suffering from psoriasis often complain of disgusting appearance, chronic itch, and joint pain [1–3]. Itch is one of the most troublesome symptoms of psoriasis, affecting the quality of life and sleep of patients. It is probably unrelated to the severity of psoriasis due to its particular mechanisms [4].

The pathophysiological mechanism of itch in psoriasis, which is mainly related to mental stress and neurogenic inflammation, remains poorly understood. Studies have shown that itch-related molecules released by epidermal keratinocytes and other cells in the dermis such as calcitonin gene-related peptide (CGRP), substance P (SP), nerve growth factor (NGF), and TRPV1 and inflammatory cytokines (IL-17 and IL-22), as well as chemokine CCL20, are important in mechanisms of itch [5–10]. Their expressions are significantly increased in the skin

specimens of psoriasis patients, involved in the occurrence and development of psoriatic itch [2, 11].

In the last few decades, considerable progress has been made in the treatment of psoriasis including topical or oral traditional medications, novel biologics, and phototherapies. With the in-depth study of psoriasis, psoriatic itch has gradually been noticed. However, traditional antipruritic therapies (such as antihistamines) are limited in the treatment of itch in psoriasis. Traditional topical drugs like vitamin D3 derivatives and coal tar for clinical treatment of psoriasis have little effect on itch or even aggravate it [12]. Biological agents, such as TNF- α and IL-17 inhibitors, can quickly and effectively relieve itch, but some patients could not afford them because of high prices or high-risk adverse reactions [13], such as infection, urticaria, and tumor in the long term [14]. Therefore, successful treatment of psoriatic itch is still challenging. It is necessary to further explore and develop treatment strategies and drugs to relieve psoriatic itch.

Nowadays, the use of botanical therapeutics has been taken attention by dermatologists, such as *Tripterygium wilfordii* and *Colquhounia Root* (CR) [15]. CR is a traditional Chinese medicine, containing several bioactive ingredients such as triptolide and tripterine [16], is widely used in the treatment of autoimmune-related diseases such as systemic lupus erythematosus, rheumatoid arthritis, chronic nephritis, vasculitis, and psoriasis, with anti-inflammatory and analgesic effects [17–19]. However, it has not been reported whether CR has the effect of inhibiting itch in psoriasis. Therefore, we aim to explore the effects and mechanisms of topical treatment with CR.

2. Materials and Methods

2.1. Mice. Forty-one female C57BL/6J mice, weighing 18–20 g, were purchased from Xi'an Jiaotong University Laboratory Animal Center and were kept at a standardized breeding environment. Standard diet and water were available to all mice anytime. All animal experiments were approved by the Institutional Animal Ethics Committee of Xi'an Jiaotong University.

2.2. Preparation of CR. CR tablets (Z20027411) were provided by Pharmaceutical Factory of the Chongqing Academy of Chinese Materia Medica. We grounded 5 g CR tablets into powder and then mixed it in 250 g Vaseline to keep the effective concentration which was 0.002%, and then stored it at 4°C.

2.3. Imiquimod- (IMQ-) Induced Psoriasisform Dermatitis (PsD) in Mice and Treatment. Mice were randomly divided into three groups, the normal control group, disease group (IMQ), and CR treated group (IMQ+CR). We followed the methods of William et al. to establish the IMQ-induced psoriasisform dermatitis mouse model [20]. Mice were anesthetized with isoflurane, and their hair on the back skin was shaved (3 cm \times 3 cm). Then, 62.5 mg of IMQ creams (Mingxin Pharmaceutical Co., Ltd., Sichuan, China) was applied daily onto the dorsal skins for 7 consecutive days to induce psoriasisform dermatitis in the IMQ group and IMQ+CR

group mice. CR were daily administered to the dorsal skins for 9 consecutive days from two days before IMQ application. Mice in the normal group were treated with Vaseline. A blinded observer measured the thickness of the dorsal skins by a vernier caliper daily and observed and photographed the back skin with a dermoscope simultaneously. Psoriasis Severity Index (PSI) scores were used to evaluate the severity of skin lesions every day [21], which were graded from 0 to 4 for erythema, thickness, scaling, and total. All mice were euthanized, and their skin specimens were stored for determination and further experiments. The experiment scheme is shown in Figure 1(a). Liver and renal injury biomarkers were carried out by an autoanalyzer (LABOSPECT 008 ASi, Hitachi, Japan).

2.4. Behavioral Tests. We did the behavioral tests following the methods of Sakai et al. [22]. Firstly, we pretreated and habituated all mice to a transparent acrylic box for 30 min twice. Twenty hours after each topical application, we videotaped the number of scratch bouts of mice for 30 minutes. Then, the scratch bouts of mice in videos were counted by a blinded observer. A scratch bout was defined as once or more times rapidly front and backward pointing and touching movement with hind claws in the skin lesions and ending by licking or biting the toes or placing the back claws on the floor. Other movements away from the treated area as ear scratching and grooming were excluded.

2.5. Histopathology and Immunohistochemistry (IHC). Skin specimens in paraformaldehyde-fixed (4%) were embedded in paraffin for haematoxylin and eosin staining (H&E) and IHC. Mast cells were stained by Toluidine blue following the way of Puebla-Osorio et al. [23]. We assessed the histopathological alterations with computer-assisted quantitative image analysis in lesions, including epidermal thickness, area of Munro's microabscesses (MM), and the number of mast cells. Tissue sections were prepared for IHC with SP (Cat, No. sc-21715, 1:50, Santa Cruze), CGRP (Cat, No. sc-57053, 1:50, Santa Cruze), and NGF (Cat, No. sc-32300, 1:50, Santa Cruze) antibodies. The integrated optical density (IOD) of SP, CGRP, and NGF in the image was measured by Image Pro plus 6 software.

2.6. mRNA Quantification. RNA, extracted from skin specimens with TRIzol reagent (Thermo Fisher Scientific) according to the instruction, was converted into cDNA with the RevertAid First Strand cDNA Synthesis kit (Thermo Fisher Scientific). Quantitative real-time polymerase chain reaction (qPCR) was performed on a PCR machine (CFX CCONNECT Real-time system; Bio Rad, Hercules, CA, USA). The gene-specific primers are summarized in Table 1. The data were analyzed with the $2^{-\Delta\Delta CT}$ method and normalized by GAPDH.

2.7. Flow Cytometry. Skin samples from each group were cut into pieces using ophthalmic scissors and digested using collagenases (2.6 mg/ml, Sigma) and DNase (0.1 mg/ml, Sigma) for 1.5 h. The cell suspension was filtered by a 40 μ m nylon net. Then, cells from the skin were stained with anti-mouse-BV785-CD45.2 (Cat, No. 109839, 1:200, BioLegend), anti-

mouse-AF700-TCR β (Cat, No. 109224, 1:200, BioLegend), anti-mouse-PE-Cy5-CD4 (Cat, No. 100514, 1:200, BioLegend), anti-mouse-BV711-CD8 (Cat, No. 100759, 1:200, BioLegend), anti-mouse-APC-CD11b (Cat, No. 101212, 1:200, BioLegend), anti-mouse-FITC-F4/80 (Cat, No. 123108, 1:200, BioLegend), anti-mouse-Pacific blue-Ly6G (Cat, No. 127612, 1:200, BioLegend), and anti-mouse-PE- γ δ T (Cat, No. 553178, 1:200, Becton Dickinson). Finally, we detected and analyzed all samples with a flow cytometer. Gating strategy of cells in flow cytometry is shown in supplementary Figure 1.

2.8. Cell Culture and Treatment. We performed all culture experiments on the normal human epidermal keratinocytes (NHEKs) which were obtained from ATCC (Manassas, VA). Cells were cultured with Dulbecco's modified Eagle's medium (DMEM, Hyclone) supplemented with 10% heat-inactivated fetal bovine serum (FBS), 100 U/ml of penicillin, and 100 μ g/ml of streptomycin and were placed in an incubator at a 37°C humidified atmosphere with 5% CO₂. NHEKs were treated with 10 ng/ml of M5 cocktail (IL-17A, IL-22, Oncostatin M, IL-1 α , and TNF- α) [24], with or without CR dissolved in DMSO for 24 h.

2.9. Cell Viability Assay. We tested the effect of CR on the growth of NHEKs by CCK-8 assay following the methods of Ru et al. 2020 [25]. We seeded NHEKs onto 96-well plates at a density of 2000 cells per well. Then, the medium was replaced with fresh medium containing 10 ng/ml M5 and various concentrations (0, 0.25 μ g/ml, 0.5 μ g/ml, 1 μ g/ml, and 2 μ g/ml) of CR and medium containing 0.1% DMSO were used as the vehicle control after 24 h. After 24 h incubation, 10 μ l of CCK8 solution (Cat. No. AR1160, Boster) was added to each well. Following 4 h incubation at 37°C, the absorbance of each well at 450 nm was determined.

2.10. Statistical Analysis. Results are expressed as the mean \pm SEM and were analyzed statistically using Graphpad Prism software. A *t*-test was used to compare the differences between two groups. One-way ANOVA with a post hoc comparison (Tukey's HSD) test was used to compare the differences in more than two groups. Statistical significance was defined as $P < 0.05$.

3. Results

3.1. Topical Treatment of CR Alleviates the Psoriasis-Like Lesions Induced by IMQ. The IMQ-induced PsD model is one of the best psoriatic mouse models with similar immunological alteration to human [26]. In order to understand the anti-inflammatory effects of CR, we applied CR to IMQ-induced mice. Topical treatment of CR has shown no obvious damage to liver and renal function of mice or even improved related index compared with the IMQ group (Supplementary figure 2).

The erythema, thickness, and scaling were observed after IMQ application (Figures 1(b) and 1(c)). The severity of these lesions was increased continuously with daily IMQ application (Figure 1(d)). By comparison, the severity of the skin lesions observed in the IMQ-induced PsD mice

was reduced by the coadministration of CR (Figures 1(b) and 1(c)). In these mice, reduced scales, skin thickness, and cumulative scores were observed from day 5 to day 7 compared with mice in the model group (Figure 1(d)). However, the erythema of skin in the CR-treated group was not relieved (Figure 1(d)). Under the dermoscope, regularly distributed dotted vessels and scales were observed in the IMQ group, while they were diminished in the CR-treated group.

The sections of the IMQ-treated group showed the representative histopathological changes of psoriasis with hyperkeratosis, parakeratosis, and acanthosis, while these features were absent in normal mice (Figure 2(a)). However, CR treatment partially inhibited these characteristic changes in psoriatic lesions (Figure 2(a)). Statistical analysis also showed a significant decrease in the epidermal thickness in CR-treated mice (Figure 2(b)). In human psoriasis, neutrophils aggregation in the cornified layer known as MM, indicated that neutrophils may play an important role in disease pathogenesis [27]. IMQ-treated skins also showed MM formation (Figure 2(c)). MM in the model group were larger and more numerous than those observed in CR-treated mice (Figure 2(c)). The average area of total MM of each mouse was dramatically diminished in CR-treated mice vs. model mice ($P < 0.01$) (Figure 2(d)).

Taken together, these results suggest that CR treatment could alleviate the severity of IMQ-induced PsD in mice. Therefore, it is necessary to study how this treatment exerts its therapeutic effect on psoriasis.

3.2. CR Treatment Improves the Immune Microenvironment of the Psoriatic Skins of Mice. The immune cell infiltration in mouse skins was then evaluated by flow cytometry. After administration of IMQ cream for 7 days, a significant increase of CD45⁺ cells ratio was observed in the IMQ group ($P < 0.001$) compared with the normal group (Figure 3(a)). The ratio of neutrophils located in the skins was also increased after applying IMQ ($P < 0.01$) (Figure 3(a)). CR treatment significantly decreased both CD45⁺ cells and neutrophils ($P < 0.01$). However, the ratio of macrophages and α β T cells in the skin showed no statistical differences between each group, whereas the proportion of CD4⁺ and CD8⁺ α β T cells was increased in the IMQ model group and decreased in the CR treatment group (Figure 3(a)).

Th17-related cells play an important role in inducing dermal inflammation and epidermal hyperplasia in psoriasis [28], so we analyzed the expression levels of inflammatory cytokines and chemokines in the mouse skins. IMQ treatment significantly induced the expression of *Il17a*, *Il22*, and *Ccl20* compared with the normal group, which showed the proinflammatory effect of IMQ by promoting the release of inflammatory factors. Moreover, a significant decrease in the levels of *Il17a*, *Il22*, and *Ccl20* was observed after CR treatment (Figure 3(b)).

These results suggest that topical CR treatment is more likely to have a direct anti-inflammatory effect on IMQ-induced PsD in mice.

3.3. Topical CR Application Relieves Psoriatic Itch and Reduces Itch-Related Mediators of Skins. As the IMQ mouse

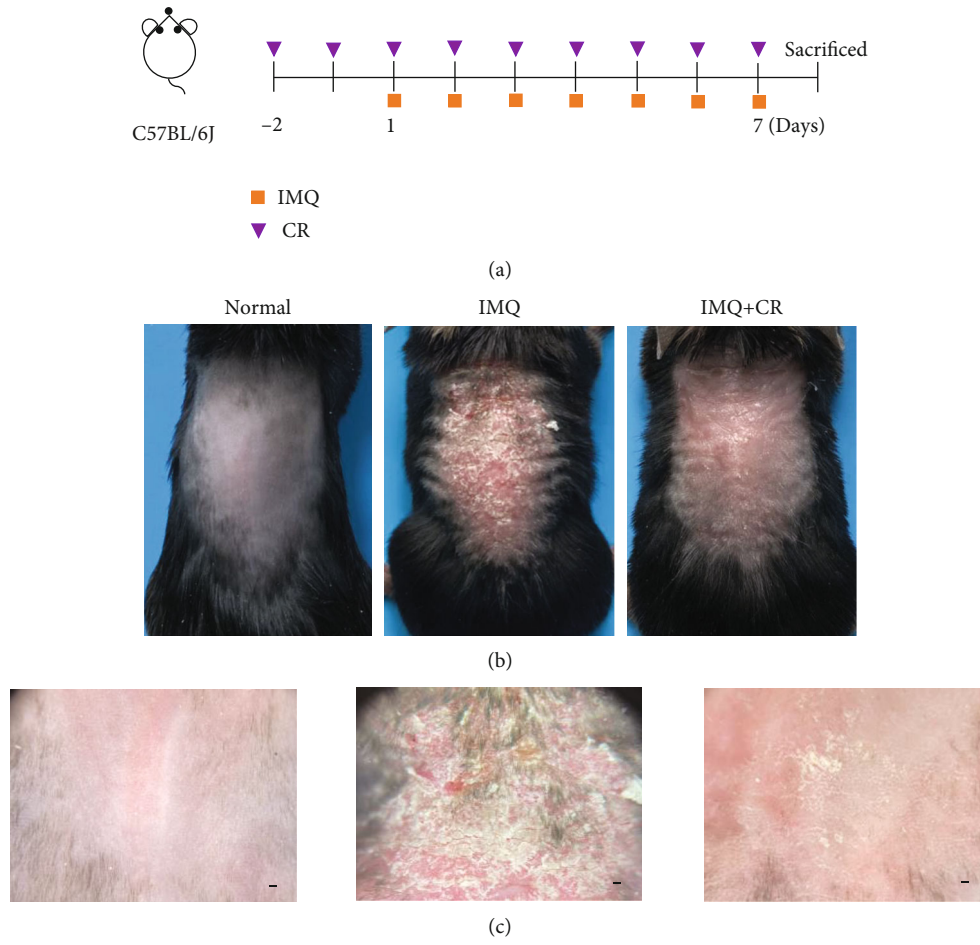
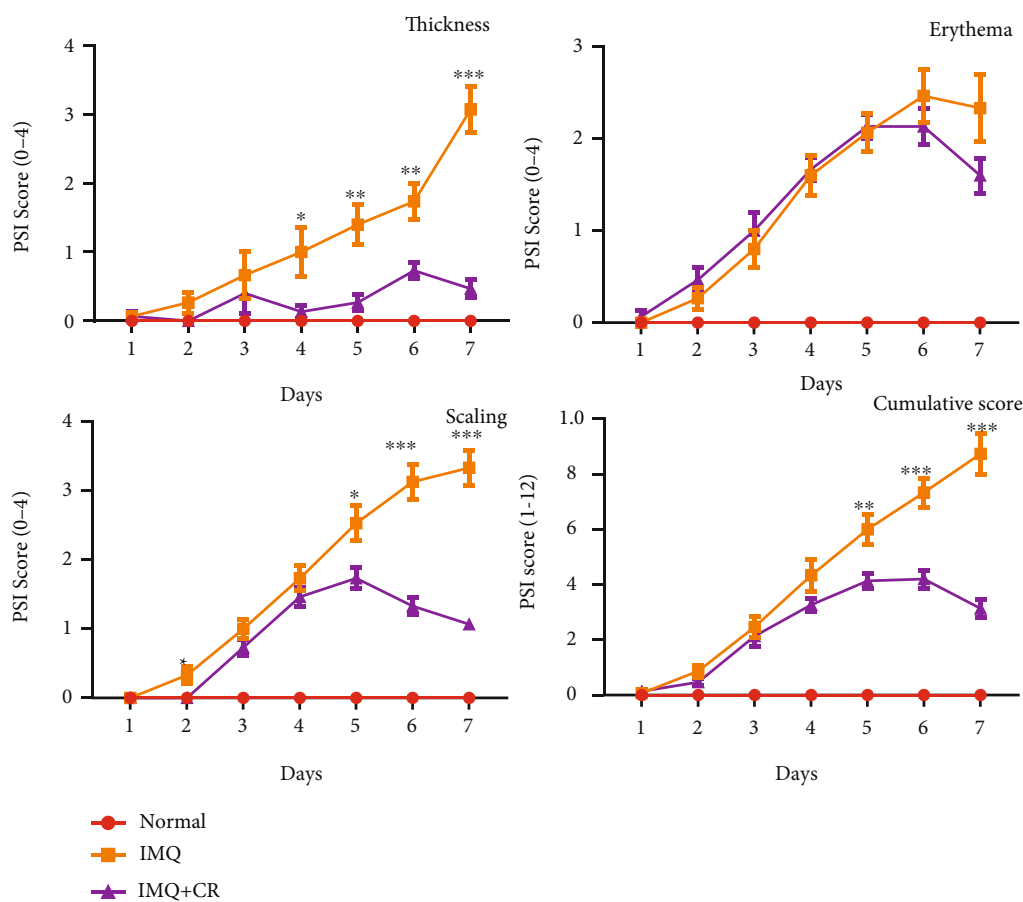


FIGURE 1: Continued.



(d)

FIGURE 1: CR treatment attenuated the severity of IMQ-induced PsD in mice. (a) The scheme of IMQ-induced murine model and CR treatment. Clinical presentation of mice (b) and dermoscopic presentation (scale bar = 1 mm) (c) of the back skin of mice after 7 days of IMQ treatment with or without the topical application CR. (d) The daily scores of erythema, skin thickness, scaling of back skin, and PSI scores were compared among normal group ($n = 11$), IMQ group ($n = 15$), and IMQ+CR group ($n = 15$). Data are shown as the Mean \pm SEM and were analyzed by using t -test. * $P < 0.05$, ** $P < 0.01$, and *** $P < 0.001$, showing the difference between the IMQ group and IMQ+CR group.

model is widely used in itch research of psoriasis, we observed the CR's effect on mice's itch behavior [22]. The counts of spontaneous scratch bouts were gradually increased in IMQ-treated mice compared with the control group (Figure 4(a)). CR application significantly reduced the scratch bouts since day 2 to day 7 (Figure 4(a)) and also diminished mast cells in dermis (Figures 4(b) and 4(c)). Mast cells are found to play a role in the induction or aggravation of psoriatic itch in previous studies [29]. The number of mast cells in the IMQ group was significantly higher than that in the normal control group. The reduction of mast cells by CR treatment was consistent with the results of itch behavioral test (Figures 4(b) and 4(c)). Both results suggest that CR can alleviate itch in psoriatic mice.

The pathogenesis of itch in psoriasis is still not fully understood. Nowadays, it is reported to be closely related with neurogenic inflammation [2]. To determine how CR treatment regulated itch in the IMQ model, we measured mRNA expression of itch-related genes *Sp*, *Cgrp*, and *Ngf*

by RT-qPCR in skins. *Sp* ($P < 0.01$) and *Cgrp* ($P < 0.05$) in the IMQ group were increased vs. those in the control group (Figure 5(a)). Of note, *Sp* ($P < 0.05$) and *Cgrp* ($P < 0.05$) in the CR group were both reduced compared with those in the IMQ group (Figure 5(a)). But there were no differences in mRNA levels of *Ngf* among the three groups ($P > 0.05$) (Figure 5(a)). The same results were also confirmed from protein level by IHC. The *Sp*, *Cgrp*, and *Ngf* in the epidermis of psoriatic lesions were all increased markedly ($P < 0.01$) with IMQ application compared with the normal group, which were reduced ($P < 0.01$) after CR treatment (Figures 5(b) and 5(c)). Thus, it suggests that CR could negatively regulate itch-related molecules in PsD mice's skin to control itch.

3.4. CR Downregulates M5-Induced Inflammatory Cytokines and Itch-Related Molecules in NHEKs. Hyperproliferative keratinocytes not only mediate inflammation but also influence itch during psoriasis [30]. Consequently, the effects of

CR on keratinocytes were then investigated. The cell viability of NHEKs treated with CR was measured using CCK-8 assay. After NHEKs being treated with different concentrations of CR, no significant toxicity was observed. In contrast, 0.5, 1, and 2 $\mu\text{g/ml}$ of CR could slightly promote cell viability ($P < 0.05$) (Figure 6(a)). In M5 (10 ng/ml) induced inflammatory condition *in vitro*, the viability of NHEKs was significantly enhanced after 24h ($P < 0.001$) (Figure 6(a)). However, when we combined CR (0.5 or 2 $\mu\text{g/ml}$) with M5 to treat keratinocytes, the induced cell viability was inhibited (Figure 6(a)). In addition, the inflammatory cytokines and itch-related molecules were determined in NHEKs with M5 stimulation. We found that M5 (10 ng/ml) could significantly upregulate mRNA levels of *IL-6*, *CXCL8*, *IL-1 β* , and *CCL20* ($P < 0.05$) (Figure 6(b)). The expression of *NGF* was also increased in the M5 group ($P < 0.05$), while *SP* and *CGRP* did not. Interestingly, CR treatment partially decreased expression of inflammatory cytokines *IL-6*, *CXCL8*, *IL-1 β* , and *CCL20* and itch-related molecules *SP*, *CGRP*, and *NGF* induced by M5 ($P < 0.05$) (Figure 6(b)). In general, these results suggest that CR treatment could regulate keratinocytes viability and reduce inflammation and the expression of some itch mediators in a psoriatic cell model.

4. Discussion

Nowadays, most treatment protocols are targeted at the inflammatory response of psoriasis, only a few of them specifically for improving psoriasis itch. The main compositions of CR tablets were analyzed by HPLC as triptolide and epicatechin in Zhou et al.'s study in 2018 [16]. Oral administration of CR has also been successfully used in the treatment of psoriasis [19]. However, the mechanisms of topical treatment with CR in psoriasis are still unclear. Long-term oral CR always accompanies with liver, kidney, and reproductive systemic damage, so that topical preparations of CR could be a better choice preventing these side effects.

Itch is a subjective sensation, which could be quantified by observing the spontaneous behaviors of experimental animals. Rapid back-and-forth movements of the hind paw around skin lesions in mice can imitate patients' scratching behaviors. Therefore, we apply this model in our research. The results showed that scales and thickness of skin were significantly reduced in CR-treated mice, consistent with previous studies of *Tripterygium wilfordii* [31]. However, the erythema in the CR group was not improved than that in the IMQ group. We speculate that it may be related to irritant contact dermatitis with external application by CR. Even so, the overall inflammation of the psoriatic lesions was greatly improved, and the number of scratches was significantly reduced in the CR group. These observations suggest that CR can relieve inflammation and pruritus in psoriasis.

Excessive inflammatory response in psoriasis has been confirmed to be related with itch [2]. Several studies reported that CD4^+ T cells were crucial for initiating and maintaining the pathogenic process of psoriasis. The percentage of CD4^+ T cells was increased in the blood of psoriasis patients [32]. CD4^+ T cells in skins consist of different helper T (Th) cells (Th1, Th2, Th9, Th17, Th22, and Treg cells) [33]. In psoriasis, keratinocytes regulate differentiation and activation of Th17 and Th22 cells by producing IL-1 β and IL-6 [28]. In our study, the total ratio of $\alpha\beta\text{T}$ cells did not change significantly among three groups. However, the increased proportion of $\text{CD4}^+/\text{CD8}^+\alpha\beta\text{T}$ cells in the IMQ group was decreased by topical application of CR. The ratio of $\text{CD4}^+/\text{CD8}^+\alpha\beta\text{T}$ cells is positively related with Koebner phenomenon caused by scratching in psoriasis [34, 35]. Scratch-induced skin injury is definitely correlated with itch. Consistent with previous research, we observed an increase in neutrophil infiltration in IMQ-induced PsD in mice, as well as scratch behaviors [22, 27]. Previous studies have shown that scratch injury to

TABLE 1: Primer sequences for quantitative reverse-transcription polymerase chain reaction.

Gene symbol	Sequence
<i>Il17a</i>	F: 5'-TTTTCAGCAAGGAATGTGGA-3'
	R: 5'-TTCATTGTGGAGGGCAGAC-3'
<i>Il22</i>	F: 5'-ATGAGTTTTCCCTTATGGGGAC-3'
	R: 5'-GCTGGAGTTGGACACCTCAA-3'
<i>Ccl20</i>	F: 5'-GCCTCTCGTACATACAGACGC-3'
	R: 5'-CCAGTTCGCTTTGGATCAGG-3'
<i>Sp</i>	F: 5'-AAGCGGGATGCTGATTCCCTC-3'
	R: 5'-TCTTTCGTAGTTCTGCATTGCG-3'
<i>Cgrp</i>	F: 5'-GAGGGCTCTAGCTTGGACAG-3'
	R: 5'-AAGGTGTGAAACTTGTTGAGGT-3'
<i>Ngf</i>	F: 5'-TGATCGGGCTACAGGCAGA-3'
	R: 5'-GCTGAAGTTTAGTCCAGTGGG-3'
<i>Gapdh</i>	F: 5'-AGTTCGGTGTGAACGGATTG-3'
	R: 5'-TGTAGACCATGTAGTTGAGGTCA-3'
<i>IL6</i>	F: 5'-CCAAGAGGTGAGTGCTTCCC-3'
	R: 5'-CTGTTGTTCCAGACTCTCTCCCT-3'
<i>CXCL8</i>	F: 5'-CAAGGCTGGTCCATGCTCC-3'
	R: 5'-TGCTATCACTTCCCTTCTGTTGC-3'
<i>IL1β</i>	F: 5'-GCAACTGTTCCCTGAACTCAACT-3'
	R: 5'-ATCTTTTGGGGTCCGTCAACT-3'
<i>CCL20</i>	F: 5'-CTGCTACTCCACCTCTGCG-3'
	R: 5'-TTGCGCACACAGACAACCTTT-3'
<i>SP</i>	F: 5'-TGATCTGAATTACTGGTCCGACT-3'
	R: 5'-TCCGGCAGTTCCTCCTTGA-3'
<i>CGRP</i>	F: 5'-ATGCAGCACCATTTCAGTCTG-3'
	R: 5'-CCAGCCGATGAGTCACACAG-3'
<i>NGF</i>	F: 5'-GGCAGACCCGCAACATTACT-3'
	R: 5'-CACCACCGACCTCGAAGTC-3'
<i>GAPDH</i>	F: 5'-CTGGGCTACTGAGCACC-3'
	R: 5'-AAGTGGTCGTTGAGGGCAATG-3'

riasis, keratinocytes regulate differentiation and activation of Th17 and Th22 cells by producing IL-1 β and IL-6 [28]. In our study, the total ratio of $\alpha\beta\text{T}$ cells did not change significantly among three groups. However, the increased proportion of $\text{CD4}^+/\text{CD8}^+\alpha\beta\text{T}$ cells in the IMQ group was decreased by topical application of CR. The ratio of $\text{CD4}^+/\text{CD8}^+\alpha\beta\text{T}$ cells is positively related with Koebner phenomenon caused by scratching in psoriasis [34, 35]. Scratch-induced skin injury is definitely correlated with itch. Consistent with previous research, we observed an increase in neutrophil infiltration in IMQ-induced PsD in mice, as well as scratch behaviors [22, 27]. Previous studies have shown that scratch injury to

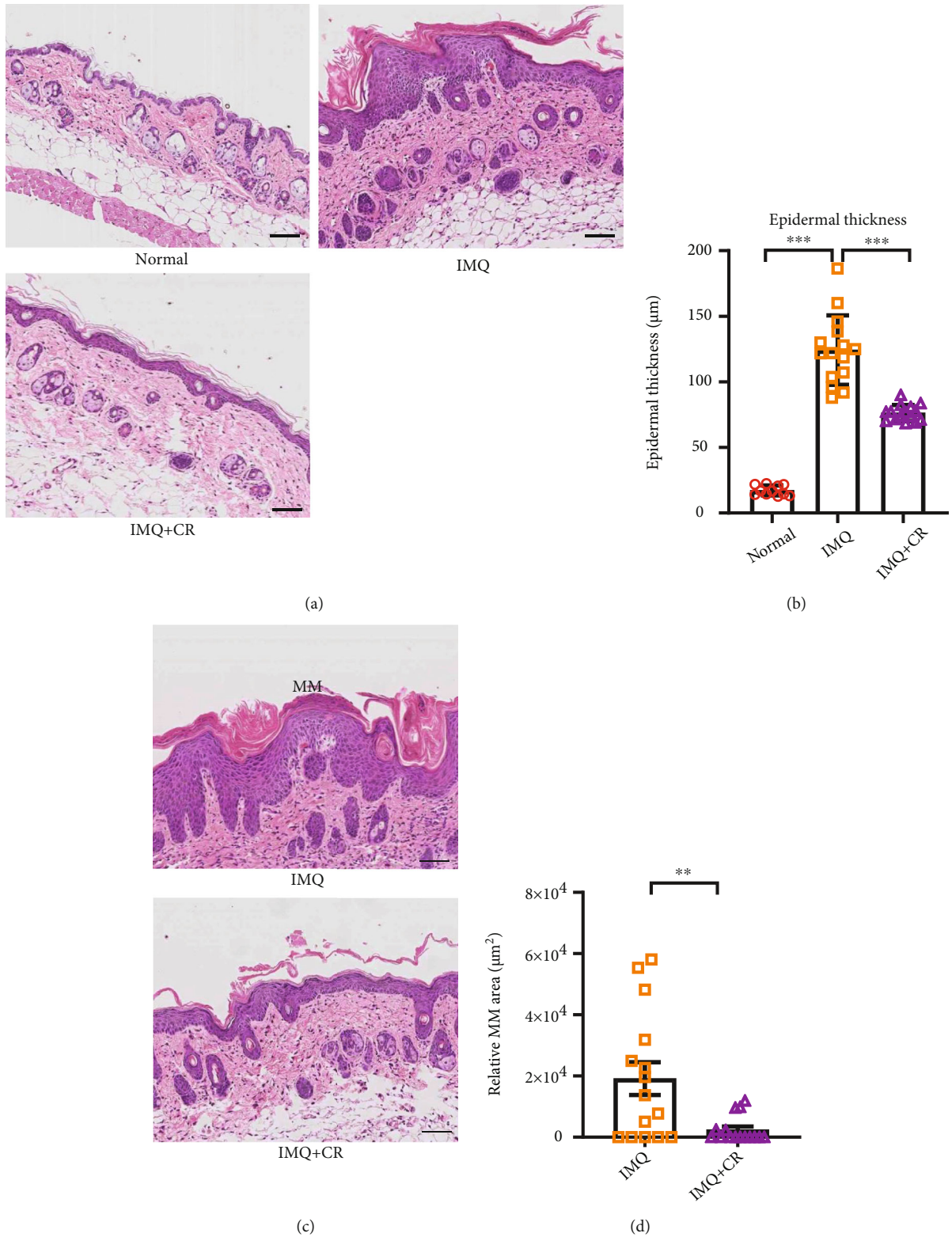


FIGURE 2: CR treatment reduced the epidermal thickness and diminished neutrophil accumulation in IMQ-induced PsD in mice. (a) Representative microscopic images of H&E-stained skin sections from each group (scale bar = 145 µm). (b) Epidermal thickness was evaluated using Leica Microsystems software under a microscope. $n = 11$ in the normal group; $n = 15$ in IMQ group and IMQ+CR group. (c) Representative image of MM (scale bar = 145 µm). (d) Quantification of MM area. $n = 15$ in both the IMQ and IMQ+CR group. Epidermal thicknesses were compared by using one-way ANOVA and post hoc Tukey's test, and MM areas were compared using a t -test. Data are shown as the Mean \pm SEM. ** $P < 0.01$ and *** $P < 0.001$.

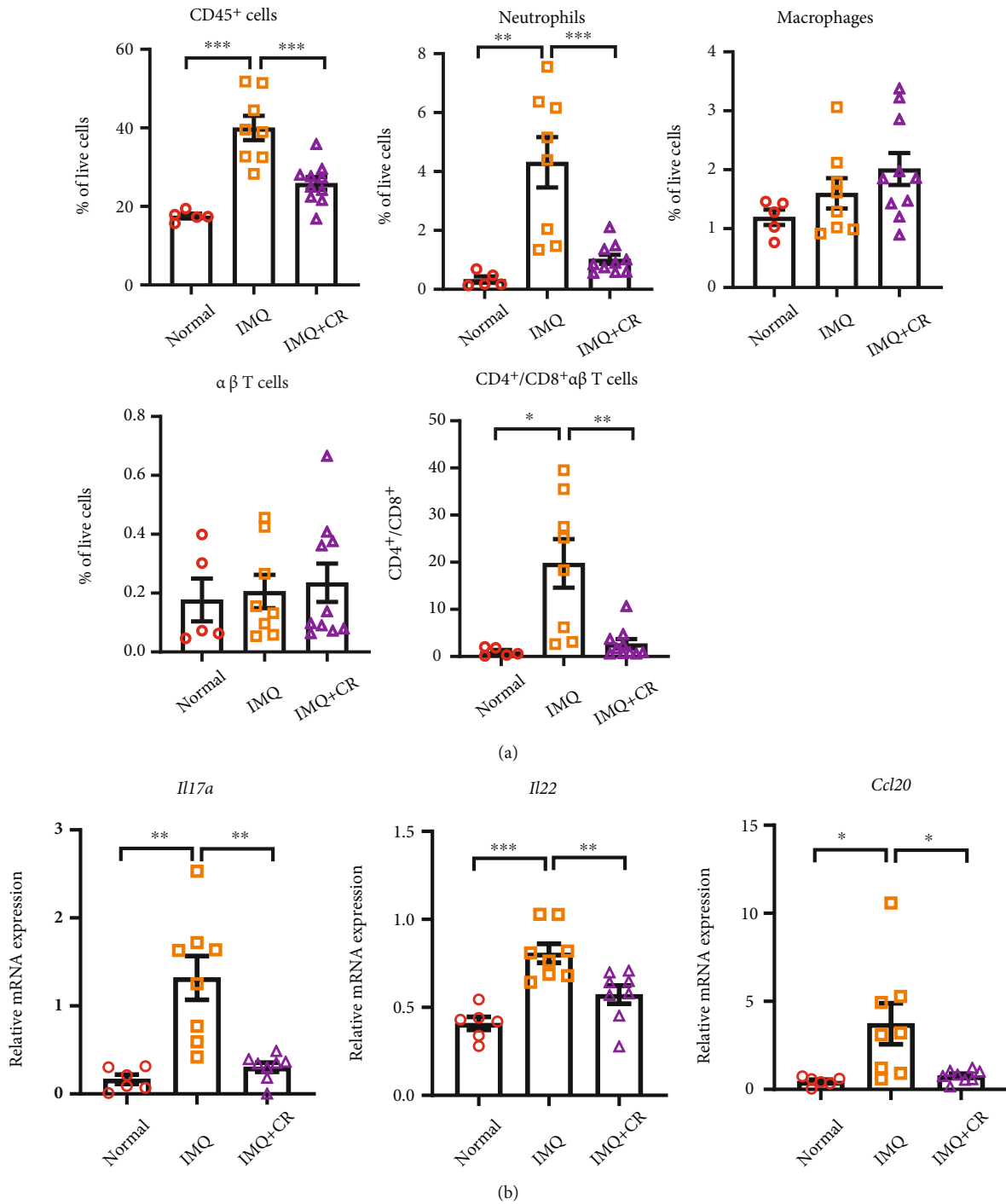


FIGURE 3: CR treatment decreased immune cell infiltration and cytokine production in murine skins of IMQ-induced PsD. (a) Flow cytometry analysis of immune cells (CD45⁺ immune cells, neutrophils, macrophages, $\alpha\beta$ T cells, and CD4⁺/CD8⁺ $\alpha\beta$ T cells) from skin tissues among groups. $n = 5$ in the normal group, $n = 8$ in the IMQ group, and $n = 10$ in the IMQ+CR group. (b) mRNA expression of *Il17a*, *Il22*, and *Ccl20* in mouse skin was measured via RT-qPCR, and the relative mRNA expression was normalized to *Gapdh* expression. $n = 6$ in the normal group, $n = 8$ in the IMQ group, and $n = 8$ in the IMQ+CR group. Statistical analysis was performed using one-way ANOVA followed by post hoc Tukey's test. Data are shown as the Mean \pm SEM. * $P < 0.05$, ** $P < 0.01$, and *** $P < 0.001$.

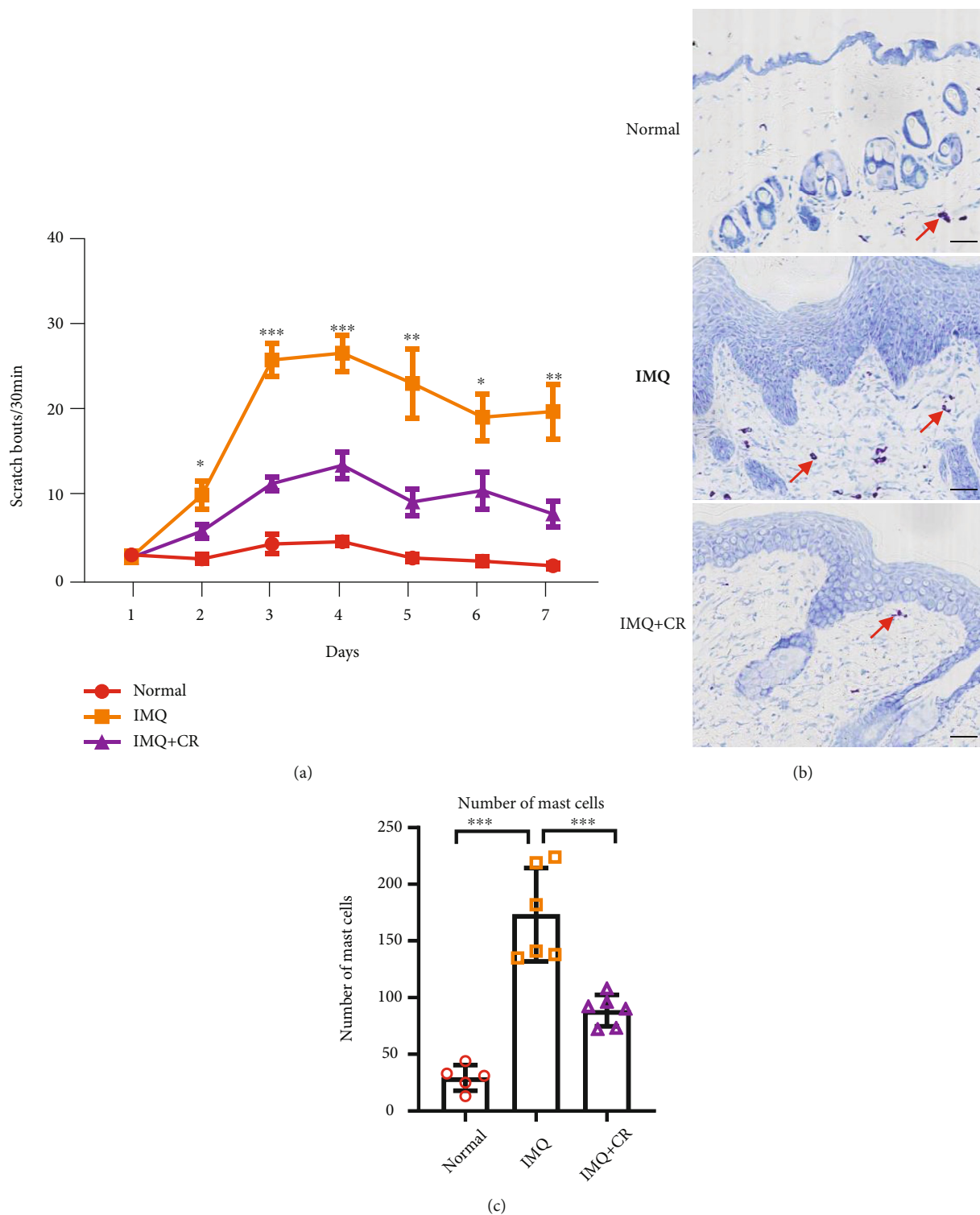


FIGURE 4: Pruritus was improved after CR treatment in IMQ-induced PsD in mice. (a) Spontaneous scratching was measured and compared among groups. $n = 11$ in the normal group and $n = 15$ in both the IMQ group and IMQ+CR group. (b) Mast cells were stained using Toluidine blue (scale bar = $73 \mu\text{m}$). (c) Numbers of mast cells in each group were counted. $n = 5$ in the normal group and $n = 6$ in both the IMQ group and IMQ+CR group. Statistical analysis was performed using one-way ANOVA followed by post hoc Tukey's test. Data are shown as the Mean \pm SEM. * $P < 0.05$, ** $P < 0.01$, and*** $P < 0.001$.

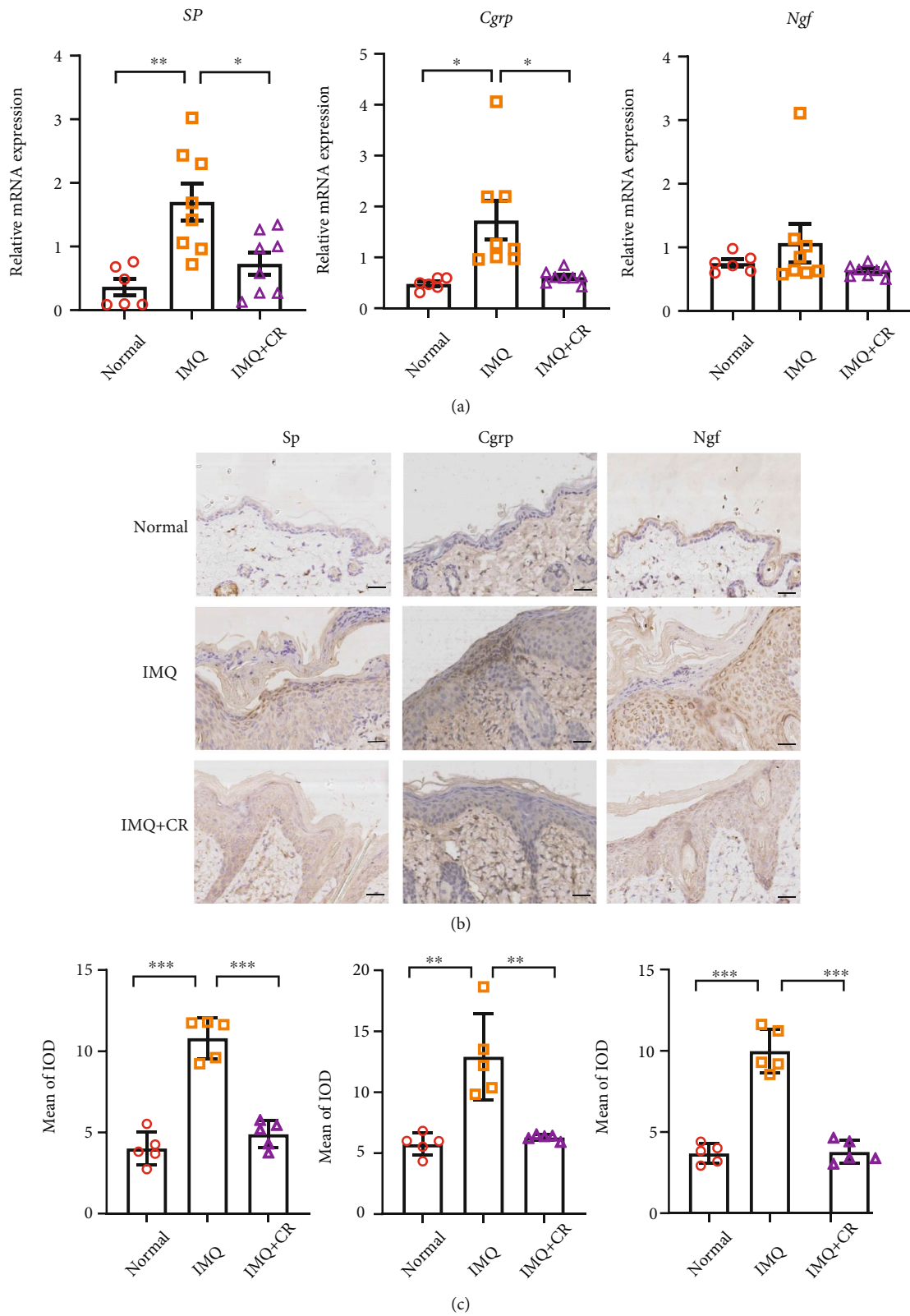


FIGURE 5: CR treatment reduced the expression of itch-related molecules in IMQ-induced PsD in mice. (a) mRNA expression of *Sp*, *Cgrp*, and *Ngf* in skins was detected by RT-qPCR. $n = 6$ mice in the control group and $n = 8$ mice in both the IMQ group and IMQ+CR group. Results of mRNA were normalized to *Gapdh* expression. (b) Representative immunohistochemical images of SP, CGRP, and NGF expression from the epidermis of back skins among groups (scale bar = 73 μ m). (c) Mean of integrated optical density (IOD) of *Sp*, *Cgrp*, and *Ngf* in skins from each group. $n = 5$ mice in three groups. Statistical analysis was performed using one-way ANOVA followed by post hoc Tukey's test. Mean \pm SEM values are indicated, * $P < 0.05$, ** $P < 0.01$, and *** $P < 0.001$.

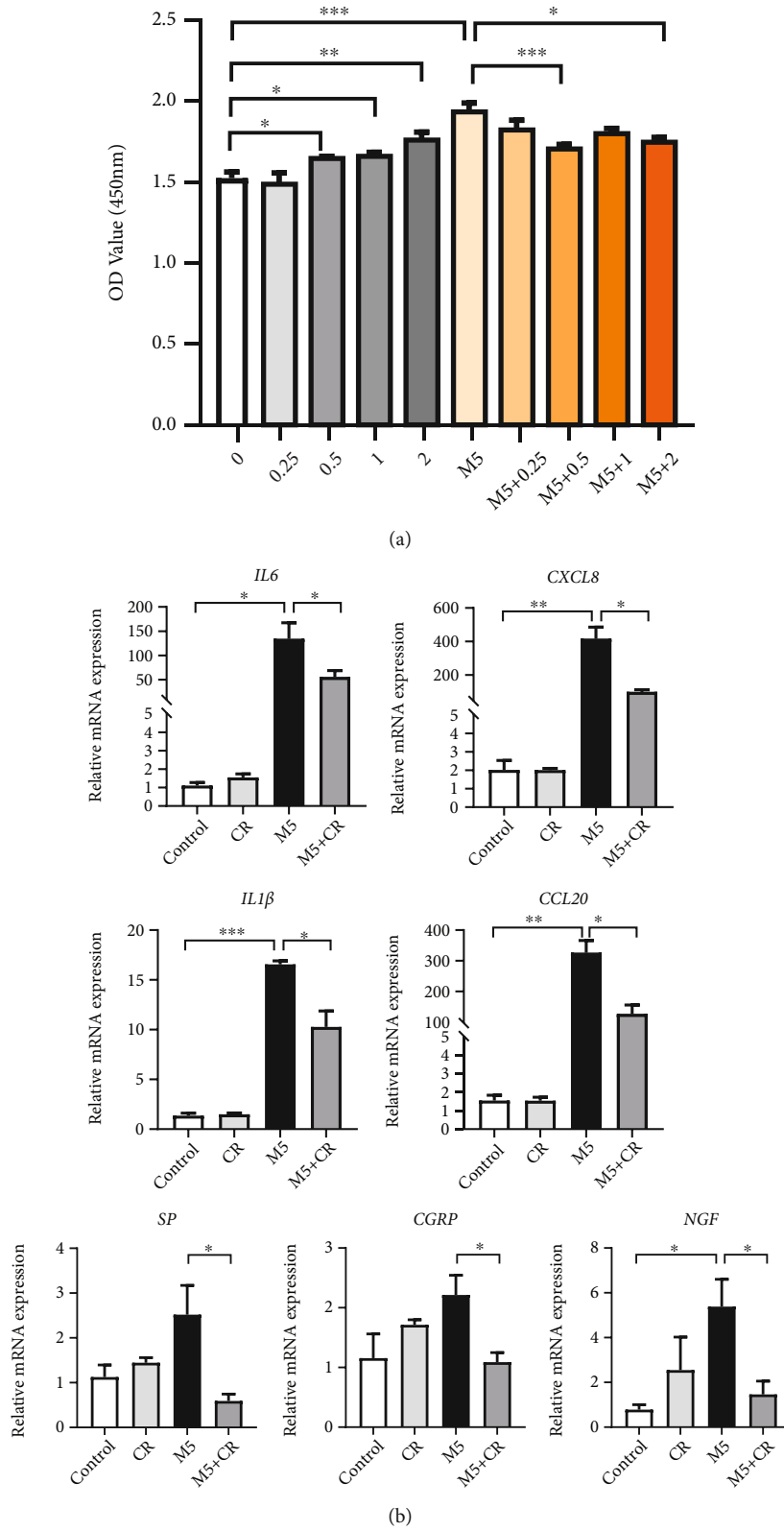


FIGURE 6: CR treatment regulated cell viability and function of M5-induced keratinocytes *in vitro*. M5 (10 ng/ml) was used to stimulate NHEKs with or without CR treatment ((a): 0, 0.25 $\mu\text{g/ml}$, 0.5 $\mu\text{g/ml}$, 1 $\mu\text{g/ml}$, and 2 $\mu\text{g/ml}$; (b): 0.5 $\mu\text{g/ml}$). (a) Cell viability was measured by using CCK-8 ($n = 4$). (b) The mRNA expression of *IL-6*, *CXCL8*, *IL-1 β* , *CCL20*, *SP*, *CGRP*, and *NGF* was detected by RT-qPCR ($n = 3$). The relative mRNA expression was normalized to *GAPDH* expression. Statistical analysis was performed using one-way ANOVA followed by post hoc Tukey's test. Mean \pm SEM values are indicated. * $P < 0.05$, ** $P < 0.01$, and *** $P < 0.001$.

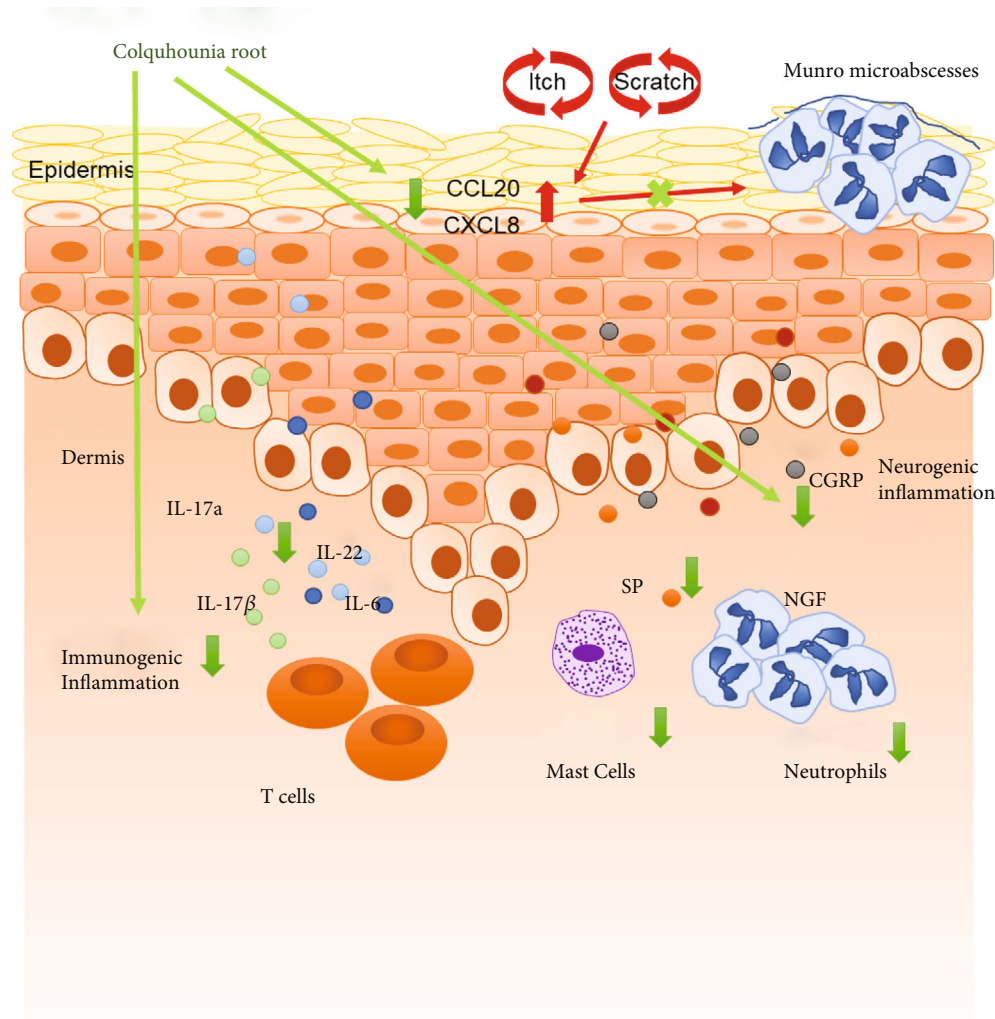


FIGURE 7: Characterization of the mechanism of CR for psoriasis pruritus improvement. CR treatment relieves the symptoms of psoriasis pruritus by inhibiting increased mast cells and neutrophils, as well as the upregulation of the inflammatory factors *IL-17a*, *IL-22*, *IL-6*, *CXCL8*, *IL-1β*, and *CCL20* and itch-related molecules *SP*, *CGRP*, and *NGF* in psoriasis.

epidermal keratinocytes promoted the release of CCL20 and CXCL8, which was related to the recruitment of both neutrophils and IL-17a-producing immune cells [36]. CCL20 was expressed abundantly in human psoriatic epidermis [9, 37]. Dupilumab inhibits the IL-4/IL-13 signaling pathway to reduce itching and itching in atopic dermatitis, which may reduce the release of CCL20 from keratinocytes and also reduce Th17 cell infiltration [38]. As well as in psoriasis, the enrichment of IL-17A-producing immune cells leads to produce high levels of IL-17A, which further stimulates keratinocytes producing CCL20, CXCL8, and IL-36 γ to recruit more IL-17A-producing immune cells and neutrophils [39]. In our findings, the neutrophil infiltration and also increasing expression of CCL20 in IMQ treated mice were both inhibited by CR. As well in vitro, dexamethasone partially inhibited scratch-induced CXCL8 and CCL20 secretion in the keratinocyte model [36]. In order to mimic a psoriatic environment, we chose an M5-induced keratinocyte model to investigate the effects of CR. As expected, CR reduced the expression levels of inflammatory cytokines *IL-6*, *IL-8*, *CXCL8*, and *CCL20*. Interestingly, we

observed that CR could promote cell viability slightly in NHEKs, while in NHEKs treated with M5, CR inhibited cell viability. We speculate that CR might regulate the viability of keratinocytes under different circumstances, which should be explored in further study.

Notably, the number of mast cells was significantly reduced in lesions of CR application. Several researches observed that mast cells are hyperactivated in psoriatic lesions of progressive stage. The use of certain medications to treat psoriasis, such as glucocorticosteroids, may lead a decline of the mast cell count [11]. Our observation indicates that CR may function as an inhibitor of itch in psoriasis by decreasing the number of mast cells in skin lesions.

In addition, the itch sensation is transmitted to the brain via itch neural pathways from skin lesions [40, 41]. Sensory nerve fibers increased in the psoriatic epidermis and dermal papilla, which were stimulated (endogenous or exogenous) by various neuropeptides and neurotrophic molecule, such as CGRP, SP, and NGF. Also, in the epidermis, neuropeptides released from the nerve fibers stimulate keratinocytes

to release proinflammatory cytokines such as IL-6 and IL-8. On the other hand, CGRP and SP induce the release of vasoactive amine by mast cells, promoting the infiltration of neutrophils and T cells closely related with itch [42–45]. The main source of NGF in the skin is keratinocytes [46]. The expression of NGF in psoriatic patients with pruritus is higher than that without pruritus [47]. These molecules work directly or indirectly on the nerve and lead to or aggravate the degree of itch in psoriasis [48, 49]. In our research, topical CR preparation can significantly relieve itch accompanied with reduced levels of CGRP, SP, and NGF in lesions from psoriatic mice. Additionally, in a psoriatic cell model, itch-related molecules SP, CGRP, and NGF were found decreased in NHEK cotreated with CR and M5. However, the expression of CGRP and SP in vitro was not upregulated by M5. We speculate that M5-induced keratinocytes may not be an optimal itching cell model in psoriasis.

5. Conclusion

In summary, we firstly prove that CR can not only inhibit the increased mast cells and neutrophils in lesions but also down-regulate the inflammatory factors and neuropeptides and neurotrophic molecule to reduce the inflammation and itch in IMQ-induced murine model of psoriasis, which is also validated in a psoriatic cell model (Figure 7). In conclusion, CR is considered to be an ideal topical therapeutic drug for anti-itch treatment not just anti-inflammation in psoriasis.

Data Availability

The datasets generated during and/or analyzed during the current study are available from the corresponding author on reasonable request.

Conflicts of Interest

The authors declare no commercial or financial conflict of interest.

Authors' Contributions

Fei Li and Dan Han designed the study, performed the majority of the experiments, analyzed the data, and wrote the manuscript; Bo Wang, Wentao Zhang, Yan Zhao, and Jing Xu performed experiments and analyzed data; Liesu Meng and Shemin Lu provided expert technical assistance; Kuanhou Mou provided clinical advice and critical discussion of work; Wenhua Zhu and Yan Zhou designed the study, supervised the project, and wrote the manuscript.

Acknowledgments

This work is supported by the National Natural Science Foundation of China (81703130 and 82171724), Key Research and Development Program of Shaanxi Province of China (2020KW-047), and the Clinical Research Award of the First Affiliated Hospital of Xi'an Jiaotong University, China (XJTU1AF-CRF-2019-027 and 2021ZXY-12).

Supplementary Materials

Supplementary 1 Supplementary Figure 1: gating strategy of skin cells in flow cytometry. *Supplementary 2* Supplementary Figure 2: effect of psoriatic inflammation and CR on liver and renal function of mice. (*Supplementary Materials*)

References



- [1] J. C. Szepietowski and A. Reich, "Pruritus in psoriasis: an update," *European Journal of Pain*, vol. 20, no. 1, pp. 41–46, 2016.
- [2] E. Komiya, M. Tominaga, Y. Kamata, Y. Suga, and K. Takamori, "Molecular and cellular mechanisms of itch in psoriasis," *International Journal of Molecular Sciences*, vol. 21, no. 21, p. 8406, 2020.
- [3] G. Yosipovitch, A. Goon, J. Wee, Y. H. Chan, and C. L. Goh, "The prevalence and clinical characteristics of pruritus among patients with extensive psoriasis," *The British Journal of Dermatology*, vol. 143, no. 5, pp. 969–973, 2000.
- [4] B. Elewski, A. F. Alexis, M. Lebwohl et al., "Itch: an under-recognized problem in psoriasis," *Journal of the European Academy of Dermatology and Venereology*, vol. 33, no. 8, pp. 1465–1476, 2019.
- [5] B. Amatya, H. el-Nour, M. Holst, E. Theodorsson, and K. Nordlind, "Expression of tachykinins and their receptors in plaque psoriasis with pruritus," *The British Journal of Dermatology*, vol. 164, no. 5, pp. 1023–1029, 2011.
- [6] R. Saraceno, C. E. Kleyn, G. Terenghi, and C. E. M. Griffiths, "The role of neuropeptides in psoriasis," *The British Journal of Dermatology*, vol. 155, no. 5, pp. 876–882, 2006.
- [7] J. Yamaguchi, M. Aihara, Y. Kobayashi, T. Kambara, and Z. Ikezawa, "Quantitative analysis of nerve growth factor (NGF) in the atopic dermatitis and psoriasis horny layer and effect of treatment on NGF in atopic dermatitis," *Journal of Dermatological Science*, vol. 53, no. 1, pp. 48–54, 2009.
- [8] F. Cevikbas, X. Wang, T. Akiyama et al., "A sensory neuron-expressed IL-31 receptor mediates T helper cell-dependent itch: involvement of TRPV1 and TRPA1," *The Journal of Allergy and Clinical Immunology*, vol. 133, no. 2, pp. 448–460.e7, 2014.
- [9] J. Pène, S. Chevalier, L. Preisser et al., "Chronically inflamed human tissues are infiltrated by highly differentiated Th17 lymphocytes," *Journal of Immunology*, vol. 180, no. 11, pp. 7423–7430, 2008.
- [10] B. Strober, B. Sigurgeirsson, G. Popp et al., "Secukinumab improves patient-reported psoriasis symptoms of itching, pain, and scaling: results of two phase 3, randomized, placebo-controlled clinical trials," *International Journal of Dermatology*, vol. 55, no. 4, pp. 401–407, 2016.
- [11] K. Jaworecka, J. Muda-Urban, M. Rzepko, and A. Reich, "Molecular aspects of pruritus pathogenesis in psoriasis," *International Journal of Molecular Sciences*, vol. 22, no. 2, p. 858, 2021.
- [12] A. W. Armstrong and C. Read, "Pathophysiology, clinical presentation, and treatment of psoriasis: a review," *JAMA*, vol. 323, no. 19, pp. 1945–1960, 2020.
- [13] G. Yosipovitch, J. Soung, J. Weiss et al., "Secukinumab provides rapid relief from itching and pain in patients with moderate-to-severe psoriasis: patient symptom diary data from two phase 3, randomized, placebo-controlled clinical

- trials," *Acta Dermato-Venereologica*, vol. 99, no. 9, pp. 820–821, 2019.
- [14] M. Kamata and Y. Tada, "Safety of biologics in psoriasis," *The Journal of Dermatology*, vol. 45, no. 3, pp. 279–286, 2018.
- [15] B. Farahnik, D. Sharma, J. Alban, and R. K. Sivamani, "Topical botanical agents for the treatment of psoriasis: a systematic review," *American Journal of Clinical Dermatology*, vol. 18, no. 4, pp. 451–468, 2017.
- [16] W. Zhou, G. Shi, J. Bai, S. Ma, Q. Liu, and X. Ma, "Colquhounia Root Tablet Protects Rat Pulmonary Microvascular Endothelial Cells against TNF-Induced Injury by Upregulating the Expression of Tight Junction Proteins Claudin-5 and ZO-1," *Evidence-based Complementary and Alternative Medicine*, vol. 2018, Article ID 1024634, 11 pages, 2018.
- [17] M. Jiang, H. Zhang, and Y. Ding, "Research progress on pharmacological activities and clinical applications of Tripterygium glycosides," *Chinese Archives of Traditional Chinese Medicine*, vol. 39, no. 3, pp. 59–63, 2021.
- [18] X. L. Wu, J. B. Li, and S. L. Mo, "Clinical observation on colquhounia root tablet in treating lipid metabolism disturbance secondary to nephrotic syndrome," *Zhongguo Zhong Xi Yi Jie He Za Zhi*, vol. 22, no. 1, pp. 30–32, 2002.
- [19] X. Han, H. Mou, and L. M. Wang, "Clinical effect analysis of colquhounia root tablet in the treatment of 46 cases of psoriasis vulgaris," *China Journal of Leprosy and Skin Diseases*, vol. 6, pp. 588–589, 2004.
- [20] W. R. Swindell, K. A. Michaels, A. J. Sutter et al., "Imiquimod has strain-dependent effects in mice and does not uniquely model human psoriasis," *Genome Medicine*, vol. 9, no. 1, p. 24, 2017.
- [21] S. R. Feldman, D. M. Bushnell, P. A. Klekotka et al., "Differences in psoriasis signs and symptom severity between patients with clear and almost clear skin in clinical practice," *The Journal of Dermatological Treatment*, vol. 27, no. 3, pp. 224–227, 2016.
- [22] K. Sakai, K. M. Sanders, M. R. Youssef et al., "Mouse model of imiquimod-induced psoriatic itch," *Pain*, vol. 157, no. 11, pp. 2536–2543, 2016.
- [23] N. Puebla-Osorio, S. N. E. Sarchio, S. E. Ullrich, and S. N. Byrne, "Detection of infiltrating mast cells using a modified toluidine blue staining," *Methods in Molecular Biology*, vol. 1627, pp. 213–222, 2017.
- [24] K. Guilloteau, I. Paris, N. Pedretti et al., "Skin inflammation induced by the synergistic action of IL-17A, IL-22, Oncostatin M, IL-1{alpha}, and TNF-{\alpha} recapitulates some features of psoriasis," *Journal of Immunology*, vol. 184, no. 9, pp. 5263–5270, 2010.
- [25] Y. Ru, H. Li, R. Zhang et al., "Role of keratinocytes and immune cells in the anti-inflammatory effects of *Tripterygium wilfordii* Hook. f. in a murine model of psoriasis," *Phytomedicine*, vol. 77, article 153299, 2020.
- [26] K. Nakajima and S. Sano, "Mouse models of psoriasis and their relevance," *The Journal of Dermatology*, vol. 45, no. 3, pp. 252–263, 2018.
- [27] L. van der Fits, S. Mourits, J. S. A. Voerman et al., "Imiquimod-induced psoriasis-like skin inflammation in mice is mediated via the IL-23/IL-17 axis," *Journal of Immunology*, vol. 182, no. 9, pp. 5836–5845, 2009.
- [28] R. Yoshiki, K. Kabashima, T. Honda et al., "IL-23 from Langerhans Cells Is Required for the Development of Imiquimod-Induced Psoriasis-Like Dermatitis by Induction of IL-17A-Producing $\gamma\delta$ T Cells," *The Journal of Investigative Dermatology*, vol. 134, no. 7, pp. 1912–1921, 2014.
- [29] K. Gupta and I. T. Harvima, "Mast cell-neural interactions contribute to pain and itch," *Immunological Reviews*, vol. 282, no. 1, pp. 168–187, 2018.
- [30] H. S. Kim and G. Yosipovitch, "The skin microbiota and itch: is there a link?," *Journal of Clinical Medicine*, vol. 9, no. 4, p. 1190, 2020.
- [31] J. Zhao, T. di, Y. Wang et al., "Multi-glycoside of *Tripterygium wilfordii* Hook. f. ameliorates imiquimod-induced skin lesions through a STAT3-dependent mechanism involving the inhibition of Th17-mediated inflammatory responses," *International Journal of Molecular Medicine*, vol. 38, no. 3, pp. 747–757, 2016.
- [32] R. M. El-Gharabawy, A. S. Ahmed, and A. H. Al-Najjar, "Mechanism of action and effect of immune-modulating agents in the treatment of psoriasis," *Biomedicine & Pharmacotherapy*, vol. 85, pp. 141–147, 2017.
- [33] T. Nomura, K. Kabashima, and Y. Miyachi, "The panoply of $\alpha\beta$ T cells in the skin," *Journal of Dermatological Science*, vol. 76, no. 1, pp. 3–9, 2014.
- [34] E. Theodorakopoulou, Z. Z. N. Yiu, C. Bundy et al., "Early- and late-onset psoriasis: a cross-sectional clinical and immunocytochemical investigation," *The British Journal of Dermatology*, vol. 175, no. 5, pp. 1038–1044, 2016.
- [35] B. S. Baker, A. V. Powles, S. Lambert, H. Valdimarsson, and L. Fry, "A prospective study of the Koebner reaction and T lymphocytes in uninvolved psoriatic skin," *Acta Dermato-Venereologica*, vol. 68, no. 5, pp. 430–434, 1988.
- [36] K. Furue, T. Ito, Y. Tanaka et al., "Cyto/chemokine profile of in vitro scratched keratinocyte model: implications of significant upregulation of CCL20, CXCL8 and IL36G in Koebner phenomenon," *Journal of Dermatological Science*, vol. 94, no. 1, pp. 244–251, 2019.
- [37] T. G. Kim, H. Jee, J. Fuentes-Duculan et al., "Dermal clusters of mature dendritic cells and T cells are associated with the CCL20/CCR6 chemokine system in chronic psoriasis," *The Journal of Investigative Dermatology*, vol. 134, no. 5, pp. 1462–1465, 2014.
- [38] E. L. Simpson, T. Bieber, E. Guttman-Yassky et al., "Two phase 3 trials of dupilumab versus placebo in atopic dermatitis," *The New England Journal of Medicine*, vol. 375, no. 24, pp. 2335–2348, 2016.
- [39] E. G. Harper, C. Guo, H. Rizzo et al., "Th17 Cytokines Stimulate CCL20 Expression in Keratinocytes *In Vitro* and *In Vivo*: Implications for Psoriasis Pathogenesis," *The Journal of Investigative Dermatology*, vol. 129, no. 9, pp. 2175–2183, 2009.
- [40] S. Bourane, B. Duan, S. C. Koch et al., "Gate control of mechanical itch by a subpopulation of spinal cord interneurons," *Science*, vol. 350, no. 6260, pp. 550–554, 2015.
- [41] M. Lay and X. Dong, "Neural mechanisms of itch," *Annual Review of Neuroscience*, vol. 43, no. 1, pp. 187–205, 2020.
- [42] A. Dallos, M. Kiss, H. Polyánka, A. Dobozy, L. Kemény, and S. Husz, "Effects of the neuropeptides substance P, calcitonin gene-related peptide, vasoactive intestinal polypeptide and galanin on the production of nerve growth factor and inflammatory cytokines in cultured human keratinocytes," *Neuropeptides*, vol. 40, no. 4, pp. 251–263, 2006.
- [43] G. J. Burbach, K. H. Kim, A. S. Zivony et al., "The neurosensory tachykinins substance P and neurokinin A directly induce

- keratinocyte nerve growth factor,” *The Journal of Investigative Dermatology*, vol. 117, no. 5, pp. 1075–1082, 2001.
- [44] I. S. Song, N. W. Bunnett, J. E. Olerud et al., “Substance P induction of murine keratinocyte PAM 212 interleukin 1 production is mediated by the neurokinin 2 receptor (NK-2R),” *Experimental Dermatology*, vol. 9, no. 1, pp. 42–52, 2000.
- [45] Y. M. Park and C. W. Kim, “The effects of substance P and vasoactive intestinal peptide on interleukin-6 synthesis in cultured human keratinocytes,” *Journal of Dermatological Science*, vol. 22, no. 1, pp. 17–23, 1999.
- [46] C. Pincelli, “Nerve growth factor and keratinocytes: a role in psoriasis,” *European Journal of Dermatology*, vol. 10, no. 2, pp. 85–90, 2000.
- [47] M. Nakamura, M. Toyoda, and M. Morohashi, “Pruritogenic mediators in psoriasis vulgaris: comparative evaluation of itch-associated cutaneous factors,” *The British Journal of Dermatology*, vol. 149, no. 4, pp. 718–730, 2003.
- [48] K. Sakai, K. M. Sanders, M. R. Youssef et al., “Role of neurturin in spontaneous itch and increased nonpeptidergic intraepidermal fiber density in a mouse model of psoriasis,” *Pain*, vol. 158, no. 11, pp. 2196–2202, 2017.
- [49] X. Kodji, K. L. Arkless, Z. Kee et al., “Sensory nerves mediate spontaneous behaviors in addition to inflammation in a murine model of psoriasis,” *The FASEB Journal*, vol. 33, no. 2, pp. 1578–1594, 2019.

Research Article

A Variant of sNASP Exacerbates Lymphocyte Subset Disorder and Nephritis in a Spontaneous Lupus Model Sle1.Yaa Mouse

Jianye Zhang,¹ Xiaoping Du,^{2,3} Hui Wang,¹ Yatao Bao,¹ Meng Lian,¹ Zhiwei Xu ¹,
and Jiyu Ju ¹

¹School of Basic Medical Science, Weifang Medical University, Weifang 261053, China

²Medical Control Office, The Second Affiliated Hospital of Weifang Medical University, Weifang 261041, China

³Medical Control Office, Weifang No. 2 Hospital, Weifang 261041, China

Correspondence should be addressed to Zhiwei Xu; xuzhiwei51888@hotmail.com and Jiyu Ju; jujiyu@163.com

Received 22 April 2021; Accepted 23 September 2021; Published 21 October 2021

Academic Editor: Bingjie Gu

Copyright © 2021 Jianye Zhang et al. This is an open access article distributed under the Creative Commons Attribution License, which permits unrestricted use, distribution, and reproduction in any medium, provided the original work is properly cited.

A variant of somatic nuclear autoantigenic sperm protein (sNASP) was identified from the murine lupus susceptibility locus Sle2c1 by whole exome sequencing (WES). Previous studies have shown that mutant sNASP could synergize with the Fas^{lpr} mutation in exacerbating autoimmunity and aggravating end-organ inflammation. In the current study, the sNASP mutation was introduced into Sle1.Yaa mice to detect whether it has a synergistic effect with Sle1 or Yaa loci. As expected, compared with Sle1.Yaa mice, Sle1.Yaa.ΔsNASP mice showed enlarged lymph nodes, aggravated renal inflammation, and shortened survival time. The proportions of CD3⁺ T cells, activated CD19⁺CD86⁺ B cells, Th1 cells in the spleen and lymph nodes, and Th17 cells in lymph nodes in Sle1.Yaa.ΔsNASP mice were increased compared to those in Sle1.Yaa mice. The levels of IFN-γ and TNF-α in the serum of Sle1.Yaa.ΔsNASP mice were higher than those of Sle1.Yaa mice. The above results show that mutant sNASP can interact with different lupus susceptibility genes and promote the disease process of systemic lupus erythematosus.

1. Introduction

Systemic lupus erythematosus (SLE) is a highly heterogeneous autoimmune disorder that causes damage to multiple organ systems. The interactions between susceptibility genes and environmental factors play a dominant role and result in an irreversible loss of immunologic self-tolerance [1]. So far, genome-wide association studies (GWAS) have identified more than 100 alleles (SNPs), which increase the risk of developing lupus in humans [2]. However, due to the inherent limitations of human clinical studies, the role of these genes is rarely elucidated. Because the clinical manifestations of spontaneous lupus mice are comparable to those of human SLE patients, various mouse models have been developed to dissect the genetic and cellular mechanisms of SLE [2], as well as to identify and validate therapeutic targets [3].

The murine lupus susceptibility locus Sle2c1 derived from the NZM2410 strain has been proven to promote the

proliferation of B1a cells in the abdominal cavity and synergism with lpr mutation in the B6.Sle2.lpr mice, leading to more severe lupus nephritis and marked lymphadenopathy compared to B6.lpr mice [4]. Recently, a variant of somatic nuclear autoantigenic sperm protein (sNASP), which is a chaperone of histones, was identified from the Sle2c1 locus by whole exome sequencing (WES). A nonsynonymous mutation of two adjacent bases on the sNASP gene resulted in changes of the 281 and 282 amino acids in the histone binding region from valine and leucine to isoleucine and phenylalanine. In our previous study, we revealed that the mutant sNASP has a greater affinity to the H4 histone or H3.1/H4 tetramer than the normal sNASP protein *in vitro*, suggesting that the amino acid changes alter its three-dimensional structure and function. To confirm the role of mutant sNASP in Sle2-mediated autoimmune phenotypes, we generated B6.ΔsNASP.lpr mice by introgressing the mutant sNASP onto B6.lpr mice and examined evidence of

disease at 6 months of age [5]. Our results demonstrate that the variant of sNASP in the B6.lpr strain was responsible for aggravating inflammatory pathology alterations in the kidney and lung and the majority of the cellular dysfunction in the spleen and lymph nodes.

Sle1.Yaa mice contain Sle1 and Y-linked autoimmune accelerator (Yaa) loci and develop a lupus-like disease with splenomegaly and glomerular nephritis in males [6]. Although the Yaa locus translocated from the X chromosome may contain as many as 16 genes, the major candidate gene for causation of the Yaa-associated autoimmune phenotype has been TLR7 [7]. Decreased autoantigen tolerance is part of the manifestation of SLE. Polymorphisms of the SLAM/CD2 gene cluster identified in the Sle1 locus are responsible for the loss of tolerance to the H2A/H2B/DNA subnucleosome antigen [8]. Yaa is highly epistatic with the Sle1 locus, culminating in severe pathology and fatal disease at a relatively young age and release of inflammatory cytokines.

Whether mutant sNASP works synergistically with other lupus genes to promote the inflammatory response and progression is unknown. Therefore, we introduced the mutant sNASP into Sle1.Yaa mice to determine whether it has epistatic product effect with Sle1 or Yaa loci. The synergistic effect between the sNASP mutant and the Sle1.Yaa locus was determined by measuring the changes of lymphocyte subsets in peripheral immune organs, terminal organ damage, levels of serum inflammatory cytokines, and survival time of mice.

2. Materials and Method

2.1. Mice. Sle1.Yaa mice were purchased from the Jackson Laboratory (Bar Harbor, ME, USA). The Sle1.Yaa. Δ sNASP line was derived by breeding female B6. Δ sNASP mice to male B6.Sle1.Yaa mice and subsequent intercrossing of progeny. All animals were cared for under experimental protocols approved by the Weifang Medical University Animal Care Committee and housed in a specific pathogen-free (SPF) facility.

2.2. Data and Sample Collection. Mice were sacrificed at 6 months after birth, and the spleen, lymph nodes, kidney, and lung were collected. Weight of fresh organs was compared between the two genotypes. Spleen and lymph nodes were ground to prepare single-cell suspension, and cell subsets were determined by flow cytometry. Pathological lesions of the kidney and lung were evaluated after staining. Proteinuria was measured using Coomassie brilliant blue G-250 (Solarbio, Beijing, China) as per the manufacturer's instructions. Bull serum albumin (BSA) serial dilutions were prepared for a standard curve.

2.3. Kidney and Lung Histopathology. For histology, tissues of the kidney and right upper lobe lung were fixed in 4% paraformaldehyde and embedded in paraffin, and the sections were stained with hematoxylin and eosin (H&E). In addition, the sections of kidney were also stained with periodic acid Schiff (PAS). Renal and lung lesions were scored in

a blind method as the previous reports [9, 10]; glomerular lesions and lung pathology alterations were rated as grades 0-4 from normal to severe as previously described [5]. For immunohistochemistry, kidneys were embedded in an optimal cutting temperature (OCT) compound and stored at -80°C . Frozen sections were fixed in cold acetone at 4°C for 10 min and blocked with 2% newborn bovine serum (NBS) for 10 min. Sections were stained with FITC-conjugated rat anti-mouse C3 (SC-58926, Santa Cruz Biotechnology, Dallas, TX) and IgG κ BP-CFL 488 (SC-516176, Santa Cruz Biotechnology, Dallas, TX). All images were obtained by Olympus BX53 fluorescence microscope and a DP80 camera. On average, 20 glomeruli were randomly selected from each sample and semiquantitatively assessed as 0-4 grades according to staining intensity using ImageJ software (NIH).

2.4. Cytokine ELISA. Serum concentrations of the cytokines IL-1 β , IL-6, IL-17, IFN- γ , and TNF- α were determined by mouse uncoated ELISA kits (Invitrogen, Carlsbad, CA, USA) according to the manufacturer's instructions.

2.5. Flow Cytometry. lymphocyte subsets in the spleen and lymph nodes were analyzed by flow cytometry as previously described. In brief, the isolated immunocytes were first blocked with excessive rat anti-mouse CD16/32 antibody (2.4G2) for 30 min at 4°C , then stained with antibodies for 30 min at 4°C , washed and determined by a BD FACSVerser flow cytometer (BD Biosciences, San Jose, CA, USA). The antibodies used for flow cytometry were CD3 (17A2), CD4 (RM), CD8 (53-6.7), CD19 (1D3), CD86 (GL1), CD5 (53-7.3), CXCR5 (2G8), PD-1 (J43), CD1d (1B1), IFN- γ (XMG1.2), IL-4 (11B11), IL-17A (TC11-18H10), and CD69 (H1.2F3). All antibodies were purchased from BD Pharmingen (San Jose, CA, USA) or eBioscience (San Diego, CA, USA). For intracellular staining, cells were first stimulated with the leukocyte activation cocktail (BD Biosciences, San Jose, CA, USA) for 4 h, then fixed with the fixation/perm dilution (Invitrogen, Carlsbad, CA, USA) before intracellular staining.

2.6. Statistical Analysis. Data analyses and graphs were performed with Prism 5.0 software (GraphPad). Student's paired *t*-test was used for comparison between the two groups. All values were reported as mean \pm SEM, and *P* < 0.05 was considered significant.

3. Results

3.1. The sNASP Variant Aggravates End-Organ Damage in Sle1.Yaa. Δ sNASP Mice. To confirm whether the mutant sNASP has epistatic interactions with the Sle1 and Yaa loci, we analyzed the pathological alterations of the Sle1.Yaa. Δ sNASP strain compared to the control Sle1.Yaa mice at 6 months of age. The spleen sizes of Sle1.Yaa. Δ sNASP were comparable to that of Sle1.Yaa mice (Figure 1(a)), but Sle1.Yaa. Δ sNASP mice presented larger pooled lymph nodes (385.04 ± 81.92 mg), about 3 times larger than that of Sle1.Yaa mice (145.02 ± 50.78 mg). Sle1.Yaa. Δ sNASP mice also presented larger kidneys than that of Sle1.Yaa mice

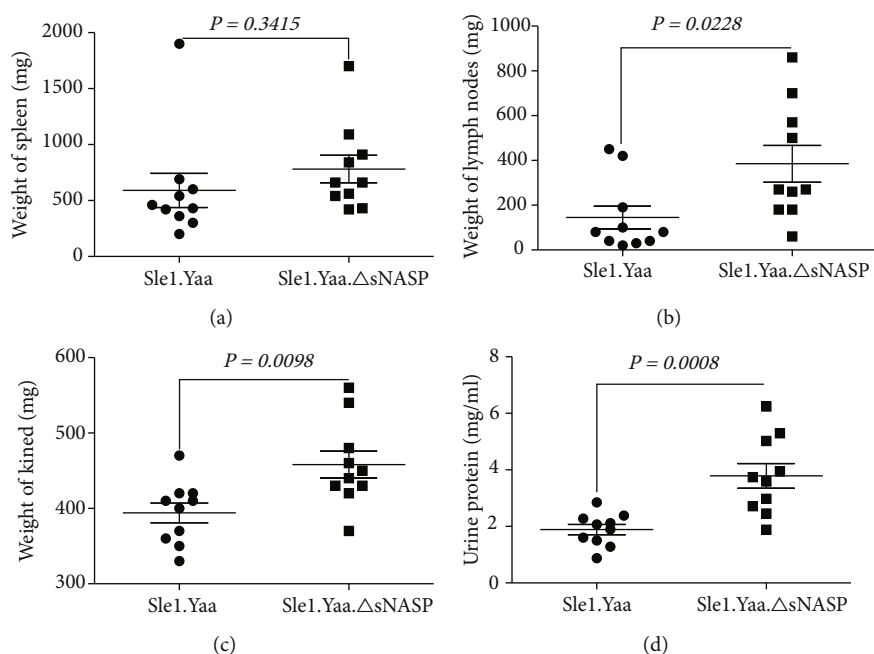


FIGURE 1: The sNASP variant promotes end-organ damage in Sle1.Yaa mice. The weight of the spleen (a), lymph nodes (b), and kidney (c). Determination of urine protein (d).

(Figure 1(c)), which were consistent with the increase of proteinuria in Sle1.Yaa.ΔsNASP mice (Figure 1(d)).

The pathology of their kidneys and lungs was also examined in our studies and showed more severe end-organ damage in sNASP mutant mice. Glomerular enlargement, mesangial cell proliferation, mesangial expansion, glomerular necrosis, tubular edema, and necrosis were observed in both groups. However, the degree of glomerular endovascular hyperplasia, mesangial cell proliferation, inflammatory cell infiltration, and renal tubular lesions, such as edema and necrosis of renal tubular epithelial cells, was higher than in Sle1.Yaa mice. We measured the long axis of the glomerulus and compared the size of the glomeruli of the two groups of mice. The results showed that the glomeruli of Sle1.Yaa.ΔsNASP mice were significantly larger than those of Sle1.Yaa mice (Sle1.Yaa: $83.15 \pm 3.485 \mu\text{m}$, Sle1.Yaa.ΔsNASP: $92.33 \pm 2.474 \mu\text{m}$, $P = 0.0455$) (Figure 2(a)). Immune complexes in the kidney were detected using the indirect immunofluorescence staining. The Sle1.Yaa.ΔsNASP mice showed significantly more C3 deposition in glomeruli than Sle1.Yaa (Figure 2(c)), yet there was no statistical difference for IgG deposition in glomeruli between Sle1.Yaa.ΔsNASP and Sle1.Yaa mice (Figure 2(b)). Pathological manifestations of inflammatory cell exudation, alveolar wall thickness, and fibrosis were observed in the lungs of both groups. Sle1.Yaa.ΔsNASP mice appeared to have developed more severe lung inflammation and fibrosis; however, no significant statistical difference in the histopathological score was observed (Figure 2(d)).

3.2. The sNASP Variant Can Increase the Levels of Serum Inflammatory Cytokines in Sle1.Yaa.ΔsNASP Mice. Cytokines play an important role in SLE initiation and progression, so we measured the expression of serum IL-1 β , IL-6,

IL-17, IFN- γ , and TNF- α using ELISA. Interestingly, IL-1 β was decreased in Sle1.Yaa.ΔsNASP mice (Figure 3(a)), while IFN- γ (Figure 3(b)) and TNF- α (Figure 3(c)) were increased compared with Sle1.Yaa mice, and there was no difference in the levels of IL-17 (Figure 3(d)) and IL-6 (Figure 3(e)) between the two groups. These results reveal that IFN- γ and TNF- α may play a major role in the exacerbation of inflammation led by mutant sNASP.

3.3. Sle1.Yaa.ΔsNASP Mice Developed More Severe Lymphocyte Subset Disorder. The imbalance and dysfunction of T and B lymphocyte subsets is an important cause of SLE. Therefore, we compared the main lymphocyte subsets in the spleen and lymph nodes between two groups of mice (Table 1). Compared with the Sle1.Yaa mice, the percentages of CD3⁺ T cells, activated CD19⁺CD86⁺ B cells, Th1 (CD4⁺IFN- γ ⁺) cells (Figure 4(a)), and CD19⁺CD5⁺CD1d^{high} Breg cells (Figure 4(b)) increased significantly while CD19⁺B cells decreased in the spleen of Sle1.Yaa.ΔsNASP mice. In the lymph nodes, the percentages of activated CD19⁺CD86⁺ B cells, CD4⁺IFN- γ ⁺ Th1 cells (Figure 4(c)), and CD4⁺IL-17A⁺ Th17 cells (Figure 4(d)) in the Sle1.Yaa.ΔsNASP mice were greater than those in the Sle1.Yaa mice. Other subsets, such as CD3⁺CD4⁺ T cells, CD3⁺CD4⁺ T cells, Tfh, activated CD4⁺CD69⁺ T, and CD4⁺IL-4⁺ Th2 cells, were comparable between Sle1.Yaa.ΔsNASP and Sle1.Yaa mice.

3.4. Effect of sNASP Gene Mutation on the Survival Rate of Sle1.Yaa Mice. An overall survival trend for Sle1.Yaa.ΔsNASP compared to the Sle1.Yaa mice up to 12 months is shown in Figure 5. Kaplan-Meier lifespan analysis indicated a significant P value of 0.0411 for overall survival differences. The variant of sNASP decreased the survival rate of Sle1.Yaa mice from 72.973% to 66.667% by month 6, 56.757% to

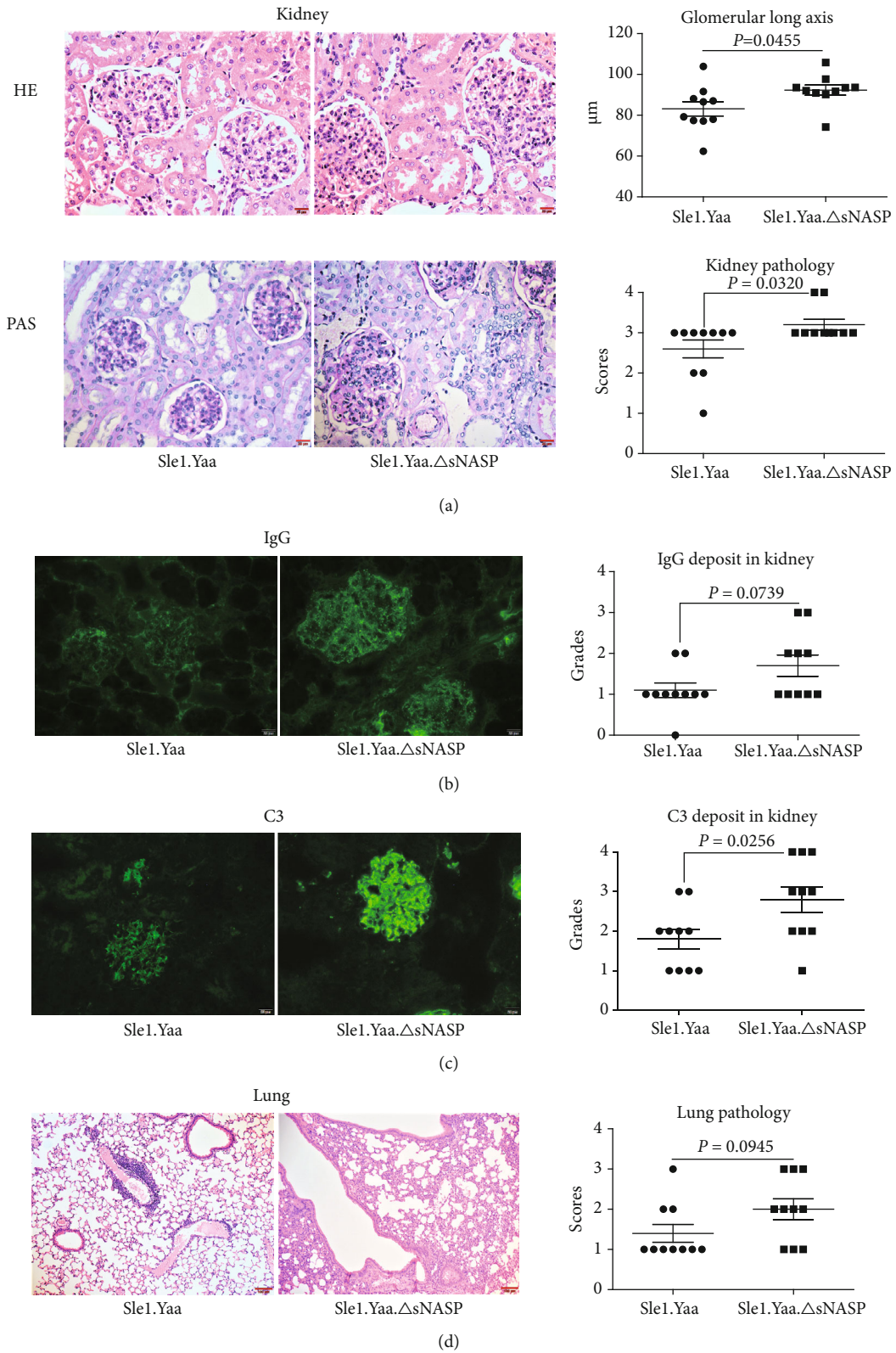


FIGURE 2: Pathological changes of the kidney and lung in mice. Representative HE-stained and PAS-stained kidney section ($\times 400$ magnification) and renal histopathology scores (a). Representative images of mouse IgG (b) and C3 (c) deposit in glomeruli from Sle1.Yaa and Sle1.Yaa. Δ sNASP mice ($\times 400$ magnification) and their respective fluorescence intensity grades. Representative H&E-stained lung section ($\times 100$ magnification) and pulmonary histopathology scores (d).

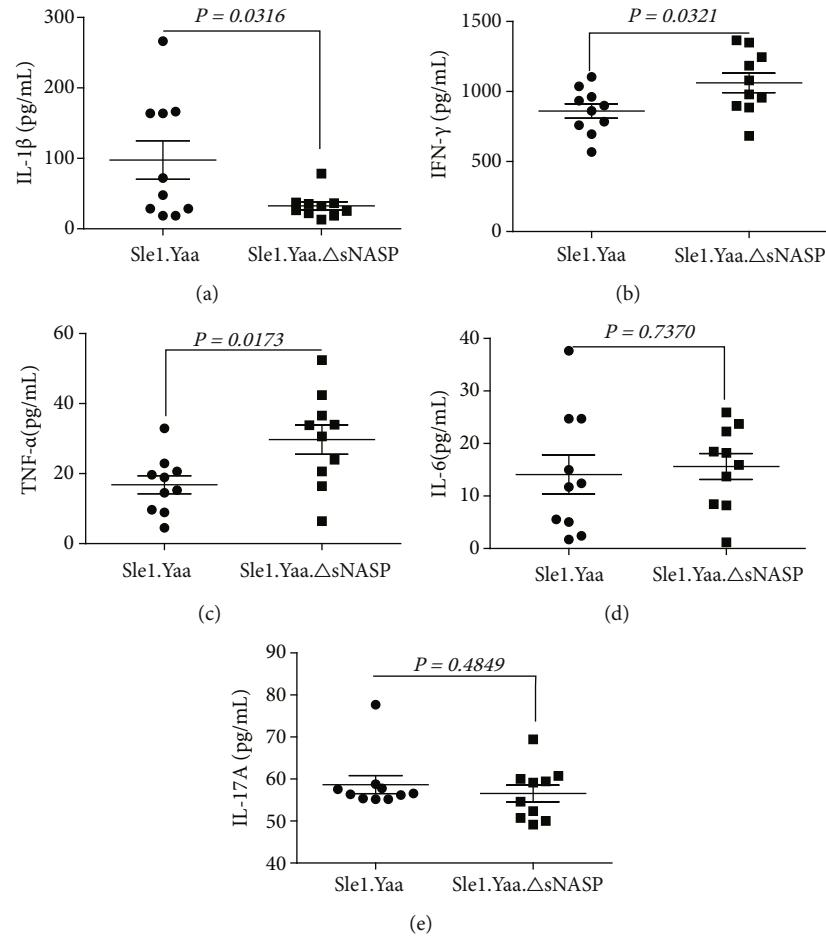


FIGURE 3: The level of serum inflammatory cytokines in mice. Decreased level of IL-1 β in Sle1.Yaa. Δ sNASP mice compared with Sle1.Yaa mice (a), but the levels of IFN- γ (b) and TNF- α (c) were increased in Sle1.Yaa. Δ sNASP mice compared with Sle1.Yaa mice. The levels of IL-6 (d) and IL-17A (e) had no significant change.

TABLE 1: Effects of NASP variant on splenic and lymph nodes' lymphocyte subsets.

Lymphocyte subsets	Spleen		Lymph nodes	
	Sle1.Yaa ($n = 10$)	Sle1.Yaa Δ sNASP ($n = 10$)	Sle1.Yaa ($n = 10$)	Sle1.Yaa Δ sNASP ($n = 10$)
CD3 ⁺	32.12 \pm 2.377	39.90 \pm 1.661*	48.35 \pm 3.245	47.54 \pm 3.400
CD19 ⁺	52.85 \pm 2.984	44.01 \pm 1.633*	42.73 \pm 3.195	42.77 \pm 3.306
CD3 ⁺ CD4 ⁺	66.09 \pm 2.272	63.54 \pm 1.080	57.11 \pm 4.764	61.26 \pm 2.177
CD3 ⁺ CD8 ⁺	19.87 \pm 1.715	24.06 \pm 0.9000	33.09 \pm 4.928	27.39 \pm 1.980
CD19 ⁺ CD86 ⁺	32.95 \pm 2.352	52.54 \pm 2.678**	39.00 \pm 3.660	49.88 \pm 3.172*
CD4 ⁺ CD69 ⁺	37.70 \pm 5.005	35.86 \pm 3.319	28.61 \pm 2.023	24.54 \pm 4.058
Tfh (CD4 ⁺ CXCR5 ⁺ PD-1 ⁺)	6.308 \pm 1.349	5.210 \pm 1.487	2.154 \pm 0.2812	2.408 \pm 0.5558
Breg (CD19 ⁺ CD5 ⁺ CD1d ^{high})	4.762 \pm 0.4781	7.664 \pm 0.5883**	3.133 \pm 0.3116	3.892 \pm 0.2756
Th1 (CD4 ⁺ IFN- γ ⁺)	39.29 \pm 1.980	46.75 \pm 2.217*	23.36 \pm 2.333	31.36 \pm 2.180*
Th2 (CD4 ⁺ IL-4 ⁺)	1.193 \pm 0.2066	0.9120 \pm 0.0969	0.5752 \pm 0.1106	0.4593 \pm 0.0573
Th17 (CD4 ⁺ IL-17A ⁺)	0.4778 \pm 0.1230	0.5944 \pm 0.0679	0.5990 \pm 0.0725	1.130 \pm 0.1004**

Results are mean \pm SEM; * $P < 0.05$ vs. Sle1.Yaa mice; ** $P < 0.01$ vs. Sle1.Yaa mice.

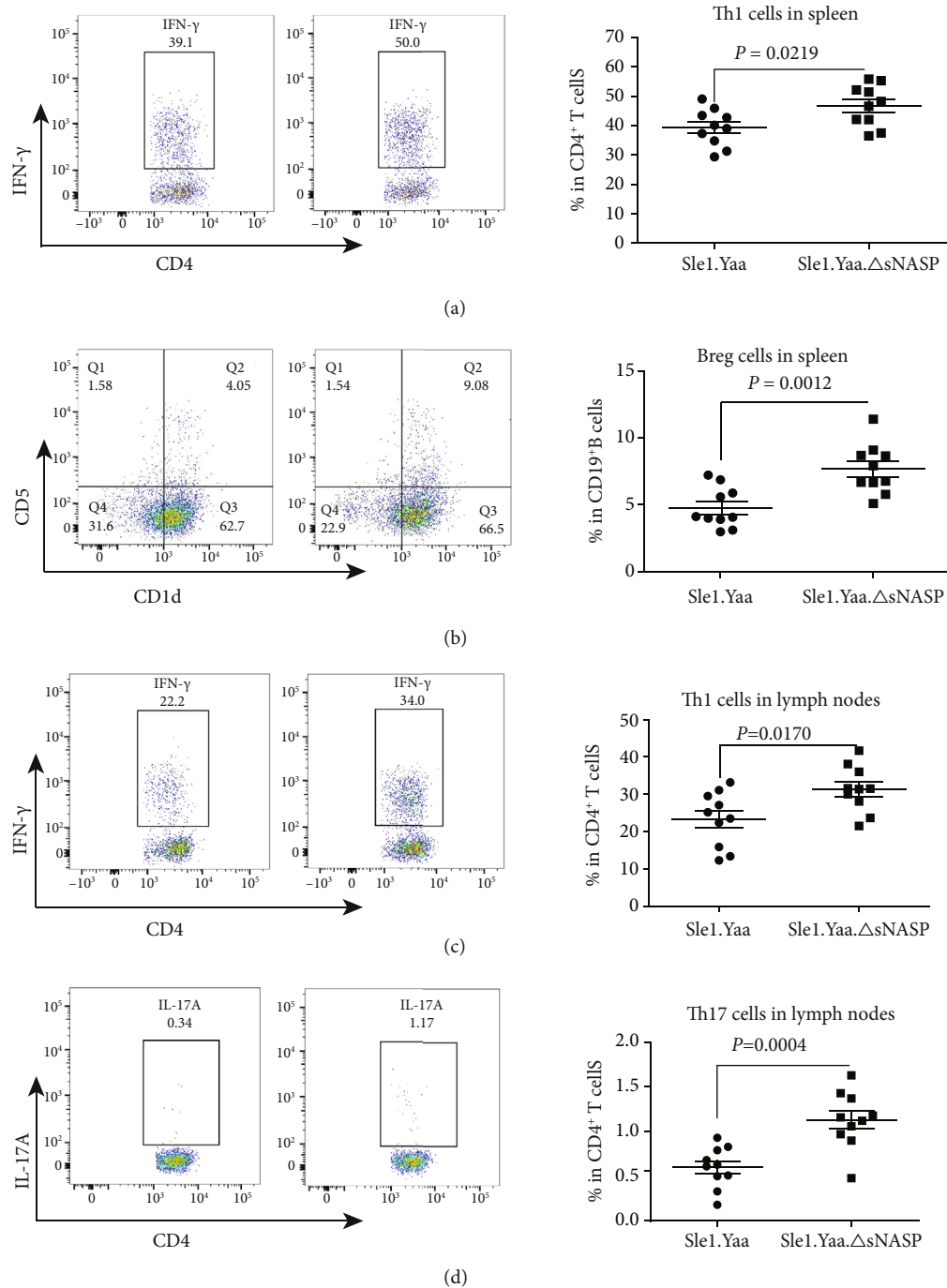


FIGURE 4: Changes of lymphocyte subsets in spleen and lymph nodes of mice. Representative FACS plots and percentages of Th1 ($CD4^+IFN-\gamma^+$) cells (a) and Breg ($CD19^+CD5^+CD1d^{high}$) cells (b) in the spleen, as well as Th1 ($CD4^+IFN-\gamma^+$) cells (c) and Th17 ($CD4^+IL-17A^+$) cells (d) in lymph nodes.

37.255% by month 9, and 45.946% to 23.529% by month 12 (Figure 5).

4. Discussion

Spontaneous mouse lupus models, such as NZB/W F1, NZM2410, MRL/lpr, and BXSB/Yaa, are useful tools for the study of the etiology of the disease. A series of gene alterations found in these models are deemed to be related to

lupus, such as the Fas gene in MRL/lpr and TLR7 in BXSB/Yaa mice. In the past decade, three lupus susceptibility genes, CDKN2c, CSF3R, and mutant Skint6, have been identified from the Sle2c1 locus of the NZM2410 strain [4, 5, 10, 11]. Recently, we revealed a novel mutant sNASP in the Sle2c1 locus, which can cooperate with Fas^{lpr} mutation to amplify autoimmunity and greatly exacerbate kidney and lung damage in the B6.lpr strain [5]. Whether mutant sNASP works synergistically with other lupus genes to

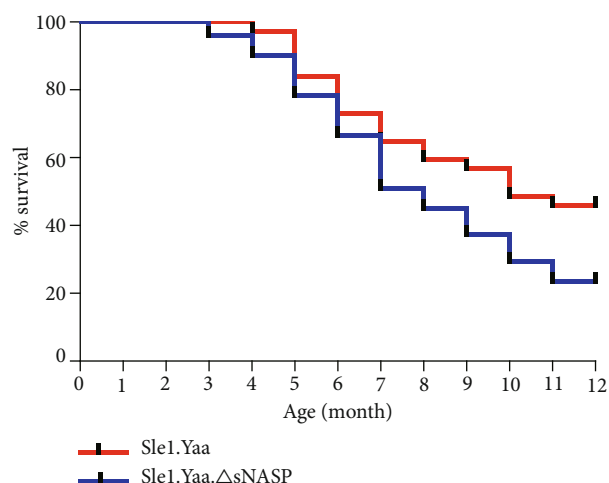


FIGURE 5: Effect of sNASP gene mutation on the survival rate of Sle1.Yaa mice. Survival was monitored in two groups of Sle1.Yaa ($n = 37$) and Sle1.Yaa.ΔsNASP ($n = 51$) mice up to 12 months. A Kaplan-Meier survival analysis was shown. The log-rank (Mantel-Cox) test was applied with a P value = 0.0411.

promote the inflammatory response and progression is unknown. Therefore, we introduced the mutant sNASP into Sle1.Yaa mice to determine whether it has an epistatic product effect with Sle1 or Yaa loci. As predicted, the mutant sNASP further aggravated the immune disorders in Sle1.Yaa.ΔsNASP mice and led to a stronger autoimmune response, which was reflected in the hyperplasia of peripheral lymphoid organs, especially lymph nodes.

T cells have been found to play a crucial role in the pathogenesis of SLE [12, 13], among which $CD4^+$ T cells are active mediators for the pathogenesis of SLE [13, 14]. Cytokine dysregulation promotes immune dysfunction, and tissue inflammation is one of the hallmarks of SLE [15, 16]. Th1 cells secrete cytokines such as $IFN-\gamma$ and $TNF-\alpha$, which can activate macrophages and inflammatory T lymphocytes. Uncontrolled Th1 activity devotes to a wide range of autoimmune disorders [17, 18]. A host of reports on spontaneous and induced lupus models pointed to the onset of SLE associated with high levels of $IFN-\gamma$ and $TNF-\alpha$ [18, 19]. Compared to Sle1.Yaa mice, the proportion of Th1 cells secreting $IFN-\gamma$ in peripheral lymphoid organs in Sle1.Yaa.ΔsNASP mice was significantly higher, and the levels of $IFN-\gamma$ and $TNF-\alpha$ in the serum were also increased. We hypothesize that the Th1 subset is one of the main targets of the mutant sNASP and contributes to the lupus pathogenesis, and the variant leads to uncontrolled $IFN-\gamma$ and $TNF-\alpha$ transcription. In addition to Th1 cell subsets, more and more studies have confirmed that IL-17 plays a momentous role in human SLE patients and murine lupus models [20, 21]. Our results indicated that the proportion of Th17 cells in the lymph nodes of Sle1.Yaa.ΔsNASP mice increased significantly and almost twice that of Sle1.Yaa mice. Studies have shown that IL-17 can promote autoreactive B cell proliferation and differentiation and autoantibody production alone or in combination with the B cell activating factor (BAFF) [22]. As a potent proinflammatory cytokine, IL-17

can induce various cells such as epithelial cells and fibroblasts to secrete chemokines and cytokines to mediate tissue damage [23, 24]. Thus, IL-17 may be another contributor among the $CD4^+$ T lymphocyte subsets to more end-organ severe glomerular mesangial expansion and pulmonary interstitial fibrosis in sNASP mutant mice. We were surprised to find that there was no difference in the proportion of $CD4^+CD69^+$ T cells in Sle1.Yaa.ΔsNASP compared to Sle1.Yaa. The variant not only affects T cell subsets, we also found that the increased $CD19^+CD86^+$ B cells in both the spleen and lymph nodes indicate enhanced activation of B cells in Sle1.Yaa.ΔsNASP mice. Interestingly, the proportion of Breg cells in the spleen of Sle1.Yaa.ΔsNASP increased slightly than those in Sle1.Yaa mice. Breg cells mainly mediate immunosuppression by secreting IL-10, while IL-10 can affect the development of T helper lymphocytes by inhibiting Th1 cells secreting $IFN-\gamma$ and IL-2 [25]. We consider that the hyperproliferation of Th1 cells disrupts the balance between Th1 and Breg cells and that increased secretion of $IFN-\gamma$ feedback promotes proliferation and differentiation of Breg cells to inhibit Th1 cells [26, 27].

Similar to what has been reported previously in B6.ΔNASP.lpr mice, we found that Sle1.Yaa.ΔsNASP mice have more severe renal damage than Sle1.Yaa mice. The proteinuria and C3 disposition of Sle1.Yaa.ΔsNASP mice were also increased. In previous studies, we have substantiated that the *rec1c* allele and the variant of sNASP promote the lung inflammation when coexpressed with the *Fas^{lpr}* mutation [5]. However, in our present study, we observed that the sNASP mutation only slightly exacerbated lung inflammation in Sle1.Yaa.ΔsNASP mice. The above results suggest that mutant sNASP seems to only aggravate the existing inflammatory response rather than start a new inflammatory response, because there is already intense renal inflammation in Sle1.Yaa mice. Along with these manifestations, the survival rate of Sle1.Yaa.ΔsNASP mice declined significantly compared to that of Sle1.Yaa mice.

How the mutant NASP promotes inflammation has yet to be further elucidated. As a key molecule in chromosome assembly, sNASP plays an important role in the late stage of DNA replication and chromosome folding [28–30]. It binds to H3, H4, and H1, participates in histone transport, and promotes cell proliferation [30, 31]. The sNASP also regulates chromatin accessibility through maintaining histone H3K9me1 [32], and DNA methylation has been shown to affect the function of T cells in lupus mice [33, 34]. Many studies have shown that the sNASP is involved in the chemical modification of histones H3 and H4. After binding the histone H3-H4 heterodimer, the sNASP mediates histone acetyltransferase activity 1 (HAT1) to the carboxyl end of histone H4 and catalyzes the acetylation of lysine at positions 5 and 12 (h4k5ac, h4k12ac). A recent study showed that sNASP can negatively regulate toll-like receptor signaling by binding tumor necrosis factor receptor associated factor 6 (TRAF6) and preventing its ubiquitination in the cytoplasm of the macrophage [35]. As a candidate gene for human SLE [36], TRAF6 has a central role in the nuclear factor $NF-\kappa B$ activation pathway. It regulates inflammation, survival, and activation of multiple immune cell subsets.

In conclusion, the mutant sNASP may participate in the disease process by changing the acetylation modification of the histone, DNA methylation of immune cells, or TRAF6-centered signaling transduction pathway. At least one point, as in our preliminary study, the mutant sNASP enhances the response of macrophages to LPS stimulation and leads to increased release of inflammatory cytokines (data not listed). On the whole, this study further confirmed that the mutant sNASP is a unique lupus susceptibility gene, which can cooperate with different lupus susceptibility genes to aggravate inflammatory response and promote disease progression.

Data Availability

The data used to support the findings of this study are included within the article.

Conflicts of Interest

The authors declare that they have no competing interests.

Authors' Contributions

Jianye Zhang and Xiaoping Du are co-first authors.

Acknowledgments

This work was supported by grants from the National Natural Science Foundation of China (81373185); Shandong Provincial Natural Science Foundation, China (ZR2018MH014); and Weifang Science and Technology Development Program (2018YX005, 2019YX030).

References

- [1] M. F. Shaikh, N. Jordan, and D. P. D'Cruz, "Systemic lupus erythematosus," *Clinical Medicine (London, England)*, vol. 17, no. 1, pp. 78–83, 2017.
- [2] J. Y. Ju and Z. W. Xu, "Potential genetic basis of B cell hyperactivation in murine lupus models," *Lupus*, vol. 30, no. 9, pp. 1438–1448, 2021.
- [3] S. K. Datta, "Harnessing tolerogenic histone peptide epitopes from nucleosomes for selective down-regulation of pathogenic autoimmune response in lupus (past, present, and future)," *Frontiers in Immunology*, vol. 12, article 629807, 2021.
- [4] L. Morel, U. H. Rudofsky, J. A. Longmate, J. Schifflbauer, and E. K. Wakeland, "Polygenic control of susceptibility to murine systemic lupus erythematosus," *Immunity*, vol. 1, no. 3, pp. 219–229, 1994.
- [5] J. Ju, J. Xu, Y. Zhu, X. Fu, L. Morel, and Z. Xu, "A variant of the histone-binding protein sNASP contributes to mouse lupus," *Frontiers in Immunology*, vol. 10, p. 637, 2019.
- [6] S. D. Yoachim, J. S. Nuxoll, K. K. Bynoté, and K. A. Gould, "Estrogen receptor alpha signaling promotes *Sle1*-induced loss of tolerance and immune cell activation and is responsible for sex bias in B6. *Sle1* congenic mice," *Clinical Immunology*, vol. 158, no. 2, pp. 153–166, 2015.
- [7] S. Subramanian, K. Tus, Q. Z. Li et al., "A *Tlr7* translocation accelerates systemic autoimmunity in murine lupus," *Proceedings of the National Academy of Sciences of the United States of America*, vol. 103, no. 26, pp. 9970–9975, 2006.
- [8] C. Mohan, E. Alas, L. Morel, P. Yang, and E. K. Wakeland, "Genetic dissection of SLE pathogenesis. *Sle1* on murine chromosome 1 leads to a selective loss of tolerance to H2A/H2B/DNA subnucleosomes," *The Journal of clinical investigation*, vol. 101, no. 6, pp. 1362–1372, 1998.
- [9] Z. Xu, C. M. Cuda, B. P. Croker, and L. Morel, "The NZM2410-derived lupus susceptibility locus *Sle2c1* increases Th17 polarization and induces nephritis in *fas*-deficient mice," *Arthritis and Rheumatism*, vol. 63, no. 3, pp. 764–774, 2011.
- [10] Z. Xu, J. Xu, J. Ju, and L. Morel, "A *Skint6* allele potentially contributes to mouse lupus," *Genes and Immunity*, vol. 18, no. 3, pp. 111–117, 2017.
- [11] Z. Xu, H. H. Potula, A. Vallurupalli et al., "Cyclin-dependent kinase Inhibitor *Cdkn2c* Regulates B cell homeostasis and function in the NZM2410-derived murine lupus susceptibility Locus *Sle2c1*," *Journal of Immunology*, vol. 186, no. 12, pp. 6673–6682, 2011.
- [12] P. M. Chen and G. C. Tsokos, "T cell abnormalities in the pathogenesis of systemic lupus erythematosus: an update," *Current Rheumatology Reports*, vol. 23, no. 2, 2021.
- [13] A. Sharabi and G. C. Tsokos, "T cell metabolism: new insights in systemic lupus erythematosus pathogenesis and therapy," *Nature Reviews Rheumatology*, vol. 16, no. 2, pp. 100–112, 2020.
- [14] M. Li, C. Yang, Y. Wang et al., "The expression of P2X7 receptor on Th1, Th17, and regulatory T cells in patients with systemic lupus erythematosus or rheumatoid arthritis and its correlations with active disease," *Journal of Immunology*, vol. 205, no. 7, pp. 1752–1762, 2020.
- [15] K. Ohl and K. Tenbrock, "Inflammatory cytokines in systemic lupus erythematosus," *Journal of Biomedicine & Biotechnology*, vol. 2011, Article ID 432595, 14 pages, 2011.
- [16] F. Chasset and L. Arnaud, "Targeting interferons and their pathways in systemic lupus erythematosus," *Autoimmunity Reviews*, vol. 17, no. 1, pp. 44–52, 2018.
- [17] A. Fava, J. Buyon, C. Mohan et al., "Integrated urine proteomics and renal single-cell genomics identify an IFN- γ response gradient in lupus nephritis," *JCI Insight*, vol. 5, no. 12, 2020.
- [18] A. N. Theofilopoulos, S. Koundouris, D. H. Kono, and B. R. Lawson, "The role of IFN-gamma in systemic lupus erythematosus: a challenge to the Th1/Th2 paradigm in autoimmunity," *Arthritis Research*, vol. 3, no. 3, pp. 136–141, 2001.
- [19] K. M. Pollard, D. M. Cauvi, C. B. Toomey, K. V. Morris, and D. H. Kono, "Interferon- γ and systemic autoimmunity," *Discovery Medicine*, vol. 16, no. 87, pp. 123–131, 2013.
- [20] T. Koga, K. Ichinose, A. Kawakami, and G. C. Tsokos, "The role of IL-17 in systemic lupus erythematosus and its potential as a therapeutic target," *Expert Review of Clinical Immunology*, vol. 15, no. 6, pp. 629–637, 2019.
- [21] J. Clarke, "IL-17 sustains plasma cells in SLE," *Nature Reviews Rheumatology*, vol. 16, no. 12, p. 666, 2020.
- [22] A. Doreau, A. Belot, J. Bastid et al., "Interleukin 17 acts in synergy with B cell-activating factor to influence B cell biology and the pathophysiology of systemic lupus erythematosus," *Nature Immunology*, vol. 10, no. 7, pp. 778–785, 2009.
- [23] S. L. Gaffen, "An overview of IL-17 function and signaling," *Cytokine*, vol. 43, no. 3, pp. 402–407, 2008.
- [24] R. M. Onishi and S. L. Gaffen, "Interleukin-17 and its target genes: mechanisms of interleukin-17 function in disease," *Immunology*, vol. 129, no. 3, pp. 311–321, 2010.

- [25] E. Oleszycka, S. McCluskey, F. A. Sharp et al., “The vaccine adjuvant alum promotes IL-10 production that suppresses Th1 responses,” *European Journal of Immunology*, vol. 48, no. 4, pp. 705–715, 2018.
- [26] K. Ma, W. du, X. Wang et al., “Multiple functions of B cells in the pathogenesis of systemic lupus erythematosus,” *International Journal of Molecular Sciences*, vol. 20, no. 23, p. 6021, 2019.
- [27] E. C. Rosser and C. Mauri, “Regulatory B cells: origin, phenotype, and function,” *Immunity*, vol. 42, no. 4, pp. 607–612, 2015.
- [28] R. T. Richardson, O. M. Alekseev, G. Grossman et al., “Nuclear Autoantigenic Sperm Protein (NASP), a Linker Histone Chaperone That Is Required for Cell Proliferation*,” *Journal of Biological Chemistry*, vol. 281, no. 30, pp. 21526–21534, 2006.
- [29] R. M. Finn, K. Browne, K. C. Hodgson, and J. Ausió, “sNASP, a Histone H1-Specific Eukaryotic Chaperone Dimer that Facilitates Chromatin Assembly,” *Biophysical Journal*, vol. 95, no. 3, pp. 1314–1325, 2008.
- [30] M. J. Apta-Smith, J. R. Hernandez-Fernaund, and A. J. Bowman, “Evidence for the nuclear import of histones H3.1 and H4 as monomers,” *The EMBO Journal*, vol. 37, no. 19, 2018.
- [31] A. J. Cook, Z. A. Gurard-Levin, I. Vassias, and G. Almouzni, “A specific function for the histone chaperone NASP to fine-tune a reservoir of soluble H3-H4 in the histone supply chain,” *Molecular Cell*, vol. 44, no. 6, pp. 918–927, 2011.
- [32] X. Kang, Y. Feng, Z. Gan et al., “NASP antagonize chromatin accessibility through maintaining histone H3K9me1 in hepatocellular carcinoma,” *Biochimica et Biophysica Acta - Molecular Basis of Disease*, vol. 1864, no. 10, pp. 3438–3448, 2018.
- [33] H. Li, M. G. Tsokos, S. Bickerton et al., “Precision DNA demethylation ameliorates disease in lupus-prone mice,” *JCI Insight*, vol. 3, no. 16, 2018.
- [34] M. Vecellio, H. Wu, Q. Lu, and C. Selmi, “The multifaceted functional role of DNA methylation in immune-mediated rheumatic diseases,” *Clinical Rheumatology*, vol. 40, no. 2, pp. 459–476, 2021.
- [35] F. M. Yang, Y. Zuo, W. Zhou et al., “sNASP inhibits TLR signaling to regulate immune response in sepsis,” *Journal of Clinical Investigation*, vol. 128, no. 6, pp. 2459–2472, 2018.
- [36] B. Namjou, C. B. Choi, I. T. Harley et al., “Evaluation of TRAF6 in a large multiethnic lupus cohort,” *Arthritis and Rheumatism*, vol. 64, no. 6, pp. 1960–1969, 2012.

Research Article

Endangered Lymphocytes: The Effects of Alloxan and Streptozotocin on Immune Cells in Type 1 Induced Diabetes

Luiz A. D. Queiroz ¹, Josiane B. Assis ², João P. T. Guimarães ¹,
Emanuella S. A. Sousa ¹, Anália C. Milhomem ³, Karen K. S. Sunahara ⁴,
Anderson Sá-Nunes ² and Joilson O. Martins ¹

¹Laboratory of Immunoendocrinology, School of Pharmaceutical Sciences, Department of Clinical and Toxicological Analyses, University of São Paulo, São Paulo, SP, Brazil

²Laboratory of Experimental Immunology, Institute of Biomedical Sciences, Department of Immunology, University of São Paulo, São Paulo, SP, Brazil

³Institute of Tropical Pathology and Public Health, Department of Microbiology, Immunology, Parasitology and Pathology, Federal University of Goiás, Goiânia, GO, Brazil

⁴Experimental Physiopathology, Department of Sciences/Experimental Physiopathology, Medical School, University of São Paulo, São Paulo, SP, Brazil

Correspondence should be addressed to Anderson Sá-Nunes; sanunes@usp.br and Joilson O. Martins; martinsj@usp.br

Received 3 June 2021; Revised 6 September 2021; Accepted 16 September 2021; Published 19 October 2021

Academic Editor: Shushan Yan

Copyright © 2021 Luiz A. D. Queiroz et al. This is an open access article distributed under the Creative Commons Attribution License, which permits unrestricted use, distribution, and reproduction in any medium, provided the original work is properly cited.

Alloxan (ALX) and streptozotocin (STZ) are extensively used to induce type 1 diabetes (T1D) in animal models. This study is aimed at evaluating the differences in immune parameters caused by ALX and STZ. T1D was induced either with ALX or with STZ, and the animals were followed for up to 180 days. Both ALX and STZ induced a decrease in the total number of circulating leukocytes and lymphocytes, with an increase in granulocytes when compared to control mice (CT). STZ-treated mice also exhibited an increase in neutrophils and a reduction in the lymphocyte percentage in the bone marrow. In addition, while the STZ-treated group showed a decrease in total CD3⁺, CD4⁺CD8⁺, and CD4⁺CD8⁺ T lymphocytes in the thymus and CD19⁺ B lymphocytes in the pancreas and spleen, the ALX group showed an increase in CD4⁺CD8⁺ and CD19⁺ only in the thymus. Basal levels of splenic interleukin- (IL-) 1 β and pancreatic IL-6 in the STZ group were decreased. Both diabetic groups showed atrophy of the thymic medulla and degeneration of pancreatic islets of Langerhans composed of inflammatory infiltration and hyperemia with vasodilation. ALX-treated mice showed a decrease in reticuloendothelial cells, enhanced lymphocyte/thymocyte cell death, and increased number of Hassall's corpuscles. Reduced *in vitro* activation of splenic lymphocytes was found in the STZ-treated group. Furthermore, mice immunized with ovalbumin (OVA) showed a more intense antigen-specific paw edema response in the STZ-treated group, while production of anti-OVA IgG1 antibodies was similar in both groups. Thereby, important changes in immune cell parameters *in vivo* and *in vitro* were found at an early stage of T1D in the STZ-treated group, whereas alterations in the ALX-treated group were mostly found in the chronic phase of T1D, including increased mortality rates. These findings suggest that the effects of ALX and STZ influenced, at different times, lymphoid organs and their cell populations.

1. Introduction

Diabetes mellitus is a chronic disorder characterized by persistent levels of hyperglycemia caused by an insufficient production of insulin by the β cells of the pancreas due to a

destruction of these cells in type 1 diabetes (T1D) or by ineffective insulin action in type 2 diabetes (T2D) [1–3]. Rodents have been extensively used as diabetes experimental models [4]—chemically induced diabetes is mainly useful for studying T1D. Alloxan (ALX) and streptozotocin (STZ) bind to

the glucose transporter- (GLUT-) 2 receptor, causing cell death by reactive oxygen species (ROS) generation (ALX) or inducing DNA damage (STZ) directly [5]. These diabetogenic agents, however, may have different toxicological effects depending on the dose and route of administration [6]. Although they have been used for quite a long time, the immunotoxicological effects of ALX and STZ are not fully clear yet.

One of the obnoxious effects of STZ is its toxicity to lymphocytes, diminishing T cell proliferation [7, 8], reducing the CD8⁺ T cell population in the blood and causing lymphopenia in the spleen and blood [7]. Gaulton et al. compared the toxicity of ALX and STZ in immune cells, both *in vivo* and *in vitro*, and found a greater impairment of lymphocyte function even when STZ was administered in doses lower than necessary for T1D onset. In contrast, a 10-fold increase in the ALX dose was not harmful to lymphoid cells [9]. Diab et al. conducted a similar study to evaluate the cytotoxicity of both agents, finding *in vitro* changes in blood cell populations, reduction of splenocytes, and immunosuppressive effects on graft transplantation in individuals treated with STZ [10].

A database search carried out by Muller et al. showed that in 131 articles on murine islet transplantation, 76.3% used the STZ diabetic model, while 3.8% used ALX [7]. STZ is the preferred model because it has a longer half-life, with prolonged hyperglycemia and lower mortality rates [10, 11]. Although less expensive, ALX is very unstable and may induce a reversible hyperglycemia that is undesirable and sometimes lethal [12].

Since the study of immune cell responses is of paramount significance/importance in T1D models, the comparison of different immune cell variables is vital to better understand the behavior of these cells and how they could be influenced by the choice of diabetogenic agents. To clarify these effects, this study is aimed at evaluating the differences in immune parameters caused by ALX and STZ, with special attention to T cell phenotype and function in lymphoid and nonlymphoid tissues.

2. Methods

2.1. Animal Model. Wild-type C57BL/6J male mice (12-14 weeks old, 25 ± 2 g at baseline) were housed at 22°C under a 12/12-hour light-dark cycle and given *ad libitum* access to food and water. This study was carried out in strict accordance with the principles and guidelines of the National Council for the Control of Animal Experimentation (CONCEA) and approved by the Ethics Committee on Animal Use (CEUA) at the Faculty of Pharmaceutical Sciences, University of São Paulo (FCF/USP), Brazil (protocol number: CEUA/FCF/338).

2.2. Induction of Diabetes. The animals were divided into three groups: (1) wild-type C57BL/6J control mice (CT), (2) ALX-treated mice, and (3) STZ-treated mice. Briefly, to induce T1D with ALX, the animals were fasted for 12 hours, followed by an intravenous (i.v.) injection of 60 mg/kg of alloxan monohydrate (Sigma-Aldrich, San Louis, MO,

USA) dissolved in 100 μ L of sterile saline solution (0.9% NaCl) [13] using insulin syringes with 12.7 mm \times 29G needle (BD Ultra-Fine, Franklin Lakes, New Jersey, USA); for STZ, the animals were fasted for 5 hours, followed by an intraperitoneal (i.p.) injection of 65 mg/kg of streptozotocin (ChemCruz®, Santa Cruz, CA, USA) dissolved in 300 μ L of 0.1 M citrate buffer, pH 4.5, for 5 consecutive days [3], using insulin syringes with 12.7 mm \times 29G needle. After 15 days from the start of the induction protocol, the glycemia of the animals was measured using Accu-Chek Advantage II (Roche Diagnostics, São Paulo, SP, Brazil). Only the animals with glycemia above 300 mg/dL were considered diabetic for this study.

2.3. Physical Observation. In one set of experiments, daily observation throughout the study was carried out for mortality and general well-being in all groups. The consumption of water and food was monitored by weighing the average amount of food (g) and water (mL) consumed per mouse, for 5 days [14]. Following diabetes induction, glycemia and body weight were monitored at various time points (15th, 30th, 60th, 90th, and 180th days) and compared to CT mice.

2.4. Insulin Tolerance Test (ITT). Insulin tolerance tests were performed after 6 hours and on the 90th and 180th days after inducing T1D. Initial blood glucose levels were determined followed by intraperitoneal injection of human insulin (Humulin®, Fegersheim, France) (0.75 unit/kg) using insulin syringes with 12.7 mm \times 29G needle. Blood glucose levels were measured via tail vein blood at 5, 10, 15, 20, 25, and 30 minutes after the injection [15–17].

2.5. Glucose Tolerance Test (GTT). Glucose tolerance tests were performed after an overnight fast (12 hours) and on the 90th and 180th days after inducing T1D. Initial blood glucose levels were determined followed by intraperitoneal injection of glucose solution (Thermo Fisher Scientific, Rockford, IL, USA) (1 g/kg) using insulin syringes with 12.7 mm \times 29G needle. Blood glucose levels were measured via tail vein blood at 15, 30, 60, 90, and 120 minutes after the injection [16, 18].

2.6. Hematological Parameters. Blood samples were collected via a facial plexus route on the 15th, 30th, 90th, and 180th days after inducing T1D. Samples of EDTA-anticoagulated blood (1:10) were used to determine the following hematological parameters [19]: red blood cells (RBC), hemoglobin (HGB), hematocrit (HCT), mean corpuscular volume (MCV), mean corpuscular hemoglobin (MCH), mean corpuscular hemoglobin concentration (MCHC), red cell distribution width (RDW), platelets (PLT), leukocytes (WBC), lymphocytes (Lymph), monocytes (Mon), granulocytes (Gran), and the percentage of lymphocytes (Lymph%), monocytes (Mon%) and granulocytes (Gran%). All analyses were performed using an automated hematology counter (BC-2800Vet Mindray, Shenzhen, GD, China).

Bone marrow was collected from femurs on the 15th day after inducing T1D, and cell suspensions were centrifuged in glass slides at 400 \times g, 4°C, for 5 minutes, using a Cytospin centrifuge (Thermo Fisher Scientific), and allowed to dry for

20 minutes at room temperature [20]. The slides were stained using fast panoptic (LB Laborclin, Pinhais, PR, Brazil). A total of 100 cells were counted based on morphological criteria, classified as either mononuclear or polymorphonuclear [21, 22], using a conventional optical microscope (CX31RBSFA, Tokyo, Japan).

2.7. Histopathological Analysis. Histopathological analyses were performed in fragments of thymus, spleen, and pancreas tissue collected on the 15th day after inducing T1D. Samples were fixed in a solution of 10% paraformaldehyde, dehydrated with alcohol, diaphanized in xylol, and embedded in paraffin. Blocks were cut into 3 μm width slices, and fragments were captured with glass slides and stained with hematoxylin and eosin (H&E) [23].

General toxicity processes were described and classified according to structural changes by a semiquantitative analysis, as follows: absent, when there was no compromise of the tissue, score = 0; discrete, with up to 25% of area commitment, score = 1; moderate, from 26% to 50% of area commitment, score = 2; and accentuated, with more than 50% of area commitment, score = 3 [23–25].

2.8. Spleen and Pancreas Homogenates. Tissue samples of spleen and pancreas were separately collected from the mice on the 15th day after inducing T1D and homogenized in radioimmunoprecipitation assay (RIPA) buffer (50 mM Tris, pH 8.0, 150 mM NaCl, 1% Triton X-100, and 0.1% SDS) containing a protease inhibitor (Sigma-Aldrich), with a tissue homogenizer (Polytron PT 1600E, Cincinnati, OH, USA). Supernatants were separated from the cellular debris by centrifugation at $239 \times g$ for 5 minutes, collected and stored at -80°C .

Protein concentration in the homogenates was determined using Pierce™ BCA Protein Assay Kit (Thermo Fisher Scientific), according to the manufacturer's instructions.

2.9. Cytokine Determination. ELISA was used to determine the concentration of the following cytokines: interleukin-(IL-) 1β , IL-4, IL-12p70, tumor necrosis factor- (TNF-) α , and interferon- (IFN-) γ (Duo-set ELISA, R&D Systems Inc., Minneapolis, MN, USA); IL-2, IL-6, and IL-10 (BD OptEIA™ ELISA Set, BD Biosciences, San Diego, CA, USA); and IL-17A (ELISA MAX Deluxe Set, Biolegend, San Diego, CA, USA) in pancreas and spleen homogenates on the 15th day after inducing T1D. The assays were performed according to the manufacturers' instructions.

2.10. Flow Cytometry. Following euthanasia, pancreas, spleen, and thymus were removed on the 15th day after inducing T1D and macerated through a 40 μm cell strainer. Spleen cell suspension was lysed using ACK Lysing Buffer (Gibco, Grand Island, NY, USA), and cell suspensions containing 1.5×10^6 cells/mL were prepared in PBS containing 1% fetal bovine serum (FBS) and stained at 4°C for 30 minutes with fluorochrome-conjugated monoclonal antibodies against the following molecules (cell clone): CD3-PE (17A2), CD19-PE-Cy7 (6D5), CD25-PB (PC61), and CD11b-APC-Cy7 (M10/70) (Biolegend) and CD4-APC (RM4-5) and CD8-PE-Cy5 (53-6.7) (BD Biosciences). The

cells were acquired in a FACSCanto II cytometer (BD Biosciences), and analysis was performed using the FlowJo software, version 10.0.7 (Tree Star, Ashland, OR, USA).

2.11. Immunization of Mice and Induction of Antigen-Specific Paw Edema. In another set of experiments, mice received three subcutaneous (s.c.) immunizations, with a 15-day interval between each one, consisting of 20 μg /mice of OVA (Sigma-Aldrich) emulsified in 100 μL of squalene adjuvant (Sigma-Aldrich). Doses were administered with a 15-day interval from one another [26]. Thirty days after the last immunization, the mice were submitted to the protocol of diabetes induction with either ALX or STZ.

The diabetic animals, together with the immunized CT and naïve mice, were challenged with s.c. injection of OVA (10 μg in 30 μL of saline) on the right paw. As a control, the mice also received a s.c. injection of 30 μL saline on the left paw. Footpad thickness was measured immediately before and 6 hours after the inoculation using a caliper (Mitutoyo, Kawasaki, OL, Japan). The results are expressed as the mean difference between the measurements, as described [27].

2.12. Determination of OVA-Specific Anti-IgG1 and Anti-IgG2a Antibodies. After the immunization and antigenic challenge described above, blood samples were collected to determine OVA-specific anti-IgG1 and anti-IgG2a antibodies. The plates were coated overnight at 4°C with OVA (20 $\mu\text{g}/\text{mL}$) in sodium carbonate buffer (pH 9.5), washed with PBS/0.05% Tween-20, and blocked with assay diluent PBS/10% FCS for 1 hour. Following washing, serum samples were added to the plates and incubated at room temperature (RT) for 2 hours. After new washing, anti-IgG1 or anti-IgG2a (BD Biosciences) conjugated with peroxidase was added and incubated for 1-hour RT. After washing, 3,3',5,5'-Tetramethylbenzidine (TMB) Substrate Reagent Set (BD Biosciences) was added and the plates were left for 30 minutes RT in the dark [26]. Colorimetric reaction was stopped by adding 2 NH_2SO_4 . Absorbance was acquired at 450 nm in the microplate reader SpectraMax 190. The data are shown in optical density (O.D) units.

2.13. Spleen Cell Proliferation. Spleen cell proliferation was evaluated at different stages of the study and by different methodologies. In all cases, spleens were removed, individually macerated through a 40 μm cell strainer, and the cell suspensions were lysed using ACK Lysing Buffer (Gibco) before the respective assay.

On the 15th day after inducing T1D in naïve mice, spleen cell suspensions containing 10^7 cells/mL were stained with carboxyfluorescein succinimidyl ester (CFSE)-FITC (eBioscience, San Diego, CA, USA) according to the manufacturer's protocols. The cells were plated with complete medium (RPMI 1640 supplemented with 10% FBS, 1% penicillin/streptomycin, 2 mM L-glutamine, and 25 mM HEPES, all from Gibco) and stimulated with Concanavalin A (Con A—0.5 and 1 $\mu\text{g}/\text{mL}$, Sigma-Aldrich) for 72 hours at 37°C and 5% CO_2 [26]. After that, the cells were stained at 4°C for 30 minutes with anti-mouse CD4-APC and CD8-PE-

cy5 (BD Biosciences), acquired in a FACSCanto II cytometer and analyzed as described above.

In mice immunized with OVA, spleen cell suspensions containing 10^6 cells/mL were prepared in complete medium and stimulated with Con A (0.5 and $1\ \mu\text{g}/\text{mL}$, Sigma-Aldrich) for polyclonal activation or with OVA (1 and $10\ \mu\text{g}/\text{mL}$, Sigma-Aldrich) for antigen-specific proliferation. Proliferation was evaluated by a colorimetric assay using resazurin (Sigma-Aldrich), as previously described [28]. The results are expressed as the difference between the absorbance reading at 570 and 600 nm by a spectrophotometer (SpectraMax 190, San Jose, CA, USA) [29, 30].

2.14. Statistical Analysis. Statistical analyses were performed using the GraphPad 6 software (San Diego, CA, USA), and the data are presented as mean \pm standard error of the mean (SEM) using analysis of variance (ANOVA), two-way for GTT and ITT and one-way for the other evaluations, followed by Bonferroni's multiple comparison test when appropriate. The significance level was set at $p \leq 0.05$.

3. Results

3.1. ALX and STZ Increased Blood Glucose Levels, Induced Bodyweight Loss, and Changed Blood Cell Counts. The effects of ALX and STZ treatment for T1D induction in mice were identified by measuring body weight and glycemia after a 15-day protocol. Both ALX- and STZ-treated animals exhibited glycemia above 300 mg/dL until the 180th day, with the ALX-induced animals maintaining higher levels of hyperglycemia until the 90th day (Figure 1(a)). The group treated with STZ showed a greater and more pronounced weight loss than the ALX group during the whole period evaluated (Figure 1(b)). Both diabetic groups showed an increase in water intake (Figures 1(i)), but not food intake (Figures 1(h)) compared to the CT group. After 180 days from T1D induction, there was no signal of insulin or glucose tolerance in the ALX and STZ groups (Figures 1(d)–1(g)). However, some animals from the ALX group started to die after 60 days (Figure 1(c)) and presented tumor nodules throughout the body (data not shown), as it has already been reported by other authors [31–33].

In order to explore the impacts of ALX and STZ on the population of blood cells in the early and chronic phases of T1D, we analyzed the whole blood count at different time points—15th, 30th, 90th, and 180th days—and identified that both the ALX- and STZ-treated groups revealed a decrease in leukocytes (Figure 2(i)) and lymphocytes (Figure 2(j)) on the 15th day. A lower percentage of lymphocytes (Figure 2(m)) and an increased percentage of granulocytes (Figure 2(o)) were found on the first 15 days in both the T1D-induced groups; despite fluctuating during the study, the number of lymphocytes remained lower in the last measurement (180th day) when compared to the CT group (Figure 2(j)). The total leukocyte count varied over the study period. For monocytes, however, while ALX lowered their count by the 15th day, this alteration only occurred after the 30th day in the STZ-induced group (Figure 2(k)). ALX-induced animals showed consistently increased parameter

values on the 30th day for red blood cell count (Figure 2(a)), hemoglobin (Figure 2(b)), and hematocrit (Figure 2(c)), while their mean corpuscular hemoglobin concentration (Figure 2(f)) was lower in the same period. In addition, a differential count of nucleated cells in the bone marrow showed a decreased percentage of lymphocytes in the STZ-induced group in comparison with CT and ALX groups, suggesting its toxicity (Table 1). In parallel, the STZ-induced group presented an increased percentage of neutrophils in the bone marrow when compared to the other groups (Table 1).

3.2. STZ Impaired the Basal Production of IL-1 β in the Pancreas and IL-6 in the Spleen. To assess whether ALX and STZ can influence the immunological steady-state profile of the animals, the basal levels of IL-1 β , IL-2, IL-4, IL-6, IL-10, IL-12, IL-17, IFN- γ , and TNF- α in spleen (Figure 3(a)) and pancreas (Figure 3(b)) homogenates were measured. A significant reduction of IL-6 in the spleen and IL-1 β in the pancreas in the STZ group was found, while all other cytokines were not altered. This could be a result of an imbalance of secretory cells due to the hyperglycemic environment rather than a toxicity of STZ.

3.3. Lymphocyte Populations in the Thymus, Spleen, and Pancreas Were Affected by STZ. Knowing that lymphocytes are the cell type most affected by the toxicity of ALX and STZ, T and B cell populations were determined in the thymus, spleen, and pancreas. It was found that the STZ-induced group showed a reduction in the percentage of total CD3⁺, CD4⁺CD8⁺ T lymphocytes, and CD4⁺CD8⁺ double-positive cells in the thymus (Figure 4(a)). A reduction in CD19⁺ B lymphocytes in the spleen (Figure 5(a)) and pancreas (Figure 6(a)) was also found. The ALX-induced group only showed changes in the thymus, including an increase in CD4⁺CD8⁺ cells, as well as CD19⁺ B lymphocytes (Figure 4(a)). This suggests that the diabetogenic agents influence lymphocyte subpopulations differently in the evaluated organs.

3.4. ALX and STZ Induced Morphological Changes in the Thymus and Pancreas, but Not in the Spleen. We also investigated whether ALX and STZ induced morphological changes in the pancreas, spleen, and thymus. In the pancreas, it was possible to identify, in both diabetic groups, atrophy of the islets of Langerhans (Figures 6(b) and 6(c)), inflammatory infiltration, and hyperemia with vascular dilation (Figure 6(b)). Being the pancreas a target organ of the diabetogenic agents, this may indicate that the destruction of the β cells was effective, followed by an inflammatory process as a side effect. The treatment seemed not to affect the integrity of the spleen in any diabetic group (Figure 5(c)). In the thymus, it was observed atrophy of the medullary region in both the ALX- and STZ-induced groups (Figures 4(b) and 4(c)). Enhanced death of lymphocytes/thymocytes, with an increase in Hassall's corpuscles and a decrease in the number of reticulum and epithelial cells in the ALX-induced group (Figure 4(b)), might indicate a

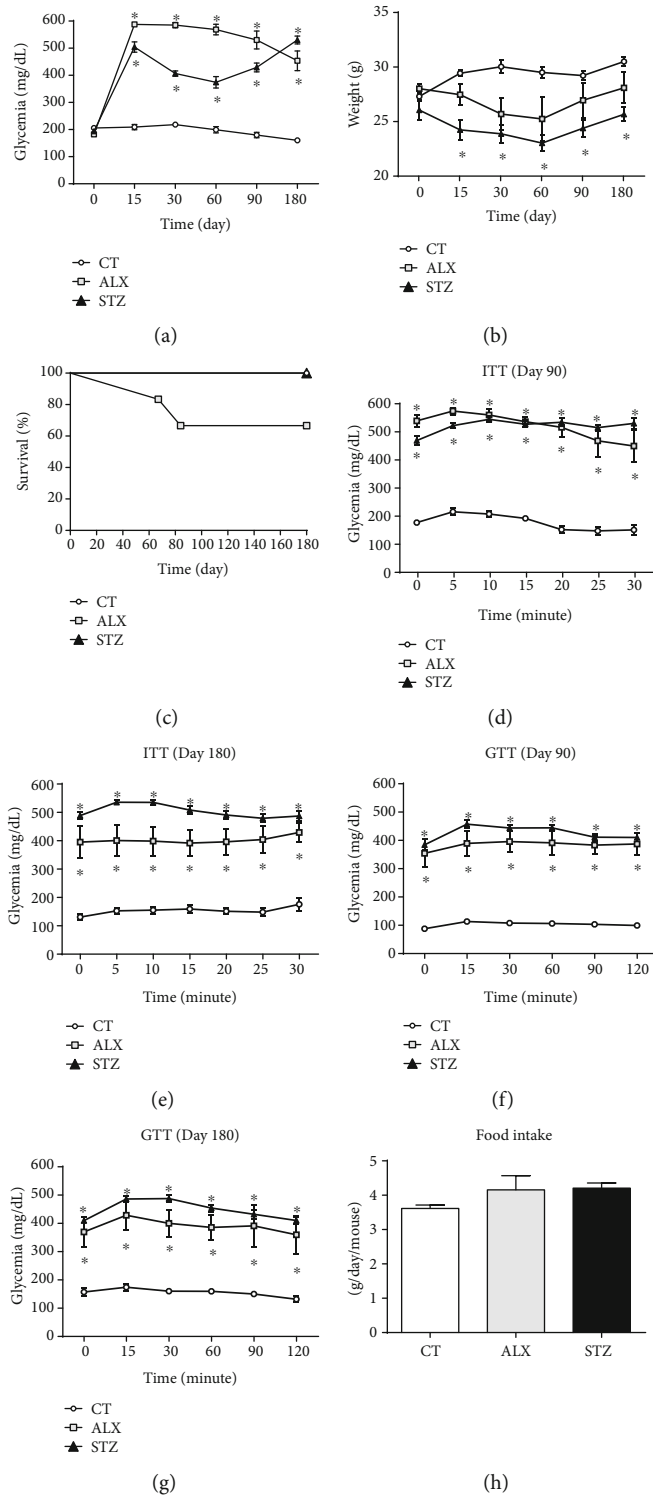


FIGURE 1: Continued.

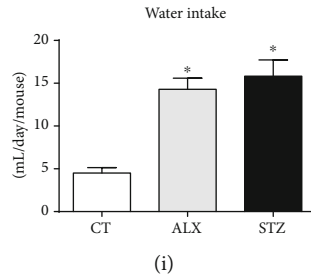


FIGURE 1: Long-term diabetogenic effects of ALX and STZ on mice. T1D was induced as described in Methods, and parameters were evaluated at different time points. (a) Blood glucose levels and (b) body weight were evaluated on the 15th, 30th, 60th, 90th, and 180th days following administration of the drugs. (c) Survival rate was monitored for 180 days (CT and STZ groups represented as overlapping lines). (d, e) Insulin tolerance test and (f, g) glucose tolerance test were evaluated on the 90th and 180th days. (h) Food and (i) water intake was evaluated for five days. Data are presented as mean \pm SEM, * $p \leq 0.05$ (5-6 animals per group).

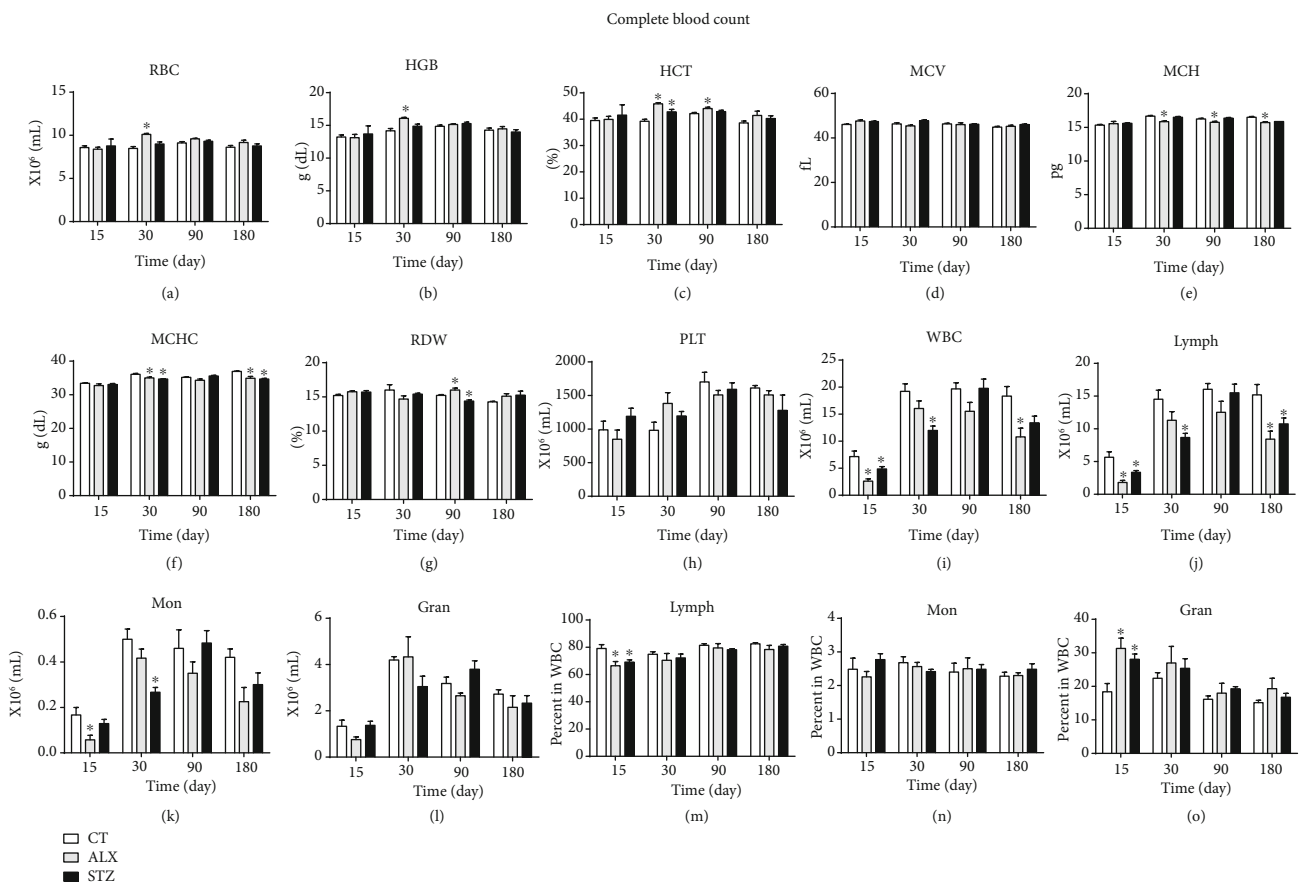


FIGURE 2: STZ effects on hematimetric parameters of immunological cells in the early phase of T1D are restored in the chronic phase of the disease. T1D was induced as described in Methods, and blood samples were collected in EDTA on the 15th, 30th, 90th, and 180th days, to evaluate the following parameters: (a) red blood cells; (b) hemoglobin; (c) hematocrit; (d) mean corpuscular volume; (e) mean corpuscular hemoglobin; (f) mean corpuscular hemoglobin concentration; (g) red cell distribution width; (h) platelets; (i) leukocytes; (j) lymphocytes; (k) monocytes; (l) granulocytes; (m) percentage of lymphocytes; (n) percentage of monocytes; (o) percentage of granulocytes. Data are presented as mean \pm SEM, * $p < 0.05$ (11-13 animals per group).

change in the epithelial component of the thymus and the natural process of replacement of lymphocytes/thymocytes.

3.5. ALX and STZ Did Not Affect the *In Vitro* Proliferative Activity of CD4⁺ and CD8⁺ T Lymphocytes in the Spleen. In order to determine whether the diabetogenic agents were

capable of influencing the functional status of lymphocytes, *in vitro* polyclonal proliferation was tested. Both CD4⁺ and CD8⁺ T lymphocytes showed no difference in activation induced by Con A after induction of T1D with ALX or STZ (Figure 5(b)), indicating that the agents did not interfere with *in vitro* cell proliferation.

TABLE 1: STZ-treated animals showed an increase in the percentage of neutrophils and a decrease in lymphocytes in the bone marrow. Data are presented as percentage \pm SEM, * $p \leq 0.05$ (5-6 animals per group).

Cells (%)	Percentage \pm SEM		
	CT	ALX	STZ
Blast	0.2 \pm 0.2	0.0 \pm 0.0	0.0 \pm 0.0
Ring forms	3.3 \pm 0.6	3.2 \pm 1.0	1.5 \pm 0.7
Segmented neutrophils	67.0 \pm 1.9	75.6 \pm 4.2	81.0 \pm 2.1*
Monocytes	2.0 \pm 0.7	2.0 \pm 0.5	1.0 \pm 0.4
Lymphocytes	27.5 \pm 2.3	19.2 \pm 4.0	16.5 \pm 2.5*

3.6. STZ Caused Changes in the Immune Response Behavior *In Vivo* and *In Vitro* of Immunized Animals. To assess whether ALX and STZ acted on the cellular and humoral acquired immune responses already established *in vivo*, mice were immunized with OVA and T1D was induced using both agents. Immunized mice from the STZ-induced group displayed an increased footpad thickness following challenge with OVA in comparison with mice from the CT and ALX-induced groups (Figure 7(a)). In addition, while all animals produced similarly increased levels of specific anti-OVA IgG1, anti-OVA IgG2a was virtually absent in immunized animals (Figure 7(b)). However, when the lymphocyte proliferative activity was evaluated *in vitro*, the immunized animals in the STZ-treated group showed a reduced polyclonal activation under Con A stimulation, but not OVA-specific activation, when compared to the CT and ALX-induced groups (Figure 7(c)). Together, these findings suggest an effect of STZ on the cell-mediated immune response of immunized animals while the humoral immune response did not seem to be affected.

4. Discussion

Animal models have been responsible for knowledge improvement and medical advances in several areas and from different perspectives. Chemically induced diabetes in rodent models has been developed to study not just the illness but also to better understand aspects of the condition. Because diabetes is a multifaceted and multifactorial disorder, animal models help to demystify different characteristics of its pathophysiology [13, 34, 35]. Since an immunopathogenic component in T1D had been previously described [36], much attention converged on choosing a model that could better contribute to the study of lymphocytes and their physiology. Although ALX and STZ are the most common pharmacological agents used to induce T1D, many toxicological effects on lymphoid organs and cells have been described [9, 10, 37–44].

Both agents were capable of maintaining the animals under T1D conditions during the whole study without causing reversible diabetes or inducing insulin or glucose tolerance effects [45, 46]. Therefore, it was possible to evaluate acute and chronic effects of T1D. Regarding blood cell counts, in the early phase of T1D, alterations in the propor-

tion of immune cells were found in both the STZ- and ALX-treated groups. This initial phase was marked by an acute stress response which correlated to a reduction in the number of lymphocytes and monocytes and an increase in the percentage of granulocytes in animals treated with STZ during the first 30 days of diabetes induction, when compared to the CT group. The initial alteration in the blood cell count was spontaneously compensated during the study timeline and became very close to CT parameters, suggesting that there is a natural ability, even for diabetic animals, to adapt to this adverse condition. Interestingly, in the chronic phase of diabetes, the ALX group started to present subcutaneous tumor nodules after 90 days (data not shown), which might have contributed to the ~30% mortality observed in this group [31–33].

While some studies state that alterations in T1D animals are a consequence of drug pharmacodynamics [9, 10, 37–44], others claim that these changes are due to the hyperglycemic environment triggered by each agent [47–52]. Indeed, hyperglycemia affects the immune system [53] and can lead to defects in host immunity, such as impaired cell migration, phagocytosis, and intracellular killing [54]. A hyperglycemic state also increases the synthesis of advanced glycation end products (AGEs), secretion of proinflammatory cytokines, and oxidative stress pathways [55]. Whether these changes are connected to our findings remains to be determined.

Regarding the diabetogenic drugs used in this work, STZ might have some level of toxicity to bone marrow precursor cells since, in animals treated with this agent, a reduction in the percentage of lymphocytes and an increase in neutrophils were found. This toxic influence has already been described and may be explained by the STZ ability to cause endogenous suppression in the DNA of cells recently isolated from the bone marrow of healthy animals, showing that it might not be a change related to insulin deficiency [44]. This toxicity is reversible, as the harmful effects that ALX exerts on erythropoietic cells are compensated after one week of treatment [56]. In addition, a fluctuation in cell population might occur. Here, there was no difference in the number of neutrophils and lymphocytes in the bone marrow of the ALX-treated group when compared to the CT group, as confirmed by flow cytometer analyses conducted in bone marrow samples from ALX-treated BALB/C mice [57].

While changes in bone marrow precursors are thought to be correlated to STZ toxicity, alterations in red blood cell parameters in the ALX-treated group are most likely linked to an early exposure to a hyperglycemic environment and, later, to the renal function failure caused by the ALX ability to promote kidney injury [58, 59]. Moreover, since the ALX-treated group presented higher glycemia, this might be associated to a higher oxidative stress induction and vascular complications found in diabetic patients [60].

Lymphocytes from spleen and pancreas, however, were little affected, with only a slight reduction in the population of B lymphocytes in the STZ-treated group, which have already been described as sensitive to the agent [7]. *In vitro* activation of CD4⁺ and CD8⁺ T lymphocytes isolated from the spleen did not show proliferation impairment in any of

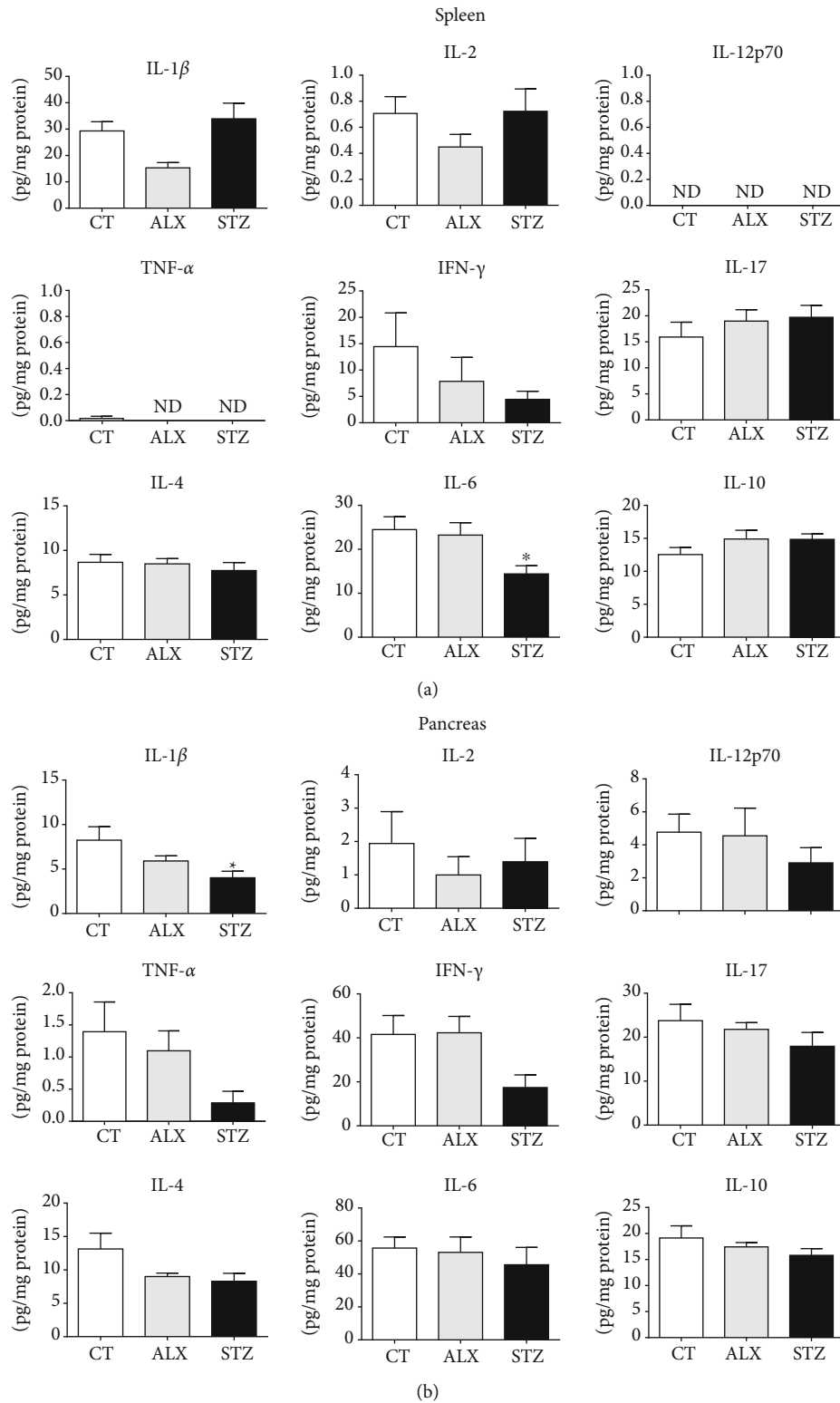


FIGURE 3: Short-term diabetogenic effects of ALX and STZ on the basal levels of cytokines in spleen and pancreas homogenates. T1D was induced as described in Methods, and (a) spleens and (b) pancreases were collected on the 15th day. Tissue homogenates from the CT, ALX-, and STZ-treated groups were evaluated for the presence of the cytokines IL-1 β , IL-2, IL-4, IL-6, IL-10, IL-12p70, IL-17, TNF- α , and IFN- γ . Data are presented as mean \pm SEM, * $p \leq 0.05$ (5-6 animals per group).

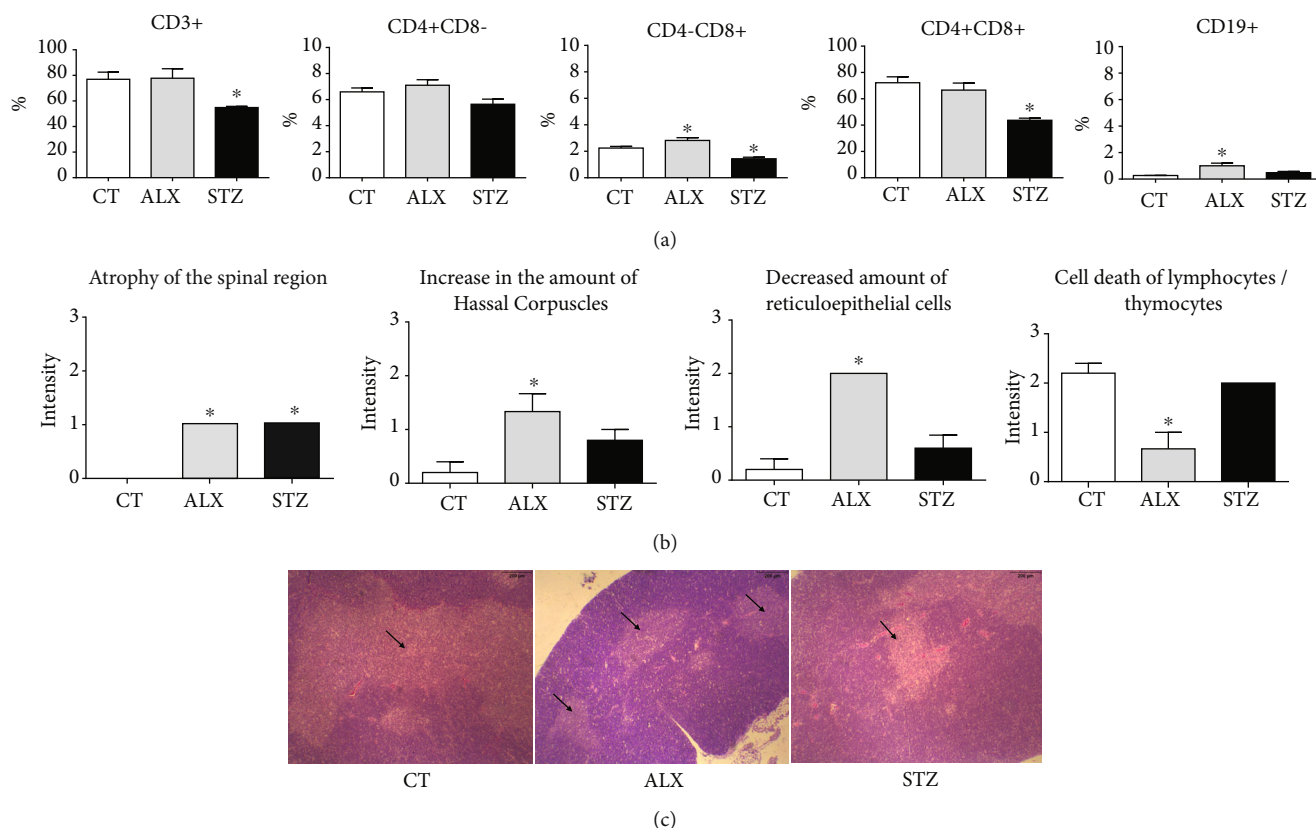


FIGURE 4: Short-term diabetogenic effects of ALX and STZ on the thymus. T1D was induced as described in Methods, and (a) thymuses from the CT, ALX, and STZ groups were collected on the 15th day and characterized according to the percentage of CD3⁺, CD4⁺CD8⁻, CD4⁻CD8⁺, CD4⁺CD8⁺, T lymphocytes, and CD19⁺ B lymphocytes. (b) Evaluation of structural changes in the thymus. (c) Representative microphotographs of 3 μ m sections of thymus tissue stained with H&E (scale 200 μ m). The arrows indicate atrophy of the spinal region in diabetic animals induced with ALX or STZ. Data are presented as mean \pm SEM, * $p \leq 0.05$ (6-13 animals per group).

the groups, suggesting low to no toxicity of the diabetogenic agents in secondary lymphoid organs. After immunization, however, *in vitro* activation of lymphocytes was shown to be more affected in animals induced with STZ. Similar results have been described by Itoh et al. [52], credited as an early deterioration in the immunological function [47], which later was shown to be a consequence of changes in the mitochondrial function that interfered with the metabolism of immune cells [61]. Lymphocyte proliferation impairment for animals treated with STZ was also described in other studies [9, 42, 43, 62], reinforcing the idea of STZ toxicity to lymphocytes.

Knowing that STZ might interfere with different immune cell populations and that lymphocytes present greater sensitivity to STZ, we showed a reduction in the total percentage of CD3⁺, CD8⁺, and double-positive CD4⁺CD8⁺ T lymphocytes in the thymus of the STZ group. These findings suggest that STZ impairs the development and maturation process of T lymphocytes. The double-positive stage precedes positive selection in the thymus that determines the differentiation either into CD4⁺ or CD8⁺ T cells through the continuous interaction between TCR and MHC/peptide complexes expressed by thymic epithelial cells [63]. Thus, it is possible that our findings are somehow related to the ability of the STZ to promote up or downregulation of MHC, as

previously identified by Klinkhammer et al. who found that STZ induced an increase in class II antigen expression in different tissues, presumably due to its alkylating potential, which influenced MHC gene methylation [64]. Although we have not evaluated the expression of MHC in cells from the different organs, it is reasonable to expect that the aforementioned findings are also occurring in our experimental system. Nevertheless, the changes found in the ALX-treated group seem to make more sense in the context of diabetes, since a hyperglycemic environment leads to an increase in proinflammatory cytokines, causing deleterious effects in the body, followed by an increase in CD8⁺ T cells [65], which might be correlated with a profuse expression of MHC class I observed in autoimmune diabetes [66]. Corollary, there may be an enhancement in the number of B lymphocytes in order to restrain the damage, as they are responsible for inducing T lymphocyte tolerance in the thymus.

Atrophy of the thymus after treatment with diabetogenic agents was found in other studies with ALX [41, 67] and STZ [44, 68], which can partially explain our results. In addition, other thymic alterations were observed in the ALX-treated group, involving the lymphocyte/thymocyte natural replacement process by the epithelial component [24]. Here, in the ALX-induced group, however, these changes were not

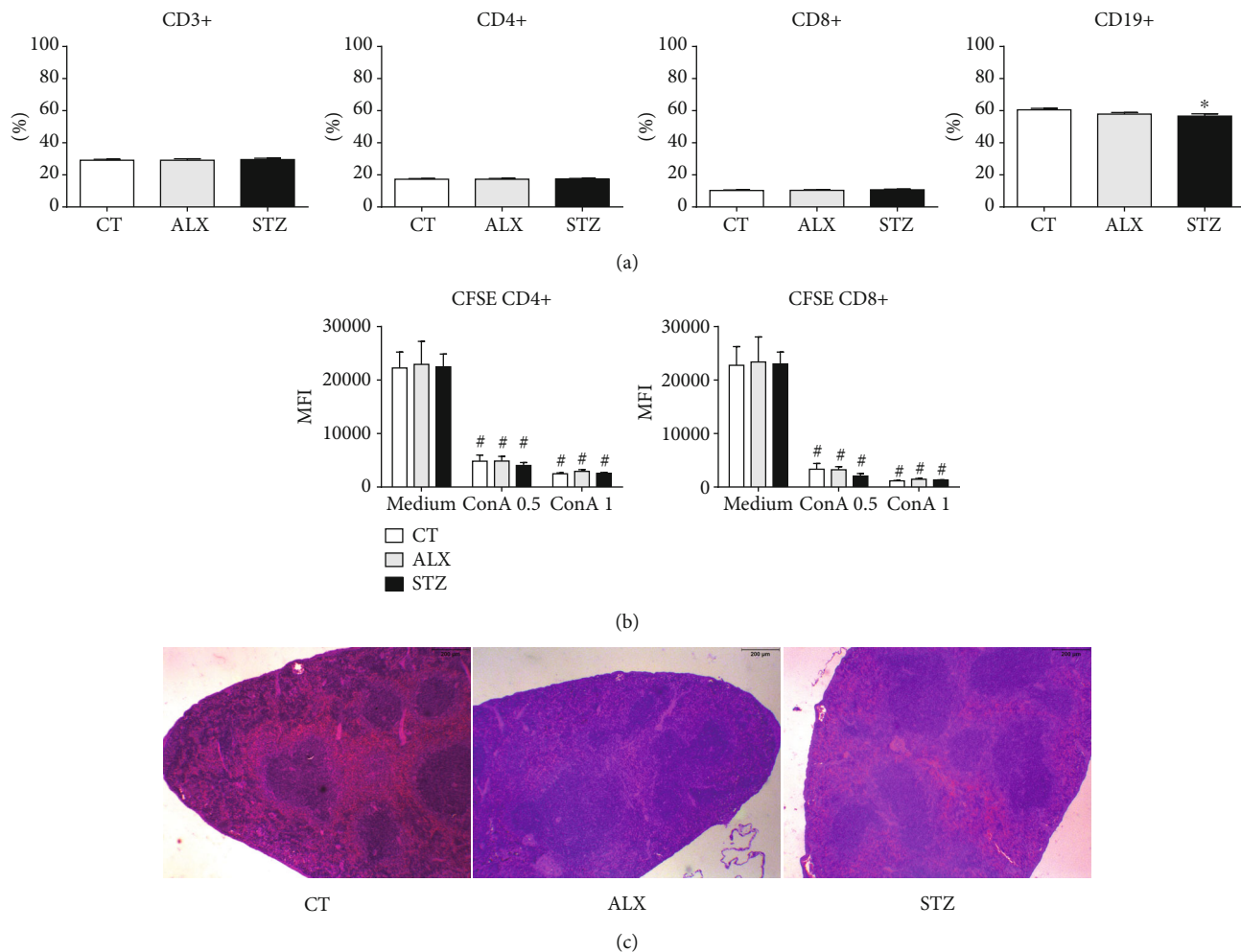


FIGURE 5: STZ has short-term diabetogenic impact on the population of B lymphocytes in the spleen. T1D was induced as described in Methods, and (a) spleens from the CT, ALX-, and STZ-treated groups were collected on the 15th day, and the total spleen cells were characterized according to the cell surface markers CD3, CD4, CD8, and CD19 by flow cytometry. (b) Spleen cells from each group were also stained with CFSE, incubated with medium, Con A (0.5 and 1 $\mu\text{g}/\text{mL}$ —final concentration), for 72 hours, and had T cell proliferation evaluated by flow cytometry. (c) Representative microphotographs of 3 μm sections of spleen tissue stained with H&E (scale 200 μm). Data are presented as mean \pm SEM, * $p \leq 0.05$, and # $p < 0.05$ versus respective control medium (6-13 animals per group).

found when performing proliferation assays using mature lymphocytes.

Therefore, hyperglycemia itself may not be completely responsible for the changes found in the STZ-induced group, contrary to the findings by Sinzato et al. [51], indicating that a direct toxic effect of the agent on the lymphocyte population might occur, as stated in other studies [7, 8]. According to Muller et al., STZ is an analog of the glucose molecule and, therefore, may eventually be captured by glucose transporters in lymphocytes [7]. It is important to highlight that STZ is an agent that can possibly react with the genetic material of cells [69] and may also interfere with lymphocyte precursor populations in the bone marrow.

A chronic low-grade inflammation profile is a common feature of the T1D state [37, 65], contributing to the side effects of the disease. In our hands, however, this low-grade inflammation was not detected, as none of the agents was able to interfere with normal physiological concentra-

tions of the cytokines evaluated in the spleen and pancreas, except for the decrease in the expression of IL-6 in the spleen and IL-1 β in the pancreas, both in the group treated with STZ. Considering that IL-6 has the ability to promote activation and expansion of T cells, as well as differentiation of B cells [70], and that almost all stromal cells and cells of the immune system produce IL-6 [71], it is reasonable to assume that the reduction in their physiological concentration derives from the indirect effects of STZ, since the major producers of this cytokine do not belong to the lymphoid cell lineage (the cell population involved in the STZ toxicity). As such, changes in the feedback between lymphocytes and this cytokine may lead to impaired innate and adaptive immunity in viral, parasitic, and bacterial infections [72]. In spite of this, the decrease in IL-1 β in the pancreas can be linked to intrinsic cellular defects of diabetic cells related to the induction of tolerance to stimulation [73] that somehow does not seem to be manifested in animals induced with

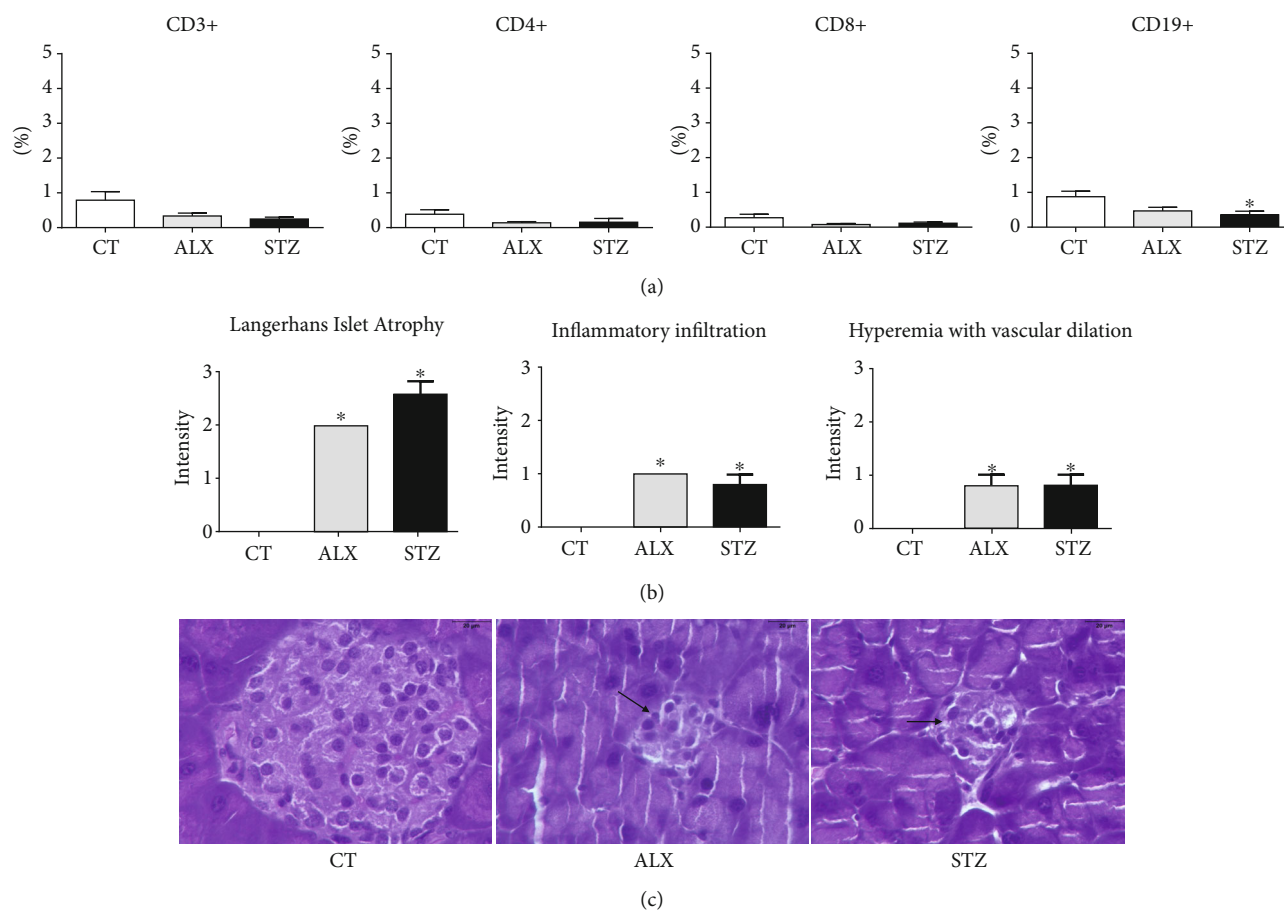


FIGURE 6: Short-term diabetogenic effects of ALX and STZ on the pancreas. T1D was induced as described in Methods, and (a) pancreases from the CT, ALX-, and STZ-treated groups were collected on the 15th day, and the pancreatic cells were characterized according to the cell surface markers CD3, CD4, CD8, and CD19 by flow cytometry. (b) Evaluation of structural changes in the pancreas. (c) Representative microphotographs of 3 μm sections of pancreas tissue stained with HE (scale 20 μm). The arrows indicate atrophy of the islets of Langerhans in diabetic animals induced with ALX or STZ. Data are presented as mean \pm SEM, * $p \leq 0.05$ (6-9 animals per group).

ALX, although it might not be derived from a direct effect of STZ, since this agent has its toxicity mainly associated with lymphocytes.

We have observed a similar polyclonal spleen cell proliferation in the CT, ALX-treated, and STZ-treated groups after 15 days from T1D induction. Rubinstein et al. described similar findings at a similar time point and also at 1 and 3 months after T1D induction with STZ in rats, although a decreased proliferation was observed after 6 months [74]. On the other hand, Liu et al. observed that spleen cells of STZ-diabetic rats could proliferate more or less than cells from control rats depending on the Con A concentration used in the assay [75]. We have tested only two Con A concentrations in our assay with no differences observed and no later time points were evaluated. Regarding ALX-induced T1D, we have not found any study with a similar experimental approach to compare our findings.

In animals immunized with OVA, we observed an increased paw edema induced by antigenic challenge in the STZ group. Even though our findings contrast with those by Ishibashi et al., who found an increased antigen-specific paw edema in STZ-induced diabetic mice [76], there are

many fundamental differences between their experimental protocol and ours: (I) Ishibashi et al. used sheep red blood cells (SRBCs) as an immunogen (a complex antigen with multiple epitopes), while we used OVA (a single protein with fewer epitopes); (II) immunization with SRBC was performed without adjuvant, while OVA immunization was done in the presence of squalene; (III) SRBC immunization was carried out after T1D induction with STZ, while OVA immunization was performed previous to STZ induction. Thus, a direct comparison between the two studies is not possible.

Regarding humoral responses in diabetic animals, the literature varies from impaired IgG responses following immunization [77, 78], to differences observed only after 6 months of T1D induction [74], to no differences [79]. Such findings differ from ours because we induced T1D after the immunization of the animals. Thus, once the antibody response is already established, the development of diabetes does not impact the production of IgG subclasses. Our results are in line with a previous case-control study that matched children with and without T1D, showing that no significant differences were observed in the antibody levels to

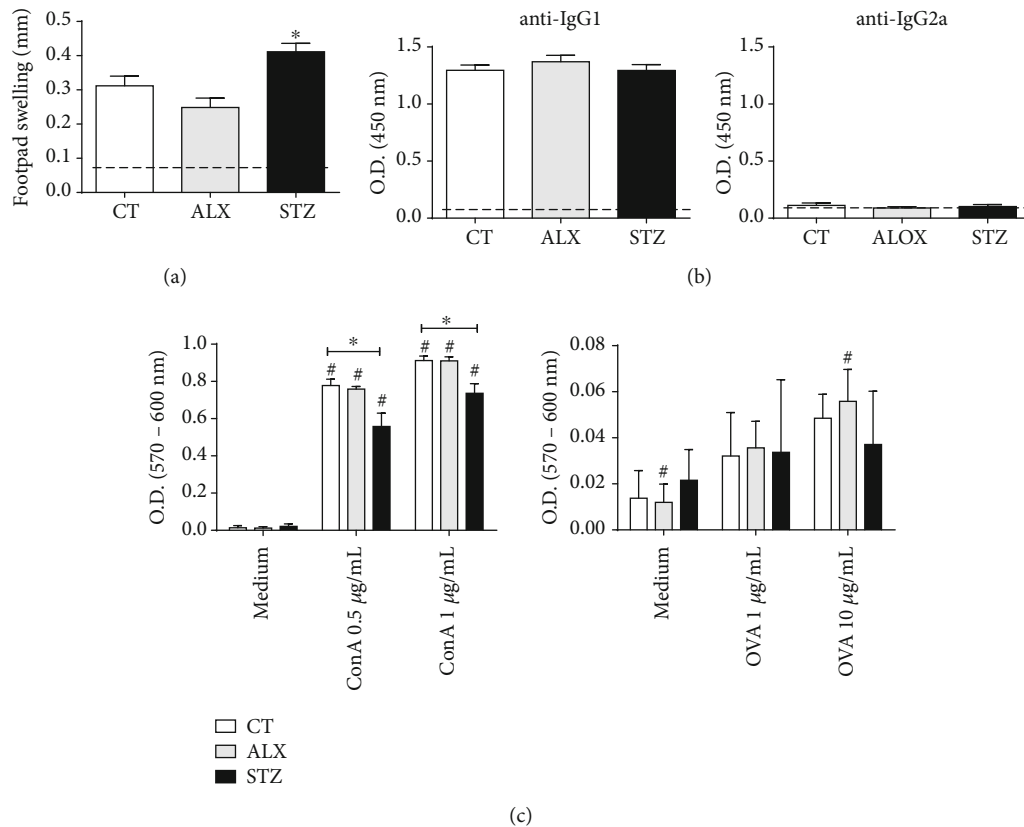


FIGURE 7: STZ short-term diabetogenic effects promote alterations in immune responses *in vitro* and *in vivo*. Mice were immunized with OVA, and 30 days later, T1D was induced as described in Methods. Fifteen days later, (a) antigen-specific paw edema was induced by footpad injection with OVA, (b) OVA-specific anti-IgG1 and anti-IgG2a were determined in the serum, and (c) *in vitro* spleen cell proliferation was performed by stimulation with medium, Con A (0.5 and 1 µg/mL—final concentration) and OVA (1 and 10 µg/mL—final concentration). Dashed line represents the mean of naïve mice not immunized with OVA. Data are presented as mean ± SEM, * $p < 0.05$ (3-6 animals per group).

pneumococcal serotypes, *Haemophilus influenzae*, as well as tetanus and diphtheria toxoids, that could be below the protective threshold between groups [80].

Choosing an appropriate animal model when planning a study is vital, as it is responsible for providing relevant and understandable scientific data. Although it is important to ensure the beneficial use of the model, there is not a perfect one yet and animals are not analogous to humans. Considering our study and the literature, animals induced with STZ would not be the best choice to study viral infections such as severe acute respiratory syndrome caused by coronavirus 2 (SARS-CoV-2). Here, where the model is only evaluated after T1D is established, it is not possible to conclude that the changes found were caused directly by the action of ALX or STZ or in response to T1D itself. Although it is clear that the immune response of animals induced with ALX or STZ is different after induction, further studies are needed to investigate the toxicity trigger of agents in immune cells during the development of T1D, to identify and separate direct effects of the agents and secondary effects of T1D. However, this does not compromise or diminish our findings, as it is necessary to consider that both groups of animals treated with ALX or STZ present a hyperglycemic environment in their conditions, which makes clear a greater

influence of the STZ agent on aspects of the immune response.

5. Conclusions

In summary, we observed that both diabetogenic agents, ALX and STZ, influenced the architecture of lymphoid and non-lymphoid organs, as well as the relative proportion of certain cell populations. Nevertheless, the changes in the immune response profile *in vivo* and *in vitro* were more intense in the animals treated with STZ and in the early phase of diabetes. In the animals induced with ALX, there was a natural ability to balance most of the alterations observed. This was not observed in the animals induced with STZ, probably due to the greater toxicity of STZ to lymphoid organs, which may be associated with reactions in the STZ methyl group with the genetic material of lymphoid precursors.

Data Availability

The data in this study are available upon reasonable request to the corresponding authors (Dr. Anderson Sá-Nunes, sanunes@usp.br or/and Joilson O. Martins, martinsj@usp.br).

Conflicts of Interest

The authors declare that the research was conducted in the absence of any commercial or financial relationships that could be construed as a potential conflict of interest.

Authors' Contributions

K.K.S.S., A.S.N., and J.O.M. conceived and designed the experiments. L.A.D.Q., J.B.A., J.P.T.G., E.S.A.S., A.C.M., and A.S.N. performed the experiments. L.A.D.Q., K.K.S.S., A.S.N., and J.O.M. analyzed the data. A.S.N. and J.O.M. contributed with reagents/materials/analysis tools. L.A.D.Q., K.K.S.S., A.S.N., and J.O.M. wrote the paper with the assistance of all the authors. Anderson Sá-Nunes and Joilson O. Martins contributed equally to this work.

Acknowledgments

The authors are supported by the Fundação de Amparo à Pesquisa do Estado de São Paulo (FAPESP: 2017/11540-7 and 2020/03175-0), Conselho Nacional de Desenvolvimento Científico e Tecnológico (CNPq: 301617/2016-3, 163410/2018-6, 310993/2020-2, 465678/2014-9, and 311204/2018-0), Núcleo de Pesquisa em Moléculas Bioativas de Artrópodes Vetores, Universidade de São Paulo (NAP-MOBIARVE/USP: 12.1.17661.1.7), and Coordenação de Aperfeiçoamento de Pessoal de Nível Superior (CAPES: Finance Code 001). The authors would like to thank Silene Migliorini, for the acquisition and organization of the reagents used in this project, and Priscila Yumi Sakagami, for her essential help with the critical reading and formatting of the manuscript.

References

- [1] C. D. Deshmukh and A. Jain, "Diabetes mellitus: a review," *International Journal of Pure & Applied Bioscience*, vol. 3, no. 3, pp. 224–230, 2015.
- [2] B. Deepthi, K. Sowjanya, B. Lidiya, R. S. Bhargavi, and O. S. Babu, "A modern review of diabetes mellitus: an annihilatory metabolic disorder," *Journal of In Silico & In Vitro Pharmacology*, vol. 3, no. 1, pp. 1–5, 2017.
- [3] J. P. T. Guimarães, L. R. Filgueiras, J. O. Martins, and S. Jancar, "Leukotriene involvement in the insulin receptor pathway and macrophage profiles in muscles from type 1 diabetic mice," *Mediators of Inflammation*, vol. 2019, Article ID 4596127, 8 pages, 2019.
- [4] A. J. King, "The use of animal models in diabetes research," *British Journal of Pharmacology*, vol. 166, no. 3, pp. 877–894, 2012.
- [5] S. Lenzen, "The mechanisms of alloxan-and streptozotocin-induced diabetes," *Diabetologia*, vol. 50, no. 6, pp. 537–546, 2008.
- [6] A. Mostafavinia, A. Amini, S. K. Ghorishi, R. Pouriran, and M. Bayat, "The effects of dosage and the routes of administrations of streptozotocin and alloxan on induction rate of type 1 diabetes mellitus and mortality rate in rats," *Laboratory Animal Research*, vol. 32, no. 3, pp. 160–165, 2016.
- [7] Y. D. Muller, D. Golshayan, D. Ehrchiou et al., "Immunosuppressive effects of streptozotocin-induced diabetes result in absolute lymphopenia and a relative increase of T regulatory cells," *Diabetes*, vol. 60, no. 9, pp. 2331–2340, 2011.
- [8] M. Sakowicz-burkiewicz, K. Kocbuch, M. Grden, A. Szutowicz, and T. Pawelczyk, "Diabetes-induced decrease of adenosine kinase expression impairs the proliferation potential of diabetic rat T lymphocytes," *Immunology*, vol. 117, no. 4, pp. 433–442, 2006.
- [9] G. N. Gaulton, J. L. Schwartz, and D. D. Eardley, "Assessment of the diabetogenic drugs alloxan and streptozotocin as models for the study of immune defects in diabetic mice," *Diabetologia*, vol. 28, no. 10, pp. 769–775, 1985.
- [10] R. A. H. Diab, M. Fares, M. Abedi-valuggerdi, M. Kumagai-braesch, J. Holgersson, and M. Hassan, "Immunotoxicological effects of streptozotocin and alloxan: in vitro and in vivo studies," *Immunology Letters*, vol. 163, no. 2, pp. 193–198, 2015.
- [11] M. Islam and Q. CODE, "Streptozotocin is more convenient than alloxan for the induction of Type 2 diabetes," *IJPR*, vol. 7, no. 1, 2017.
- [12] O. M. Ighodaro, A. M. Adeosun, and O. A. Akinloye, "Alloxan-induced diabetes, a common model for evaluating the glycemic-control potential of therapeutic compounds and plants extracts in experimental studies," *Medicina*, vol. 53, no. 6, pp. 365–374, 2017.
- [13] F. H. Tessaro, T. S. Ayala, E. L. Nolasco, L. M. Bella, and J. O. Martins, "Insulin influences LPS-Induced TNF- α and IL-6 release through distinct pathways in mouse macrophages from different compartments," *Cellular Physiology and Biochemistry*, vol. 42, no. 5, pp. 2093–2104, 2017.
- [14] Y. B. Jarrar, L. Al-Essa, A. Kilani, M. Hasan, and W. Al-Qerem, "Alterations in the gene expression of drug and arachidonic acid-metabolizing Cyp450 in the livers of controlled and uncontrolled insulin-dependent diabetic mice," *Diabetes, Metabolic Syndrome and Obesity: Targets and Therapy*, vol. 11, p. 483, 2018.
- [15] J. Gao, J. Song, M. Du, and X. Mao, "Bovine α -lactalbumin hydrolysates (α -LAH) ameliorate adipose insulin resistance and inflammation in high-fat diet-fed C57BL/6J mice," *Nutrients*, vol. 10, no. 2, p. 242, 2018.
- [16] T. Alquier and V. Poytout, "Considerations and guidelines for mouse metabolic phenotyping in diabetes research," *Diabetologia*, vol. 61, no. 3, pp. 526–538, 2018.
- [17] A. Rafacho, V. A. Giozzet, A. C. Boschero, and J. R. Bosqueiro, "Functional alterations in endocrine pancreas of rats with different degrees of dexamethasone-induced insulin resistance," *Pancreas*, vol. 36, no. 3, pp. 284–293, 2008.
- [18] J. Xue, W. Ding, and Y. Liu, "Anti-diabetic effects of emodin involved in the activation of PPAR γ on high-fat diet-fed and low dose of streptozotocin-induced diabetic mice," *Fitoterapia*, vol. 81, no. 3, pp. 173–177, 2010.
- [19] F. du, T. Zhao, H. C. Ji et al., "Dioxin-like (DL-) polychlorinated biphenyls induced immunotoxicity through apoptosis in mice splenocytes via the AhR mediated mitochondria dependent signaling pathways," *Food and Chemical Toxicology*, vol. 134, p. 110803, 2019.
- [20] R. C. Furze and S. M. Rankin, "The role of the bone marrow in neutrophil clearance under homeostatic conditions in the mouse," *The FASEB Journal*, vol. 22, no. 9, pp. 3111–3119, 2008.
- [21] A. P. Bolliger, "Cytologic evaluation of bone marrow in rats: indications, methods, and normal morphology," *Veterinary Clinical Pathology*, vol. 33, no. 2, pp. 58–67, 2004.

- [22] M. Yang, G. Büsche, A. Ganser, and Z. Li, "Morphology and quantitative composition of hematopoietic cells in murine bone marrow and spleen of healthy subjects," *Annals of Hematology*, vol. 92, no. 5, pp. 587–594, 2013.
- [23] R. Shah, F. Subhan, S. M. Sultan, G. Ali, I. Ullah, and S. Ullah, "Comparative evaluation of pancreatic histopathology of rats treated with olanzapine, risperidone and streptozocin," *Brazilian Journal of Pharmaceutical Sciences*, vol. 54, no. 3, 2018.
- [24] A. S. Elmore, "Enhanced histopathology of the thymus," *Toxicologic Pathology*, vol. 34, no. 5, pp. 656–665, 2006.
- [25] S. A. Elmore, "Enhanced histopathology of the spleen," *Toxicologic Pathology*, vol. 34, no. 5, pp. 648–655, 2006.
- [26] M. M. Koga, B. Bizzarro, A. Sá-Nunes, F. J. Rios, and S. Jancar, "Boosting adaptive immunity: a new role for PAFR antagonists," *Scientific Reports*, vol. 6, no. 1, pp. 1–9, 2016.
- [27] A. Sá-Nunes, A. I. Medeiros, R. Nicolete et al., "Efficacy of cell-free antigens in evaluating cell immunity and inducing protection in a murine model of histoplasmosis," *Microbes and Infection*, vol. 7, no. 4, pp. 584–592, 2005.
- [28] B. Bizzarro, M. S. Barros, C. Maciel et al., "Effects of *Aedes aegypti* salivary components on dendritic cell and lymphocyte biology," *Parasites & Vectors*, vol. 6, no. 1, pp. 1–13, 2013.
- [29] S. A. Ahmed, R. M. Gogal Jr., and J. E. Walsh, "A new rapid and simple non-radioactive assay to monitor and determine the proliferation of lymphocytes: an alternative to [3H] thymidine incorporation assay," *Journal of Immunological Methods*, vol. 170, no. 2, pp. 211–224, 1994.
- [30] B. J. Quah, H. S. Warren, and C. R. Parish, "Monitoring lymphocyte proliferation *in vitro* and *in vivo* with the intracellular fluorescent dye carboxyfluorescein diacetate succinimidyl ester," *Nature Protocols*, vol. 2, no. 9, pp. 2049–2056, 2007.
- [31] D. L. Ribeiro, S. F. G. Marques, S. Alberti et al., "Malignant lesions in the ventral prostate of alloxan-induced diabetic rats," *International Journal of Experimental Pathology*, vol. 89, no. 4, pp. 276–283, 2008.
- [32] Y. Kodama, K. Ozaki, T. Sano, T. Matsuura, H. Akagi, and I. Narama, "Induction of squamous cell carcinoma of forestomach in diabetic rats by single alloxan treatment," *Cancer Science*, vol. 97, no. 10, pp. 1023–1030, 2006.
- [33] T. Sano, K. Ozaki, Y. Kodama, T. Matsuura, and I. Narama, "Prevention of proliferative changes of forestomach mucosa by blood glucose control with insulin in alloxan-induced diabetic rats," *Cancer Science*, vol. 100, no. 4, pp. 595–600, 2009.
- [34] J. O. Martins, M. Ferracini, D. B. Anger et al., "Signaling pathways and mediators in LPS-induced lung inflammation in diabetic rats: role of insulin," *Shock*, vol. 33, no. 1, pp. 76–82, 2010.
- [35] K. K. Sunahara, F. P. Nunes, M. A. Baptista et al., "Insulin influences autophagy response distinctively in macrophages of different compartments," *Cellular Physiology and Biochemistry*, vol. 34, no. 6, pp. 2017–2026, 2014.
- [36] P. Pozzilli, R. Strollo, and I. Barchetta, "Natural history and immunopathogenesis of type 1 diabetes," *Endocrinología y Nutrición*, vol. 23, no. 2, pp. 115–124, 2009.
- [37] F. Song, W. Chen, W. Jia et al., "A natural sweetener, *Momordica grosvenori*, attenuates the imbalance of cellular immune functions in alloxan-induced diabetic mice," *Phytotherapy Research*, vol. 20, no. 7, pp. 552–560, 2006.
- [38] Q. Xiangyang, C. Weijun, L. Liegang, Y. Ping, and X. Bijun, "Effect of a *Siraitia grosvenori* extract containing mogrosides on the cellular immune system of type 1 diabetes mellitus mice," *Molecular Nutrition & Food Research*, vol. 50, no. 8, pp. 732–738, 2006.
- [39] Z. Luo, C. Soläng, M. Mejia-Cordova et al., "Kinetics of immune cell responses in the multiple low-dose streptozotocin mouse model of type 1 diabetes," *FASEB BioAdvances*, vol. 1, no. 9, pp. 538–549, 2019.
- [40] A. Muller, P. Schott-ohly, C. Dohle, and H. Gleichmann, "Differential regulation of Th1-type and Th2-type cytokine profiles in pancreatic islets of C57BL/6 and BALB/c mice by multiple low doses of streptozotocin," *Immunobiology*, vol. 205, no. 1, pp. 35–50, 2002.
- [41] P. R. Nagib, J. Gameiro, L. Guilherme Stivanin-Silva et al., "Thymic microenvironmental alterations in experimentally induced diabetes," *Immunobiology*, vol. 215, no. 12, pp. 971–979, 2010.
- [42] W. K. Nichols, J. B. Spellmann, and R. A. Daynes, "Immune responses of diabetic animals," *Diabetologia*, vol. 14, no. 5, pp. 343–349, 1978.
- [43] S. M. Jang, S. T. Yee, J. Choi et al., "Ursolic acid enhances the cellular immune system and pancreatic β -cell function in streptozotocin-induced diabetic mice fed a high-fat diet," *International Immunopharmacology*, vol. 9, no. 1, pp. 113–119, 2009.
- [44] S. R. Wellhausen, "Definition of streptozocin toxicity for primary lymphoid tissues," *Diabetes*, vol. 35, no. 12, pp. 1404–1411, 1986.
- [45] A. Ar'Rajab and B. Ahrén, "Long-term diabetogenic effect of streptozotocin in rats," *Pancreas*, vol. 8, no. 1, pp. 50–57, 1993.
- [46] B. Ahrén and G. Sundkvist, "Long-term effects of alloxan in mice," *International Journal of Pancreatology*, vol. 17, no. 2, pp. 197–201, 1995.
- [47] K. Chatamra, P. M. Daniel, M. D. Kendall, and D. K. C. Lam, "Atrophy of the thymus in rats rendered diabetic by streptozotocin," *Hormone and Metabolic Research*, vol. 17, no. 12, pp. 630–632, 1985.
- [48] B. Luo, W. F. N. Chan, S. J. Lord et al., "Diabetes induces rapid suppression of adaptive immunity followed by homeostatic T-cell proliferation," *Scandinavian Journal of Immunology*, vol. 65, no. 1, pp. 22–31, 2007.
- [49] K. Pavelić, M. Slijepčević, and J. Pavelić, "Recovery of immune system in diabetic mice after treatment with insulin," *Hormone and Metabolic Research*, vol. 10, no. 5, pp. 381–386, 1978.
- [50] A. A. Mic, F. A. Mic, C. A. Tatu, M. Ionac, V. L. Ordodi, and V. Paunescu, "Indomethacin inhibits thymic involution in mice with streptozotocin-induced diabetes," *Comparative Medicine*, vol. 57, no. 5, pp. 476–481, 2007.
- [51] Y. K. Sinzato, R. B. Gelaleti, G. T. Volpato, M. V. C. Rudge, E. Herrera, and D. C. Damasceno, "Streptozotocin-induced leukocyte DNA damage in rats," *Drug and Chemical Toxicology*, vol. 43, no. 2, pp. 165–168, 2020.
- [52] M. Itoh, M. Funachi, K. Sato et al., "Abnormal lymphocyte function precedes hyperglycaemia in mice treated with multiple low doses of streptozotocin," *Diabetologia*, vol. 27, no. S1, pp. 109–112, 1984.
- [53] N. Jafar, H. Edriss, and K. Nugent, "The effect of short-term hyperglycemia on the innate immune system," *The American Journal of the Medical Sciences*, vol. 351, no. 2, pp. 201–211, 2016.
- [54] W. Abu-Ashour, L. K. Twells, J. E. Valcour, and J. M. Gamble, "Diabetes and the occurrence of infection in primary care: a matched cohort study," *BMC Infectious Diseases*, vol. 18, no. 1, p. 67, 2018.

- [55] A. Hussain, B. Bhowmik, and N. C. do Vale Moreira, "COVID-19 and diabetes: knowledge in progress," *Diabetes Research and Clinical Practice*, vol. 162, p. 108142, 2020.
- [56] J. C. Baiardi, "Some effects of alloxan on hemopoiesis in the mouse," *American Journal of Physiology-Legacy Content*, vol. 183, no. 2, pp. 209–213, 1955.
- [57] S. S. Ferreira, M. A. Oliveira, M. Tsujita et al., "Insulin modulates the immune cell phenotype in pulmonary allergic inflammation and increases pulmonary resistance in diabetic mice," *Frontiers in Immunology*, vol. 11, 2020.
- [58] A. P. Evan, S. A. Mong, B. A. Connors, G. R. Aronoff, and F. C. Luft, "The effect of alloxan, and alloxan-induced diabetes on the kidney," *The Anatomical Record*, vol. 208, no. 1, pp. 33–47, 1984.
- [59] E. Costa, S. Rocha, P. Rocha-Pereira et al., "Changes in red blood cells membrane protein composition during hemodialysis procedure," *Renal Failure*, vol. 30, no. 10, pp. 971–975, 2008.
- [60] C. P. Domingueti, L. M. S'. A. Dusse, M. . G. Carvalho, L. P. de Sousa, K. B. Gomes, and A. P. Fernandes, "Diabetes mellitus: the linkage between oxidative stress, inflammation, hypercoagulability and vascular complications," *Journal of Diabetes and its Complications*, vol. 30, no. 4, pp. 738–745, 2016.
- [61] K. Anupam, J. Kaushal, N. Prabhakar, and A. Bhatnagar, "Effect of redox status of peripheral blood on immune signature of circulating regulatory and cytotoxic T cells in streptozotocin induced rodent model of type I diabetes," *Immunobiology*, vol. 223, no. 10, pp. 586–597, 2018.
- [62] K. Bettermann, K. Sinha, R. Kumari, C. Fox, and I. A. Simpson, "The peripheral immune response in hyperglycemic stroke," *Clinical Neurology and Neurosurgery*, vol. 195, p. 106061, 2020.
- [63] A. A. Freitas and B. Rocha, "Population biology of lymphocytes: the flight for survival," *Annual Review of Immunology*, vol. 18, no. 1, pp. 83–111, 2000.
- [64] C. Klinkhammer, C. Dohle, and H. Gleichmann, "T Cell-Dependent Class II Major Histocompatibility Complex Antigen Expression in *_vivo_* Induced by the Diabetogen Streptozotocin," *Immunobiology*, vol. 180, no. 1, pp. 1–11, 1989.
- [65] G. Badr, "Blocking type I interferon signaling rescues lymphocytes from oxidative stress, exhaustion, and apoptosis in a streptozotocin-induced mouse model of type I diabetes," *Oxidative Medicine and Cellular Longevity*, vol. 2013, Article ID 148725, 12 pages, 2013.
- [66] T. W. H. Kay, H. L. Chaplin, J. L. Parker, L. A. Stephens, and H. E. Thomas, "CD4⁺ and CD8⁺ T lymphocytes: clarification of their pathogenic roles in diabetes in the NOD mouse," *Research in Immunology*, vol. 148, no. 5, pp. 320–327, 1997.
- [67] E. O. Barreto, I. Riederer, A. C. S. Arantes et al., "Thymus involution in alloxan diabetes: analysis of mast cells," *Memórias do Instituto Oswaldo Cruz*, vol. 100, suppl 1, pp. 127–130, 2005.
- [68] D. Ozerkan, N. Ozsoy, and S. Cebesoy, "Response of thymus lymphocytes to streptozotocin-induced diabetes and exogenous vitamin C administration in rats," *Journal of Electron Microscopy*, vol. 63, no. 6, pp. 409–417, 2014.
- [69] A. D. Bolzán and M. S. Bianchi, "Genotoxicity of streptozotocin," *Mutation Research, Reviews in Mutation Research*, vol. 512, no. 2-3, pp. 121–134, 2002.
- [70] F. Eddahri, S. Denanglaire, F. Bureau et al., "Interleukin-6/STAT3 signaling regulates the ability of naive T cells to acquire B-cell help capacities," *Blood, The Journal of the American Society of Hematology*, vol. 113, no. 11, pp. 2426–2433, 2009.
- [71] M. Najjar, R. Rouas, G. Raicevic et al., "Mesenchymal stromal cells promote or suppress the proliferation of T lymphocytes from cord blood and peripheral blood: the importance of low cell ratio and role of interleukin-6," *Cytotherapy*, vol. 11, no. 5, pp. 570–583, 2009.
- [72] C. A. Hunter and S. A. Jones, "IL-6 as a keystone cytokine in health and disease," *Nature Immunology*, vol. 16, no. 5, pp. 448–457, 2015.
- [73] S. E. Geerlings and A. I. Hoepelman, "Immune dysfunction in patients with diabetes mellitus (DM)," *FEMS Immunology and Medical Microbiology*, vol. 26, no. 3-4, pp. 259–265, 1999.
- [74] R. Rubinstein, A. M. Genaro, A. Motta, G. Cremaschi, and M. R. Wald, "Impaired immune responses in streptozotocin-induced type I diabetes in mice. Involvement of high glucose," *Clinical and Experimental Immunology*, vol. 154, no. 2, pp. 235–246, 2008.
- [75] C. T. Liu, K. M. Chen, S. H. Lee, and L. J. Tsai, "Effect of supplemental L-arginine on the function of T lymphocytes and the formation of advanced glycosylated end products in rats with streptozotocin-induced diabetes," *Nutrition*, vol. 21, no. 5, pp. 615–623, 2005.
- [76] T. Ishibashi, Y. Kitahara, Y. Harada, S. Harada, M. Takamoto, and T. Ishibashi, "Immunologic features of mice with streptozotocin-induced diabetes: depression of their immune responses to sheep red blood cells," *Diabetes*, vol. 29, no. 7, pp. 516–523, 1980.
- [77] M. I. Yattoo, U. Dimri, A. Gopalakrishnan, A. Saxena, S. A. Wani, and K. Dhama, "In vitro and in vivo immunomodulatory potential of *Pedicularis longiflora* and *Allium carolinianum* in alloxan-induced diabetes in rats," *Biomedicine & Pharmacotherapy*, vol. 97, pp. 375–384, 2018.
- [78] B. L. Fletcher-McGruder and G. C. Gerritsen, "Deficient humoral antibody response of the spontaneously diabetic Chinese hamster," *Proceedings of the Society for Experimental Biology and Medicine*, vol. 175, no. 1, pp. 74–78, 1984.
- [79] R. E. Dolkart, B. Halpern, and J. Perlman, "Comparison of antibody responses in normal and alloxan diabetic mice," *Diabetes*, vol. 20, no. 3, pp. 162–167, 1971.
- [80] M. Eisenhut, A. Chesover, R. Misquith, N. Nathwani, and A. Walters, "Antibody responses to immunizations in children with type I diabetes mellitus: a case-control study," *Clinical and Vaccine Immunology*, vol. 23, no. 11, pp. 873–877, 2016.

Review Article

Gut Microbiota and Type 2 Diabetes Mellitus: Association, Mechanism, and Translational Applications

Lili Zhang,¹ Jinjin Chu,¹ Wenhao Hao,² Jiaojiao Zhang,¹ Haibo Li,¹ Chunjuan Yang,³ Jinghan Yang,³ Xiaohua Chen ,⁴ and Honggang Wang ⁵

¹Central Laboratory, Weifang People's Hospital, Weifang 261000, China

²Department of Scientific Research Management, Weifang People's Hospital, Weifang 261000, China

³Central Laboratory of the First Affiliated Hospital, Weifang Medical University, Weifang 261000, China

⁴Department of Nuclear Medicine, Weifang People's Hospital, Weifang 261000, China

⁵Clinical Laboratory, Weifang People's Hospital, Weifang 261000, China

Correspondence should be addressed to Xiaohua Chen; 2760370581@qq.com and Honggang Wang; wf661188@163.com

Received 14 April 2021; Accepted 26 July 2021; Published 17 August 2021

Academic Editor: Bingjie Gu

Copyright © 2021 Lili Zhang et al. This is an open access article distributed under the Creative Commons Attribution License, which permits unrestricted use, distribution, and reproduction in any medium, provided the original work is properly cited.

Gut microbiota has attracted widespread attention due to its crucial role in disease pathophysiology, including type 2 diabetes mellitus (T2DM). Metabolites and bacterial components of gut microbiota affect the initiation and progression of T2DM by regulating inflammation, immunity, and metabolism. Short-chain fatty acids, secondary bile acid, imidazole propionate, branched-chain amino acids, and lipopolysaccharide are the main molecules related to T2DM. Many studies have investigated the role of gut microbiota in T2DM, particularly those butyrate-producing bacteria. Increasing evidence has demonstrated that fecal microbiota transplantation and probiotic capsules are useful strategies in preventing diabetes. In this review, we aim to elucidate the complex association between gut microbiota and T2DM inflammation, metabolism, and immune disorders, the underlying mechanisms, and translational applications of gut microbiota. This review will provide novel insight into developing individualized therapy for T2DM patients based on gut microbiota immunometabolism.

1. Introduction

Diabetes mellitus (DM) is a group of chronic metabolic diseases characterized by hyperglycemia. There are two most common forms, namely, type 1 diabetes mellitus (T1DM) and type 2 diabetes mellitus (T2DM). T2DM accounts for about 90% of all diabetes cases, resulting from insulin resistance combined with impaired insulin secretion. DM can cause a variety of acute and chronic complications, such as blindness, amputation, heart disease, kidney failure, and premature death. According to the latest version of the diabetes map released by the International Diabetes Federation (IDF) in 2019, about 463 million adults worldwide suffer from diabetes, with an average growth rate of 51%. The number of diabetic patients will reach 700 million by 2045 with increasing economic burden for diabetes worldwide [1]. The pathogenesis of diabetes is complex and unclear. Accumulated evidence has implicated genetics,

infection, immune disorders, obesity, and diet are closely related to diabetes. Diet control, reasonable exercise, oral anti-diabetic drugs, and insulin injection are routine options for the prevention and treatment of diabetes. However, none of them can fundamentally prevent the development of diabetes and associated complications. During the last decade, the role of gut microbiome has drawn much attention across the world. Understanding the interplay of gut microbiome and diabetes would provide new insight into developing therapeutics for diabetes.

With the development of high-throughput sequence, research on gut microbiota breaks through the shackles of the traditional manner of living bacterium cultivation. The whole picture of gut microbiota is gradually revealed. Gut microbiota consists of more than 1000 bacterial species, mainly distributing in 9 phyla, most of which belong to the *Firmicutes*, *Bacteroidetes*, *Proteobacteria*, and *Actinobacteria* [2].

The main physiological functions of gut microbiota include the following: food digestion and absorption, enhanced host immune, biological antagonism, strengthened antitumor responses, and synthesized beneficial compounds [3, 4]. Once the gut microbiota is out of balance, a series of diseases would be induced, including metabolic diseases, cardiovascular and cerebrovascular diseases, autoimmune diseases, inflammatory bowel disease, psychotic disorders, and cancer [5].

A number of studies have demonstrated that gut microbiota plays an important role in T2DM. Gut microbiota participates in regulating glucose and insulin sensitivity. Symptoms of diabetic patients can be improved by modifying gut microbiota, which helps to reverse the impaired glucose tolerance and fasting glucose in prediabetes. This review will focus on elucidating the correlation between gut microbiota and T2DM, the pathogenesis of T2DM mediated by gut microbiota, and the therapeutic interventions based on gut microbiota.

2. Gut Microbiota of T2DM

The first study on gut microbiota of T2DM was reported in 2010 [6]. It has been found that the abundance of class *Clostridia* and phylum *Firmicutes* in T2DM patients considerably declined, while the level of class *Betaproteobacteria* was highly increased and positively associated with plasma glucose. Additionally, the ratios of *Bacteroidetes* to *Firmicutes* and *Bacteroides-Prevotella* to *C. coccoides-E. rectale* are positive correlation with plasma glucose, suggesting that T2DM is correlated with the intestinal microbiota composition. In 2012, a metagenome-wide association study (MGWAS) has revealed the characterization of gut microbiota in T2DM [7]. Herein, moderate gut microbial dysbiosis is applied to characterize the gut microbiota of T2DM patients. The abundance of butyrate-producing bacteria (*Clostridiales* sp. SS3/4, *Faecalibacterium prausnitzii*, *Roseburia intestinalis*, *Eubacterium rectale*, and *Roseburia inulinivorans*) is decreased, while the abundance of opportunistic pathogen bacteria (*Bacteroides caccae*, *Clostridium hathewayi*, *Clostridium symbiosum*, *Eggerthella*, *lenta Clostridium ramosum*, and *Escherichia coli*), mucin-degrading bacteria (*Akkermansia muciniphila*), and sulfate-reducing bacteria (*Desulfovibrio* sp. 3_1_syn3) is increased. A gut-microbiota-based T2DM classifier system can accurately classify T2D individuals, and the area under the receiver operating characteristic (ROC) curve is 0.81. Functional analysis has shown that glucose membrane transport, methane metabolism, heterogeneous biomass degradation, branched-chain amino acid transport and metabolism, and sulfate reduction pathways are enriched in patients with T2DM. Some functional genes related to flagella assembly, bacterial chemotaxis, butyrate biosynthesis, cofactors, and vitamin metabolism are decreased, while the activity of seven antioxidative stress-related enzymes is upregulated in T2DM [7]. A previous study has suggested that four intestinal *Lactobacillus* species increased in patients with diabetes, while the abundance of five *Clostridium* species decreased [8]. *Lactobacillus* is positively correlated with fasting blood glucose (FBG) and glycosylated hemoglobin (HbA1c), while *Clostridium* is negatively associated with HbA1c, FBG, C peptide, insulin, and plasma triglyceride and positively correlated with high-

density lipoprotein (HDL) and adiponectin [8]. The metagenomic-cluster-based T2DM identification model showed superior discriminatory power (AUC = 0.83), in which *Roseburia* and *Faecalibacterium prausnitzii* displayed highly discriminant for T2DM. Regarding the gut barrier function, signaling pathways regarding energy metabolism and absorption, glycerides, and fatty acid synthesis, cysteine and methionine metabolism are also activated [8]. Taken together, different cohort studies have shown inconsistent findings. It has also been found that the differences were mainly associated with metformin treatment, rather than diabetes itself. Excluding the biological interference of metformin, the reduction of *Roseburia* spp., *Subdoligranulum* spp., and *Clostridiales* spp. was significantly correlated with T2DM, and the trend of enriched *Lactobacillus* was reversed [9]. In addition, metformin treatment leads to higher abundance of *Escheria* and lower abundance of *Intestinibacter*, which can be explained by the adverse gastrointestinal reactions such as diarrhea, nausea, vomiting, and abdominal distension [9]. Further analysis based on gut microbial function showed that metformin treatment reduced the intestinal lipid absorption and LPS-induced inflammatory response and increased the production of butyrate and propionate [9]. In addition, many studies have further confirmed the importance of metformin in regulating gut microbiota [10, 11]. It is suggested that the study of the correlation between gut microbiota and diabetes has been proved as an alarm for the impact of antidiabetic agents on gut microbiota homeostasis with T2DM; therefore, any treatment on gut microbiota should be carefully applied.

During the past few years, researchers have investigated the role of gut microbiota in prediabetes patients or newly diagnosed without antidiabetic drugs, hoping to better explain the correlation between diabetes and gut microbiota. Allin et al. have found that the level of *Clostridium* and *Akkermansia muciniphila* decreased significantly, while the level of *Dorea*, *Ruminococcus*, *Sutterella*, and *Streptococcus* increased, implicating that abnormal changes in gut microbiota occurred in the period of prediabetes [12]. Another study performed in the Swedish population has demonstrated that compared with the normal glucose tolerance (NGT) group, the composition of intestinal flora in impaired glucose tolerance (IGT), impaired fasting glucose and glucose tolerance (CGT), and untreated diabetes (T2D) groups has significantly changed, but no significant change was observed in the impaired fasting glucose (IFG) group [13]. It could be concluded that gut microbiota plays an important role in leading to diabetes by regulating systemic insulin resistance. Besides, in cases of prediabetes and T2D patients, the abundance of several butyrate producers decreased, such as *Pseudoflavonifractor* spp., *Clostridium* spp., *Alistipes* spp., *Faecalibacterium* spp., and *Oscillibacter* spp. The AUC of this gut-microbiota-based T2DM classifier model was 0.7. Therefore, its prediction power in distinguishing individuals with T2DM from those with NGT was moderate. However, an improved model for distinguishing T2DM and CGI had better AUC (AUC = 0.78), implicating the gut-microbiota-based classifier system could accurately assess the blood glucose status. Moreover, the ability of certain gut microbiota producing butyrate was inhibited, while genes involved in the biosynthetic pathway of intestinal biotin were

significantly upregulated [13]. Accordingly, gut microbial dysbiosis plays a critical role in the pathogenesis of diabetes, which can change IGT rather than IFG.

In summary, the gut microbiota has been considered as a marker of metabolic diseases including T2DM [14]. Butyrate, metabolites of intestinal bacteria, can affect the insulin sensitivity. A decrease of butyrate has been proved to be positively correlated with diabetes [15]. Therefore, increasing the abundance of butyrate-producing bacteria or improving the butyrate synthesis ability of intestinal bacteria may be an effective method to prevent or treat diabetes.

3. Causality between Gut Microbiota and T2DM

Gut microbiota studies in large cohorts have emphasized the complex association between intestinal flora and T2DM. Animal studies from sterile mice have determined that gut microbiota is the vital cause of disease [16]. The sterile mice have lower insulin resistance and lower level of body fat than conventional mice. Subsequent gut microbiota transplantation tests have also confirmed that obesity and insulin resistance are significantly increased in sterile mice treated with ob/ob mice gut microbiota [17]. However, the results presented in sterile mice could not be used as a direct proof for human research due to the different genetic backgrounds [18]. A human study from 952 volunteers in the Netherlands finally knocked down the real hammer for the causal relationship between gut microbiota and T2DM [15]. Researchers have analyzed the whole genome and intestinal metagenome of subjects, measured fecal short-chain fatty acid (SCFA) levels, and counted clinical parameters. The causality between microbial characteristics and blood glucose characteristics was evaluated by bidirectional Mendelian Randomization (MR) analyses. It has been found that the increase of butyrate driven by host genetics was related to the improvement of insulin response after the oral glucose tolerance test. The abundance of *Eubacterium* and *Roseburia intestinalis* increased, and the abnormal level of production or absorption of propionate was related to the increased risk of T2DM. Accordingly, butyrate can promote postprandial insulin secretion and propionate generation in feces, which elevates the risk of T2DM. Nevertheless, more prospective cohort studies are warranted in different regions for deep exploration.

4. The Function of Gut Microbiota in T2DM Pathophysiology

Metabolites and components of gut microbiota affect the progress of various diseases primarily through distinct signaling pathways (Figure 1). It has been well documented that SCFAs, bile acid, branched-chain amino acids (BCAAs), imidazole propionate, and lipopolysaccharide (LPS) are important regulators in T2DM. We have discussed the detailed mechanism as follows.

4.1. SCFAs. SCFA is a metabolite produced by intestinal bacteria to metabolize dietary fiber, including acetate, propionate acid, and butyrate [19]. As one of the most extensively studied metabolites, SCFAs affect glucose metabolism and

insulin sensitivity by participating in a variety of pathways, thereby affecting the development of diabetes. Their core functions can be summarized as follows: (1) Stimulating the secretion of intestinal hormones: SCFAs can be used as energy-regulated signaling molecules, directly bound to the free fatty acid receptor (FFAR2 or FFAR3) on the surface of intestinal L cells, and stimulate the secretion of peptide YY (PYY) and glucagon-like peptide-1 (GLP-1) by colon L cells. These two intestinal hormones are responsible for delaying gastric emptying, inhibiting appetite, promoting insulin secretion, and reducing glucagon [20–23]. (2) Energy supply: SCFAs account for 5%–10% of total energy consumption in normal colon, especially butyrate [24]. (3) Increasing the intestinal gluconeogenesis: by acting in a cAMP-dependent mechanism, butyrate is able to promote the expression of intestinal gluconeogenesis-related genes. Besides, propionate is an important substrate of gluconeogenesis, which activates the intestinal gluconeogenesis-related genes through the intestinal-brain nerve circuit including FFAR3 regulating blood glucose and lipid metabolism [25]. (4) Maintaining the integrity of the intestinal barrier: the intestinal barrier in T2DM patients is damaged by proinflammatory components, including LPS resulting in insulin resistance [26, 27]. Butyrate enhances the integrity of intestinal barrier by increasing the expression of Claudin-1 mediated by the interaction between transcription factor SP1 and specific modification in the promoter region of binding protein Claudin-1, which leads to the redistribution of ZO-1 and Occludin on cell membrane [28]. Gut microbiota has been proved to operate host-secreted mucus glycoproteins as a source of nutrients under dietary fiber deficiency, and it can cause the degradation of colonic mucus barrier [29]. The addition of butyrate and propionate to human goblet-like LS174T cells can increase the expression of MUC2 mediated by acetylation/methylation of AP-1 and MUC2 promoter histones. MUC2 synthesis increases intestinal mucus thickness, ultimately leading to a decrease of intestinal permeability and protection of the integrity of intestinal barrier [30]. Moreover, acetate has been implicated as a good regulator in reducing mucosal permeability and enhancing intestinal barrier [31]. (5) Maintenance of intestinal anaerobic environment: butyrate activates peroxisome proliferator-activated receptor α (PPAR- α) in colon cells and drives the energy metabolism of colon cells to transform to β -oxidation. In addition, butyrate reduces the bioavailability of respiratory electron receptors of *Enterobacteriaceae* in the colon cavity and prevents the abnormal proliferation of opportunistic pathogen bacteria, *ca. Escherichia coli* and *Salmonella*, and maintains the intestinal microecological balance in T2DM patients [32]. (6) Enhanced immunity: patients with T2DM are associated with chronic low-grade inflammation [33, 34]. Symptoms of patients can be alleviated by inhibiting inflammation. Propionate can change the hematopoietic function of bone marrow in mice and increase the production of macrophages and dendritic cells [35]. Butyrate has an anti-inflammatory effect by promoting the production of regulatory T cells (Treg) and reducing inflammation [36–39].

4.2. Bile Acid. The primary bile acids are synthesized from cholesterol in the liver. Primary bile acids are secreted into

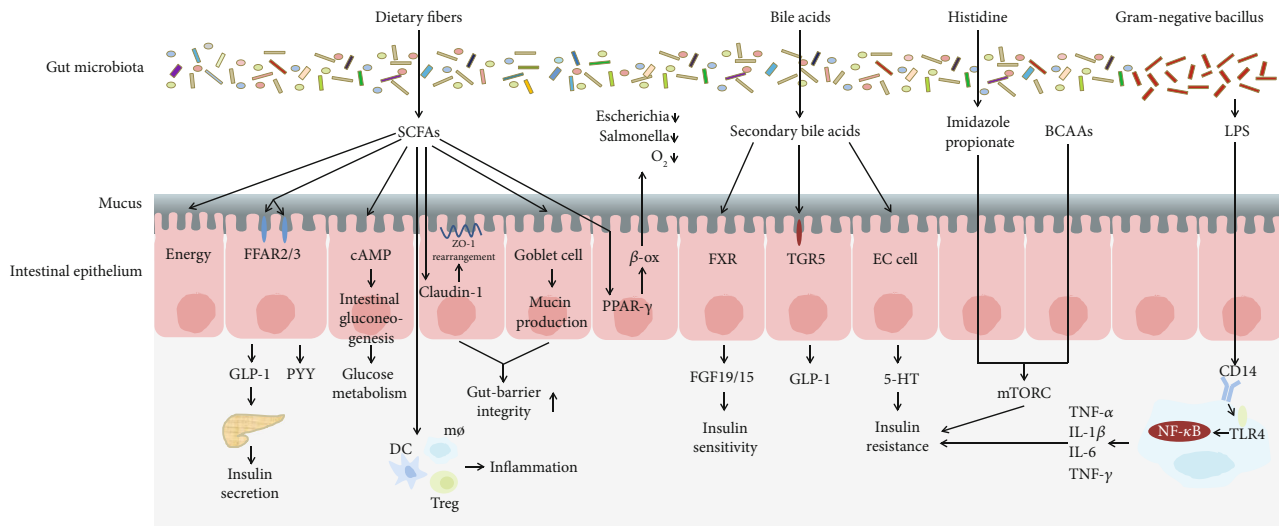


FIGURE 1: The main mechanisms between gut microbiota and T2DM. SCFAs mediate glucose homeostasis by energy supply for colonocytes, increasing intestinal hormone secretion and gluconeogenesis, decreasing gut permeability, maintaining intestinal anaerobic environment, and regulating host immune. Imidazole propionate and BCAAs can block insulin signaling and activate mTORC1 responsible for insulin resistance. Bile acids have effects on glucose metabolism by binding to FXR and TGR5 and stimulate the release of 5-hydroxy tryptamine in enterochromaffin cells to induce insulin resistance. LPS induces low-grade inflammation and insulin resistance by binding to TLR4.

the intestine and often converted into secondary bile acids by gut microbiota, affecting glucose metabolism and insulin sensitivity through different signaling pathways [40]. Secondary bile acid stimulates the farnesoid X receptor (FXR) and leads to the release of fibroblast growth factor 19/15 (FGF19/15). FGF19/15 acts as ligands to improve insulin sensitivity and glucose tolerance. Secondary bile acid can also activate the thiol guanosine receptor-5 (TGR-5) receptor, promote muscle energy consumption and the secretion of GLP-1 by intestinal L cells, and rescue insulin resistance and abnormal glucose metabolism [41, 42]. Gut microbiota can transform primary bile acids into secondary bile acids, regulate bile acid diversity, and decouple them through bile salt hydrolase, which is essential in bile acid synthesis, modification, and signal transduction. Abnormal bile acid metabolism mediated by gut microbiota will affect the role of bile acid in the regulation of glucose metabolism [43, 44]. Recent studies have shown that the metabolism of bile acid is abnormal in patients with gut microbial dysbiosis with increased secretion of secondary bile acids such as lithocholic acid and deoxycholic acid. Bile acid stimulates the release of 5-hydroxy tryptamine by enterochromaffin cells, resulting in reduced insulin release and enhanced glucagon secretion [45]. Furthermore, bile acid can also directly cause altered structure, function, and stability of intestinal flora [46].

4.3. *LPS*. A number of studies have shown that T2DM patients have a low degree of inflammation due to increased LPS in the peripheral circulation [47–49]. High levels of serum LPS are mainly produced by gram-negative bacteria, which increases the intestinal permeability and leads to elevated LPS in the peripheral circulation. LPS recognizes the receptor TLR4 with the help of CD14, which leads to macrophage aggregation and NF- κ B inflammatory signaling pathway activation, character-

ized by elevated production of inflammatory factors such as TNF- γ , IL-1 β , IL-6, and TNF- α . After that, abnormal phosphorylation of insulin receptor substrate and insulin resistance occur [50]. Furthermore, β cells are damaged followed by inhibited insulin secretion and downregulated expression of the Homeobox1 (PDX1) gene in the pancreas and duodenum [51, 52].

4.4. *BCAAs*. BCAAs mainly include leucine, isoleucine, and valine, which are essential amino acids for the human body. They cannot be synthesized by the host, must be obtained from diet, and are mainly produced by gut microbiota metabolism [53]. Elevated plasma level of BCAAs is a risk factor for T2DM [54–56]. Increased intake of BCAAs in diet promotes the development of T2DM and insulin resistance [57, 58]. The metagenome of gut microbiota in 277 nondiabetic and 75 diabetic patients has suggested that the functional genes of BCAA synthase and internal transport proteins were enriched in T2DM patients [59]. The main driving bacteria for the synthesis of BCAAs are *Prevotella copri* and *Bacteroides vulgatus*. Feces microbiota transplantation of *P. copri* in a mouse model can cause the insulin resistance, decrease glucose tolerance, and increase plasma BCAAs. The mechanism of insulin resistance induced by BCAA is found to be closely related to the mTOR signaling pathway. High expression of phosphorylated mTOR-Ser2448, phosphorylated S6K1^{Thr389}, and phosphorylated IRS1-Ser302 has been found in mice fed with BCAAs, which can block the normal conduction of insulin signaling and cause insulin resistance [60]. In addition, BCAAs can increase the oxidation of free fatty acids and activate phosphatidylinositol 3 kinase (PI3K). PI3K activation can further induce insulin resistance through AKT phosphorylation [61]. However, further research is needed in that the exact molecular mechanism remains unclear.

4.5. Imidazole Propionate. The study by Koh et al. has elaborated the new mechanism that imidazole propionate, a product of histidine metabolism in the intestinal flora, affected glucose metabolism through the mTORC1 signaling pathway [62]. It has been clarified that imidazole propionate directly exerts effects on p38 γ mitogen-activated protein kinase (MAPK), promotes p62 protein phosphorylation, and then induces mTORC1^{S2448} phosphorylation. The downstream S6K1 protein phosphorylation is further activated, which causes abnormal serine phosphorylation of insulin receptor substrate, IRS degradation, and insulin resistance. A recent multicenter cohort study has revealed that imidazole propionate increased in prediabetes and T2DM patients with *Bacteroides* 2 enterotype and low abundance of microbial genes. It is positively associated with the richness of *Clostridium baumannii*, *Clostridium parasymbiotics*, and *Ruminococcus gnavus* and negatively associated with anti-inflammatory bacteria [63]. Imidazole propionate was also positively correlated with systemic inflammation [63].

5. Therapies for T2DM Based on Gut Microbiota

In view of the important role of gut microbiota in T2DM pathophysiology, the prevention and treatment of diabetes by regulating intestinal flora is currently a research hotspot. Many studies have found that the characteristics of individual intestinal flora can affect the effect of traditional treatment.

5.1. Fecal Microbiota Transplantation. Fecal microbiota transplantation (FMT) is a useful treatment strategy for gastrointestinal diseases with ineffective antibiotic treatment, including ulcerative colitis, *Clostridium difficile* infection, and irritable bowel syndrome [64]. It is very effective in the treatment of *C. difficile* infection [65], and 60% of patients were cured within 1 month without serious adverse consequences [66]. In 2012, the first clinical trial of FMT in the treatment of metabolic syndrome was reported, in which nine patients with metabolic syndrome received fecal microbiota from healthy lean donors [66]. After six weeks of treatment, the insulin sensitivity was significantly improved, and the butyrate-producing bacteria increased [67]. Another larger study has demonstrated the beneficial effect of FMT in the treatment of metabolic syndrome [68]. The fecal microbiota transplantation from healthy donors to patients can effectively improve peripheral insulin resistance in the short term (6 weeks), with a decrease in HbA1c and an increase of plasma γ -aminobutyric acid (GABA) level. However, there was individual difference in patients' response to FMT. Patients with low baseline intestinal flora diversity showed a more significant effect, suggesting that the characteristics of patients' gut microbiota were crucial factors affecting the treatment. de Groot et al. have further demonstrated the effect of homologous FMT donors' own metabolic characteristics on FMT by using gastric bypass donor (RYGB-D) and metabolic syndrome donor (METS-D) [69]. The results showed that the insulin sensitivity of patients with metabolic syndrome after 2 weeks of transplantation of METS-D intestinal flora was significantly reduced, accompanied by the increase of lithocholic acid, deoxycholic acid, and

isolithocholic acid. However, the intestinal transit time of patients receiving RYGB-D intestinal flora was reduced, and the expression and plasma level of chemokine ligand 2 (CCL2) were increased, implicating that the donor should be carefully selected in the treatment of FMT.

5.2. Dietary Fiber. Change of food structure is the most basic auxiliary means for the treatment of diabetes, among which dietary fiber has attracted much attention due to its strong effect on improving T2DM [70, 71]. According to the *Chinese Diabetes Dietary Guidelines 2019*, T2DM patients should increase dietary fiber intake by 25-30 g/d, and whole grains and legume carbohydrates should account for 1/3 of the staple food. A large-scale long-term study from three forthcoming cohorts has found that the increasing amount of total whole-grain intake and commonly consumed whole-grain foods results in a decreased risk of type 2 diabetes, providing strong support for daily food recommendations of sufficient whole-grain consumption as a health-giving diet style to prevent type 2 diabetes [72]. Ma-pi diet is rich in complex carbohydrates, beans, fermented products, sea salt, and green tea, which can increase the diversity of gut microbiota, enrich short-chain fatty acid-producing bacteria and mucus-producing bacteria, such as *Faecalibacterium*, *Akkermansia*, *Lachnospira*, *Bacterioides*, and *Roseburia*, inhibit *Collinsella* and *Streptococcus* bacteria with proinflammatory effect, and reduce inflammation in T2DM [73, 74]. WTP diet is a high dietary fiber diet based on whole grain, supplemented by traditional Chinese medicine homologous food and probiotics [75]. The dietary fiber can enrich SCFA-producing bacteria, improve the level of intestinal SCFAs, prevent the growth of harmful bacteria, activate intestinal cells to secrete GLP-1, and increase insulin and HbA1c levels in patients. The abundance of SCFA-producing bacteria is higher with reduced HbA1c. It is worth noting that gut microbiota will also affect the response of individuals to dietary fiber. The analysis of gut microbiota between individuals with well or poor glucose metabolism after eating barley bread has revealed that *Prevotella* exists in most individuals who respond to barley bread compared with those without response to dietary intervention [76]. *Prevotella* is considered to be directly related to the effect of high fiber intake.

5.3. Probiotics. Probiotics, generally gram-positive bacteria, are defined as live microorganisms which confer health benefits on human health at an adequate level. According to current research, there are mainly three types of probiotics for diabetes: (1) common probiotics. These types of bacteria mainly from *Lactobacillus* and *Bifidobacterium* are widely used in food fermentation and have high safety in use [77, 78]. The intervention of probiotics in T2DM patients has been carried out in many clinical trials, but the results are inconsistent. Meta-analysis of multiple clinical trials showed that probiotics could effectively reduce FBG, fasting insulin, and HbA1c and improve the efficacy of HOMA-IR [79]. Another meta-analysis found that probiotics effectively reduced oxidative stress markers (TAS, TAS and MDA), and the benefits in reducing HbA1c were not clear, suggesting that probiotics mainly alleviated diabetes by improving oxidative stress rather

than glucose metabolism [80]. Sun et al. meta-analysis showed that multistrains combined with probiotic capsules were able to effectively reduce FBG and HbA1c in patients with T2DM, but the effect was not significant in patients with other risk factors [81]. The inconsistent results might be attributed to the use of strains, doses, intervention time, and single or multiple strains; thus, more clinical trials are needed to evaluate the role of conventional probiotics in preventing and improving T2DM [82]. (2) Novel probiotics. *A. muciniphila* has recently become the new candidate for probiotics to improve a variety of diseases [83–85]. The abundance of *A. muciniphila* in T2DM patients is significantly reduced [86]. Oral administration of *A. muciniphila* in mice can improve the secretion of GLP-1 in mouse colon cells [87], improve glucose tolerance [88], restore intestinal barrier, and reduce inflammation [89]. In addition, the application of *A. muciniphila* pasteurization agent and specific membrane proteins isolated from *A. muciniphila* in obese mice with diabetes significantly reduces the fat content in mice and improves insulin resistance and dyslipidemia [90]. Depommier et al. have reported *A. muciniphila* in obese patients with insulin resistance [91]. Supplementation of pasteurized *A. muciniphila* significantly improved insulin resistance and lipid metabolism but reduced liver damage and inflammation-related plasma markers. Another potential probiotic for T2DM is *Faecalibacterium prausnitzii*, an important butyrate-producing bacterium, which is negatively correlated with T2DM [13]. In db/db mice, its anti-inflammatory metabolite AMA restores the structure and function of the intestinal barrier by regulating the tight junction pathway and the expression of ZO-1 [92]. In addition, *F. prausnitzii* was significantly enriched in the treatment of diabetes through diet, fecal transplantation, drugs, and other measures (described below), which suggested that *F. prausnitzii* was very important in the treatment of T2DM. However, the application safety of this bacterium is still not clear due to a lack of effective human research. (3) Genetic engineering bacteria. The strain was genetically modified to produce biological factors for the disease. One example related to T2DM is the application of *Lactococcus lactis* as a carrier to produce GLP-1 [93]. Oral administration of the *Lactococcus lactis* can reduce blood glucose and increase insulin concentrations in rats. Nevertheless, there is still a long way to go for clinical applications of probiotics in T2DM in the future.

5.4. Exercise. Exercise is essential for improving insulin sensitivity, reducing blood glucose, and inhibiting inflammation [94, 95]. According to the *Guideline for prevention and treatment of type 2 diabetes in China*, adult patients with T2DM walk fast at least 150 min per week, play Taijiquan, cycling, table tennis, and golf, and exercise muscle strength and endurance by resistance exercise 2-3 times per week. The study of gut microbiota provides a new perspective to the mechanism by which exercise regulating diabetes. Exercise not only increases the diversity of gut microbiota but also increases the abundance of *A. muciniphila* in athletes' intestinal flora, which is negatively correlated with obesity and T2DM [96]. Accumulated studies have shown that the abundance of *Bacteroides* increased after exercise training, while the abundance of *Clostridium* genus and *Blautia* decreased

[97]. The change of gut microbiota has positive correlation with the absorption of glucose, implicating that exercise decreased the blood glucose level of diabetic patients through gut microbiota. Gut microbiota can regulate diabetes through the SCFA/FFAR/GLP-1 signaling pathway [98]. The antidiabetic efficacy of exercise is also affected by individual gut microbiota. Studies on drug-naive and overweight diabetic patients showed that the glucose homeostasis and insulin sensitivity regulated by exercise have significant relationship to the feature of gut microbiota and the ability to metabolize and ferment proteins and carbohydrates [99]. The gut microbiota of the responders who benefit from exercise has enhanced the ability to synthesize SCFAs, GABA, and decompose BCAAs, while the gut microbiota of the nonresponders has produced more harmful metabolites. The fecal microbiota transplantation in mice has confirmed that gut microbiota improved insulin resistance by exercise. The baseline gut microbiota characteristics of patients, such as the abundance of *Bacteroides* and concentration of GABA, can accurately predict the response to exercise intervention.

6. Gut Microbiota and Antidiabetic Drugs

6.1. Metformin. Since the inception of metformin in the mid-20th century, it has become the first choice for the treatment of T2DM, which can inhibit liver gluconeogenesis and improve insulin sensitivity. However, the specific mechanism of action of metformin is still under exploration. Numbers of studies have shown that the hypoglycemic mechanism of metformin may be mediated by gut microbiota. To the best of our knowledge, metformin affects glucose metabolism targeting gut microbiota in the following aspects: (1) Balancing the ecology of intestinal microorganism, improving the disorder of gut microbiota in T2DM patients, and making it closer to healthy individuals [9]. (2) Improving the synthesis ability of SCFAs, increasing the abundance of SCFA-producing bacteria, such as *Shewanella*, *Lactobacillus*, *Blautia*, *Bifidobacterium*, *Akkermansia*, *Prevotella*, *Megasphaera*, and *Butyrivibrio* species [9, 11, 100]. As mentioned above, SCFAs can improve insulin sensitivity and exert a hypoglycemic effect by increasing the secretion of GLP-1 and PYY. Studies have shown that metformin can indeed improve the plasma and intestinal GLP-1 levels in T2DM patients [101–103]. (3) Regulating the glucose metabolism through the bile acid pathway. Sun et al. elaborated that metformin played a hypoglycemic effect through intestinal *Bacteroides fragilis*-bile acid GUDCA-intestinal FXR metabolic axis [10]. Metformin inhibited the growth of *B. fragilis* by modifying the metabolism of folic acid and methionine, thereby reducing the activity of bile acid hydrolase BSH and increasing the level of GUDCA. As an endogenous competitive antagonist of intestinal FXR receptor, GUDCA inhibited the FXR signaling pathway. Inhibition of the intestinal FXR signaling pathway could increase the secretion of GPL-1 and regulate glucose metabolism [104]. (4) Increasing the abundance of probiotics. In the study of gut microbiota, the increase in the abundance of probiotics (such as *Lactobacillus* and *Bifidobacterium*) after metformin administration is common [8, 10, 100]. A recent study on mice showed that SGLT1 activated in the

TABLE 1: Baseline gut microbiota or bacterial metabolite characteristics of responders and nonresponders.

Treatment	Responders		Nonresponders		Predictors
	Increase	Decrease	Increase	Decrease	
Exercise	<i>Lanchospiraceae</i> <i>bacterium</i>	<i>Bacteroides xyloxylosum</i> <i>Alistipes shahii</i> <i>Prevotella copri</i> SCFAs BCAAs	<i>Alistipes shahii</i> Detrimental metabolites	<i>Alistipes putredinis</i> <i>Ruminococcus</i> <i>gnavus</i> GABA SCFAs	<i>Bacteroides xyloxylosum</i> <i>Bacteroides cellulosilyticus</i> GABA
	<i>Streptococcus mitis</i>				
	<i>Bacteroides</i>				
	SCFAs				
	GABA				
FMT	<i>Subdoligranulum</i> <i>variabile</i>	<i>Eubacterium ventriosum</i>	<i>Ruminococcus</i> <i>torques</i>		Low baseline diversity <i>Subdoligranulum</i> <i>variabile</i>
	<i>Dorea longicatena</i>	<i>Ruminococcus torques</i>			
Barley bread	<i>Prevotella</i> species		<i>Bacteroides</i> species		<i>Prevotella copri</i>
Drugs					
Metformin		Imidazole propionate	Imidazole propionate		Imidazole propionate
Acarbose	<i>Bacteroides</i>	LCA and DCA	<i>Prevotella</i>		<i>Bacteroides/Prevotella</i>
	UDCA	12- α OH/non-12 α OH BA			
	PBA/SBA ratio	ratio			

SCFAs: short-chain fatty acids; GABA: γ -aminobutyric acid; BCAAs: branched-chain amino acids; FMT: fecal microbiota transplantation; UDCA: ursodeoxycholic acid; PBA: primary bile acids; SBA: secondary bile acids; LCA: lithocholic acid; DCA: deoxycholic acid; BA: bile acid.

proximal intestine of mice through glucose induction could reduce glucose production. A high-fat diet reduced the expression of SGLT1 in the proximal ileum of mice and reduced the abundance of *Lactobacillus*. Metformin offsets these microbial changes and restores glucose sensing [105], but whether this phenomenon exists in humans needs further study. (5) Effected by imidazole propionate. As described above, imidazole propionate blocks insulin conduction through the mTORC1 signaling pathway and then induces diabetes. Recent studies showed that imidazole propionate also determines the hypoglycemic effect of metformin [106]. In T2DM patients who take metformin but still have high blood glucose, the concentration of imidazole propionate is higher. The mouse experiment confirmed that imidazole propionate destroyed the hypoglycemic effect of metformin. Further cytological experiments revealed that imidazole propionate inhibited metformin-induced adenosine 5'-monophosphate-activated protein kinase (AMPK) activation by inhibiting AMPK phosphorylation through the p38 γ /Akt pathway. The p38 γ kinase inhibitor could effectively block the inhibitory effect of imidazole propionate on metformin, which provided a new idea for the individualized treatment of diabetic patients. In addition, up to a third of patients who take metformin were reported to have gastrointestinal side effects, such as diarrhea, abdominal distension, and nausea. It has been demonstrated that metformin significantly increased the abundance of *Escherichia coli* and upregulated the corresponding virulence factors and gas metabolism genes [9, 11].

6.2. Acarbose. Acarbose is an α -glucosidase inhibitor, which reduces the digestion and absorption of carbohydrates in the small intestine, thereby reducing the postprandial blood glucose level. Acarbose completely acts in the intestine, which may partially affect the composition of distal gut microbiota. A previous study has shown that the gut micro-

biota of prediabetes who took acarbose changed significantly, where the abundance of *Lactobacillus*, *Faecalibacterium*, and *Dialister* was enriched [107]. Among them, *Dialister* was negatively correlated with HbA1c in prediabetes patients, indicating its potential role in glucose metabolism regulation [107]. Acarbose can also increase the abundance of *Bifidobacterium longum* and *Enterococcus faecalis* in patients with T2DM. *E. faecalis* were negatively correlated with LPS concentration, while *B. longum* was positively correlated with HDL cholesterol concentration [108]. The data from newly diagnosed T2DM patients showed that acarbose increased the abundance of probiotics *Lactobacillus* and *Bifidobacterium*, while the content of *Bacteroides* was significantly reduced. The metabolic spectrum of bile acid in plasma and feces has changed, suggesting that acarbose may affect the gut-mediated bile acid signal pathway and improve the glucose metabolism [109]. In addition, similar to metformin, the baseline characteristics of individual gut microbiota determine the therapeutic effect of acarbose. The metabolic parameters of patients with intestinal flora dominated by *Bacteroides*, including FBG, insulin, C-peptide levels, and insulin resistance, are improved more significantly compared with patients with intestinal flora dominated by *Prevotella* [109]. Accordingly, stratification of T2DM patients according to gut microbiota characteristics before treatment is useful for individualized treatment.

6.3. Traditional Chinese Medicine. Traditional Chinese medicine has shown some advantages in improving the life quality of T2DM patients by influencing insulin resistance [110, 111]. Therefore, the *Guideline for prevention and treatment of type 2 diabetes in China* takes traditional Chinese medicine as an adjuvant drug for T2DM treatment. Many components of traditional Chinese medicine do not enter the blood, but it has a clear effect. Increasing data has suggested that its efficacy may be mediated by gut microbiota [112]. Gegenqinlian

decoction can significantly enrich the abundance of *F. prausnitzii* in the intestinal tract of T2DM patients, which has significantly negative correlation with FBG, HbA1c, and postprandial 2 h blood glucose levels and has positive correlation with HOMA- β [113]. AMC, an herbal formula containing eight traditional Chinese medicines, can effectively alleviate hyperglycemia and hyperlipidemia in diabetic patients and alter the gut microbiota of T2DM patients [114]. They significantly increase the symbiotic bacteria utilized by *Blautia* spp., which is associated with lipid homeostasis and glucose. AMC shows superior effects in improving insulin resistance (HOMA-IR) and plasma triglycerides and plays a vital role in regulating gut microbiota, and only AMC increases the symbiotic bacteria using *Faecalibacterium* spp. It has been shown that berberine can effectively reduce the HbA1c of patients, and the effect of berberine in inhibiting the biotransformation of dicarboxylic acid is mediated by *Ruminococcus bromii* in T2DM [115].

7. Conclusion

Gut microbiota plays an important role in T2DM by exerting effects both in composition and function. A decrease of butyrate-producing bacteria, such as *Faecalibacterium* and *Roseburia*, and reduction of butyrate are common in T2DM, which may be the principal causes of T2DM. Several factors associated with gut microbiota have been elucidated in T2DM, including SCFAs, bile acids, LPS, BCAAs, and imidazole propionate. Gut microbiota can not only be used as a diagnostic biomarker but a potential therapeutic target for T2DM. Nevertheless, characteristics of individual gut microbiota have an important influence on different treatments, particularly the ratio of *Prevotella/Bacteroides*. As a result, the treated subjects can be divided into responders and nonresponders (Table 1). However, the exact core driving bacteria or flora is still unclear. Therefore, multicenter and comprehensive studies are warranted for further investigation. Additionally, the multiomics has been extensively applied for gut microbiota research, such as metagenomics, transcriptomics, proteomics, and metabolomics exploring the role of gut microbiota in T2DM. Elucidation of the precise role and mechanism of gut microbiota in T2DM will provide novel insight into developing individualized therapy for T2DM patients.

Data Availability

No data were used to support this study.

Conflicts of Interest

The authors declare that there is no conflict of interest regarding the publication of this paper.

Acknowledgments

We acknowledge funds from Shandong Natural Science Foundation (ZR2020KC001), Shandong Science and Technology Development Program (2016WS0657), and the Sci-

ence and Technology Development Program of Weifang (2020TX084). We thank very much Professor Lili Lu for her great help for revising the manuscript.

References

- [1] P. Saedi, I. Petersohn, P. Salpea et al., "Global and regional diabetes prevalence estimates for 2019 and projections for 2030 and 2045: Results from the International Diabetes Federation Diabetes Atlas, 9th edition," *Diabetes Research and Clinical Practice*, vol. 157, article 107843, 2019.
- [2] S. Schloissnig, M. Arumugam, S. Sunagawa et al., "Genomic variation landscape of the human gut microbiome," *Nature*, vol. 493, no. 7430, pp. 45–50, 2013.
- [3] S. M. Jandhyala, R. Talukdar, C. Subramanyam, H. Vuyyuru, M. Sasikala, and D. Nageshwar Reddy, "Role of the normal gut microbiota," *World Journal of Gastroenterology*, vol. 21, no. 29, pp. 8787–8803, 2015.
- [4] A. M. O'Hara and F. Shanahan, "The gut flora as a forgotten organ," *EMBO Reports*, vol. 7, no. 7, pp. 688–693, 2006.
- [5] A. M. Valdes, J. Walter, E. Segal, and T. D. Spector, "Role of the gut microbiota in nutrition and health," *BMJ*, vol. 361, article k2179, 2018.
- [6] N. Larsen, F. K. Vogensen, F. W. van den Berg et al., "Gut microbiota in human adults with type 2 diabetes differs from non-diabetic adults," *PLoS One*, vol. 5, no. 2, article e9085, 2010.
- [7] J. Qin, Y. Li, Z. Cai et al., "A metagenome-wide association study of gut microbiota in type 2 diabetes," *Nature*, vol. 490, no. 7418, pp. 55–60, 2012.
- [8] F. H. Karlsson, V. Tremaroli, I. Nookaew et al., "Gut metagenome in European women with normal, impaired and diabetic glucose control," *Nature*, vol. 498, no. 7452, pp. 99–103, 2013.
- [9] MetaHIT consortium, K. Forslund, F. Hildebrand et al., "Disentangling type 2 diabetes and metformin treatment signatures in the human gut microbiota," *Nature*, vol. 528, no. 7581, pp. 262–266, 2015.
- [10] L. Sun, C. Xie, G. Wang et al., "Gut microbiota and intestinal FXR mediate the clinical benefits of metformin," *Nature Medicine*, vol. 24, no. 12, pp. 1919–1929, 2018.
- [11] H. Wu, E. Esteve, V. Tremaroli et al., "Metformin alters the gut microbiome of individuals with treatment-naive type 2 diabetes, contributing to the therapeutic effects of the drug," *Nature Medicine*, vol. 23, no. 7, pp. 850–858, 2017.
- [12] the IMI-DIRECT consortium, K. H. Allin, V. Tremaroli et al., "Aberrant intestinal microbiota in individuals with prediabetes," *Diabetologia*, vol. 61, no. 4, pp. 810–820, 2018.
- [13] H. Wu, V. Tremaroli, C. Schmidt et al., "The Gut Microbiota in Prediabetes and Diabetes: A Population-Based Cross-Sectional Study," *Cell Metabolism*, vol. 32, no. 3, pp. 379–390.e3, 2020.
- [14] M. Gurung, Z. Li, H. You et al., "Role of gut microbiota in type 2 diabetes pathophysiology," *eBioMedicine*, vol. 51, article 102590, 2020.
- [15] S. Sanna, N. R. van Zuydam, A. Mahajan et al., "Causal relationships among the gut microbiome, short-chain fatty acids and metabolic diseases," *Nature Genetics*, vol. 51, no. 4, pp. 600–605, 2019.
- [16] F. Backhed, H. Ding, T. Wang et al., "The gut microbiota as an environmental factor that regulates fat storage,"

Proceedings of the National Academy of Sciences of the United States of America, vol. 101, no. 44, pp. 15718–15723, 2004.

- [17] P. J. Turnbaugh, R. E. Ley, M. A. Mahowald, V. Magrini, E. R. Mardis, and J. I. Gordon, “An obesity-associated gut microbiome with increased capacity for energy harvest,” *Nature*, vol. 444, no. 7122, pp. 1027–1031, 2006.
- [18] W. Z. Li, K. Stirling, J. J. Yang, and L. Zhang, “Gut microbiota and diabetes: from correlation to causality and mechanism,” *World Journal of Diabetes*, vol. 11, no. 7, pp. 293–308, 2020.
- [19] J. H. Cummings, E. W. Pomare, W. J. Branch, C. P. Naylor, and G. T. Macfarlane, “Short chain fatty acids in human large intestine, portal, hepatic and venous blood,” *Gut*, vol. 28, no. 10, pp. 1221–1227, 1987.
- [20] A. Psichas, M. L. Sleeth, K. G. Murphy et al., “The short chain fatty acid propionate stimulates GLP-1 and PYY secretion via free fatty acid receptor 2 in rodents,” *International Journal of Obesity*, vol. 39, no. 3, pp. 424–429, 2015.
- [21] I. Kaji, S. Karaki, and A. Kuwahara, “Short-chain fatty acid receptor and its contribution to glucagon-like peptide-1 release,” *Digestion*, vol. 89, no. 1, pp. 31–36, 2014.
- [22] G. Tolhurst, H. Heffron, Y. S. Lam et al., “Short-chain fatty acids stimulate glucagon-like peptide-1 secretion via the G-protein-coupled receptor FFAR2,” *Diabetes*, vol. 61, no. 2, pp. 364–371, 2012.
- [23] H. V. Lin, A. Frassetto, E. J. Kowalik Jr et al., “Butyrate and propionate protect against diet-induced obesity and regulate gut hormones via free fatty acid receptor 3-independent mechanisms,” *PLoS One*, vol. 7, no. 4, article e35240, 2012.
- [24] A. Koh, F. De Vadder, P. Kovatcheva-Datchary, and F. Backhed, “From dietary fiber to host physiology: short-chain fatty acids as key bacterial metabolites,” *Cell*, vol. 165, no. 6, pp. 1332–1345, 2016.
- [25] F. de Vadder, P. Kovatcheva-Datchary, D. Goncalves et al., “Microbiota-generated metabolites promote metabolic benefits via gut-brain neural circuits,” *Cell*, vol. 156, no. 1–2, pp. 84–96, 2014.
- [26] S. Sharma and P. Tripathi, “Gut microbiome and type 2 diabetes: where we are and where to go?,” *Journal of Nutritional Biochemistry*, vol. 63, pp. 101–108, 2019.
- [27] F. Horton, J. Wright, L. Smith, P. J. Hinton, and M. D. Robertson, “Increased intestinal permeability to oral chromium (51 Cr) -EDTA in human type 2 diabetes,” *Diabetic Medicine*, vol. 31, no. 5, pp. 559–563, 2014.
- [28] H. B. Wang, P. Y. Wang, X. Wang, Y. L. Wan, and Y. C. Liu, “Butyrate enhances intestinal epithelial barrier function via up-regulation of tight junction protein Claudin-1 transcription,” *Digestive Diseases and Sciences*, vol. 57, no. 12, pp. 3126–3135, 2012.
- [29] M. S. Desai, A. M. Seekatz, N. M. Koropatkin et al., “A dietary fiber-deprived gut microbiota degrades the colonic mucus barrier and enhances pathogen susceptibility,” *Cell*, vol. 167, no. 5, pp. 1339–1353.e21, 2016.
- [30] N. Burger-van Paassen, A. Vincent, P. J. Puiman et al., “The regulation of intestinal mucin MUC2 expression by short-chain fatty acids: implications for epithelial protection,” *Biochemical Journal*, vol. 420, no. 2, pp. 211–219, 2009.
- [31] T. Suzuki, S. Yoshida, and H. Hara, “Physiological concentrations of short-chain fatty acids immediately suppress colonic epithelial permeability,” *The British Journal of Nutrition*, vol. 100, no. 2, pp. 297–305, 2008.
- [32] M. X. Byndloss, E. E. Olsan, F. Rivera-Chávez et al., “Microbiota-activated PPAR- γ signaling inhibits dysbiotic Enterobacteriaceae expansion,” *Science*, vol. 357, no. 6351, pp. 570–575, 2017.
- [33] T. de las Heras Gala, C. Herder, F. Rutters et al., “Association of changes in inflammation with variation in glycaemia, insulin resistance and secretion based on the KORA study,” *Diabetes/Metabolism Research and Reviews*, vol. 34, no. 8, article e3063, 2018.
- [34] P. D. Cani, M. Osto, L. Geurts, and A. Everard, “Involvement of gut microbiota in the development of low-grade inflammation and type 2 diabetes associated with obesity,” *Gut Microbes*, vol. 3, no. 4, pp. 279–288, 2012.
- [35] A. Trompette, E. S. Gollwitzer, K. Yadava et al., “Gut microbiota metabolism of dietary fiber influences allergic airway disease and hematopoiesis,” *Nature Medicine*, vol. 20, no. 2, pp. 159–166, 2014.
- [36] D. Takahashi, N. Hoshina, Y. Kabumoto et al., “Microbiota-derived butyrate limits the autoimmune response by promoting the differentiation of follicular regulatory T cells,” *eBioMedicine*, vol. 58, article 102913, 2020.
- [37] N. Arpaia, C. Campbell, X. Fan et al., “Metabolites produced by commensal bacteria promote peripheral regulatory T-cell generation,” *Nature*, vol. 504, no. 7480, pp. 451–455, 2013.
- [38] P. M. Smith, M. R. Howitt, N. Panikov et al., “The microbial metabolites, short-chain fatty acids, regulate colonic Treg cell homeostasis,” *Science*, vol. 341, no. 6145, pp. 569–573, 2013.
- [39] Y. Furusawa, Y. Obata, S. Fukuda et al., “Commensal microbe-derived butyrate induces the differentiation of colonic regulatory T cells,” *Nature*, vol. 504, no. 7480, pp. 446–450, 2013.
- [40] S. Fiorucci and E. Distrutti, “Bile acid-activated receptors, intestinal microbiota, and the treatment of metabolic disorders,” *Trends in Molecular Medicine*, vol. 21, no. 11, pp. 702–714, 2015.
- [41] H. Shapiro, A. A. Kolodziejczyk, D. Halstuch, and E. Elinav, “Bile acids in glucose metabolism in health and disease,” *Journal of Experimental Medicine*, vol. 215, no. 2, pp. 383–396, 2018.
- [42] X. Zheng, T. Chen, R. Jiang et al., “Hyocholeic acid species improve glucose homeostasis through a distinct TGR5 and FXR signaling mechanism,” *Cell Metabolism*, vol. 33, no. 4, pp. 791–803.e7, 2021.
- [43] S. I. Sayin, A. Wahlström, J. Felin et al., “Gut Microbiota Regulates Bile Acid Metabolism by Reducing the Levels of Tauro-beta-muricholic Acid, a Naturally Occurring FXR Antagonist,” *Cell Metabolism*, vol. 17, no. 2, pp. 225–235, 2013.
- [44] J. R. Swann, E. J. Want, F. M. Geier et al., “Systemic gut microbial modulation of bile acid metabolism in host tissue compartments,” *Proceedings of the National Academy of Sciences*, vol. 108, Supplement_1, pp. 4523–4530, 2011.
- [45] A. M. Martin, J. M. Yabut, J. M. Choo et al., “The gut microbiome regulates host glucose homeostasis via peripheral serotonin,” *Proceedings of the National Academy of Sciences of the United States of America*, vol. 116, no. 40, pp. 19802–19804, 2019.
- [46] G. Kakiyama, W. M. Pandak, P. M. Gillevet et al., “Modulation of the fecal bile acid profile by gut microbiota in cirrhosis,” *Journal of Hepatology*, vol. 58, no. 5, pp. 949–955, 2013.

- [47] J. Gomes, J. A. Costa, and R. Alfenas, "Metabolic endotoxemia and diabetes mellitus: a systematic review," *Metabolism-Clinical and Experimental*, vol. 68, pp. 133–144, 2017.
- [48] B. Jayashree, Y. S. Bibin, D. Prabhu et al., "Increased circulatory levels of lipopolysaccharide (LPS) and zonulin signify novel biomarkers of proinflammation in patients with type 2 diabetes," *Molecular and Cellular Biochemistry*, vol. 388, no. 1–2, pp. 203–210, 2014.
- [49] P. J. Pussinen, A. S. Havulinna, M. Lehto, J. Sundvall, and V. Salomaa, "Endotoxemia is associated with an increased risk of incident diabetes," *Diabetes Care*, vol. 34, no. 2, pp. 392–397, 2011.
- [50] S. J. Creely, P. G. McTernan, C. M. Kusminski et al., "Lipopolysaccharide activates an innate immune system response in human adipose tissue in obesity and type 2 diabetes," *American Journal of Physiology. Endocrinology and Metabolism*, vol. 292, no. 3, pp. E740–E747, 2007.
- [51] D. Salamon, A. Sroka-Oleksiak, P. Kapusta et al., "Characteristics of gut microbiota in adult patients with type 1 and type 2 diabetes based on next-generation sequencing of the 16S rRNA gene fragment," *Polish Archives of Internal Medicine-Polskie Archiwum Medycyny Wewnetrznej*, vol. 128, no. 6, pp. 336–343, 2018.
- [52] L. Rodes, A. Khan, A. Paul et al., "Effect of probiotics Lactobacillus and Bifidobacterium on gut-derived lipopolysaccharides and inflammatory cytokines: an in vitro study using a human colonic microbiota model," *Journal of Microbiology and Biotechnology*, vol. 23, no. 4, pp. 518–526, 2013.
- [53] C. S. Katsanos, H. Kobayashi, M. Sheffield-Moore, A. Aarsland, and R. R. Wolfe, "A high proportion of leucine is required for optimal stimulation of the rate of muscle protein synthesis by essential amino acids in the elderly," *American Journal of Physiology. Endocrinology and Metabolism*, vol. 291, no. 2, pp. E381–E387, 2006.
- [54] P. Giesbertz and H. Daniel, "Branched-chain amino acids as biomarkers in diabetes," *Current Opinion in Clinical Nutrition and Metabolic Care*, vol. 19, no. 1, pp. 48–54, 2016.
- [55] T. Chen, Y. Ni, X. Ma et al., "Branched-chain and aromatic amino acid profiles and diabetes risk in Chinese populations," *Scientific Reports*, vol. 6, no. 1, article 20594, 2016.
- [56] T. J. Wang, M. G. Larson, R. S. Vasan et al., "Metabolite profiles and the risk of developing diabetes," *Nature Medicine*, vol. 17, no. 4, pp. 448–453, 2011.
- [57] G. Asghari, H. Farhadnejad, F. Teymoori, P. Mirmiran, M. Tohidi, and F. Azizi, "High dietary intake of branched-chain amino acids is associated with an increased risk of insulin resistance in adults," *Journal of Diabetes*, vol. 10, no. 5, pp. 357–364, 2018.
- [58] Y. Zheng, Y. Li, Q. Qi et al., "Cumulative consumption of branched-chain amino acids and incidence of type 2 diabetes," *International Journal of Epidemiology*, vol. 45, no. 5, pp. 1482–1492, 2016.
- [59] H. K. Pedersen, V. Gudmundsdottir, H. B. Nielsen et al., "Human gut microbes impact host serum metabolome and insulin sensitivity," *Nature*, vol. 535, no. 7612, pp. 376–381, 2016.
- [60] C. B. Newgard, J. An, J. R. Bain et al., "A branched-chain amino acid-related metabolic signature that differentiates obese and lean humans and contributes to insulin resistance," *Cell Metabolism*, vol. 9, no. 4, pp. 311–326, 2009.
- [61] T. Kawaguchi, N. Izumi, M. R. Charlton, and M. Sata, "Branched-chain amino acids as pharmacological nutrients in chronic liver disease," *Hepatology*, vol. 54, no. 3, pp. 1063–1070, 2011.
- [62] A. Koh, A. Molinaro, M. Ståhlman et al., "Microbially produced imidazole propionate impairs insulin signaling through mTORC1," *Cell*, vol. 175, no. 4, pp. 947–961.e17, 2018.
- [63] The MetaCardis Consortium, A. Molinaro, P. Bel Lassen et al., "Imidazole propionate is increased in diabetes and associated with dietary patterns and altered microbial ecology," *Nature Communications*, vol. 11, no. 1, article 5881, 2020.
- [64] H. Antushevich, "Fecal microbiota transplantation in disease therapy," *Clinica Chimica Acta*, vol. 503, pp. 90–98, 2020.
- [65] E. Gough, H. Shaikh, and A. R. Manges, "Systematic review of intestinal microbiota transplantation (fecal bacteriotherapy) for recurrent *Clostridium difficile* infection," *Clinical Infectious Diseases*, vol. 53, no. 10, pp. 994–1002, 2011.
- [66] B. Cui, Q. Feng, H. Wang et al., "Fecal microbiota transplantation through mid-gut for refractory Crohn's disease: safety, feasibility, and efficacy trial results," *Journal of Gastroenterology and Hepatology*, vol. 30, no. 1, pp. 51–58, 2015.
- [67] A. Vrieze, E. van Nood, F. Holleman et al., "Transfer of intestinal microbiota from lean donors increases insulin sensitivity in individuals with metabolic syndrome," *Gastroenterology*, vol. 143, no. 4, pp. 913–916.e7, 2012.
- [68] R. S. Koote, E. Levin, J. Salojärvi et al., "Improvement of insulin sensitivity after lean donor feces in metabolic syndrome is driven by baseline intestinal microbiota composition," *Cell Metabolism*, vol. 26, no. 4, pp. 611–619.e6, 2017.
- [69] P. de Groot, T. Scheithauer, G. J. Bakker et al., "Donor metabolic characteristics drive effects of faecal microbiota transplantation on recipient insulin sensitivity, energy expenditure and intestinal transit time," *Gut*, vol. 69, no. 3, pp. 502–512, 2020.
- [70] M. P. Mcrae, "Dietary Fiber Intake and Type 2 Diabetes Mellitus: An Umbrella Review of Meta-analyses," *Journal of Chiropractic Medicine*, vol. 17, no. 1, pp. 44–53, 2018.
- [71] L. Velázquez-López, A. V. Muñoz-Torres, C. García-Peña, M. López-Alarcón, S. Islas-Andrade, and J. Escobedo-de la Peña, "Fiber in diet is associated with improvement of glycated hemoglobin and lipid profile in Mexican patients with type 2 diabetes," *Journal of Diabetes Research*, vol. 2016, Article ID 2980406, 9 pages, 2016.
- [72] Y. Hu, M. Ding, L. Sampson et al., "Intake of whole grain foods and risk of type 2 diabetes: results from three prospective cohort studies," *BMJ*, vol. 370, p. m2206, 2020.
- [73] M. Candela, E. Biagi, M. Soverini et al., "Modulation of gut microbiota dysbioses in type 2 diabetic patients by macrobiotic Ma-Pi 2 diet," *The British Journal of Nutrition*, vol. 116, no. 1, pp. 80–93, 2016.
- [74] F. Fallucca, C. Porrata, S. Fallucca, and M. Pianesi, "Influence of diet on gut microbiota, inflammation and type 2 diabetes mellitus. First experience with macrobiotic Ma-Pi 2 diet," *Diabetes/metabolism research and reviews*, vol. 30, Supplement 1, pp. 48–54, 2014.
- [75] L. Zhao, F. Zhang, X. Ding et al., "Gut bacteria selectively promoted by dietary fibers alleviate type 2 diabetes," *Science*, vol. 359, no. 6380, pp. 1151–1156, 2018.
- [76] P. Kovatcheva-Datchary, A. Nilsson, R. Akrami et al., "Dietary Fiber-Induced Improvement in Glucose Metabolism Is

- Associated with Increased Abundance of *Prevotella*,” *Cell Metabolism*, vol. 22, no. 6, pp. 971–982, 2015.
- [77] R. George Kerry, J. K. Patra, S. Gouda, Y. Park, H. S. Shin, and G. Das, “Benefaction of probiotics for human health: a review,” *Journal of Food and Drug Analysis*, vol. 26, no. 3, pp. 927–939, 2018.
- [78] V. P. Singh, J. Sharma, S. Babu, Rizwanulla, and A. Singla, “Role of probiotics in health and disease: a review,” *Journal of the Pakistan Medical Association*, vol. 63, no. 2, pp. 253–257, 2013.
- [79] Y. W. Tao, Y. L. Gu, X. Q. Mao, L. Zhang, and Y. F. Pei, “Effects of probiotics on type II diabetes mellitus: a meta-analysis,” *Journal of Translational Medicine*, vol. 18, no. 1, p. 30, 2020.
- [80] E. Ardeshirlarijani, O. Tabatabaei-Malazy, S. Mohseni, M. Qorbani, B. Larijani, and R. Baradar Jalili, “Effect of probiotics supplementation on glucose and oxidative stress in type 2 diabetes mellitus: a meta-analysis of randomized trials,” *DARU-Journal of Pharmaceutical Sciences*, vol. 27, no. 2, pp. 827–837, 2019.
- [81] J. Sun and N. J. Buys, “Glucose- and glycaemic factor-lowering effects of probiotics on diabetes: a meta-analysis of randomised placebo-controlled trials,” *The British Journal of Nutrition*, vol. 115, no. 7, pp. 1167–1177, 2016.
- [82] Z. Sun, X. Sun, J. Li et al., “Using probiotics for type 2 diabetes mellitus intervention: advances, questions, and potential,” *Critical Reviews in Food Science and Nutrition*, vol. 60, no. 4, pp. 670–683, 2020.
- [83] D. Cheng and M. Z. Xie, “A review of a potential and promising probiotic candidate-*Akkermansia muciniphila*,” *Journal of Applied Microbiology*, vol. 130, no. 6, pp. 1813–1822, 2021.
- [84] Q. Zhai, S. Feng, N. Arjan, and W. Chen, “A next generation probiotic, *Akkermansia muciniphila*,” *Critical Reviews in Food Science and Nutrition*, vol. 59, no. 19, pp. 3227–3236, 2019.
- [85] E. Ansaldo, L. C. Slayden, K. L. Ching et al., “*Akkermansia muciniphila* induces intestinal adaptive immune responses during homeostasis,” *Science*, vol. 364, no. 6446, pp. 1179–1184, 2019.
- [86] M. C. Dao, A. Everard, J. Aron-Wisnewsky et al., “*Akkermansia muciniphila* and improved metabolic health during a dietary intervention in obesity: relationship with gut microbiome richness and ecology,” *Gut*, vol. 65, no. 3, pp. 426–436, 2016.
- [87] C. H. Hansen, L. Krych, D. S. Nielsen et al., “Early life treatment with vancomycin propagates *Akkermansia muciniphila* and reduces diabetes incidence in the NOD mouse,” *Diabetologia*, vol. 55, no. 8, pp. 2285–2294, 2012.
- [88] S. Zhao, W. Liu, J. Wang et al., “*Akkermansia muciniphila* improves metabolic profiles by reducing inflammation in chow diet-fed mice,” *Journal of Molecular Endocrinology*, vol. 58, no. 1, pp. 1–14, 2017.
- [89] A. Everard, C. Belzer, L. Geurts et al., “Cross-talk between *Akkermansia muciniphila* and intestinal epithelium controls diet-induced obesity,” *Proceedings of the National Academy of Sciences of the United States of America*, vol. 110, no. 22, pp. 9066–9071, 2013.
- [90] H. Plovier, A. Everard, C. Druart et al., “A purified membrane protein from *Akkermansia muciniphila* or the pasteurized bacterium improves metabolism in obese and diabetic mice,” *Nature Medicine*, vol. 23, no. 1, pp. 107–113, 2017.
- [91] C. Depommier, A. Everard, C. Druart et al., “Supplementation with *Akkermansia muciniphila* in overweight and obese human volunteers: a proof-of-concept exploratory study,” *Nature Medicine*, vol. 25, no. 7, pp. 1096–1103, 2019.
- [92] J. Xu, R. Liang, W. Zhang et al., “*Faecalibacterium prausnitzii*-derived microbial anti-inflammatory molecule regulates intestinal integrity in diabetes mellitus mice via modulating tight junction protein expression,” *Journal of Diabetes*, vol. 12, no. 3, pp. 224–236, 2020.
- [93] P. Agarwal, P. Khatri, B. Billack, W. K. Low, and J. Shao, “Oral delivery of glucagon like peptide-1 by a recombinant *Lactococcus lactis*,” *Pharmaceutical Research*, vol. 31, no. 12, pp. 3404–3414, 2014.
- [94] T. Teich, D. P. Zaharieva, and M. C. Riddell, “Advances in exercise, physical activity, and diabetes mellitus,” *Diabetes Technology & Therapeutics*, vol. 21, Supplement 1, pp. S-112–S-122, 2019.
- [95] D. W. Jenkins and A. Jenks, “Exercise and diabetes: a narrative review,” *Journal of foot surgery*, vol. 56, no. 5, pp. 968–974, 2017.
- [96] S. F. Clarke, E. F. Murphy, O. O’Sullivan et al., “Exercise and associated dietary extremes impact on gut microbial diversity,” *Gut*, vol. 63, no. 12, pp. 1913–1920, 2014.
- [97] K. K. Motiani, M. C. Collado, J. J. Eskelinen et al., “Exercise training modulates gut microbiota profile and improves endotoxemia,” *Medicine and Science in Sports and Exercise*, vol. 52, no. 1, pp. 94–104, 2020.
- [98] H. Hamasaki, “Exercise and glucagon-like peptide-1: does exercise potentiate the effect of treatment?,” *World Journal of Diabetes*, vol. 9, no. 8, pp. 138–140, 2018.
- [99] Y. Liu, Y. Wang, Y. Ni et al., “Gut microbiome fermentation determines the efficacy of exercise for diabetes prevention,” *Cell Metabolism*, vol. 31, no. 1, pp. 77–91.e5, 2020.
- [100] J. de la Cuesta-Zuluaga, N. T. Mueller, V. Corrales-Agudelo et al., “Metformin is associated with higher relative abundance of mucin-degrading *Akkermansia muciniphila* and several short-chain fatty acid-producing microbiota in the gut,” *Diabetes Care*, vol. 40, no. 1, pp. 54–62, 2017.
- [101] E. Mannucci, F. Tesi, G. Bardini et al., “Effects of metformin on glucagon-like peptide-1 levels in obese patients with and without type 2 diabetes,” *Diabetes, Nutrition & Metabolism*, vol. 17, no. 6, pp. 336–342, 2004.
- [102] W. C. Knowler, E. Barrett-Connor, S. E. Fowler et al., “Reduction in the incidence of type 2 diabetes with lifestyle intervention or metformin,” *The New England Journal of Medicine*, vol. 346, no. 6, pp. 393–403, 2002.
- [103] L. J. McCreight, C. J. Bailey, and E. R. Pearson, “Metformin and the gastrointestinal tract,” *Diabetologia*, vol. 59, no. 3, pp. 426–435, 2016.
- [104] M. S. Trabelsi, M. Daoudi, J. Prawitt et al., “Farnesoid X receptor inhibits glucagon-like peptide-1 production by enteroendocrine L cells,” *Nature Communications*, vol. 6, no. 1, p. 7629, 2015.
- [105] P. V. Bauer, F. A. Duca, T. Waise et al., “Metformin Alters Upper Small Intestinal Microbiota that Impact a Glucose-SGLT1-Sensing Glucoregulatory Pathway,” *Cell Metabolism*, vol. 27, no. 1, pp. 101–117.e5, 2018.
- [106] A. Koh, L. Mannerås-Holm, N. O. Yunn et al., “Microbial Imidazole Propionate Affects Responses to Metformin through p38 γ -Dependent Inhibitory AMPK Phosphorylation,” *Cell Metabolism*, vol. 32, no. 4, pp. 643–653.e4, 2020.

- [107] X. Zhang, Z. Fang, C. Zhang et al., “Effects of acarbose on the gut microbiota of prediabetic patients: a randomized, double-blind, controlled crossover trial,” *Diabetes Therapy*, vol. 8, no. 2, pp. 293–307, 2017.
- [108] B. Su, H. Liu, J. Li et al., “Acarbose treatment affects the serum levels of inflammatory cytokines and the gut content of bifidobacteria in Chinese patients with type 2 diabetes mellitus,” *Journal of Diabetes*, vol. 7, no. 5, pp. 729–739, 2015.
- [109] Y. Gu, X. Wang, J. Li et al., “Analyses of gut microbiota and plasma bile acids enable stratification of patients for antidiabetic treatment,” *Nature Communications*, vol. 8, no. 1, article 1785, 2017.
- [110] J. Wang, Q. Ma, Y. Li et al., “Research progress on traditional Chinese medicine syndromes of diabetes mellitus,” *Biomedicine & Pharmacotherapy*, vol. 121, article 109565, 2020.
- [111] J. Tian, D. Jin, Q. Bao et al., “Evidence and potential mechanisms of traditional Chinese medicine for the treatment of type 2 diabetes: a systematic review and meta-analysis,” *Diabetes Obesity & Metabolism*, vol. 21, no. 8, pp. 1801–1816, 2019.
- [112] Q. Nie, H. Chen, J. Hu, S. Fan, and S. Nie, “Dietary compounds and traditional Chinese medicine ameliorate type 2 diabetes by modulating gut microbiota,” *Critical Reviews in Food Science and Nutrition*, vol. 59, no. 6, pp. 848–863, 2019.
- [113] J. Xu, F. Lian, L. Zhao et al., “Structural modulation of gut microbiota during alleviation of type 2 diabetes with a Chinese herbal formula,” *ISME Journal*, vol. 9, no. 3, pp. 552–562, 2015.
- [114] X. Tong, J. Xu, F. Lian et al., “Structural alteration of gut microbiota during the amelioration of human type 2 diabetes with hyperlipidemia by metformin and a traditional Chinese herbal formula: a multicenter, randomized, open label clinical trial,” *mBio*, vol. 9, no. 3, 2018.
- [115] Y. Zhang, Y. Gu, H. Ren et al., “Gut microbiome-related effects of berberine and probiotics on type 2 diabetes (the PREMOTÉ study),” *Nature Communications*, vol. 11, no. 1, article 18414, p. 5015, 2020.

Research Article

Serum IgE Predicts Difference of Population and Allergens in Allergic Diseases: Data from Weifang City, China

Zhang Xu-De ¹, Guo Bei-Bei ¹, Wang Xi-Juan ¹, Li Hai-Bo ², Zhang Li-Li ²,
and Liu Feng-Xia ¹

¹Department of Allergy, The First Affiliated Hospital of Weifang Medical University/Weifang People's Hospital, Weifang, China

²Department of Central Laboratory, The First Affiliated Hospital of Weifang Medical University/Weifang People's Hospital, Weifang, China

Correspondence should be addressed to Liu Feng-Xia; wf_lfx@163.com

Received 31 December 2020; Revised 8 April 2021; Accepted 9 June 2021; Published 28 June 2021

Academic Editor: Ulrich Eisel

Copyright © 2021 Zhang Xu-De et al. This is an open access article distributed under the Creative Commons Attribution License, which permits unrestricted use, distribution, and reproduction in any medium, provided the original work is properly cited.

Background. Immunoglobulin E (IgE) is the most important promoter of allergic inflammation. However, there are few systematic studies on IgE in age range, genders, disease spectrum, and time regularity. **Aim.** To screen the common allergens, allergen spectrum, and IgE difference between type 2 inflammatory allergic diseases and other allergic diseases in Weifang, China. **Methods.** A retrospective study was performed by estimating patients' clinical data suffering from allergic diseases (urticaria, pollinosis, allergic rhinitis, atopic dermatitis, and bronchial asthma) between May 2019 and April 2020 using an allergen detection kit of Macro-Union Pharmaceutical. **Results.** 732 of the 1367 patients showed different antigen positive, and the positive rate was 53.5%. The most common allergens were dust mites, mixed fungi, Artemisia pollen, cat/dog dander, and cockroaches. There were 27.0% (369/1367) of the patients with single positive allergen-specific IgE (sIgE), 26.5% (363/1367) with multiple-positive IgE. The total immunoglobulin E (tIgE) levels varied with gender, age, and type of disease. There was a difference in the distribution of allergens between children and adults. A positive correlation between the serum-specific IgE and the corresponding local inhaled allergen density was observed. **Conclusions.** In this study, we found that type 2 inflammatory allergic diseases have higher serum IgE and a higher probability of inhaled sIgE positive. According to age, gender, and condition, serological IgE detection of allergens provides new insight into the early diagnosis and prevention of allergic diseases.

1. Introduction

IgE-mediated allergic diseases are usually multisymptomatic, including allergic rhinitis (AR), allergic asthma (AS), urticaria, atopic dermatitis (AD), and eczema, which have become significant public health issues. The pathogenesis remains largely unknown. Allergic inflammation induced by certain inhaled substances or food antigens in the environment has been implicated in IgE-mediated allergic diseases. Based on the biological mechanisms that underline these diseases, AR, atopic dermatitis, and AS are widely regarded as classic type 2 inflammatory (Th2-dominated response) with the increase of circulating IgE level-eosinophilic inflammation in the human body [1–4]. Long

sustained exposure to airborne allergens is known to result in persistent inflammation in AR and AS. Regarding urticaria, IgE-mediated mast cell activation, degranulation, and release of histamine and inflammatory mediators play critical roles in the pathogenesis of allergic diseases [5]. Many studies have suggested that IgE plays a crucial role in immune and inflammatory responses, which is a Th2 biomarker and participates in regulating Th2 inflammatory response.

The prevalence of allergic diseases has been raised due to increased environmental and industrial exposures in recent decades [6–8]. Environmental factors play an important role in the pathogenesis of AR and other respiratory and skin allergic diseases [9–11]. The prevalence of IgE-mediated allergic diseases increased progressively in the developed

countries, which currently account for 10% of children subject to food allergy [12], and 40% of the population with allergic rhinitis [13, 14]. There are over 330 million asthma patients worldwide [15], which accounts for 20% of children and 2-18% of adults among the AD population [16]. However, up to now, the high prevalence of allergic diseases in the population has not been effectively curbed, and people are still plagued by diseases, which indicates that the human understanding of the diagnosis and treatment of such diseases is still insufficient [17–19]. The increased global prevalence of allergic diseases is mainly attributed to environmental factors, suggesting that controlling environmental exposures may protect against allergic diseases in predisposed individuals. Therefore, it is of great significance to identify allergens for the prevention and treatment of allergic diseases. With industrialization development in China, allergic diseases have become a public health concern with increasing incidence. The prevalence of allergic disorders is closely related to various environmental allergens implicated in AR and asthma, including dust mite, mold, pollen, and animal fur [20, 21]. Although the prevalence and possible causes of AR/AS have been well documented in many developed countries, little information is available in China [22]. Because of the vast territory, different topographic, climatic, and economic conditions, and plant species, allergen spectrum is different from region to region in China. In view of this, we collect data of 1367 patients with allergic diseases, including AS, AR, AD/eczema, and urticaria. In this study, we aim to explore the allergen spectrum of Weifang city in China and investigate the association between allergic reaction and specific allergens, which will thus provide a rationale for the selecting allergens to be tested based on the clinical presentations.

2. Methods

2.1. Study Subjects. This retrospective study was approved by the Ethics Review Board of Weifang People’s Hospital, Weifang, China. A total of 79 nonatopic subjects and 1367 patients with AR, AS, AD, and urticaria, who received treatment at the Department of Allergy, Respiration and Pediatrics in Weifang People’s Hospital between May 2019 and April 2020, were enrolled in the study. Only the first test report was included if the same person met the diagnostic allergen detection multiple times within the same time range. Patients with ambiguous and suspicious diagnoses were excluded. There were 638 males and 729 females aged from 2 months to 87 years old. There were 266 infants aged 0-4 years, 341 school-age children (5-11 y) and adolescents (12-17 y), and 760 adults aged over 18 years. Four hundred four cases of urticaria, 345 cases of AD and eczema, 324 cases of AS and cough variant asthma (CVA), and 233 patients of AR (including pollinosis) were all included (Table 1).

2.2. Allergen-Specific IgE Antibody Detection. 2-4 ml fresh peripheral venous blood was collected and clotted at room temperature for 20 minutes, centrifuged at 3600 rpm for 4 minutes. The serum was separated and stored at 4°C for examination. The inhaled allergens and ingested allergens

TABLE 1: Number and percentage of allergic diseases among 1367 patients.

Diseases	Number (proportions)
Urticaria (acute/chronic)	404 (29.6%)
Allergic dermatitis/eczema	345 (25.2%)
Allergic asthma/CVA/chest tightness	324 (23.7%)
Allergic rhinitis/pollinosis	233 (17.0%)
Anaphylactic reaction without clear predisposing factors	16 (1.2%)
Papular urticaria	30 (2.2%)
Allergic conjunctivitis	7 (0.5%)
Others	22 (1.6%)

were tested using an allergen sIgE antibody detection kit (Beijing Macro-Union Pharmaceutical Co. Ltd., China). The allergen-specific IgE antibody detection kit was used to detect serum sIgE by chemiluminescent immunoassay, whose clinical usefulness was documented compared to other assays for specific IgE measurement [23]. A standard curve was established for quality control. Briefly, 96-well plates coated with allergen were put into the CLIA200 automatic operation platform. 50 μ l of the sample diluent was added into each well. 50 μ l of the sample was added to the mix. The coated plate was sealed with the sealing film and incubated in a 37°C constant temperature incubator for 45 minutes. After incubation, the vessel was diluted and released. The working solution shall not be less than 350 μ l for washing, which shall be left for 30 s and pat dry for five times in total. After washing the plate, we added 100 μ l enzyme conjugates to each well and passed the plate after incubation. After that, 50 μ l luminescent substrate A and substrate B were added into each well, respectively. The vessel was shaken at room temperature for 5 minutes, avoiding light. The luminescent intensity (RLU) of each pore was measured by chemiluminescent immunoassay (Yantai Addcare Bio-Tech Co. Ltd., China). The double logarithm fitting software was used for analysis.

2.3. Diagnosis of Allergic Diseases. In this study, we have defined different allergic diseases simply and effectively according to the international consensus of diagnostics so that researchers can screen them from thousands of medical records: AR: rhinorrhea, nasal obstruction, nasal itching, and sneezing with or without ocular symptoms [24]; AS: recurrent episodes of wheeze, cough, breathlessness, and chest tightness, which are usually associated with variable airflow obstruction and bronchial (airway) hyperresponsiveness [25]; AD: xerosis, pruritus, and erythematous lesions with increased transepidermal water loss [26]; urticaria: the sudden appearance of wheals and/or angioedema, those with a course of more than six weeks are defined as chronic urticaria (CU), or acute urticaria [27, 28]; eczema: clusters of punctate erythema and needle to miliary-sized papules and papules and herpes, dense patches, basal flush, mild swelling, diffuse boundary, dry skin, and severe itching [29]; papular urticaria: typical local or systemic red papules with constant itching; anaphylactic reaction: the severe allergic reaction that is rapid

in onset and may cause death including difficulty in breathing and chest tightness, laryngeal edema, and anaphylactic shock [30].

2.4. Statistical Analysis. SPSS version 19.0 software (SPSS Inc., Chicago, IL, USA) was used for data analysis. Positive rate (%) is the percentage of the positive serum test to various allergens. Different diseases are considered as categorical variables. The chi-square test evaluates the difference among variables. A two-tailed $p < 0.05$ is considered to be statistically significant.

3. Results

3.1. Age, Gender, and Serum tIgE in All Participants. 1367 patients and 79 nonatopic subjects were included in the study. The patients' mean age was 25.1 years (95% CI, 24.0 to 26.1 years). There were 267, 338, and 762 patients in the 0-4 (infancy), 5-17y, and adult groups. The tIgE of 934 patients (68.3%) exceeded 100 IU/ml. The mean value of tIgE was 225.4 IU/ml in males and 192.3 IU/ml in females. There was a significant difference in tIgE between groups regarding gender ($p < 0.001$) (Table 2).

The mean of tIgE in the 0-4 age group was 190.6 IU/ml (95% CI, 173.9 to 207.4 IU/ml). The mean value of tIgE in the 5-17 groups was 252.0 IU/ml (95% CI, 229.7 to 274.4 IU/ml). The mean value of tIgE in the adult groups was 194.1 IU/ml (95% CI, 182.4 to 205.8 IU/ml). The difference of tIgE was significant between the adolescent and adults ($p < 0.001$). Similar results were found between the infant group and the adolescent group ($p < 0.001$). There were 544 cases of hypersensitivity of the respiratory system. The average total IgE was 263.3 IU/ml. The tIgE of 828 patients only with cutaneous symptoms was 171.7 IU/ml. When we further refined the disease into AR, AS/cough/chest distress, acute/chronic urticaria, and eczema/AD (complications excluded), the average tIgE was decreased in turn, and the differences between groups were statistically significant (Figure 1).

3.2. Average Age Associated with Single Positive Allergen in Allergic Disease Patients. As shown in Table 3, the number of allergens of allergic disease patients was as follows: dust mite (394), mixed fungi (266), Artemisia pollen (173), Humulus scandens pollen (123), cockroach (109), dog dander (104), cat dander (89), ragweed pollen (77), milk (49), egg white (42), soybeans (40), tree pollen (poplar/willow/elm) (36), sea fish/crab (30), peanuts (23), and sea shrimp (19). As a result, it could be quickly concluded that dust mites, mixed fungi, Artemisia pollen, and Humulus pollen were the main allergens causing allergic diseases in Weifang, China.

The age of the allergic population varied with different allergens: egg: 7.5 years (95% CI, 4.3 to 10.7 years), milk: 7.7 years (95% CI, 4.7 to 10.7 years), peanut: 15.8 years (95% CI, 9.2 to 22.5 years), mixed fungi: 19.1 years (95% CI, 16.9 to 21.3 years), dust mite: 22.4 years (95% CI, 20.6 to 24.3 years), Artemisia pollen: 24.2 years (95% CI, 21.4 to 27.0 years), cat: 25.4 years (95% CI, 21.3 to 29.5 years), dog: 25.5 years (95% CI, 21.8 to 29.2 years), Humulus scandens: 27.7 years (95% CI, 24.4 to 30.9 years), tree pollen: 30.1 years

(95% CI, 24.3 to 35.9 years), soybean: 27.4 years (95% CI, 20.9 to 33.9 years), ragweed pollen: 27.5 years (95% CI, 23.1 to 31.9 years), and cockroach: 32.4 years (95% CI, 28.6 to 36.2 years) (Figure 2).

3.3. sIgE Level of Inhaled Allergens and Ingestible Allergens in Different Allergic Disease Patients. The level of inhaled sIgE was significantly different between the respiratory allergic disease and the allergic skin disease ($p < 0.001$). In contrast, no statistical differences of sIgE were found between groups of AR and AS, urticaria, and eczema. There was no significant difference of sIgE between the two groups of inhaled allergens and ingestible allergens. Moreover, patients with respiratory allergies had higher levels of sIgE than those with allergic dermatosis, and most patients with respiratory allergies were aeroallergens positive (Figures 3 and 4). There was no significant correlation between tIgE and sIgE in all allergic groups.

3.4. Time Regularity of Allergic Disease Positive with Specific Allergens. The median concentration of sIgE in patients positive with 15 specific allergens in different months of the year was analyzed. There was a peak in March, June, and November for dust mite and mixed fungi, respectively. Also, patients' sIgE level positive with dust mite peaked in August, while Artemisia and Humulus pollen had only one peak in September. The peak of poplar/willow/elm's sIgE appeared in June, while the annual dispersal of tree pollen occurred in May. Accordingly, as reported in the previous study, there was one month time postponement between the air concentration of tree pollen and the corresponding serum sIgE concentration of patients [31]. A positive correlation was found between annual total pollen quantity and median sIgE values (Figure 5). In contrast, the incidence of ingestible allergens, especially regarding peanuts, soybeans, and milk, was most common in March and July (Figure 6).

4. Discussion

More and more epidemiological studies have confirmed the objective existence of "atopic march"; consequently, the early prevention and prediction of allergic diseases have become a hot issue [32–35]. Numerous studies have confirmed that antigens can sensitize the body through the damaged epidermal layer, thereby initiating local and systemic immune responses, increasing the incidence of eczema, AR, and AS [36]. It has been proposed that the observed temporal relationship between atopic diseases may help earlier diagnosis and may facilitate novel approaches to prevent the disease [34, 37]. This study found that the primary manifestation of allergic infants and young children is AD caused by ingestible allergens. Allergic adolescents mainly have respiratory disorders. The sIgE of dust mites and various airborne pollen is gradually detected, which can change with age. Recently, Belgrave et al. concluded that the developmental profiles of eczema, wheeze, and rhinitis were heterogeneous, and only a tiny proportion of children (7% of those with symptoms) followed trajectory profiles resembling the atopic march [38]. Nevertheless, each region has its unique allergen

TABLE 2: Characteristics of all participants regarding age and tIgE.

	Nonatopic subjects			Patients		
	Male	Female	Total	Male	Female	Total
Patients, no. (%)	37 (46.8)	42 (53.2)	79 (100)	638 (46.7)	729 (53.3)	1367 (100)
Age range (year (minimum-maximum))	7-75	4-76	4-76	0.3-86	0.4-87	0.3-87
Mean age (y (95% CI))	41.7 (36.0-47.5)	36.6 (30.6-42.5)	38.2 (34.0-42.5)	20.0 (18.5-21.6)	29.2 (27.8-30.6)	25.1 (24.0-26.1)
Mean total IgE (IU/ml (95% CI))	64.6 (45.7-83.5)	63.4 (51.5-75.3)	64.0 (53.3-74.6)	225.4 (211.4-239.5)	192.3 (182.2-204.4)	207.8 (198.5-217.0)
Sensitization to respiratory allergens, no. (%)	0 (0)	2 (4.8)	2 (2.5)	341 (53.4)	323 (44.3) ^a	664 (48.6)
Sensitization to ingestible allergens	0 (0)	0 (0)	0 (0)	89 (13.9)	63 (8.6) ^b	152 (11.1)

Chi-square test: ^a $p = 0.001$; ^b $p = 0.002$.

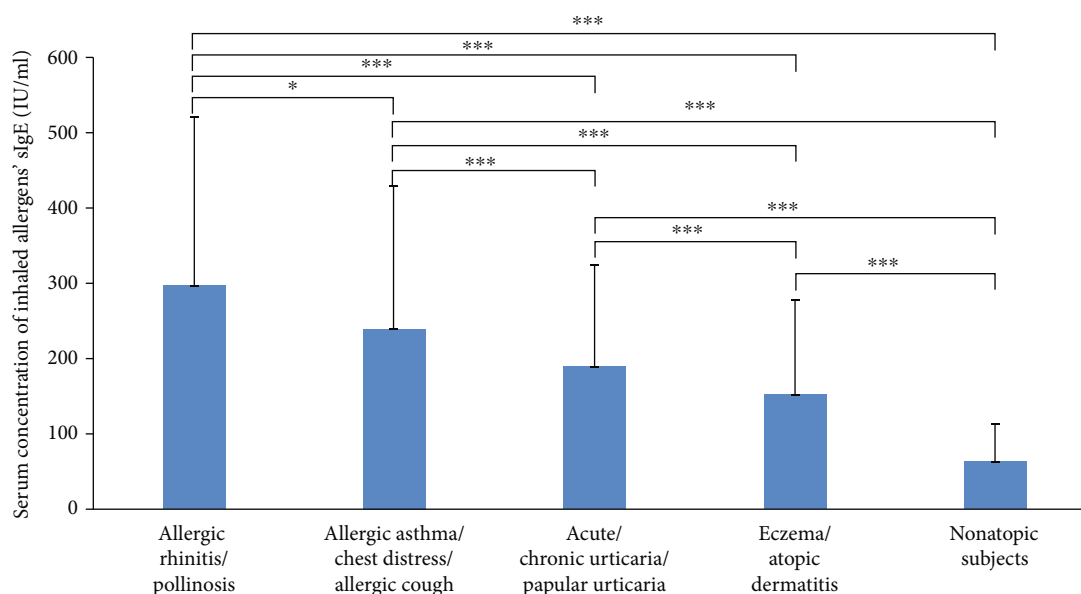


FIGURE 1: Mean value of total IgE in different diseases (** $p = 0.024$, *** $p < 0.001$).

TABLE 3: Number of allergen-positive patients with the relevant allergic diseases.

	Ar	Mite	Dog	Cat	Cr	Ra	Hu	Fungi	Tree	Egg	Milk	Peanut	Soy	Shrimp	Fish
*Allergic rhinitis/pollinosis	48	117	22	19	13	22	33	58	6	0	5	1	7	1	1
*Allergic asthma/allergic cough/chest tightness	61	130	30	23	28	22	33	95	10	8	7	6	5	1	3
*Acute/chronic urticaria, papular urticaria	26	83	25	23	33	20	26	54	14	15	19	11	14	6	9
*Eczema/allergic dermatitis	30	60	26	24	33	10	25	59	5	19	18	4	12	11	16
Anaphylactic	8	4	1	0	2	3	6	0	1	0	0	1	2	0	1

Cr: cockroach; Hu: Humulus scandens; Ra: ragweed pollen. *Jonckheere-Terpstra test: $p = 0.229$.

spectrum due to differences in heredity, diet, and lifestyle. Zhang and Zhang [39] reviewed the sensitization pattern to inhalant allergens among AR patients in the mainland of China. They found that the prevalence and type of aeroallergens were different in diverse cities and regions. This study investigates the disease spectrum of allergic diseases accord-

ing to the other areas and allergens by pooling data from 1367 patients with allergic diseases.

Although previous studies have shown the association of serum tIgE and sIgE levels with allergic diseases, few studies address this association in general. We have found that the mean tIgE in males was higher than that in females

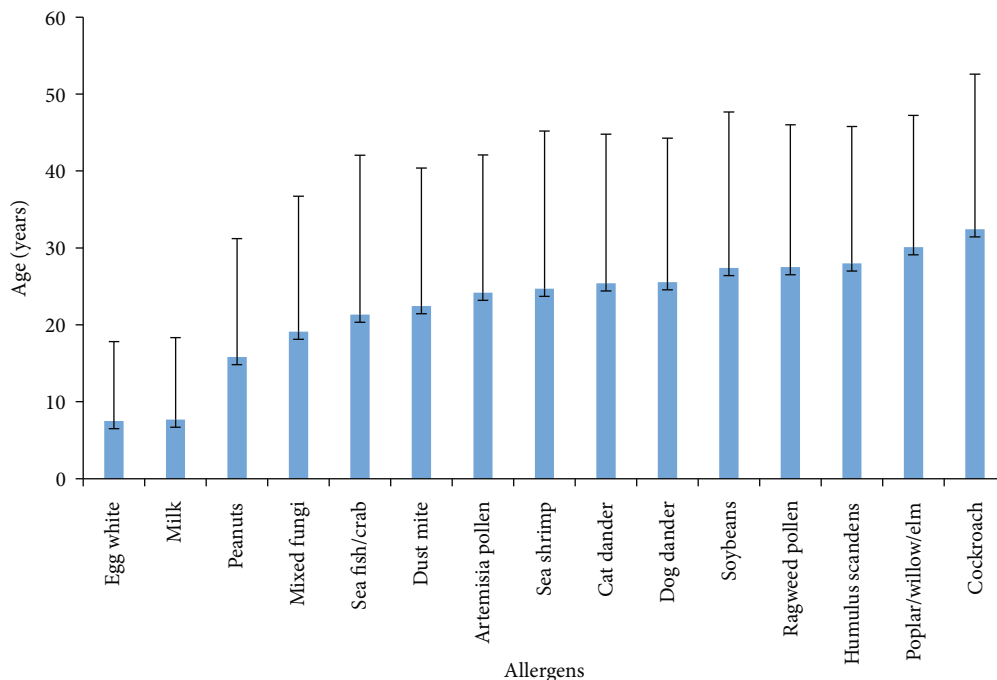


FIGURE 2: Average age of single allergen sensitization.

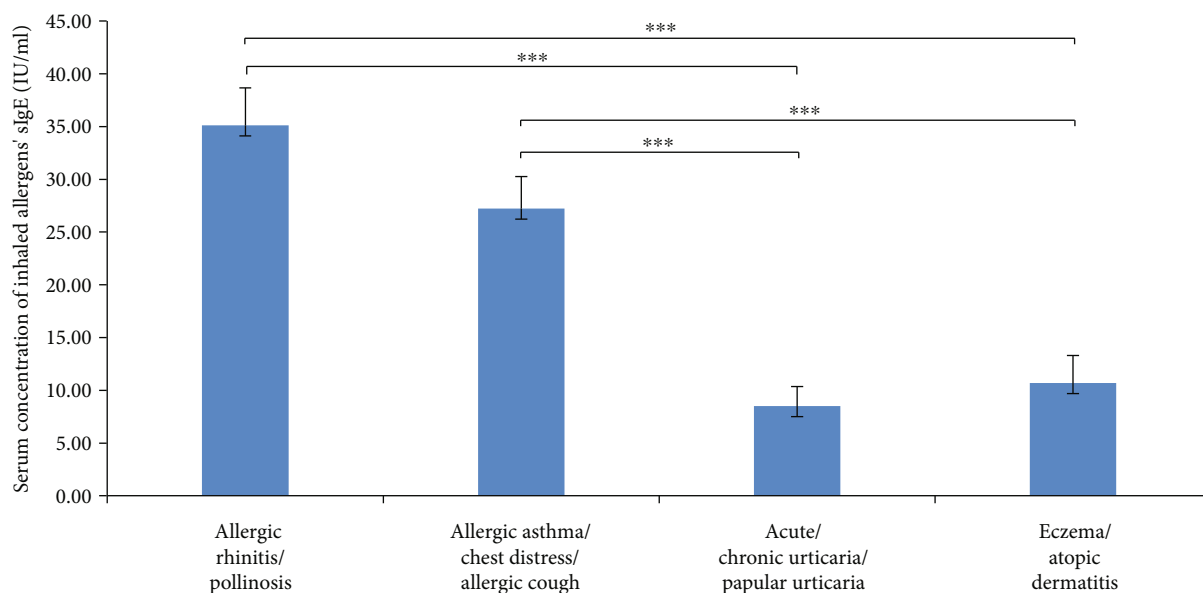


FIGURE 3: Mean value of inhaled allergens' sIgE in different diseases (***p* < 0.001).

(*p* < 0.05). We hypothesize that sex hormone may affect the level of serum IgE. In terms of age, the concentration of tIgE is observed to increase from birth to adolescence and then decrease during adulthood, which has been validated in a previous study [40, 41]. It has been suggested that the level of tIgE in Th2-driven respiratory inflammatory diseases is significantly higher than that in inflammatory skin diseases. Therefore, tIgE has developed as a Th2 biomarker, which is involved in regulating Th2 inflammatory response. The

determination of serum tIgE in asthma patients can help determine the disease's severity, thus guiding the acute attack period's treatment and preventing remission [42].

The main allergens of respiratory allergy are dust mites, mixed fungi, Artemisia pollen, and Humulus scandens pollen. Dust mites are the main allergens in north China, consistent with other reports [39, 43]. Limited by the types of allergens detected in the study, we do not have the data of the most common allergens in spring, such as Platanus

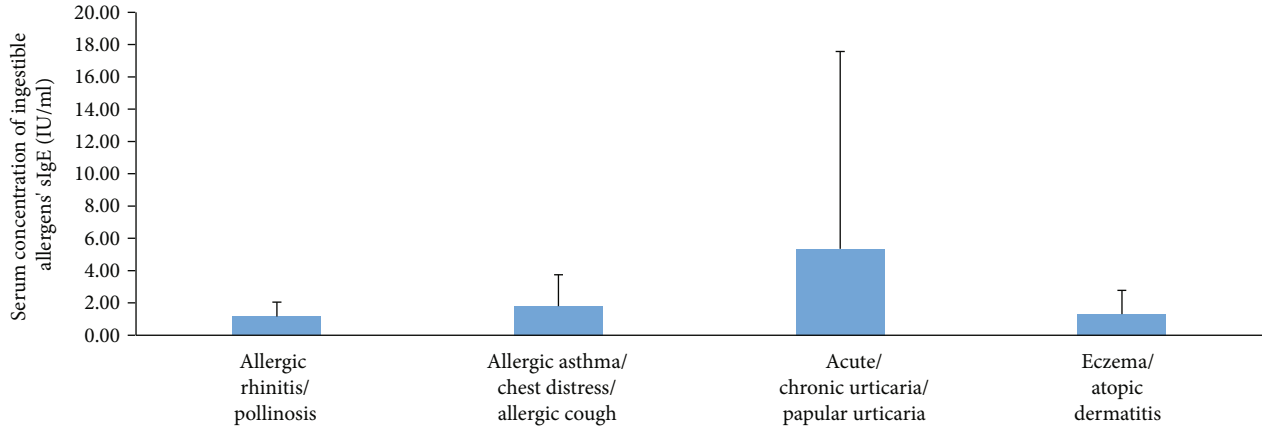


FIGURE 4: Mean value of ingestible allergen's sIgE in different diseases.

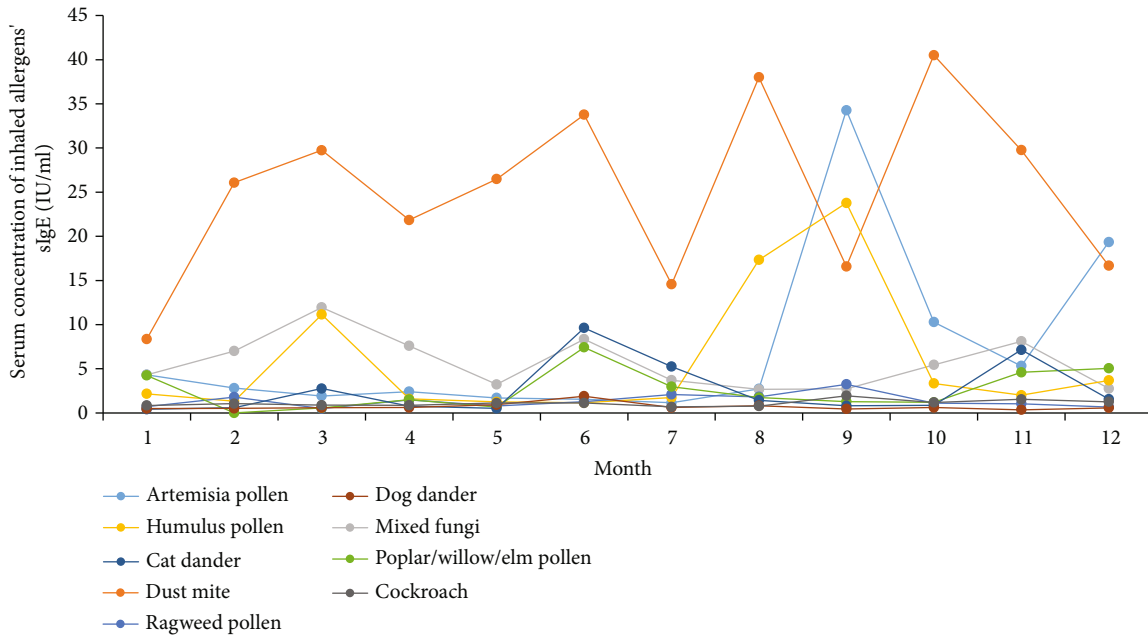


FIGURE 5: sIgE levels of 9 inhaled allergens in different months.

orientalis and ash tree pollen. Therefore, a large part of AR and pollinosis patients with negative sIgE and high tIgE in spring are diagnosed by the skin prick test (SPT). At the same time, poplar/willows, which are native trees of north China, have visible white floccules but are rarely sensitized. For inflammatory skin diseases, urticaria accounts for 29.6% of the allergic population in this study, and 37% of them are detected as allergen-positive. Although the etiology of urticaria is complex, many relevant causes and/or triggers have been discovered, such as food in infants and children [44]. We have found that ingestion of many foods, including eggs, milk, and peanuts in sensitized infants/children, may cause acute urticaria more frequently than in adults. In adult urticaria, the IgE antibody in blood is more likely to be specific for inhalant allergens, such as dust mites and airborne pollen.

In this study, 87% of allergen-related eczema appeared after childhood. Food sensitization was only present in 21%

of patients. 58% of the eczema population had more than one allergen. We also observed some IgE sensitization patterns, mainly including dust mites and molds, associated with persistent eczema/allergic dermatitis, especially in adults. The main food allergens for infantile eczema were still eggs and milk. Sensitization to sea fish/crab, sea shrimp, and peanuts among atopic children in Weifang was rarely observed. Although allergic patients will be refrained from eating spicy foods and seafood, we hypothesize that a non-IgE-mediated pathway may cause aggravation of dermatitis symptoms after seafood intake. Attributed to the gene differences with western populations, peanut and soybean nuts are not the leading causes of allergy in the Chinese population.

Among all immunoglobulin subclasses, IgE stands out concerning its low serum concentration and short half-life of 2 days. Seasonal allergen exposure can induce a rapid increase in allergen-specific IgE levels [45, 46]. This study

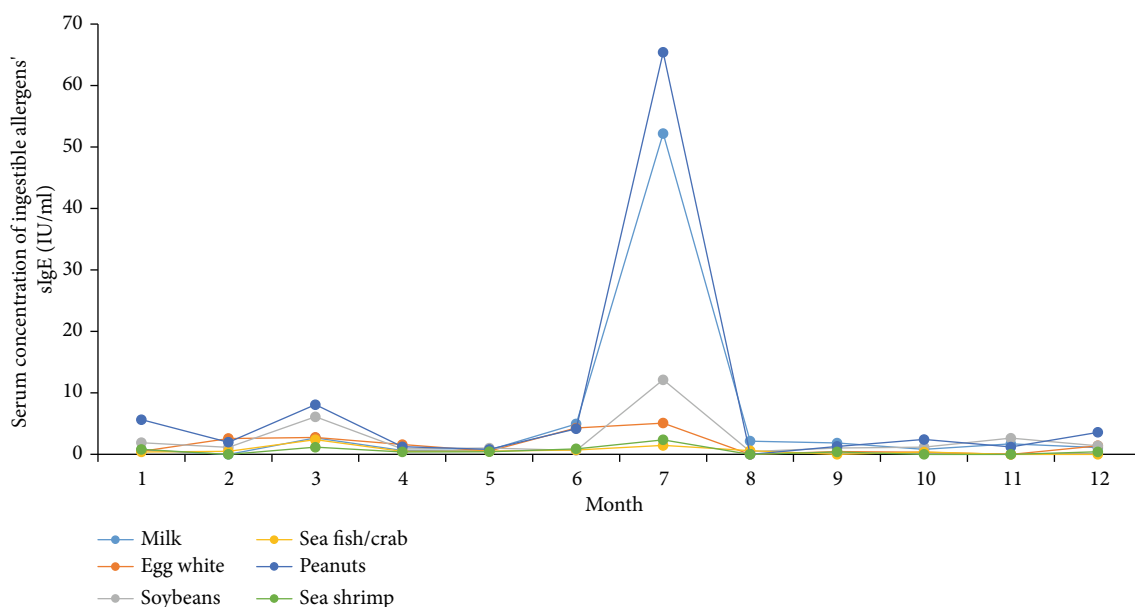


FIGURE 6: sIgE levels of 6 ingestible allergens in different months.

analyzed the time regularity of serum sIgE concentration of four main allergens, including dust mite, mixed fungi, Artemisia pollen, and Humulus pollen. There is a 1 month postponement between the serum sIgE concentration peak and the corresponding plant pollens' seasonal dissemination peak [47, 48]. Although the environmental density data of dust mites and fungi are insufficient in Weifang, the role of meteorological factors in the survival and reproduction of fungi and dust mites is critical [49, 50]. We speculate that the serum concentration of dust mites and fungi is closely related to seasonal reproduction. Therefore, it is necessary to detect airborne pollen and fungi as one of the routine meteorological forecast items and guide the allergic population to prevent and/or relocate to an allergen-free area for seasonal allergens.

Besides, sIgE levels of dust mites in inflammatory skin diseases (urticaria, eczema), classical type 2 inflammatory allergic diseases (AR and AS) are all statistically significant. The results have shown the allergic levels of dust mites in allergic skin patients were lower than those in respiratory allergic patients ($p < 0.05$). Similar findings have been found about fungi. There is a saying in China, namely, "one respiratory tract, one disease." We have found that AR patients tend to have higher sIgE antibodies than those with AS, especially in the two significant allergens of dust mites and Artemisia pollen. Recent cross-sectional studies have shown that the same individual can display different inflammation profiles in various respiratory tract sites [51]. There is an issue of whether each allergen family should be given a different cut-off. In addition to the most critical four allergens causing allergies, airborne pollen concentrations and food allergen antibodies are lower. However, their role in the allergy process is undeniable. This confusion was particularly evident after clinical verification of SPT.

Our study has some limitations. First, the patient's information is not further refined, including asthma, rhinitis, dermatitis symptom scores, and other indicators to assess the

disease's severity. Change in IgE concentration with seasons has not been accurately counted. Second, the number of patients in each group is different. Almost half of the patients are diagnosed with urticaria and patients with AD account for only 3.2% of the sample. Third, the reagent kit does not contain the most common inhaled allergens of the *Platanus orientalis* in the north of China in spring and the ingestive allergens of wheat. Finally, because most of the patients are referred from Weifang, IgE's disease entity and measurements may not represent atopic patients' general population in Shandong province. More studies are warranted to elucidate the role of serological IgE detection of allergens according to different age, gender, and other factors in allergic diseases.

Data Availability

Data in this study is available from the corresponding author upon request.

Conflicts of Interest

All authors have no conflicts of interest to disclose.

Acknowledgments

We acknowledge funds from the Science and Technology Development Program of Weifang (2020YX013 and 2020YX084) and Shandong Science and Technology Development Program (2016WS0657).

References

- [1] M. Andrea, B. Susanna, N. Francesca, M. Enrico, and V. Alessandra, "The emerging role of type 2 inflammation in asthma," *Expert Review of Clinical Immunology*, vol. 17, no. 1, pp. 63–71, 2021.

- [2] M. Kubo, "Innate and adaptive type 2 immunity in lung allergic inflammation," *Immunological Reviews*, vol. 278, no. 1, pp. 162–172, 2017.
- [3] L. M. Wheatley and A. Togias, "Clinical practice. Allergic rhinitis," *The New England Journal of Medicine*, vol. 372, no. 5, pp. 456–463, 2015.
- [4] I. Agache, K. Sugita, H. Morita, M. Akdis, and C. A. Akdis, "The complex type 2 endotype in allergy and asthma: from laboratory to bedside," *Current Allergy and Asthma Reports*, vol. 15, no. 6, p. 29, 2015.
- [5] A. V. Kudryavtseva, K. A. Neskorodova, and P. Staubach, "Urticaria in children and adolescents: an updated review of the pathogenesis and management," *Pediatric Allergy and Immunology*, vol. 30, no. 1, pp. 17–24, 2019.
- [6] J. Zhao, J. Bai, K. Shen et al., "Self-reported prevalence of childhood allergic diseases in three cities of China: a multicenter study," *BMC Public Health*, vol. 10, no. 1, 2010.
- [7] N. Ravnborg, D. Ambikaibalan, G. Agnihotri et al., "Prevalence of asthma in patients with atopic dermatitis: a systematic review and meta-analysis," *Journal of the American Academy of Dermatology*, vol. 84, no. 2, pp. 471–478, 2021.
- [8] F. Li, Y. Zhou, S. Li et al., "Prevalence and risk factors of childhood allergic diseases in eight metropolitan cities in China: a multicenter study," *BMC Public Health*, vol. 11, no. 1, 2011.
- [9] W. Feleszko, M. Ruszczyński, J. Jaworska, A. Strzelak, B. M. Zalewski, and M. Kulus, "Environmental tobacco smoke exposure and risk of allergic sensitisation in children: a systematic review and meta-analysis," *Archives of Disease in Childhood*, vol. 99, no. 11, pp. 985–992, 2014.
- [10] J. S. Kim, F. Ouyang, J. A. Pongracic et al., "Dissociation between the prevalence of atopy and allergic disease in rural china among children and adults," *Journal of Allergy and Clinical Immunology*, vol. 122, no. 5, pp. 929–935.e4, 2008.
- [11] B. Q. Sun, D. H. Chen, P. Y. Zheng et al., "Allergy-related evidences in relation to serum ige: data from the China state key laboratory of respiratory disease, 2008-2013," *Biomedical and Environmental Sciences*, vol. 27, no. 7, pp. 495–505, 2014.
- [12] S. Lee, "Ige-mediated food allergies in children: prevalence, triggers, and management," *Korean Journal of Pediatrics*, vol. 60, no. 4, pp. 99–105, 2017.
- [13] C. H. Katelaris, B. W. Lee, P. C. Potter et al., "Prevalence and diversity of allergic rhinitis in regions of the world beyond europe and north america," *Clinical and Experimental Allergy*, vol. 42, no. 2, pp. 186–207, 2012.
- [14] H. T. Wang, C. M. Warren, R. S. Gupta, and C. M. Davis, "Prevalence and characteristics of shellfish allergy in the pediatric population of the united states," *The Journal of Allergy and Clinical Immunology: In Practice*, vol. 8, no. 4, pp. 1359–1370.e2, 2020.
- [15] J. Stern, J. Pier, and A. A. Litonjua, "Asthma epidemiology and risk factors," *Seminars in Immunopathology*, vol. 42, no. 1, pp. 5–15, 2020.
- [16] M. J. Ridd, A. J. L. King, E. le Roux, A. Waldecker, and A. L. Huntley, "Systematic review of self-management interventions for people with eczema," *The British Journal of Dermatology*, vol. 177, no. 3, pp. 719–734, 2017.
- [17] A. Muraro, G. Roberts, M. Worm et al., "Anaphylaxis: guidelines from the european academy of allergy and clinical immunology," *Allergy*, vol. 69, no. 8, pp. 1026–1045, 2014.
- [18] F. E. Simons, M. Ebisawa, M. Sanchez-Borges et al., "2015 update of the evidence base: world allergy organization anaphylaxis guidelines," *World Allergy Organization Journal*, vol. 8, no. 1, p. 32, 2015.
- [19] M. A. Tejedor Alonso, M. Moro Moro, and M. V. Múgica García, "Epidemiology of anaphylaxis," *Clinical and Experimental Allergy*, vol. 45, no. 6, pp. 1027–1039, 2015.
- [20] W. Luo, H. Hu, W. Tang et al., "Allergen sensitization pattern of allergic adults and children in southern China: a survey based on real life data," *Allergy, Asthma and Clinical Immunology*, vol. 15, no. 1, 2019.
- [21] J. Wang, Z. Zhao, Y. Zhang et al., "Asthma, allergic rhinitis and eczema among parents of preschool children in relation to climate, and dampness and mold in dwellings in China," *Environment International*, vol. 130, p. 104910, 2019.
- [22] X. D. Wang, M. Zheng, H. F. Lou et al., "An increased prevalence of self-reported allergic rhinitis in major chinese cities from 2005 to 2011," *Allergy*, vol. 71, no. 8, pp. 1170–1180, 2016.
- [23] H. Mosbech, N. H. Nielsen, A. Dirksen, J. Launbjerg, I. Biering, and M. Søborg, "Comparison between specific ige measured by rast, two chemiluminescent assays and skin prick test," *Allergologia et Immunopathologia*, vol. 20, no. 6, pp. 220–224, 1992.
- [24] L. Cheng, J. Chen, Q. Fu et al., "Chinese society of allergy guidelines for diagnosis and treatment of allergic rhinitis," *Allergy, Asthma & Immunology Research*, vol. 10, no. 4, pp. 300–353, 2018.
- [25] N. G. Papadopoulos, H. Arakawa, K. H. Carlsen et al., "International consensus on (icon) pediatric asthma," *Allergy*, vol. 67, no. 8, pp. 976–997, 2012.
- [26] T. Bieber, "Atopic dermatitis," *The New England Journal of Medicine*, vol. 358, no. 14, pp. 1483–1494, 2008.
- [27] A. Wollenberg, S. Barbarot, T. Bieber et al., "Consensus-based european guidelines for treatment of atopic eczema (atopic dermatitis) in adults and children: part ii," *Journal of the European Academy of Dermatology and Venereology*, vol. 32, no. 6, pp. 850–878, 2018.
- [28] R. A. Wood, D. A. Khan, D. M. Lang et al., "American Academy of Allergy, Asthma and Immunology response to the EAACI/GA2LEN/EDF/WAO guideline for the definition, classification, diagnosis, and management of urticaria 2017 revision," *Allergy*, vol. 74, no. 2, pp. 411–413, 2019.
- [29] J. Schmitt, S. Langan, S. Deckert et al., "Assessment of clinical signs of atopic dermatitis: a systematic review and recommendation," *The Journal of Allergy and Clinical Immunology*, vol. 132, no. 6, pp. 1337–1347, 2013.
- [30] F. E. Simons and H. A. Sampson, "Anaphylaxis epidemic: fact or fiction?," *The Journal of Allergy and Clinical Immunology*, vol. 122, no. 6, pp. 1166–1168, 2008.
- [31] J. Ščevková, J. Dušička, M. Hrubíško, and K. Mičieta, "Influence of airborne pollen counts and length of pollen season of selected allergenic plants on the concentration of ige antibodies on the population of Bratislava, Slovakia," *Annals of Agricultural and Environmental Medicine*, vol. 22, no. 3, pp. 451–455, 2015.
- [32] S. C. Dharmage, A. J. Lowe, M. C. Matheson, J. A. Burgess, K. J. Allen, and M. J. Abramson, "Atopic dermatitis and the atopic march revisited," *Allergy*, vol. 69, no. 1, pp. 17–27, 2014.
- [33] S. Illi, E. von Mutius, S. Lau et al., "The natural course of atopic dermatitis from birth to age 7 years and the association with asthma," *The Journal of Allergy and Clinical Immunology*, vol. 113, no. 5, pp. 925–931, 2004.
- [34] A. S. Paller, J. M. Spergel, P. Mina-Osorio, and A. D. Irvine, "The atopic march and atopic multimorbidity: many

- trajectories, many pathways,” *The Journal of Allergy and Clinical Immunology*, vol. 143, no. 1, pp. 46–55, 2019.
- [35] M. Saunes, T. Øien, C. K. Dotterud et al., “Early eczema and the risk of childhood asthma: a prospective, population-based study,” *BMC Pediatrics*, vol. 12, no. 1, 2012.
- [36] K. A. Engebretsen and J. P. Thyssen, *Skin barrier function and allergens*, vol. 49 of Current Problems in Dermatology, Basel, Karger, 2016.
- [37] M. Shaker, “New insights into the allergic march,” *Current Opinion in Pediatrics*, vol. 26, no. 4, pp. 516–520, 2014.
- [38] D. C. Belgrave, R. Granell, A. Simpson et al., “Developmental profiles of eczema, wheeze, and rhinitis: two population-based birth cohort studies,” *PLoS Medicine*, vol. 11, no. 10, p. e1001748, 2014.
- [39] Y. Zhang and L. Zhang, “Prevalence of allergic rhinitis in China,” *Allergy, Asthma & Immunology Research*, vol. 6, no. 2, pp. 105–113, 2014.
- [40] R. A. Barbee, M. Halonen, M. Lebowitz, and B. Burrows, “Distribution of ige in a community population sample: correlations with age, sex, and allergen skin test reactivity,” *The Journal of Allergy and Clinical Immunology*, vol. 68, no. 2, pp. 106–111, 1981.
- [41] J. W. Gerrard, S. Horne, P. Vickers et al., “Serum ige levels in parents and children,” *The Journal of Pediatrics*, vol. 85, no. 5, pp. 660–663, 1974.
- [42] K. Kovač, S. Dodig, D. Tješić-Drinković, and M. Raos, “Correlation between Asthma Severity and Serum IgE in Asthmatic Children Sensitized to *Dermatophagoides pteronyssinus*,” *Archives of Medical Research*, vol. 38, no. 1, pp. 99–105, 2007.
- [43] J. Li, B. Sun, Y. Huang et al., “A multicentre study assessing the prevalence of sensitizations in patients with asthma and/or rhinitis in China,” *Allergy*, vol. 64, no. 7, pp. 1083–1092, 2009.
- [44] O. Jirapongsananuruk, S. Pongpreuksa, P. Sangacharoenkit, N. Visitsunthorn, and P. Vichyanond, “Identification of the etiologies of chronic urticaria in children: a prospective study of 94 patients,” *Pediatric Allergy and Immunology*, vol. 21, no. 3, pp. 508–514, 2010.
- [45] J. Eckl-Dorna, S. Villazala-Merino, N. J. Campion et al., “Tracing ige-producing cells in allergic patients,” *Cells*, vol. 8, no. 9, p. 994, 2019.
- [46] V. Niederberger, J. Ring, J. Rakoski et al., “Antigens drive memory ige responses in human allergy via the nasal mucosa,” *International Archives of Allergy and Immunology*, vol. 142, no. 2, pp. 133–144, 2007.
- [47] G. J. Gleich, G. L. Jacob, J. W. Yunginger, and L. L. Henderson, “Measurement of the absolute levels of IgE antibodies in patients with ragweed hay fever: effect of immunotherapy on seasonal changes and relationship to IgG antibodies,” *The Journal of Allergy and Clinical Immunology*, vol. 60, no. 3, pp. 188–198, 1977.
- [48] Y. Ouyang, Z. Yin, Y. Li, E. Fan, and L. Zhang, “Associations among air pollutants, grass pollens, and daily number of grass pollen allergen-positive patients: a longitudinal study from 2012 to 2016,” *International Forum of Allergy & Rhinology*, vol. 9, no. 11, pp. 1297–1303, 2019.
- [49] A. A. Abdel Hameed, M. I. Khoder, Y. H. Ibrahim, Y. Saeed, M. E. Osman, and S. Ghanem, “Study on some factors affecting survivability of airborne fungi,” *Science of The Total Environment*, vol. 414, pp. 696–700, 2012.
- [50] J. D. Miller, “The role of dust mites in allergy,” *Clinical Reviews in Allergy and Immunology*, vol. 57, no. 3, pp. 312–329, 2019.
- [51] L. Giovannini-Chami, A. Paquet, C. Sanfiorenzo et al., “The “one airway, one disease” concept in light of th2 inflammation,” *European Respiratory Journal*, vol. 52, no. 4, p. 1800437, 2018.

Review Article

Role of Extracellular Vesicles in Placental Inflammation and Local Immune Balance

Zengfang Wang,¹ Ruizhen Yang,² Jiaojiao Zhang,³ Pingping Wang,¹ Zengyan Wang,² Jian Gao ,⁴ and Xue Liu ²

¹Department of Gynecology and Obstetrics, Maternal and Child Health Hospital of Weifang Medical University, Weifang 261000, China

²Operating Room, Zhucheng People's Hospital, Zhucheng 262200, China

³Central Laboratory of Weifang People's Hospital, Weifang 261000, China

⁴Department of Paediatrics, Maternal and Child Health Care Hospital of Weifang, Weifang 261000, China

Correspondence should be addressed to Jian Gao; gaojian1650@126.com and Xue Liu; rmyyliuxue@163.com

Received 7 February 2021; Revised 26 April 2021; Accepted 25 May 2021; Published 19 June 2021

Academic Editor: Bingjie Gu

Copyright © 2021 Zengfang Wang et al. This is an open access article distributed under the Creative Commons Attribution License, which permits unrestricted use, distribution, and reproduction in any medium, provided the original work is properly cited.

Background. Pregnancy maintenance depends on the formation of normal placentas accompanied by trophoblast invasion and vascular remodeling. Various types of cells, such as trophoblasts, endothelial cells, immune cells, mesenchymal stem cells (MSCs), and adipocytes, mediate cell-to-cell interactions through soluble factors to maintain normal placental development. Extracellular vesicles (EVs) are diverse nanosized to microsized membrane-bound particles released from various cells. EVs contain tens to thousands of different RNA, proteins, small molecules, DNA fragments, and bioactive lipids. EV-derived microRNAs (miRNAs) and proteins regulate inflammation and trophoblast invasion in the placental microenvironment. Maternal-fetal communication through EV can regulate the key signaling pathways involved in pregnancy maintenance, from implantation to immune regulation. Therefore, EVs and the encapsulating factors play important roles in pregnancy, some of which might be potential biomarkers. **Conclusion.** In this review, we have summarized published studies about the EVs in the placentation and pregnancy-related diseases. By summarizing the role of EVs and their delivering active molecules in pregnancy-related diseases, it provides novel insight into the diagnosis and treatment of diseases.

1. Introduction

Extracellular vesicles (EVs) are secreted by cell membrane or cells with diameters ranging from 40 nm to 1000 nm [1, 2]. EVs mainly include microbubbles, ectosomes, exosomes, and microparticles according to their subcellular sources [3–5]. Exosomes with a diameter of 40~100 nm are the most commonly studied EVs, which are firstly found in sheep reticulocytes [6]. EV plays an important role in a series of biological processes by transferring lipids, proteins, nucleotides, and other bioactive components. These encapsulated bioactive molecules can be delivered to specific targeted cells (Figure 1). In particular, some EVs carrying noncoding RNAs, such as microRNA (miRNA) and long-chain noncoding RNAs (lncRNA), can be transferred to specific cells and

regulate the expression and function of target mRNA at different biological stages [7]. EVs participate in the exchange of substances and information between cells mainly through the following pathways [8–10]. Firstly, EV membrane proteins can bind to the targeted cell membrane, thereby activating the signaling pathway in cells. Secondly, EVs can be digested by proteases in extracellular matrix. The digested fragments can be used as ligands to bind to the receptors on the cell membrane, thereby regulating intracellular communication. Thirdly, EVs can be directly fused with the target cell membrane, and then, EVs containing bioactive components are nonselectively released into recipient cells.

EVs from different cell sources can exert multiple effects. EVs derived from mesenchymal stem cells (MSC) can significantly improve myocardial cell survival, prevent myocardial

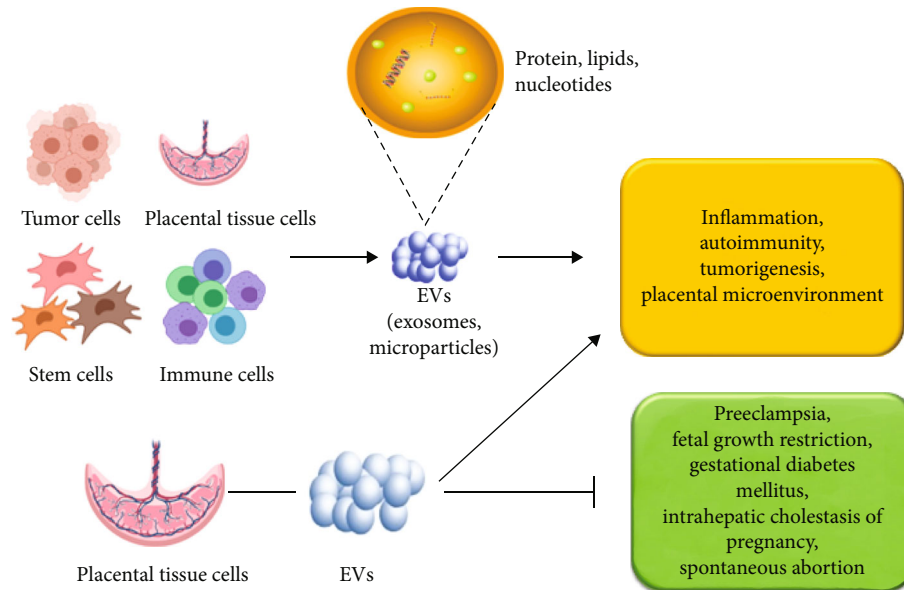


FIGURE 1: Role of EVs in placenta and pregnancy disorders. EVs mainly include exosomes and particles, which can be derived from stem cells, tumor cells, immune cells, and placental tissue cells. They participate in intercellular communication by transmitting bioactive proteins, lipids, and nucleotides to targeted cells. EVs, especially EVs derived from placental tissue cells, play a crucial role in regulating inflammation, autoimmune, tumor occurrence, and placental microenvironment balance. EVs have been used to prevent pregnancy diseases such as PE, fetal growth restriction, and spontaneous abortion.

cell injury, promote angiogenesis, and improve cardiac function by regulating inflammation and autoimmune [11–13]. Due to the advantages of nanomolecular structure and excellent biocompatibility, EVs have great application potential as drug carriers. MSC-derived EVs are used to treat chronic skin ulcers, which can promote wound healing and reduce scar formation [14]. In addition, EVs play a key role in tumor occurrence, immune surveillance, immune escape, and tumor microenvironment reprogramming [15–17]. Accordingly, EVs and their encapsulated bioactive molecules are essential for intercellular communication in many diseases, including pregnancy disorders. The role of EVs in immune regulation has been extensively studied. EVs from intestinal epithelial cells (IECs) released during sepsis have been reported to improve intestinal inflammation by transferring miRNAs into cells [18]. EVs are involved in maintaining T cell tolerance and long-term T cell memory [19]. EV-encapsulated proteins participate in immune regulation by influencing the secretion of anti-inflammatory cytokines [20]. Thyroid stimulating hormone receptor (TSHR) released by EV improves autoantibody-mediated activation of Graves disease by blocking autoantibodies [21]. Baskaran et al. reported that EVs play an indispensable role in sperm maturation by regulating autoimmunity [22]. This local immunity privilege at the maternal-fetal interface has been attributed to the expression of Fas ligand (FasL) related to placental exosomes, programmed death ligand 1 (PD-L1), and TNF-related apoptosis-inducing ligand (TRAIL), which all induce maternal T cell incompetence and death [23, 24]. Expression of NKG2D receptor ligand, UL-16-binding protein (ULBP), and MHC class I chain-related protein (MIC) on placental exosomes have been shown to downregulate NK cell activity and inhibit maternal cytotoxicity [25].

In the past decades, the role of EV in regulating placenta implantation and pregnancy diseases has attracted much attention due to its key role in regulating inflammation and immunity. The aim of this study is to summarize the current published studies on the association of EVs with placenta implantation and pregnancy-related diseases. In particular, we aim to explore the role of EVs in the diagnosis and treatment of pregnancy-related diseases.

2. EVS from Placental Tissues and Stem Cells

Placenta is the fundamental physiological barrier for maternal immune tolerance to fetus and various pathogens. EVs released by syncytiotrophoblasts, trophoblasts, extravillous trophoblasts, and placental vascular endothelial cells play a key role in pregnancy [26]. Placenta and umbilical cord are rich in MSCs, which are promising treatment strategies for various diseases [27]. It has been shown that EVs from human umbilical cord MSCs (hUC-MSCs) could protect against severe burn-induced hyperinflammation through the way of paracrine secretion [28]. Surico et al. have found that hUC-MSCs are involved in preeclampsia (PE) and affect fetal growth restriction (FGR) by delivering bioactive components encapsulated in EVs [29]. hUC-MSC-derived EVs have also been found to confer effect on the paracrine of trophoblast cells, which facilitates their use in treating pregnancy-related disorders. Decidual MSC-derived EVs can also exert inhibitory effects on angiogenesis and maintain the balance of maternal-fetal interface by regulating macrophage polarization in PE [30]. Accordingly, placenta tissue MSCs and hUC-MSC-derived EVs play key roles in maintaining placental functions and protecting against pregnancy disorders.

Accumulated data have shown that MSC transplantation may be extremely beneficial for pregnancy-associated diseases [31]. In the past few years, the use of MSC-EVs in pregnancy disorders has drawn more and more attention. Placental tissue cell-derived EVs can be produced regardless of physiological or pathological pregnancy. Reduced circulating EVs are associated with placental dysfunction [32]. Circulating EVs play a crucial role during pregnancy [33]. EVs derived from placental tissue cells increased gradually with the progress of pregnancy, especially during delivery, but significantly decreased to nonpregnancy level 48 hours after delivery [34]. EVs derived from placental tissue cells can selectively transfer bioactive molecules, such as stress-induced protein molecules, apoptosis-related molecules, cytokines, mRNA, and miRNA. EVs actively participate in maternal-fetal communication during pregnancy by regulating different processes [35]. The fetus is the mother's allogeneic graft. Successful pregnancy depends on the maintenance of maternal-fetal interface immune tolerance. Th1/Th2 balance during pregnancy is essential to maintain maternal and fetal microenvironment [36]. Placenta-derived EVs promote maternal immune tolerance by inhibiting maternal T cell response and maintaining Th1/Th2 balance [35]. Placenta-derived EVs produce Syn-2, which proves to play an immunosuppressive role in placenta [37]. Placental tissue-derived EVs and exosome inclusion factors are important regulators of placental immunity and homeostasis [37]. The delivery of bioactive molecules by EVs is beneficial to placental function. During pregnancy, EVs can be transported to the fetal side as drugs and other goods [38]. EVs also play an important role in regulating systemic inflammation by releasing cytokines. Therefore, EVs from placenta tissues and stem cells are essential for maintaining maternal-fetal immunity and protecting inflammation.

MSC-derived noncoding RNAs can serve as useful biomarkers in pregnancy disorders [28–30]. However, whether MSC-derived noncoding RNAs can exert their effects through EVs and mediate intercellular communications in maternal-fetal immunity needs to be elucidated in the future. During the past few decades, noncoding RNAs derived from placental stem cells have been demonstrated to participate in pregnancy regulation, such as lncRNAs and miRNAs [39–41]. Placental tissue-derived EV miRNAs have been implicated in the antiviral immunity at the maternal and fetal interface [42]. In addition, studies have found that EVs from placental tissue cells also have significant effects on pregnancy complications by transferring miRNAs to recipient cells [43]. Accordingly, those noncoding RNAs from placental tissues and stem cell-derived EVs serve as key biomarkers for gestational disorders.

3. EVS and Pregnant Disorders

EVs are the “fingerprints” of their primitive cells and are involved in regulating pregnancy complications. EVs derived from placental tissue may be another way for the fetus to communicate with mothers. EV regulates inflammatory cascade reactions in some complex pregnancy, such as PE and intrauterine growth restriction [44]. Here,

we summarize the research progress of the role of EVs and their encapsulated factors in some common pregnancy diseases (Table 1).

3.1. EVS and PE. PE is an idiopathic pregnancy disease characterized by hypertension and proteinuria after 20 weeks of pregnancy. The global incidence of PE is 3–8%, and its pathogenesis is still unclear. The basic pathological changes of PE are systemic vasospasm, vascular endothelial injury, and ischemia. PE leads to reduced perfusion of all organs and poses risks to both mothers and children. Its performance is often significantly improved after childbirth or termination of pregnancy, suggesting that placental-derived media play a key role in the pathogenesis of PE.

A number of studies have suggested EVs and their encapsulated factors are involved in the pathogenesis of PE [45, 46]. Bioactive molecules in placental tissue-derived EVs might be as potential biomarkers for the diagnosis and prognosis of PE [47]. Placental protein 13 (PP13) has been identified in maternal circulating exosomes or microvesicles [48]. Low serum level of PP13 predicts high risk of PE and other obstetric complication [48]. Salomon et al. have found that total plasma exosomes and placental tissue exosomes both significantly increased in patients with PE compared with normal pregnancies [49]. Similarly, placental EVs in the blood circulation of PE patients are significantly lower than that in patients with early-onset PE [50]. Chang et al. showed that exosome soluble fms-like tyrosine kinase-1 (sFlt-1) and soluble endoglin (sEng) inhibited the growth and tube formation of human umbilical vein endothelial cells in PE [51]. In addition, circulating EVs from placenta can activate immune cells and may affect the production of inflammatory cytokines in PE pregnancy [52]. As a result, EV-delivering factors are essential regulators in PE.

In the last decade, EV-encapsulated noncoding RNAs have been found to affect the development of PE [40]. Some placental tissue-derived miRNAs can be released into the maternal circulation from the trophoblast layer via EVs [53]. A few EV-encapsulated miRNAs are potential markers for PE [54]. Diverse miRNA profiles in circulating EVs from early and late onset of PE have been demonstrated, which implicates that EV-derived miRNAs are key factors associated with PE [55]. Li et al. have demonstrated there are specific miRNA expression and signals in serum exosomes from PE pregnancies, suggesting the modifying effect of plasma exosomal miRNAs in the pathogenesis of PE [56]. Increased expression of miR-201-3p has been demonstrated in the circulating EVs of patients with PE [57]. The study by Shen et al. has suggested that placental tissue cell-derived exosomal miR-155 inhibits the expression of endothelial nitric oxide synthase in PE [58]. In addition, there are many other EV-derived miRNAs demonstrated as key biomarkers in PE, such as EV-encapsulated miR-136 and miR-495 [59]. Exosomal miR-210 has been reported to be produced by trophoblasts and participates in the intercellular communication in PE [60]. Some EV-derived miRNAs have been suggested as circulating markers for PE, including miR-517-5p, miR-520a-5p, and miR-525-5p [61]. Accordingly, EV-encapsulated noncoding RNAs are key regulators in PE.

TABLE 1: EV-derived biomarkers in autoimmunity and pregnancy disorders.

Biomarker	Type of biomarker	Type of derived EVs	Diseases and pregnancy condition	Function	Reference
Thyrotropin receptor	Receptor	Exosomes	Graves' disease	Sequestering autoantibody and ameliorating autoantibody-mediated activation	[21]
UL-16-binding protein	Protein	Exosomes	Placenta during pregnancy	Downregulate NK cell activity and inhibit maternal cytotoxicity	[25]
MHC class I chain-related protein	Protein	Exosomes	Placenta during pregnancy	Downregulate NK cell activity and inhibit maternal cytotoxicity	[25]
Syncytin-2	Protein	Exosomes	Normal pregnancy	Exerting immunosuppressive effects on T cells	[37]
Placental protein 13	Protein	Exosomes or microvesicles	PE and other obstetric complications	Binding to glycosylated receptors, bringing about hemagglutination, immunoregulation and vasodilation	[48]
Soluble fms-like tyrosine kinase-1	Protein	Exosomes	PE	Attenuating the proliferation, migration, and tube formation of human umbilical vein endothelial cells	[51]
Soluble endoglin	Protein	Exosomes	PE	Inhibiting the growth and tube formation of human umbilical vein endothelial cells	[51]
MiR-201-3p	Nucleotide/noncoding RNA	Exosomes	PE	Having a role in the pathomechanism of PE	[57]
MiR-155	Nucleotide/noncoding RNA	Exosomes	PE	Inhibiting the expression of endothelial nitric oxide synthase	[58]
MiR-136 and miR-495	Nucleotide/noncoding RNA	MSC-derived exosomes	PE	Promising circulating biomarkers in early detection of PE	[59]
MiR-210	Nucleotide/noncoding RNA	Exosomes	PE	Produced by trophoblasts and participating in the intercellular communication	[60]
Phosphoenolpyruvate carboxykinase	Kinase	Urine exosomes	Gestational diabetes mellitus	Affecting insulin resistance	[66]
Sterile 20-like kinase 1	Protein	Cardiac microvascular endothelial cell-derived exosomes	Diabetes	Inhibiting autophagy, promoting apoptosis and suppressing glucose metabolism	[70]
EVs-encapsulated miRNAs	Nucleotide/noncoding RNA	EVs	Gestational diabetes mellitus	Serving as biomarkers for the diagnosis and treatment of gestational diabetes mellitus	[79–82]
MiR-150	Nucleotide/noncoding RNA	Piglet's umbilical vein-derived EVs	FGR	Promoting angiogenesis	[86]
MiR-21, miR-29a and miR-590-3p	Nucleotide/noncoding RNA	Urinary exosomes	ICP	Downregulating intercellular adhesion molecule 1	[90]
MiR-300 and miR-299-5p	Nucleotide/noncoding RNA	EVs	Congenital obstructive nephropathy	Reregulating renal fibrosis	[99]

EVs: extracellular vesicles; FGR: fetal growth restriction; ICP: intrahepatic cholestasis of pregnancy; MSCs: mesenchymal stem cells; PE: preeclampsia.

The role of stem cell EV-derived miRNAs in PE has also been extensively investigated in the past few years. It has been reported that the umbilical cord blood stem cells EV-derived miR-125a-5p plays a critical role in PE [62]. It has been demonstrated that hUC-MSC EVs can inhibit placental cell apo-

ptosis and promote angiogenesis in PE [63]. Besides, MSC-derived exosomal lncRNA H19 has been demonstrated to increase the invasion and migration of trophoblast cells by regulating let-7b through AKT signaling pathway in PE [64]. Accordingly, stem cell-derived EVs and the

encapsulated bioactive molecules can regulate angiogenesis and autoimmune balance in PE, which may be promising therapeutic strategy for patients with PE.

3.2. EVs and Gestational Diabetes Mellitus. Pregnancy can cause diabetes in pregnant women who have no diabetes previously and also exacerbate the condition of patients with existing diabetes. Gestational diabetes has a greater impact on both mothers and children, and the near-term and long-term complications of mothers and children are higher. Pregnant women with diabetes are more likely to subject to hypertension during pregnancy than nondiabetic women [65]. Diabetes can increase the chance of infection, dystocia, birth canal injury, surgery, and postpartum bleeding in pregnant women as well as elevated incidence of large children, restricted fetal growth, spontaneous abortion, embryonic termination, and premature birth.

The development of gestational diabetes mellitus is related to heredity, autoimmunity, and environmental factors. Increasing evidence has suggested the crucial role of EVs in gestational diabetes mellitus. The study by Arias et al. has demonstrated the potential role of plasma EV-encapsulated factors as early biomarkers for gestational diabetes mellitus [65]. Sharma et al. have found that human urine-derived EVs contained gluconeogenic enzymes that affect glucose metabolism [66]. Elevated phosphoenolpyruvate carboxykinase (PEPCK) in urine exosomes is related to high risk of diabetes and early insulin resistance [66]. In addition, currently available data has suggested EVs play an important role in autoimmune reaction in islets of type 1 diabetes [67]. Moreover, EVs produced by adipose tissue and muscle tissue regulate glucose and lipid balance and even the inflammatory environment by transferring specific molecules to a variety of insulin-sensitive peripheral tissues [67]. As a result, the effect of EVs in gestational diabetes mellitus is essential.

EV-encapsulated factors can be used as useful biomarkers for a variety of diseases and complications [68]. Many studies have shown EV-encapsulated proteins, mRNAs, and DNAs and are new diagnostic markers for diabetic nephropathy [68]. EVs can also be used as delivery vehicles for the treatment of diabetic nephropathy. A previous study has demonstrated that the urinary exosomal E1f3 may be an early noninvasive marker for podocyte injuries in diabetic nephropathy [69]. Mammalian sterile 20-like kinase 1- (Mst1-) enriched EVs released from cardiac microvascular endothelial cells play an important role in inhibiting autophagy, promoting apoptosis, and suppressing glucose metabolism in cardiomyocytes [70]. All these findings have supported the vital role of EVs in glucose metabolism and diabetes progression.

Insufficient myocardial angiogenesis can induce diabetes-related ischemic cardiovascular [71]. CD133⁺ exosomes derived from human umbilical cord blood improve cardiac function in diabetic stroke mice [72]. MSC EVs protect β cells from hypoxia-induced apoptosis [73]. More and more evidence suggests that EVs and delivered miRNAs have neuroprotective effects and may be a treatment for diabetes-related stroke [74]. Studies have shown that EVs extracted

from plasma of pregnant women with gestational diabetes significantly promote the production of inflammatory cytokines [75]. EVs can also regulate placental and fetal membrane endothelial dysfunction in gestational diabetes mellitus [76]. Adipose tissue-derived EVs mediate placental immunity in gestational diabetes mellitus, which may be associated with some adverse outcomes, including fetal overgrowth [77]. EVs represent a new mechanism for regulating maternal glucose homeostasis during pregnancy [78]. Taken together, the role of EVs in gestational diabetes mellitus is critical. At the same time, the mechanism of EVs wrapped bioactive factors in gestational diabetes remains to be further studied.

Increasing evidence has supported that EV-transferred miRNAs and other noncoding RNAs can be used as promising biomarkers for gestational diseases including gestational diabetes mellitus [79]. Nair et al. have reported that placental tissue-derived EV miRNAs can regulate skeletal muscle insulin sensitivity [80]. Placental tissue-derived EVs may exert effects on insulin sensitivity in normal and gestational diabetes mellitus pregnancies. Taken together, EVs offer new options for the treatment of gestational diabetes mellitus [81]. EV-encapsulated noncoding RNAs can also serve as biomarkers for the diagnosis and treatment of gestational diabetes mellitus [82].

3.3. EVs and Fetal Growth Restriction (FGR). FGR usually leads to low birthweight births. However, the underlying biological mechanism has not been fully elucidated. FGR can be secondary to various pregnancy complications, such as gestational hypertension, diabetes, and intrahepatic cholestasis. Previously found aberrantly expressed miRNAs in maternal circulation [83]. New evidence suggests that miRNAs are specifically expressed in maternal blood of FGR in the second trimester of pregnancy, suggesting possible fetal growth markers [84]. Besides, Miranda et al. reported that placental exosome-derived miRNAs in maternal plasma can predict fetal growth and can be used as indicators of placental function [85]. Studies have shown that EV miR-150 derived from umbilical vein of normal piglets can promote angiogenesis in intrauterine growth restriction pigs [86]. It is reported that circulating plasma exosomes in early pregnancy had the same C19MC microRNA as placental tissues of GH, PE, and FGR patients after delivery [87]. Maternal plasma exosome analysis of selected C19MC microRNAs [88] showed that FGR women had a new downregulated biomarker (miR-520a-5p) in the first three months of pregnancy, which was not found in maternal plasma analysis [89]. In summary, these established findings strongly demonstrate the important role of EVs and encapsulation factors including miRNAs in FGR, providing new clues for understanding the pathogenesis of FGR.

3.4. EVs and Intrahepatic Cholestasis of Pregnancy (ICP). ICP is a common complication during pregnancy. Due to bile acid toxicity, the incidence and mortality of perinatal complications increased significantly. The etiology of ICP is still unclear, which may be related to female hormones, genetic and environmental factors. The previously published data

show the pivotal role of EVs in ICP. Those active factors usually consist of lipids, proteins, and nucleotides. The upregulation of miR-21, miR-29a, and miR-590-3p in urinary exosomes can increase the incidence of ICP by downregulating intercellular adhesion molecule 1 (ICAM1) [90]. Nevertheless, more studies are needed to further clarify the role of EVs and EV-encapsulated bioactive factors in ICP.

3.5. EVS and Spontaneous Abortion or Premature Delivery. Spontaneous abortion is highly correlated with embryo chromosomal abnormalities. Premature birth will cause great harm to pregnant women and fetuses. The organ development of premature infants is not good. The smaller the gestational age at birth, the lighter the weight, and the worse the prognosis. The causes of premature delivery include infection, malnutrition, cervical insufficiency, uterine malformation, and pregnancy complications. EVs have been shown to be involved in the development of spontaneous abortion and premature delivery by regulating homeostasis imbalances, particularly inflammation and endocrine signals [91]. MSC-derived exosomes regulate maternal-fetal interface T cells and macrophage-mediated immune response, affecting the outcome of spontaneous abortion or premature delivery [92]. The key role of stem cell-derived EVs in animal models of pregnancy has also been demonstrated [93]. The exact mechanism of endometrial cell-derived EVs mediating maternal crosstalk and affecting pregnancy outcomes during implantation remains unclear. Some studies have shown that EVs derived from placental tissue can predict pregnancy outcomes, including spontaneous abortion and premature delivery. Panfoli et al. confirmed that MSC-EVs affect aerobic metabolism in term and preterm infants [94]. Most importantly, EVs are professional carriers of fetal signals that affect pregnancy outcomes [95]. Amniotic fluid EVs have been shown to deliver information to normal and abnormal births [96]. In addition, exosomal miRNAs were found in maternal circulation, which may represent the “fingerprint” of pregnancy progression [97]. In summary, the study of EVs and their bioactive factors in spontaneous abortion or premature delivery is expected to find new therapeutic strategies for these diseases.

3.6. EVS and Prenatal Diagnosis. Prenatal diagnosis includes chromosomal abnormalities, sexually related genetic diseases, genetic metabolic defects, and congenital structural abnormalities. The important role of circulating EVs has been demonstrated in prenatal and neurodegenerative diseases [98]. Studies have shown that EV miRNAs can be used as biomarkers for prenatal diagnosis of congenital hydronephrosis [99]. They found that reduced expression of EV-transmitting miR-300 and miR-299-5p in amniotic fluid of congenital hydronephrosis could predict renal fibrosis. Interestingly, studies by Goetzl et al. showed that EVs derived from fetal central nervous system could be purified from maternal plasma, which was related to the abnormal proliferation and differentiation of neural stem cells [100]. Therefore, EVs may be a potential way for early prenatal diagnosis of fetal neurological diseases. EVs, especially exosomes, are also involved in Down syndrome [101], suggest-

ing that EVs play an important role in the regulation of central nervous system development. Although EVs and the transfer of bioactive factors have been associated with some prenatal and neurodegenerative diseases, more studies need to explore their role in prenatal diagnosis.

4. Conclusion and Perspectives

At present, studies have shown that EVs play a key role in tumorigenesis, stem cell capacity maintenance, inflammation, and immune disorders. They participate in the exchange of substances and information between cells by transmitting bioactive molecules, including lipids, proteins, and nucleotides. Cellular EVs in placenta tissue have a good record in maternal circulation, thus affecting pregnancy outcomes. Targeting EVs and the encapsulated bioactive factors may be promising strategies for the treatment and prevention of pregnancy disorders. However, the molecular mechanism and function of EVs in placenta and pregnancy-related complications warrant further elucidation in the future.

Conflicts of Interest

The authors declare that they have no conflicts of interest.

Authors' Contributions

Zengfang Wang, Ruizhen Yang, Jiaojiao Zhang, and Pingping Wang contributed equally to this work.

Acknowledgments

This work is funded by the Weifang Health Science and Technology Program (wfwjsk2019-031) and Shandong Medical and Health Science and Technology Program (2018WS091 and 2015WS0085).

References

- [1] C. Théry, K. W. Witwer, E. Aikawa et al., “Minimal information for studies of extracellular vesicles 2018 (MISEV 2018): a position statement of the International Society for Extracellular Vesicles and update of the MISEV2014 guidelines,” *Journal of Extracellular Vesicles*, vol. 7, no. 1, 2018.
- [2] G. van Niel, G. D'Angelo, and G. Raposo, “Shedding light on the cell biology of extracellular vesicles,” *Nature Reviews. Molecular Cell Biology*, vol. 19, no. 4, pp. 213–228, 2018.
- [3] M. Colombo, G. Raposo, and C. Théry, “Biogenesis, secretion, and intercellular interactions of exosomes and other extracellular vesicles,” *Annual Review of Cell and Developmental Biology*, vol. 30, no. 1, pp. 255–289, 2014.
- [4] J. Meldolesi, “Exosomes and ectosomes in intercellular communication,” *Current Biology*, vol. 28, no. 8, pp. R435–R444, 2018.
- [5] Q. Qu, Y. Pang, C. Zhang, L. Liu, and Y. Bi, “Exosomes derived from human umbilical cord mesenchymal stem cells inhibit vein graft intimal hyperplasia and accelerate reendothelialization by enhancing endothelial function,” *Stem Cell Research & Therapy*, vol. 11, no. 1, 2020.
- [6] R. M. Johnstone, M. Adam, and B. T. Pan, “The fate of the transferrin receptor during maturation of sheep reticulocytes

- in vitro," *Canadian Journal of Biochemistry and Cell Biology*, vol. 62, no. 11, pp. 1246–1254, 1984.
- [7] H. Valadi, K. Ekström, A. Bossios, M. Sjöstrand, J. J. Lee, and J. O. Lötvall, "Exosome-mediated transfer of mRNAs and microRNAs is a novel mechanism of genetic exchange between cells," *Nature Cell Biology*, vol. 9, no. 6, pp. 654–659, 2007.
 - [8] G. Lia, C. di Vito, M. Cerrano et al., "Extracellular vesicles after allogeneic hematopoietic cell transplantation: emerging role in post-transplant complications," *Frontiers in Immunology*, vol. 11, p. 422, 2020.
 - [9] A. Jurj, O. Zanoaga, C. Braicu et al., "A comprehensive picture of extracellular vesicles and their contents. molecular transfer to cancer cells," *Cancers*, vol. 12, no. 2, p. 298, 2020.
 - [10] C. Yang, S. Sun, Q. Zhang et al., "Exosomes of antler mesenchymal stem cells improve postoperative cognitive dysfunction in cardiopulmonary bypass rats through inhibiting the TLR2/TLR4 signaling pathway," *Stem Cells International*, vol. 2020, Article ID 2134565, 13 pages, 2020.
 - [11] M. Khan, E. Nickoloff, T. Abramova et al., "Embryonic stem cell-derived exosomes promote endogenous repair mechanisms and enhance cardiac function following myocardial infarction," *Circulation Research*, vol. 117, no. 1, pp. 52–64, 2015.
 - [12] G. Zhao, Y. Ge, C. Zhang et al., "Progress of mesenchymal stem cell-derived exosomes in tissue repair," *Current Pharmaceutical Design*, vol. 26, no. 17, pp. 2022–2037, 2020.
 - [13] M. Shao, M. Jin, S. Xu et al., "Exosomes from long noncoding RNA-Gm37494-ADSCs repair spinal cord injury via shifting microglial M1/M2 polarization," *Inflammation*, vol. 43, no. 4, pp. 1536–1547, 2020.
 - [14] A. Casado-Diaz, J. M. Quesada-Gomez, and G. Dorado, "Extracellular vesicles derived from mesenchymal stem cells (MSC) in regenerative medicine: applications in skin wound healing," *Frontiers in Bioengineering and Biotechnology*, vol. 8, p. 146, 2020.
 - [15] C. F. Ruivo, B. Adem, M. Silva, and S. A. Melo, "The biology of cancer exosomes: insights and new perspectives," *Cancer Research*, vol. 77, no. 23, pp. 6480–6488, 2017.
 - [16] R. S. Que, C. Lin, G. P. Ding, Z. R. Wu, and L. P. Cao, "Increasing the immune activity of exosomes: the effect of miRNA-depleted exosome proteins on activating dendritic cell/cytokine-induced killer cells against pancreatic cancer," *Journal of Zhejiang University. Science. B*, vol. 17, no. 5, pp. 352–360, 2016.
 - [17] F. Fanini and M. Fabbri, "Cancer-derived exosomal microRNAs shape the immune system within the tumor microenvironment: state of the art," *Seminars in Cell & Developmental Biology*, vol. 67, pp. 23–28, 2017.
 - [18] M. G. Appiah, E. J. Park, S. Darkwah et al., "Intestinal epithelium-derived lumenally released extracellular vesicles in sepsis exhibit the ability to suppress TNF- α and IL-17A expression in mucosal inflammation," *International Journal of Molecular Sciences*, vol. 21, no. 22, p. 8445, 2020.
 - [19] G. Raposo, H. W. Nijman, W. Stoorvogel et al., "B lymphocytes secrete antigen-presenting vesicles," *The Journal of Experimental Medicine*, vol. 183, no. 3, pp. 1161–1172, 1996.
 - [20] G. Qiu, G. Zheng, M. Ge et al., "Functional proteins of mesenchymal stem cell-derived extracellular vesicles," *Stem Cell Research & Therapy*, vol. 10, no. 1, p. 359, 2019.
 - [21] N. Edo, K. Kawakami, Y. Fujita et al., "Exosomes expressing thyrotropin receptor attenuate autoantibody-mediated stimulation of cyclic adenosine monophosphate production," *Thyroid*, vol. 29, no. 7, pp. 1012–1017, 2019.
 - [22] S. Baskaran, M. K. Panner Selvam, and A. Agarwal, "Exosomes of male reproduction," *Advances in Clinical Chemistry*, vol. 95, pp. 149–163, 2020.
 - [23] A. Sabapatha, C. Gercel-Taylor, and D. D. Taylor, "Specific isolation of placenta-derived exosomes from the circulation of pregnant women and their immunoregulatory consequences," *American Journal of Reproductive Immunology*, vol. 56, no. 5-6, pp. 345–355, 2006.
 - [24] L. Frängsmyr, V. Baranov, O. Nagaeva, U. Stendahl, L. Kjellberg, and L. Mincheva-Nilsson, "Cytoplasmic microvesicular form of Fas ligand in human early placenta: switching the tissue immune privilege hypothesis from cellular to vesicular level," *Molecular Human Reproduction*, vol. 11, no. 1, pp. 35–41, 2005.
 - [25] M. Hedlund, A.-C. Stenqvist, O. Nagaeva et al., "Human placenta expresses and secretes NKG2D ligands via exosomes that down-modulate the cognate receptor expression: evidence for immunosuppressive function," *Journal of Immunology*, vol. 183, no. 1, pp. 340–351, 2009.
 - [26] M. Gill, C. Motta-Mejia, N. Kandzija et al., "Placental syncytiotrophoblast-derived extracellular vesicles carry active NEP (neprilysin) and are increased in preeclampsia," *Hypertension*, vol. 73, no. 5, pp. 1112–1119, 2019.
 - [27] S. A. Mathew, C. Naik, P. A. Cahill, and R. R. Bhande, "Placental mesenchymal stromal cells as an alternative tool for therapeutic angiogenesis," *Cellular and Molecular Life Sciences*, vol. 77, no. 2, pp. 253–265, 2020.
 - [28] X. Li, L. Liu, J. Yang et al., "Exosome derived from human umbilical cord mesenchymal stem cell mediates MiR-181c attenuating burn-induced excessive inflammation," *eBioMedicine*, vol. 8, pp. 72–82, 2016.
 - [29] D. Surico, V. Bordin, V. Cantaluppi et al., "Preeclampsia and intrauterine growth restriction: role of human umbilical cord mesenchymal stem cells-trophoblast cross-talk," *PLoS One*, vol. 14, no. 6, p. e0218437, 2019.
 - [30] S. Suvakov, H. Cubro, W. M. White et al., "Targeting senescence improves angiogenic potential of adipose-derived mesenchymal stem cells in patients with preeclampsia," *Biology of Sex Differences*, vol. 10, no. 1, p. 49, 2019.
 - [31] L. L. Wang, Y. Yu, H. B. Guan, and C. Qiao, "Effect of human umbilical cord mesenchymal stem cell transplantation in a rat model of preeclampsia," *Reproductive Sciences*, vol. 23, no. 8, pp. 1058–1070, 2016.
 - [32] S. L. Nguyen, J. W. Greenberg, H. Wang, B. W. Collaer, J. Wang, and M. G. Petroff, "Quantifying murine placental extracellular vesicles across gestation and in preterm birth data with tidyNano: a computational framework for analyzing and visualizing nanoparticle data in R," *PLoS One*, vol. 14, no. 6, article e0218270, 2019.
 - [33] S. Sarker, K. Scholz-Romero, A. Perez et al., "Placenta-derived exosomes continuously increase in maternal circulation over the first trimester of pregnancy," *Journal of Translational Medicine*, vol. 12, no. 1, p. 204, 2014.
 - [34] D. Tannetta, I. Masliukaite, M. Vatish, C. Redman, and I. Sargent, "Update of syncytiotrophoblast derived extracellular vesicles in normal pregnancy and preeclampsia," *Journal of Reproductive Immunology*, vol. 119, pp. 98–106, 2017.




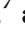

- [35] D. I. Chiarello, R. Salsoso, F. Toledo, A. Mate, C. M. Vázquez, and L. Sobrevia, "Foetoplacental communication via extracellular vesicles in normal pregnancy and preeclampsia," *Molecular Aspects of Medicine*, vol. 60, pp. 69–80, 2018.
- [36] G. E. Rice, K. Scholz-Romero, E. Sweeney et al., "The effect of glucose on the release and bioactivity of exosomes from first trimester trophoblast cells," *The Journal of Clinical Endocrinology and Metabolism*, vol. 100, no. 10, pp. E1280–E1288, 2015.
- [37] A. G. Lokossou, C. Toudic, P. T. Nguyen et al., "Endogenous retrovirus-encoded Syncytin-2 contributes to exosome-mediated immunosuppression of T cells," *Biology of Reproduction*, vol. 102, no. 1, pp. 185–198, 2020.
- [38] S. Sheller-Miller, K. Choi, C. Choi, and R. Menon, "Cyclic-recombinase-reporter mouse model to determine exosome communication and function during pregnancy," *American Journal of Obstetrics and Gynecology*, vol. 221, no. 5, pp. 502.e1–502.e12, 2019.
- [39] F. Pouresmaeli, I. Azari, S. Arsang-Jang, M. Taheri, and S. Ghafouri-Fard, "Association between expression of long noncoding RNAs in placenta and pregnancy features," *Personalized Medicine*, vol. 16, no. 6, pp. 457–466, 2019.
- [40] A. Kamrani, I. Alipourfard, H. Ahmadi-Khiavi et al., "The role of epigenetic changes in preeclampsia," *BioFactors*, vol. 45, no. 5, pp. 712–724, 2019.
- [41] D. Wu, Y. Xu, Y. Zou et al., "Long noncoding RNA 00473 is involved in preeclampsia by LSD1 binding-regulated TFPI2 transcription in trophoblast cells," *Molecular Therapy - Nucleic Acids*, vol. 12, pp. 381–392, 2018.
- [42] E. Delorme-Axford, A. Bayer, Y. Sadovsky, and C. B. Coyne, "Autophagy as a mechanism of antiviral defense at the maternal-fetal interface," *Autophagy*, vol. 9, no. 12, pp. 2173–2174, 2013.
- [43] B. Zhang, R. Liang, M. Zheng, L. Cai, and X. Fan, "Surface-functionalized nanoparticles as efficient tools in targeted therapy of pregnancy complications," *International Journal of Molecular Sciences*, vol. 20, no. 15, p. 3642, 2019.
- [44] J. E. Song, S. J. Park, K. Y. Lee, and W. J. Lee, "Amniotic fluid HIF1 α and exosomal HIF1 α in cervical insufficiency patients with physical examination-indicated cerclage," *The Journal of Maternal-Fetal & Neonatal Medicine*, vol. 32, no. 14, pp. 2287–2294, 2019.
- [45] B. Lee, I. Saadeldin, and H. J. Oh, "Embryonic–maternal cross-talk via exosomes: potential implications," *Stem Cells and Cloning: Advances and Applications*, vol. 8, pp. 103–107, 2015.
- [46] G. Truong, D. Guanzon, V. Kinhal et al., "Oxygen tension regulates the miRNA profile and bioactivity of exosomes released from extravillous trophoblast cells - liquid biopsies for monitoring complications of pregnancy," *PLoS One*, vol. 12, no. 3, article e0174514, 2017.
- [47] P. Pillay, K. Moodley, J. Moodley, and I. Mackraj, "Placenta-derived exosomes: potential biomarkers of preeclampsia," *International Journal of Nanomedicine*, vol. Volume 12, pp. 8009–8023, 2017.
- [48] R. Gadde, D. Cd, and S. R. Sheela, "Placental protein 13: an important biological protein in preeclampsia," *Journal of Circulating Biomarkers*, vol. 7, article 1849454418786159, 2018.
- [49] C. Salomon, D. Guanzon, K. Scholz-Romero et al., "Placental exosomes as early biomarker of preeclampsia: potential role of exosomal microRNAs across gestation," *The Journal of Clinical Endocrinology and Metabolism*, vol. 102, no. 9, pp. 3182–3194, 2017.
- [50] P. Pillay, N. Maharaj, J. Moodley, and I. Mackraj, "Placental exosomes and pre-eclampsia: maternal circulating levels in normal pregnancies and, early and late onset pre-eclamptic pregnancies," *Placenta*, vol. 46, pp. 18–25, 2016.
- [51] X. Chang, J. Yao, Q. He, M. Liu, T. Duan, and K. Wang, "Exosomes from women with preeclampsia induced vascular dysfunction by delivering sFlt (soluble Fms-like tyrosine kinase)-1 and sEng (soluble endoglin) to endothelial cells," *Hypertension*, vol. 72, no. 6, pp. 1381–1390, 2018.
- [52] K. Maduray, J. Moodley, and I. Mackraj, "The impact of circulating exosomes derived from early and late onset preeclamptic pregnancies on inflammatory cytokine secretion by BeWo cells," *European Journal of Obstetrics, Gynecology, and Reproductive Biology*, vol. 247, pp. 156–162, 2020.
- [53] O. Biro and J. Rigo Jr., "The pathogenetic role and expression profile of microRNAs in preeclampsia," *Orvosi Hetilap*, vol. 159, no. 14, pp. 547–556, 2018.
- [54] E. Devor, D. Santillan, S. Scroggins, A. Warriar, and M. Santillan, "Trimester-specific plasma exosome microRNA expression profiles in preeclampsia," *The Journal of Maternal-Fetal & Neonatal Medicine*, vol. 33, no. 18, pp. 3116–3124, 2020.
- [55] P. Pillay, M. Vatish, R. Duarte, J. Moodley, and I. Mackraj, "Exosomal microRNA profiling in early and late onset preeclamptic pregnant women reflects pathophysiology," *International Journal of Nanomedicine*, vol. Volume 14, pp. 5637–5657, 2019.
- [56] H. Li, Y. Ouyang, E. Sadovsky, W. T. Parks, T. Chu, and Y. Sadovsky, "Unique microRNA signals in plasma exosomes from pregnancies complicated by preeclampsia," *Hypertension*, vol. 75, no. 3, pp. 762–771, 2020.
- [57] O. Biró, B. Alasztics, A. Molvarec, J. Joó, B. Nagy, and J. Rigó Jr., "Various levels of circulating exosomal total-miRNA and miR-210 hypoxamiR in different forms of pregnancy hypertension," *Pregnancy Hypertension*, vol. 10, pp. 207–212, 2017.
- [58] L. Shen, Y. Li, R. Li et al., "Placenta-associated serum exosomal miR-155 derived from patients with preeclampsia inhibits eNOS expression in human umbilical vein endothelial cells," *International Journal of Molecular Medicine*, vol. 41, no. 3, pp. 1731–1739, 2018.
- [59] T. M. K. Motawi, D. Sabry, N. W. Maurice, and S. M. Rizk, "Role of mesenchymal stem cells exosomes derived microRNAs; miR-136, miR-494 and miR-495 in pre-eclampsia diagnosis and evaluation," *Archives of Biochemistry and Biophysics*, vol. 659, pp. 13–21, 2018.
- [60] O. Biró, Á. Fóthi, B. Alasztics, B. Nagy, T. I. Orbán, and J. Rigó Jr., "Circulating exosomal and Argonaute-bound microRNAs in preeclampsia," *Gene*, vol. 692, pp. 138–144, 2019.
- [61] I. Hromadnikova, L. Dvorakova, K. Kotlabova, and L. Krofta, "The prediction of gestational hypertension, preeclampsia and fetal growth restriction via the first trimester screening of plasma exosomal C19MC microRNAs," *International Journal of Molecular Sciences*, vol. 20, no. 12, p. 2972, 2019.
- [62] Z. Xueya, L. Yamei, C. Sha et al., "Exosomal encapsulation of miR-125a-5p inhibited trophoblast cell migration and proliferation by regulating the expression of VEGFA in preeclampsia," *Biochemical and Biophysical Research Communications*, vol. 525, no. 3, pp. 646–653, 2020.

- [63] Z. H. Xiong, J. Wei, M. Q. Lu, M. Y. Jin, and H. L. Geng, "Protective effect of human umbilical cord mesenchymal stem cell exosomes on preserving the morphology and angiogenesis of placenta in rats with preeclampsia," *Biomedicine & Pharmacotherapy*, vol. 105, pp. 1240–1247, 2018.
- [64] Y. Chen, H. Ding, M. Wei et al., "MSC-secreted exosomal H19 promotes trophoblast cell invasion and migration by downregulating let-7b and upregulating FOXO1," *Molecular Therapy - Nucleic Acids*, vol. 19, pp. 1237–1249, 2020.
- [65] M. Arias, L. J. Monteiro, S. Acuña-Gallardo et al., "Extracellular vesicle concentration in maternal plasma as an early marker of gestational diabetes," *Revista Médica de Chile*, vol. 147, no. 12, pp. 1503–1509, 2019.
- [66] R. Sharma, M. Kumari, P. Prakash, S. Gupta, and S. Tiwari, "Phosphoenolpyruvate carboxykinase in urine exosomes reflect impairment in renal gluconeogenesis in early insulin resistance and diabetes," *American Journal of Physiology. Renal Physiology*, vol. 318, no. 3, pp. F720–F731, 2020.
- [67] T. DeLong, T. A. Wiles, R. L. Baker et al., "Pathogenic CD4 T cells in type 1 diabetes recognize epitopes formed by peptide fusion," *Science*, vol. 351, no. 6274, pp. 711–714, 2016.
- [68] Y. Lytvyn, F. Xiao, C. R. J. Kennedy et al., "Assessment of urinary microparticles in normotensive patients with type 1 diabetes," *Diabetologia*, vol. 60, no. 3, pp. 581–584, 2017.
- [69] A. Sakurai, H. Ono, A. Ochi et al., "Involvement of Elf 3 on Smad 3 activation-dependent injuries in podocytes and excretion of urinary exosome in diabetic nephropathy," *PLoS One*, vol. 14, no. 5, article e0216788, 2019.
- [70] J. Hu, S. Wang, Z. Xiong et al., "Exosomal Mst1 transfer from cardiac microvascular endothelial cells to cardiomyocytes deteriorates diabetic cardiomyopathy," *Biochimica et Biophysica Acta - Molecular Basis of Disease*, vol. 1864, no. 11, pp. 3639–3649, 2018.
- [71] D. Beuzelin and B. Kaeffer, "Exosomes and miRNA-Loaded biomimetic nanovehicles, a focus on their potentials preventing type-2 diabetes linked to metabolic syndrome," *Front Immunol*, vol. 9, p. 2711, 2018.
- [72] P. Venkat, C. Cui, Z. Chen et al., "CD133+exosome treatment improves cardiac function after stroke in type 2 diabetic mice," *Translational Stroke Research*, vol. 12, pp. 112–124, 2020.
- [73] J. Chen, J. Chen, Y. Cheng et al., "Mesenchymal stem cell-derived exosomes protect beta cells against hypoxia-induced apoptosis via miR-21 by alleviating ER stress and inhibiting p38 MAPK phosphorylation," *Stem Cell Research & Therapy*, vol. 11, no. 1, p. 97, 2020.
- [74] P. Venkat, M. Chopp, and J. Chen, "Cell-based and exosome therapy in diabetic stroke," *Stem Cells Translational Medicine*, vol. 7, no. 6, pp. 451–455, 2018.
- [75] J. Liu, S. Z. Wang, Q. L. Wang, J. G. Du, and B. B. Wang, "Gestational diabetes mellitus is associated with changes in the concentration and bioactivity of placental exosomes in the maternal circulation across gestation," *European Review for Medical and Pharmacological Sciences*, vol. 22, no. 7, pp. 2036–2043, 2018.
- [76] T. Saez, P. de Vos, L. Sobrevia, and M. M. Faas, "Is there a role for exosomes in foetoplacental endothelial dysfunction in gestational diabetes mellitus?," *Placenta*, vol. 61, pp. 48–54, 2018.
- [77] N. Jayabalan, A. Lai, V. Ormazabal et al., "Adipose tissue exosomal proteomic profile reveals a role on placenta glucose metabolism in gestational diabetes mellitus," *The Journal of Clinical Endocrinology and Metabolism*, vol. 104, no. 5, pp. 1735–1752, 2019.
- [78] L. B. James-Allan, F. J. Rosario, K. Barner et al., "Regulation of glucose homeostasis by small extracellular vesicles in normal pregnancy and in gestational diabetes," *The FASEB Journal*, vol. 34, no. 4, pp. 5724–5739, 2020.
- [79] E. Guarino, C. Delli Poggi, G. E. Grieco et al., "Circulating MicroRNAs as Biomarkers of Gestational Diabetes Mellitus: Updates and Perspectives," *International Journal of Endocrinology*, vol. 2018, Article ID 6380463, 11 pages, 2018.
- [80] S. Nair, N. Jayabalan, D. Guanzon et al., "Human placental exosomes in gestational diabetes mellitus carry a specific set of miRNAs associated with skeletal muscle insulin sensitivity," *Clinical Science (London, England)*, vol. 132, no. 22, pp. 2451–2467, 2018.
- [81] J. F. Floriano, G. Willis, F. Catapano et al., "Exosomes could offer new options to combat the long-term complications inflicted by gestational diabetes mellitus," *Cells*, vol. 9, no. 3, p. 675, 2020.
- [82] A. S. Herrera-Van Oostdam, M. Salgado-Bustamante, J. A. Lopez, D. A. Herrera-Van Oostdam, and Y. Lopez-Hernandez, "Placental exosomes viewed from an 'omics' perspective: implications for gestational diabetes biomarkers identification," *Biomarkers in Medicine*, vol. 13, no. 8, pp. 675–684, 2019.
- [83] Q. Ge, Y. Zhu, H. Li, F. Tian, X. Xie, and Y. Bai, "Differential expression of circulating miRNAs in maternal plasma in pregnancies with fetal macrosomia," *International Journal of Molecular Medicine*, vol. 35, no. 1, pp. 81–91, 2015.
- [84] R. S. Rodosthenous, H. H. Burris, A. P. Sanders et al., "Second trimester extracellular microRNAs in maternal blood and fetal growth: an exploratory study," *Epigenetics*, vol. 12, no. 9, pp. 804–810, 2017.
- [85] J. Miranda, C. Paules, S. Nair et al., "Placental exosomes profile in maternal and fetal circulation in intrauterine growth restriction - liquid biopsies to monitoring fetal growth," *Placenta*, vol. 64, pp. 34–43, 2018.
- [86] J. Luo, Y. Fan, L. Shen et al., "The pro-angiogenesis of exosomes derived from umbilical cord blood of intrauterine growth restriction pigs was repressed associated with MiRNAs," *International Journal of Biological Sciences*, vol. 14, no. 11, pp. 1426–1436, 2018.
- [87] I. Hromadnikova, K. Kotlabova, M. Ondrackova et al., "Expression profile of C19MC microRNAs in placental tissue in pregnancy-related complications," *DNA and Cell Biology*, vol. 34, no. 6, pp. 437–457, 2015.
- [88] K. Kotlabova, J. Doucha, and I. Hromadnikova, "Placental-specific microRNA in maternal circulation - identification of appropriate pregnancy-associated microRNAs with diagnostic potential," *Journal of Reproductive Immunology*, vol. 89, no. 2, pp. 185–191, 2011.
- [89] I. Hromadnikova, K. Kotlabova, K. Ivankova, and L. Krofta, "First trimester screening of circulating C19MC microRNAs and the evaluation of their potential to predict the onset of preeclampsia and IUGR," *PLoS One*, vol. 12, no. 2, article e0171756, 2017.
- [90] P. Y. Jiang, X. J. Zhu, R. A. Jiang, Y. N. Zhang, L. Liu, and X. F. Yang, "MicroRNAs derived from urinary exosomes act as novel biomarkers in the diagnosis of intrahepatic cholestasis of pregnancy," *American Journal of Translational Research*, vol. 11, no. 9, pp. 6249–6261, 2019.

- [91] N. Jayabalan, A. Lai, S. Nair et al., "Quantitative proteomics by SWATH-MS suggest an association between circulating exosomes and maternal metabolic changes in gestational diabetes mellitus," *Proteomics*, vol. 19, no. 1-2, article e1800164, 2019.
- [92] Y. J. Xiang, Y. Y. Hou, H. L. Yan et al., "Mesenchymal stem cells-derived exosomes improve pregnancy outcome through inducing maternal tolerance to the allogeneic fetus in abortion-prone mating mouse," *Kaohsiung Journal of Medical Sciences*, vol. 36, no. 5, pp. 363–370, 2020.
- [93] A. Mitchell, H. Wanczyk, T. Jensen, and C. Finck, "Human induced pluripotent stem cells ameliorate hyperoxia-induced lung injury in a mouse model," *American Journal of Translational Research*, vol. 12, no. 1, pp. 292–307, 2020.
- [94] I. Panfoli, S. Ravera, M. Podestà et al., "Exosomes from human mesenchymal stem cells conduct aerobic metabolism in term and preterm newborn infants," *The FASEB Journal*, vol. 30, no. 4, pp. 1416–1424, 2016.
- [95] C. Salomon, Z. Nuzhat, C. L. Dixon, and R. Menon, "Placental exosomes during gestation: liquid biopsies carrying signals for the regulation of human parturition," *Current Pharmaceutical Design*, vol. 24, no. 9, pp. 974–982, 2018.
- [96] C. L. Dixon, S. Sheller-Miller, G. R. Saade et al., "Amniotic fluid exosome proteomic profile exhibits unique pathways of term and preterm labor," *Endocrinology*, vol. 159, no. 5, pp. 2229–2240, 2018.
- [97] R. Menon, C. Debnath, A. Lai et al., "Circulating exosomal miRNA profile during term and preterm birth pregnancies: a longitudinal study," *Endocrinology*, vol. 160, no. 2, pp. 249–275, 2019.
- [98] X. Cai, F. Janku, Q. Zhan, and J. B. Fan, "Accessing genetic information with liquid biopsies," *Trends in Genetics*, vol. 31, no. 10, pp. 564–575, 2015.
- [99] J. Xie, Y. Zhou, W. Gao, Z. Li, Z. Xu, and L. Zhou, "The relationship between amniotic fluid miRNAs and congenital obstructive nephropathy," *American Journal of Translational Research*, vol. 9, no. 4, pp. 1754–1763, 2017.
- [100] L. Goetzl, N. Darbinian, and N. Merabova, "Noninvasive assessment of fetal central nervous system insult: potential application to prenatal diagnosis," *Prenatal Diagnosis*, vol. 39, no. 8, pp. 609–615, 2019.
- [101] E. D. Hamlett, A. LaRosa, E. J. Mufson, J. Fortea, A. Ledreux, and A. C. Granholm, "Exosome release and cargo in Down syndrome," *Developmental Neurobiology*, vol. 79, no. 7, pp. 639–655, 2019.

Research Article

Investigation of Newly Diagnosed Drug-Naive Patients with Systemic Autoimmune Diseases Revealed the Cleaved Peptide Tyrosine Tyrosine (PYY 3-36) as a Specific Plasma Biomarker of Rheumatoid Arthritis

Jozsef A. Balog ^{1,2}, Agnes Kemeny ^{3,4}, Laszlo G. Puskas ^{1,5,6}, Szilard Burcsar,⁷
Attila Balog ⁷, and Gabor J. Szebeni ^{1,8,9}

¹Biological Research Centre, Szeged, Hungary

²PhD School of Biology, University of Szeged, Szeged, Hungary

³Department of Medical Biology, University of Pecs, Pecs, Hungary

⁴Department of Pharmacology and Pharmacotherapy, Medical School, University of Pecs, Pecs, Hungary

⁵Avicor Ltd. Szeged, Hungary

⁶Avidin Ltd., Szeged, Hungary

⁷Department of Rheumatology and Immunology, Faculty of Medicine, Albert Szent-Gyorgyi Health Centre, University of Szeged, Szeged, Hungary

⁸Department of Physiology, Anatomy and Neuroscience, Faculty of Science and Informatics, University of Szeged, Szeged, Hungary

⁹CS-Smartlab Devices, Kozarmisleny, Hungary

Correspondence should be addressed to Attila Balog; balog.attila@med.u-szeged.hu
and Gabor J. Szebeni; g.szebeni@avidinbiotech.com

Received 23 February 2021; Revised 24 April 2021; Accepted 11 May 2021; Published 17 June 2021

Academic Editor: Shushan Yan

Copyright © 2021 Jozsef A. Balog et al. This is an open access article distributed under the Creative Commons Attribution License, which permits unrestricted use, distribution, and reproduction in any medium, provided the original work is properly cited.

There is a current imperative to reveal more precisely the molecular pathways of early onset of systemic autoimmune diseases (SADs). The investigation of newly diagnosed drug-naive SAD patients might contribute to identify novel disease-specific and prognostic markers. The multiplex analysis of 30 plasma proteins in 60 newly diagnosed drug-naive SADs, such as RA (rheumatoid arthritis, $n = 31$), SLE (systemic lupus erythematosus, $n = 19$), and SSc (systemic sclerosis, $n = 10$) patients, versus healthy controls (HCs, $n = 40$) was addressed. Thirty plasma cytokines were quantified using the Procarta Plex™ panel. The higher expression of IL-12p40, IL-10, IL-13, IFN- γ , M-CSF, IL-4, NTproBNP, IL-17A, BMP-9, PYY (3-36), GITRL, MMP-12, and TNFRSF6 was associated with RA; IL-12p40, M-CSF, IL-4, GITRL, and NTproBNP were higher in SLE; or NTproBNP, PYY (3-36), and MMP-12 were increased in SSc over HCs, respectively. The cleaved peptide tyrosine tyrosine (PYY 3-36) was elevated in RA (361.6 ± 47.7 pg/ml) vs. HCs (163.96 ± 14.5 pg/ml, mean \pm SEM, *** $p = 4 \times 10^{-5}$). The CI (95%) was 268.05-455.16 pg/ml for RA vs. 135.55-192.37 pg/ml for HCs. The elevated PYY (3-36) level correlated significantly with the increased IL-4 or GITRL concentration but not with the clinical scores (DAS28, CRP, ESR, RF, aMCV). We are the first to report cleaved PYY (3-36) as a specific plasma marker of therapy-naive RA. Additionally, the multiplex plasma protein analysis supported a disease-specific cytokine pattern in RA, SLE, and SSc, respectively.

1. Introduction

Systemic autoimmune rheumatic diseases (SADs) including rheumatoid arthritis (RA), systemic lupus erythematosus

(SLE), and systemic sclerosis (SSc) are characterized by an abnormal immune system response, complement dysregulation, imbalance of cytokines production, and inflammation [1]. Their etiology, complex pathogenesis, heterogeneous

presentation, and unpredictable disease course are still not fully understood [2]. Therefore, the limitation in diagnosing, classifying, and treating both RA, SLE, and SSc is significant. Clinical remission is reached in less than half of the patients, the personalized therapeutic strategy is still lacking, and the gap between the first symptoms and the diagnosis may often lead to irreversible pathologic changes [3]. SADs display clinical heterogeneity as presented by variable prognosis, unpredictable susceptibility to rapid progression to structural damage in joints in RA, and severe extra-articular organ manifestations in SLE and SSc. In summary, the need for biomarkers facilitating early diagnosis and profiling those individuals at the highest risk for a poor outcome has become essential [4]. Biomarkers of RA [5, 6], SLE [7, 8], or SSc [9, 10] have been recently reviewed elsewhere. Many of the previous studies have been performed in established or late-stage disease in SADs. There is a current imperative to reveal more precisely the molecular pathways of early treatment-naïve SADs [11]. Furthermore, very few studies have reported a systematic molecular characterization in RA, SLE, and SSc parallelly, but none in early treatment-naïve patients with SADs. The investigation of newly diagnosed drug-naïve SAD patients might contribute to identify novel disease-specific and prognostic markers. The parallel investigation of SADs also could give us the possibility to recognize novel checkpoints in their pathways and unknown molecular therapeutic targets. Therefore, we aimed to assay the plasma content of thirty soluble mediators in newly diagnosed therapy-naïve RA, SLE, or SSc patients versus age- and gender-matched healthy controls.

2. Materials and Methods

2.1. Patient and Public Involvement. Patients were enrolled during regular visits at the Department of Rheumatology and Immunology (University of Szeged). Healthy controls were voluntary staff members of the BRC or University of Szeged. Subjects were informed about the research by a physician. Written informed consent was obtained from all subjects, and our study was reviewed and approved by an independent ethical committee of the university. Laboratory studies and interpretations were performed on coded samples lacking personal and diagnostic identifiers. The study adhered to the tenets of the most recent revision of the Declaration of Helsinki. Details about the study design and handling of biological materials were submitted to the Human Investigation Review Board of the University of Szeged under the 149/2019-SZTE Project Identification code.

2.2. Study Cohorts. The multiplex protein analysis of 60 drug-naïve SAD patients, RA patients ($n = 31$, age median 57, 70.9% female (F), Supplementary Table 1); SLE patients ($n = 19$, age median 51, 89.4% F, Supplementary Table 2); SSc patients ($n = 10$, age median 51, 88.9% F, Supplementary Table 3), and 40 age- and gender-matched healthy controls (age median 48.5, 72.5% F) was performed. We enrolled newly diagnosed drug-naïve RA, SLE, and SSc patients, who had not received antirheumatic treatment,

including nonsteroidal anti-inflammatory drugs (NSAIDs), disease-modifying antirheumatic drugs (DMARDs), or glucocorticoids until the time of blood sampling. The RA patients were diagnosed according to the latest ACR/EULAR criteria [12] (Supplementary Table 1). The SLE patients who met the 2012 Systemic Lupus Collaborating Clinics (SLICC) criteria and in whom active, newly diagnosed SLE was present were considered eligible [13]. Several clinical and immunoserological parameters were present at the time of diagnosis of SLE (Supplementary Table 2). Ten newly diagnosed patients fulfilling the criteria proposed by the 2013 ACR/EULAR classification criteria for SSc were enrolled [14]. Two out of ten were further classified as those with limited cutaneous SSc, and eight out of ten with diffuse cutaneous scleroderma according to LeRoy et al. [15] (Supplementary Table 3). Healthy controls were age and gender matched to the patients, having a negative history of rheumatic symptoms and negative status upon detailed physical and laboratory examination. No comorbidities were detected in patients and controls that could have influenced our investigation, nor did they take any medication that could have interfered with the measurements.

2.3. Measurement of Plasma Proteins. After the withdrawal of 20 ml blood into an EDTA vacutainer (Becton Dickinson), human peripheral blood mononuclear cells and plasma samples were purified by Leucosep tubes (Greiner Bio-One, Austria). PBMCs were used for immunophenotyping in another project. Plasma fractions were stored at -80°C in aliquots before running the assay. Luminex xMAP technology was used to determine the protein concentrations of 30 distinct cytokines/chemokines performing Procarta Plex™ Immunoassay (ThermoFisher Scientific, Waltham, MA, USA) according to the instructions of the manufacturer. The Luminex panel was designed by the authors quantifying the proteins listed in Supplementary Table 4. Briefly, all samples were thawed and diluted with sterile phosphate-buffered saline (PBS) to 1:1 and were tested in a blind fashion and in duplicate. $25\ \mu\text{l}$ volume of each sample, standard, and universal assay buffer was added to a 96-well plate (provided with the kit) containing $50\ \mu\text{l}$ of capture antibody-coated, fluorescent-coded beads. Biotinylated detection antibody mixture and streptavidin-PE were added to the plate after the appropriate incubation period. After the last washing step, $120\ \mu\text{l}$ reading buffer was added to the wells, and the plate was incubated for an additional 5 minutes and read on the Luminex MAGPIX® instrument. Luminex xPonent 4.2 software was used for data acquisition. Five-PL regression curves were generated to plot the standard curves for all analytes by the Analyst 5.1 (Merck Millipore, Darmstadt, Germany) software calculating with bead median fluorescence intensity values. The panel of the investigated 30 plasma proteins and the range of the detection (in pg/ml from the lower limit to the upper limit) are available in the Supplementary Table 4. Data were pooled from two independent measurements and plotted in GraphPad Prism.

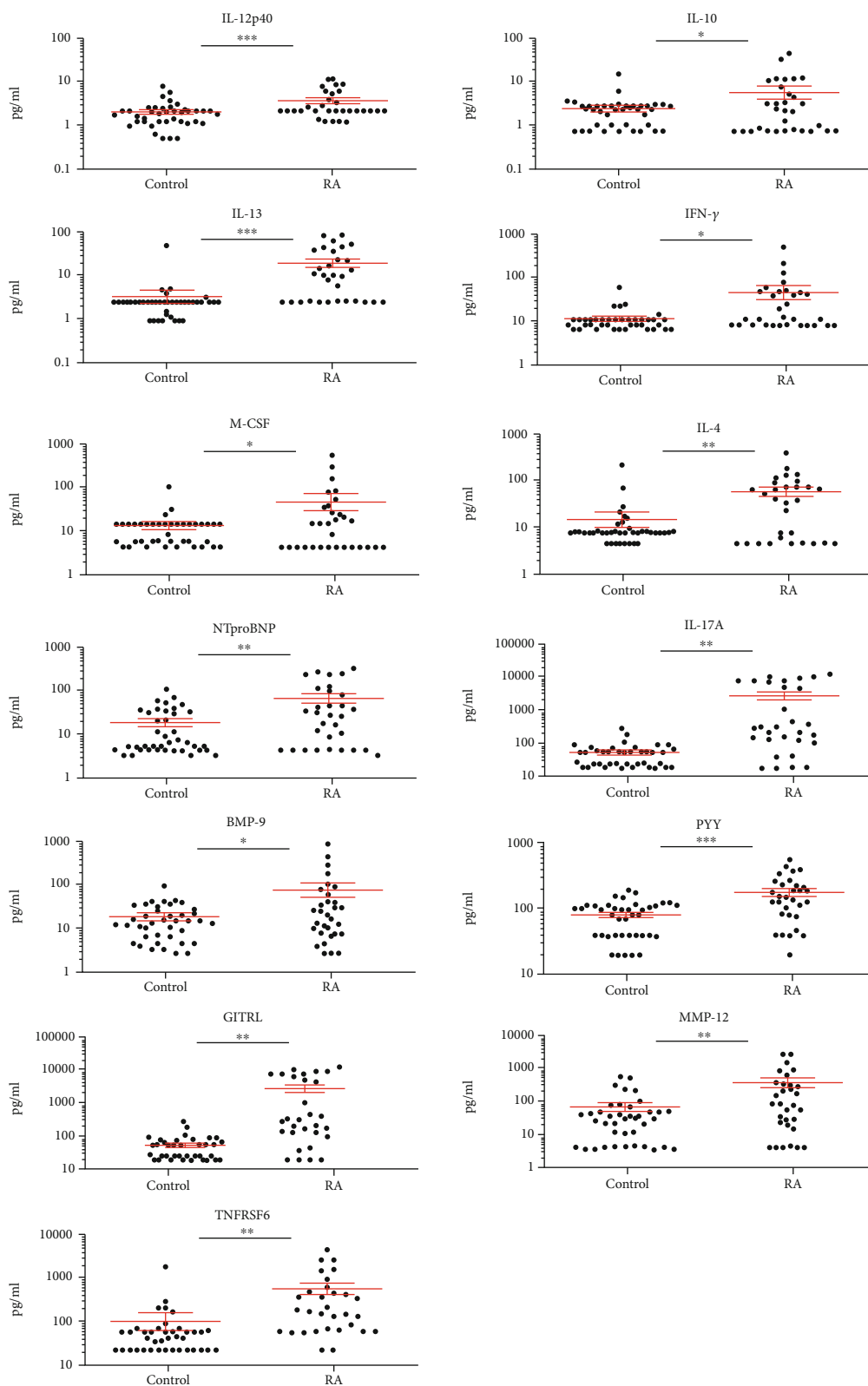


FIGURE 1: The scatter plots of the protein concentrations of plasma proteins (pg/ml) in drug-naive RA ($n = 31$) patients versus age- and gender-matched healthy controls ($n = 40$) with significant differences (one-way ANOVA, $*p < 0.05$; $**p < 0.01$, $***p < 0.001$) measured by the Luminex MAGPIX technology. The cleaved peptide tyrosine tyrosine PYY (3-36) was detected as being a novel marker of early-onset therapy-naive rheumatoid arthritis (RA) ($***p = 4 \times 10^{-5}$). The arithmetic mean \pm SEM are demonstrated for each cytokine (pg/ml) of RA ($n = 31$) patients versus age- and gender-matched healthy controls ($n = 40$). One dot is the average of two technical replicates.

TABLE 1: The summary of the significant differences of plasma cytokine concentrations between drug-naive autoimmune patients (RA, SLE, SSc) and healthy controls (HCs) in a pairwise comparison. The arithmetic means (mean), standard deviation (SD), and the standard error of the mean (SEM) of the plasma cytokine concentrations were calculated. The pairwise comparison of the concentrations of each cytokine of patients versus healthy controls (RA vs. HC; SLE vs. HC; SSc vs. HC) was carried out by one-way ANOVA (* $p < 0.05$; ** $p < 0.01$, *** $p < 0.001$). The 95% confidence intervals (CI, 95%) were calculated between patients and HCs for each cytokine separately. *Italic emphasis* corresponds to overlapping patient's CI with HCs.

Cytokine	Cohort	Mean (pg/ml)	SD	SEM	One-way ANOVA (p)	CI (95%)
IL-12p40	HC	4.18	2.85	0.45	9.7E-05	3.30-5.06
	RA	8.90	6.45	1.16		6.63-11.17
IL-10	HC	4.96	4.66	0.74	3.2E-02	<i>3.51-6.40</i>
	RA	12.02	19.69	3.54		5.09-18.95
IL-13	HC	7.25	15.53	2.46	9.7E-05	2.43-12.06
	RA	41.74	49.74	8.93		24.23-59.25
IFN- γ	HC	23.64	18.35	2.90	1.6E-02	17.96-29.33
	RA	98.83	191.03	34.31		31.58-166.07
M-CSF	HC	27.34	34.09	5.39	4.8E-02	<i>16.78-37.91</i>
	RA	100.58	227.01	40.77		20.66-180.49
IL-4	HC	31.14	69.44	10.98	1.7E-03	9.62-52.66
	RA	121.79	157.07	28.21		66.50-177.09
NTproBNP	HC	39.24	47.07	7.44	1.9E-03	24.64-53.82
	RA	142.07	194.66	34.96		73.55-210.59
IL-17A	HC	15.98	26.99	4.27	3.5E-03	7.62-24.34
	RA	154.17	288.13	51.75		52.74-255.6
BMP-9	HC	37.78	34.56	5.46	2.9E-02	27.07-48.49
	RA	160.67	347.69	62.45		38.27-283.06
PYY	HC	163.96	91.68	14.50	4.0E-05	135.55-192.37
	RA	361.60	265.77	47.73		268.05-455.16
GITRL	HC	110.19	100.94	15.96	1.4E-03	78.91-141.47
	RA	901.22	1498.96	269.22		373.54-1428.89
MMP-12	HC	154.26	278.20	43.99	7.4E-03	68.05-240.48
	RA	833.00	1525.20	273.93		296.09-1369.91
TNFRSF6	HC	209.45	574.09	90.77	3.9E-03	31.54-387.36
	RA	1200.63	1998.27	358.90		497.18-1904.07
IL-12p40	HC	4.18	2.85	0.45	5.7E-06	3.29-5.06
	SLE	10.86	7.43	1.70		7.52-14.20
M-CSF	HC	27.34	34.09	5.39	6.8E-03	<i>16.77-37.90</i>
	SLE	63.06	63.94	14.67		34.31-91.81
IL-4	HC	31.14	69.44	10.98	5.2E-02	9.61-52.65
	SLE	70.16	73.03	16.75		37.32-102.99
GITRL	HC	110.19	100.94	15.96	1.3E-02	<i>78.90-141.47</i>
	SLE	217.58	222.56	51.06		117.50-317.65
NTproBNP	HC	39.24	47.07	7.44	1.9E-02	24.64-53.82
	SLE	315.89	727.91	166.99		1.69-643.19
NTproBNP	HC	39.235	47.07	7.44	3.8E-03	24.64-53.82
	SSc	174.206	272.76	86.25		5.15-343.26
PYY	HC	163.9605	91.68	14.50	3.1E-02	135.54-192.37

TABLE 1: Continued.

Cytokine	Cohort	Mean (pg/ml)	SD	SEM	One-way ANOVA (<i>p</i>)	CI (95%)
	SSc	232.962	68.12	21.54		190.73-275.18
MMP-12	HC	154.2605	278.20	43.99	2.1E-02	68.04-240.47
	SSc	514.748	798.52	252.52		19.82-1009.66

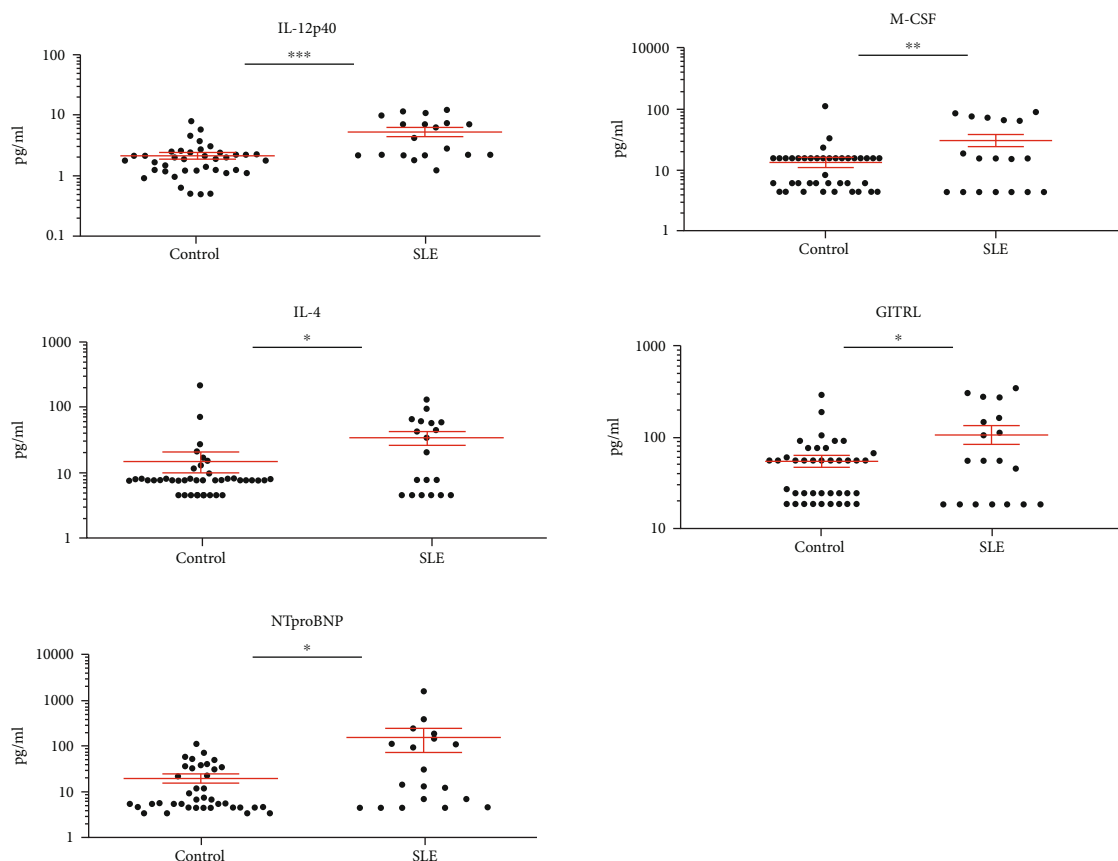


FIGURE 2: The scatter plots of the protein concentrations (pg/ml) of SLE ($n = 19$) patients versus age- and gender-matched healthy controls ($n = 40$) with significant differences (one-way ANOVA, $*p < 0.05$; $**p < 0.01$, $***p < 0.001$). One dot is the average of two technical replicates.

2.4. Statistical Analysis. The arithmetic mean (mean), standard deviation (SD), and the standard error of the mean (SEM) of the plasma cytokine concentrations were calculated. The pairwise comparison of the concentrations of each cytokine of patients versus healthy controls (RA vs. HC; SLE vs. HC; SSc vs. HC) was carried out by one-way ANOVA ($*p < 0.05$; $**p < 0.01$, $***p < 0.001$). The 95% confidence intervals (CI, 95%) were calculated between patients and HCs for each cytokine separately. Calculations were done in Microsoft Excel.

3. Results and Discussion

The following 30 plasma cytokines in the custom Procarta Plex™ panel were quantified in the RA, SLE, and SSc patients and healthy controls (HCs): SDF-1a, GITRL, IL-1b, IL-2, IL-4, IL-5, IL-33, IL-10, Insulin, PYY (3-36), CCL22, IL-13, IL-17A, Gal-3, FKN, IFN- γ , GM-CSF, Leptin, MMP-12, NTproBNP, MCP-1, APRIL, TNFRSF6,

BDNF, BMP-9, IL-12p40, BAFF, M-CSF, Survivin, and CD40-ligand (Supplementary Table 4). These markers under investigation were selected by the authors based on preliminary experiments and literature data. Thirteen cytokines were significantly elevated in RA vs. HCs (Figure 1); the concentrations of eleven cytokines in RA patients showed nonoverlapping confidence interval with HCs (Table 1).

The protein concentrations were the following (RA vs. HC, mean \pm SEM, respectively), IL-12p40: 8.90 ± 1.16 vs. 4.18 ± 0.45 pg/ml; IL-13: 41.74 ± 8.93 vs. 7.25 ± 2.46 pg/ml; IFN- γ : 98.83 ± 34.31 vs. 23.64 ± 2.9 pg/ml; IL-4: 121.79 ± 28.21 vs. 31.14 ± 10.98 pg/ml; NTproBNT: 142.07 ± 34.96 vs. 39.24 ± 7.44 pg/ml; IL-17A: 154.17 ± 51.57 vs. 15.98 ± 4.27 pg/ml; BMP-9: 160.67 ± 62.45 vs. 37.78 ± 5.46 pg/ml; PYY (3-36): 361.6 ± 47.73 vs. 163.96 ± 14.5 pg/ml; GITRL: 901.22 ± 269.22 vs. 110.19 ± 15.96 pg/ml; MMP-12: 833.00 ± 273.93 vs. 154.26 ± 43.99 pg/ml; and TNFRSF6: 1200.63 ± 358.90 vs. 209.45 ± 90.77 pg/ml (Table 1 and Figure 1).

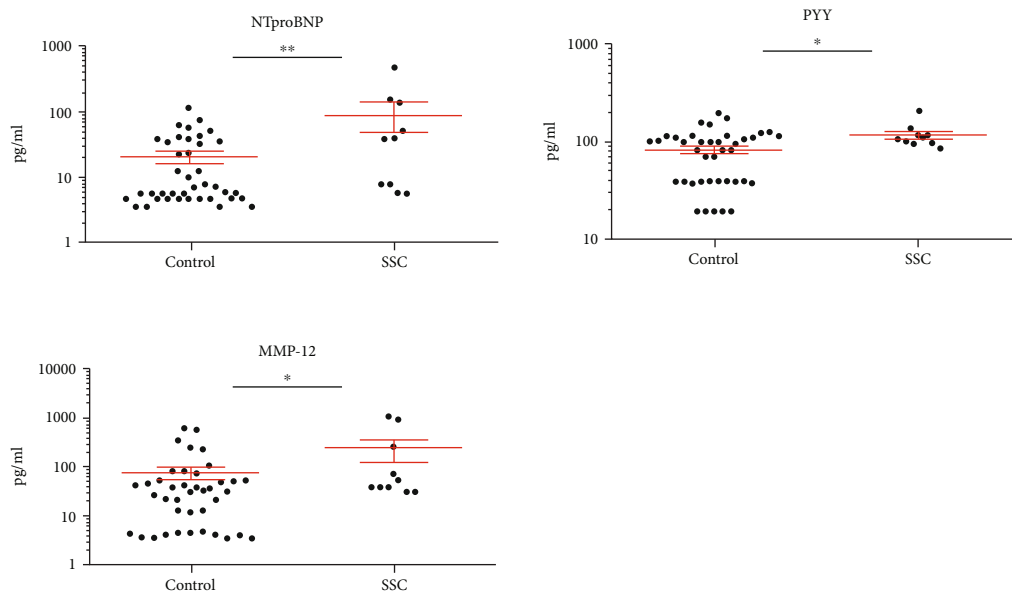


FIGURE 3: The scatter plots of the protein concentrations (pg/ml) of SSc ($n = 10$) patients versus age- and gender-matched healthy controls ($n = 40$) with significant differences (one-way ANOVA, $*p < 0.05$; $**p < 0.01$, $***p < 0.001$). One dot is the average of two technical replicates.

Five cytokines, IL-12p40, M-CSF, IL-4, GITRL, and NTproBNP, were significantly elevated in SLE vs. HC (Figure 2), and only IL-12p40 had nonoverlapping CI with HC: 10.86 ± 1.7 vs. 4.18 ± 0.45 pg/ml (Table 1).

Three cytokines, NTproBNP, PYY (3-36), and MMP-12, were significantly increased in SSc vs. HC (Figure 3), but all had overlapping CI (Table 1).

We are the first to report the cleaved peptide tyrosine tyrosine PYY (3-36) is an early marker of drug-naïve RA vs. HC. The margin of errors (ME) of the CI are 93.55 for PYY in the RA ($n = 31$) group and 28.41 for HC ($n = 40$), the 95% CI falls between 268.05 and 455.16 pg/ml (361.6 pg/ml mean \pm 93.55 ME) for RA, and the 95% CI is between 135.55 and 192.37 pg/ml for HC (163.96 pg/ml mean \pm 28.41 ME) (Table 1). Comparing the concentrations (mean \pm SEM) of PYY (3-36) in RA (361.6 ± 47.7 pg/ml) vs. SLE (189.3 ± 27.5 pg/ml), it was significantly higher in RA ($*p = 1.07 \times 10^{-2}$), and the CI is not overlapping; 95% CI falls between 268.05 and 455.16 pg/ml for RA and 135.4 and 243.3 pg/ml for SLE. The amount of the PYY (3-36) had no significant difference (mean \pm SEM) between RA (361.6 ± 47.7 pg/ml) vs. SSc (232.9 ± 21.5 pg/ml) with CI for RA (268.05-455.16 pg/ml, 95%) and SSc (190.73-275.18 pg/ml, 95%). The amount of the PYY (3-36) had no significant difference (mean \pm SEM) between SLE (189.3 ± 27.5 pg/ml) and SSc (232.9 ± 21.5 pg/ml) with CI for SLE (135.4-243.3 pg/ml, 95%) and SSc (190.73-275.18 pg/ml, 95%). There was no difference in the concentrations of the following cytokines in either RA, SLE, or SSc patients versus HCs: SDF-1a, IL-1b, IL-2, IL-5, IL-33, Insulin, CCL22, Gal-3, FKN, GM-CSF, Leptin, MCP-1, APRIL, BDNF, BAFF, Survivin, and CD40-ligand, respectively.

Thirteen cytokines showed significantly elevated concentrations in the plasma of SAD patients, distinguishing RA (Figure 1), SLE (Figure 2), or SSc (Figure 3) from HCs,

respectively. Arranging the values in an ascending order of the concentrations of the plasma cytokines as a prototype model delineates a characteristic cytokine/chemokine pattern of RA, SLE, and SSc. Therefore, after performing the assay, we propose a simple diagnostic algorithm fitting the curves of cytokine concentration values of early drug-naïve SADs patients vs. HCs to diagnose drug-naïve RA, SLE, or SSc (Figure 4). Based on these data, we propose the machine-learning automated classification of drug-naïve RA, SLE, and SSc, which should be further verified in a dedicated clinical study.

Better identification of the specific molecular players of the early stage of SADs may contribute to the recognition of novel prognostic markers and could facilitate the pathogenesis-appropriate timing of therapeutic interventions. In summary, we have quantified plasma proteins in early SAD patients, prior to therapeutic modification of the disease pathology. A characteristic pattern of soluble mediators was revealed distinguishing early diagnosed therapy-naïve RA, SLE, or SSc from HCs. These eleven markers with nonoverlapping CI (95%) were associated with RA: IL-12p40, IL-10, IL-13, IFN- γ , M-CSF, IL-4, NTproBNP, IL-17A, BMP-9, PYY, GITRL, MMP12, and TNFRSF6, and one marker, IL-12p40, with SLE versus HCs (Table 1). However, we suggest our Luminex panel for in vitro diagnostics and the development of a simple algorithm to differentiate therapy-naïve RA, SLE, or SSc based on the profile of protein concentrations (Figure 4).

There were no significant correlations in PYY (3-36) concentration (pg/ml values) compared to CRP, ESR, RF, aMVCV, and DAS28 scores in RA, separately. However, the concentration of two cytokines in the plasma of drug-naïve RA patients, the IL-4 or GITRL concentrations, showed correlation with bioactive PYY (3-36) level, respectively. (Supplementary Figure 1). The elevated GITRL or IL-4

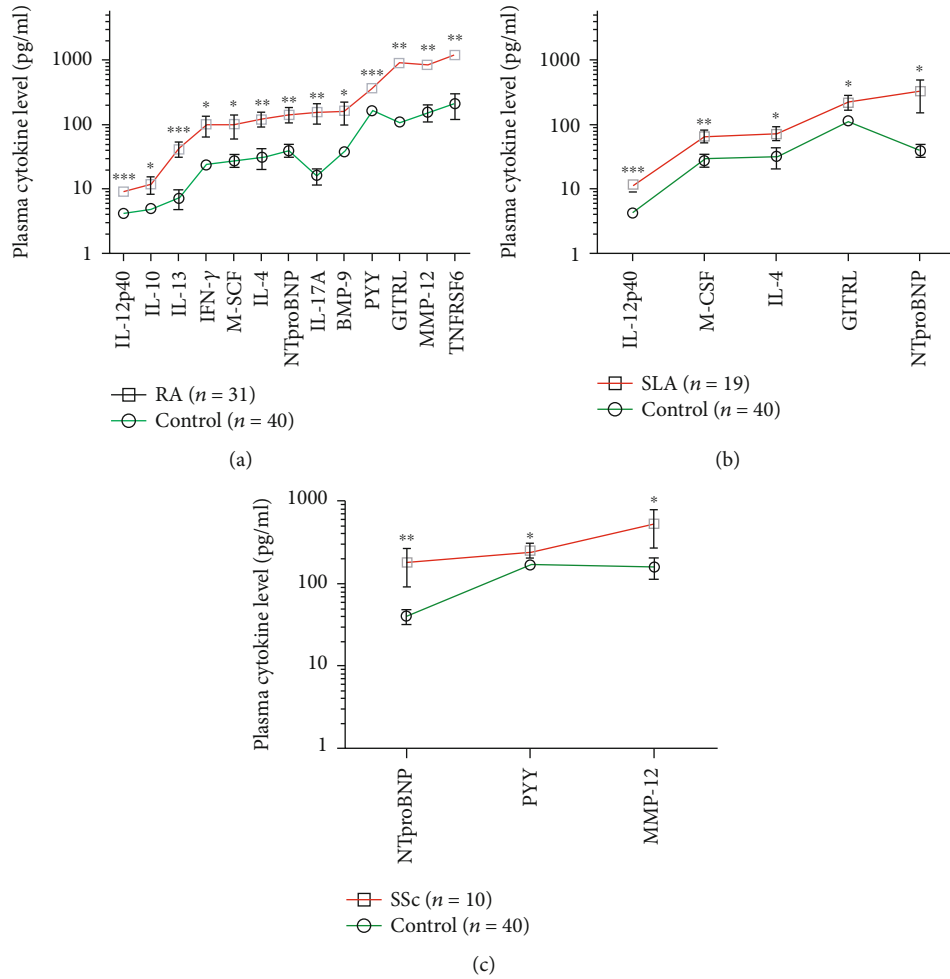


FIGURE 4: The concentrations of plasma cytokines (pg/ml) in the ascending order of (a) RA ($n = 31$), (b) SLE ($n = 19$), and (c) SSc ($n = 10$) patients versus age- and gender-matched healthy controls ($n = 40$) measured by the Luminex MAGPIX technology. The cleaved peptide tyrosine tyrosine PYY (3-36) is a novel marker of early-onset therapy-naive rheumatoid arthritis (RA) ($***p = 4 \times 10^{-5}$). The arithmetic mean \pm SEM are demonstrated for each cytokine on a log10 scale in GraphPad Prism software. The connecting lines delineate a characteristic pattern of proteins measured specific to drug-naive autoimmune diseases (red) such as (a) RA, (b) SLE, and (c) SSc or healthy controls (green).

have been thoroughly studied in RA and associated with disease severity linked to Th17-cell activation or autoantibody induction, respectively [16, 17]. However, their association with the increased concentration with PYY (3-36) needs further mechanistic studies to explain. We describe here the cleaved peptide tyrosine tyrosine (PYY 3-36) as a plasma marker of early-onset drug-naive RA. The 1-36 peptide YY (PYY) as a gut hormone has been reported to be activated by dipeptidyl peptidase-IV (DPP-IV or CD26) cleavage resulting in PYY (3-36) which binds to Y2 (coded by *NPY2R*) receptors in the hippocampus reducing appetite [18, 19]. Chen et al. showed that plasma PYY concentration was negatively correlated with the increase of body weight in RA patients followed by etanercept therapy [20]. The authors have no direct evidence, but the literature and our data may suggest that the elevated plasma PYY (3-36) level contributes to the reduced appetite and cachexia of RA patients. Chen et al. already shed light on PYY as a link between the gastrointestinal neuroendocrine axis and

the immune system [21]. The possible role of Y2 receptor + microglia, monocytes/macrophages, granulocytes, and lymphocytes on the immune homeostasis and regulation of inflammation has been recently reviewed [22]. Further research is needed to ascertain the role of PYY (3-36) in early-onset RA and its possible effect on the innate or adaptive arm of the immune system and whether it has a regulatory effect or its increase in the blood is just a consequence of the pathomechanism of RA.

4. Conclusions

We are the first to report PYY (3-36) as a specific plasma marker of drug-naive RA. Additionally, the multiplex analysis of 30 plasma proteins supported a disease-specific cytokine pattern in RA, SLE, and SSc, respectively. Based on these data, we could delineate a prototype model for the machine-learning automated classification of drug-naive RA, SLE, and SSc.

Data Availability

Additional data are in the Supplementary Files, or raw data can be requested from the corresponding author.

Conflicts of Interest

The authors declare that there is no conflict of interest regarding the publication of this paper.

Acknowledgments

This research was funded by the following grants: GINOP-2.3.2-15-2016-00001 (BRC), GINOP-2.3.2-15-2016-00030 (BRC and UoS), 2017-1.3.1-VKE-2017-00028 (Avicor), and 2018-1.3.1-VKE-2018-00024 (BRC and Avidin) from the National Research, Development and Innovation Office (NKFI), Hungary. This study was prepared with the professional support of the doctoral student scholarship program of the cooperative doctoral program of the Ministry of Innovation and Technology financed by the National Research, Development and Innovation Fund for Jozsef A. Balog (KDP-17-4/PALY-2021, 1000464).

Supplementary Materials

Supplementary 1. Supplementary Table 1: clinical characteristics of RA study participants. The median DAS28 disease activity score was 6.01, and Q1-Q3 interquartiles were 5.4-6.5. Several clinical and immunoserological parameters were present at the time of diagnosis of RA including RF: rheumatoid factor; MCV: mutated citrullinated vimentin; CRP: C-reactive protein; ESR: erythrocyte sedimentation rate. Data are expressed as median and interquartile range (Q1, Q3) for continuous variables and as number (n) and (%) for categorical variables. BLD: below the detection limit.

Supplementary 2. Supplementary Table 2: clinical characteristics of SLE study participants. The median SLEDAI-2K activity score was 16, and Q1-Q3 interquartiles were 10-21. Several clinical and immunoserological parameters were present at the time of diagnosis of SLE including ANA (antinuclear antibodies); anti-DNA antibody; LA (lupus anticoagulant) (activated partial thromboplastin time > 40 s, 8/19); hemolytic anemia (hematocrit < 0.35, 4/19); nonhemolytic anemia (hematocrit < 0.35, 4/19); leukopenia (leukocyte count < 3000/mm³, 8/19); lymphopenia (lymphocyte count < 1500/mm³, 7/19); and thrombocytopenia (thrombocyte count < 100000/×10⁶l, 7/19). Data are expressed as median and interquartile range (Q1, Q3) for continuous variables and as number (n) and (%) for categorical variables.

Supplementary 3. Supplementary Table 3: clinical characteristics of SSc study participants. Several clinical and immunoserological parameters were present at the time of diagnosis of SSc including ANA (antinuclear antibodies); anti-Scl-70, anti-Scl-70 antibodies; ACA (anticentromere antibodies); and anti-RNA polymerase III antibodies. Data are expressed as median and interquartile range (Q1, Q3) for continuous variables and as number (n) and (%) for categorical variables.

dcSSc: diffuse cutaneous SSc; lcSSc: limited cutaneous SSc; skin score^b: modified Rodnan skin thickness score.

Supplementary 4. Supplementary Table 4: the list of the proteins measured in the plasma of the human subjects enrolled in the study. The lower range of the detection corresponds to the threshold of the sensitivity of the assay. The Procarta Plex™ panel was designed by the authors, and the assay was loaded on a MAGPIX Luminex instrument.

Supplementary 5. Supplementary Figure 1: the Pearson correlations of the plasma concentrations of IL-4 vs. PYY (3-36) or GITRL vs. PYY (3-36) in RA patients were analyzed in Microsoft Excel. The Pearson correlation coefficients were 0.819 for IL-4 vs. PYY (3-36) and 0.864 for GITRL vs. PYY (3-36). The t -statistic (t) was calculated in Microsoft Excel following this equation: $t = (r * \text{SQRT}(n - 2)) / (\text{SQRT}(1 - r^2))$, where n is number of subjects and r is the Pearson coefficient. Then, the p value was calculated in Microsoft Excel following this equation: $p = \text{TDIST}(t, \text{DF}, \text{tails})$, where $\text{DF} = n - 2$, degree of freedom. The p was 1.8×10^{-8} (***) for the correlation of IL-4 vs. PYY (3-36) concentrations. The p was 3.9×10^{-10} (***) for the correlation of GITRL vs. PYY (3-36) concentrations.

References

- [1] F. Goldblatt and S. G. O'Neill, "Clinical aspects of autoimmune rheumatic diseases," *Lancet*, vol. 382, no. 9894, pp. 797–808, 2013.
- [2] M. Wahren-Herlenius and T. Dorner, "Immunopathogenic mechanisms of systemic autoimmune disease," *Lancet*, vol. 382, no. 9894, pp. 819–831, 2013.
- [3] M. G. P. Zuidgeest, P. M. J. Welsing, G. van Thiel et al., "Series: pragmatic trials and real world evidence: paper 5. Usual care and real life comparators," *Journal of Clinical Epidemiology*, vol. 90, pp. 92–98, 2017.
- [4] R. Giacomelli, A. Afeltra, A. Alunno et al., "Guidelines for biomarkers in autoimmune rheumatic diseases - evidence based analysis," *Autoimmunity Reviews*, vol. 18, no. 1, pp. 93–106, 2019.
- [5] B. Nakken, G. Papp, V. Bosnes, M. Zeher, G. Nagy, and P. Szodoray, "Biomarkers for rheumatoid arthritis: from molecular processes to diagnostic applications-current concepts and future perspectives," *Immunology Letters*, vol. 189, pp. 13–18, 2017.
- [6] B. Kolarz, D. Podgorska, and R. Podgorski, "Insights of rheumatoid arthritis biomarkers," *Biomarkers*, vol. 26, no. 3, pp. 185–195, 2021.
- [7] C. Arriens, J. D. Wren, M. E. Munroe, and C. Mohan, "Systemic lupus erythematosus biomarkers: the challenging quest," *Rheumatology*, vol. 56, article kew407, 2017.
- [8] M. Aringer, "Inflammatory markers in systemic lupus erythematosus," *Journal of Autoimmunity*, vol. 110, p. 102374, 2020.
- [9] B. Skaug and S. Assassi, "Biomarkers in systemic sclerosis," *Current Opinion in Rheumatology*, vol. 31, no. 6, pp. 595–602, 2019.
- [10] P. J. Wermuth, S. Piera-Velazquez, J. Rosenbloom, and S. A. Jimenez, "Existing and novel biomarkers for precision medicine in systemic sclerosis," *Nature Reviews Rheumatology*, vol. 14, no. 7, pp. 421–432, 2018.
- [11] M. J. Lewis, M. R. Barnes, K. Blighe et al., "Molecular portraits of early rheumatoid arthritis identify clinical and treatment

- response phenotypes,” *Cell Reports*, vol. 28, no. 9, pp. 2455–2470.e5, 2019.
- [12] D. Aletaha, T. Neogi, A. J. Silman et al., “2010 Rheumatoid arthritis classification criteria: an American College of Rheumatology/European League Against Rheumatism collaborative initiative,” *Arthritis and Rheumatism*, vol. 62, no. 9, pp. 2569–2581, 2010.
- [13] M. Petri, A. M. Orbai, G. S. Alarcon et al., “Derivation and validation of the Systemic Lupus International Collaborating Clinics classification criteria for systemic lupus erythematosus,” *Arthritis and Rheumatism*, vol. 64, no. 8, pp. 2677–2686, 2012.
- [14] F. van den Hoogen, D. Khanna, J. Fransen et al., “2013 classification criteria for systemic sclerosis: an American College of Rheumatology/European League against Rheumatism collaborative initiative,” *Arthritis and Rheumatism*, vol. 65, no. 11, pp. 2737–2747, 2013.
- [15] E. C. LeRoy, C. Black, R. Fleischmajer et al., “Scleroderma (systemic sclerosis): classification, subsets and pathogenesis,” *The Journal of Rheumatology*, vol. 15, no. 2, pp. 202–205, 1988.
- [16] J. Tian, B. Zhang, K. Rui, and S. Wang, “The role of GITR/GITRL interaction in autoimmune diseases,” *Frontiers in Immunology*, vol. 11, article 588682, 2020.
- [17] C. Dong, T. Fu, J. Ji, Z. Li, and Z. Gu, “The role of interleukin-4 in rheumatic diseases,” *Clinical and Experimental Pharmacology & Physiology*, vol. 45, no. 8, pp. 747–754, 2018.
- [18] M. Kjaergaard, C. B. G. Salinas, J. F. Rehfeld, A. Secher, K. Raun, and B. S. Wulff, “PYY(3-36) and exendin-4 reduce food intake and activate neuronal circuits in a synergistic manner in mice,” *Neuropeptides*, vol. 73, pp. 89–95, 2019.
- [19] A. De Silva and S. R. Bloom, “Gut hormones and appetite control: a focus on PYY and GLP-1 as therapeutic targets in obesity,” *Gut and Liver*, vol. 6, no. 1, pp. 10–20, 2012.
- [20] C. Y. Chen, C. Y. Tsai, P. C. Lee, and S. D. Lee, “Long-term etanercept therapy favors weight gain and ameliorates cachexia in rheumatoid arthritis patients: roles of gut hormones and leptin,” *Current Pharmaceutical Design*, vol. 19, no. 10, pp. 1956–1964, 2013.
- [21] C. Y. Chen and C. Y. Tsai, “From endocrine to rheumatism: do gut hormones play roles in rheumatoid arthritis?,” *Rheumatology*, vol. 53, no. 2, pp. 205–212, 2014.
- [22] W. C. Chen, Y. B. Liu, W. F. Liu, Y. Y. Zhou, H. F. He, and S. Lin, “Neuropeptide Y is an immunomodulatory factor: direct and indirect,” *Frontiers in Immunology*, vol. 11, article 580378, 2020.